

Durham E-Theses

The Jurassic Source Rock Potential of the Celtic Sea and Western Approaches

JACK KIERAN LEE

How to cite:

LEE, JACK KIERAN (2018) The Jurassic Source Rock Potential of the Celtic Sea and Western Approaches. Masters thesis, Durham University.

Use policy



This work is licensed under a [Creative Commons Public Domain Dedication 1.0 \(CC0\)](#)

The Jurassic Source Rock Potential of the Celtic Sea and Western Approaches



Jack Kieran Lee

Department of Earth Sciences

Durham University

One Volume

**Thesis submitted in accordance with the regulations for the
degree of Master of Science by Research in Durham
University, Department of Earth Sciences, 2017**

The Jurassic Source Rock Potential of the Celtic Sea and Western Approaches

Jack Kieran Lee

Abstract

A working petroleum system requires the presence of mature source rocks that have generated significant quantities of petroleum along with favourable timing of generation and expulsion with respect to the reservoir, trap and seal development. The Oil and Gas Authority (OGA) is currently promoting exploration in frontier basins extensional Mesozoic half graben and graben basins of the Western Approaches and Celtic Sea regions. Despite initial exploration efforts during the 1970s to 1990s, the source rock potential and likely timing of hydrocarbon generation and expulsion in the Celtic Sea and Western Approaches remain poorly understood. The Dragon Discovery, located between the North Celtic Sea and St George's Channel Basins is the only discovery (gas with minor oil shows). Analysis of legacy geochemical datasets suggests that the Jurassic mudrocks contain the main intervals of potential source rock.

The Lower Jurassic strata in the Western Approaches and Celtic Sea Basins are shown to have highly variable source rock potential. Regionally, Sinemurian to Pliensbachian mudrocks form a zone of correlatable source rock potential with Total Organic Carbon commonly greater than 2% and Hydrogen Index values of greater than 200 mg/g. The main limiting factors are the general immaturity to early maturity of Jurassic strata, and the limited preservation of Jurassic sediments, especially in the Western Approaches. Late Jurassic to Early Cretaceous uplift and erosion caused the truncation of Jurassic strata in the Western Approaches and South Celtic Sea Basin, and a cessation in the increase of the thermal maturity of the Jurassic interval. This Late Jurassic to Early Cretaceous uplift and erosion event is suggested as the main control on the preservation and maturity (0.4-0.6% R_o) of Jurassic source rocks in the UK sector of the Celtic Sea and Western Approaches. The potential also exists for the preservation of more deeply buried sections of Jurassic source rock in localised graben at greater thermal maturity (>0.55% R_o).

Declaration and Copyright

I declare that this thesis which is presented for the degree of Master of Science by Research at Durham University, is a result of my own original research, except where acknowledgement is made in the text and has not been previously submitted to Durham University or any other institution.

Jack Lee

Durham University

September 2017

The copyright of this thesis rests with the author. No quotation from it should be published without the author's prior written consent and information derived from it should be acknowledged.

Table of Contents

Contents

Abstract.....	i
Declaration and Copyright.....	ii
Table of Contents.....	iii
Acknowledgements	viii
Figure List.....	ix
Table List	xxiv
Chapter 1	1
1. Introduction	2
1.1. Aims	2
1.1.1. Objectives and Project Layout	2
1.2. Project Structure and Layout.....	3
1.2.1. Region of Interest and Geological Nomenclature	5
1.3. Source Rocks.....	6
1.4. Analogue Data.....	6
1.4.1. Wessex Basin (Wytch Farm)	6
1.4.2. St George’s Channel Basin	8
1.5. Analysis of new Oil and Gas Authority (OGA) 2D seismic lines.....	10
Chapter 2	11
2. Palaeogeography and Tectonostratigraphic Framework of the Western Approaches and Celtic Sea Basins.....	12
2.1. Introduction	12
2.1.1. Objectives	12
2.1.2. Chapter Layout.....	13
2.2. Geodynamic and Palaeogeographic Evolution	15
2.2.1. Precambrian to Early Palaeozoic.....	15
2.2.2. Caledonian Orogeny	17

2.2.3.	Variscan Orogeny.....	20
2.3.	Basin Architecture and Fabrics	26
2.3.1.	Armorican Trends	28
2.3.2.	Caledonian Trends	28
2.3.3.	Variscan Trends	29
2.3.4.	Strike-Slip Faults	30
2.3.5.	3D Architecture.....	31
2.4.	Megasequences.....	32
2.5.	Devonian & Carboniferous - Megasequence 1.....	35
2.5.1.	Early Devonian.....	35
2.5.2.	Devonian to Early Carboniferous.....	36
2.5.3.	Culm Basin and South Wales Basin.....	37
2.5.4.	Potential Source Rock Strata in Megasequence 1.....	41
2.6.	Permian to Late Jurassic - Megasequence 2	43
2.6.1.	Permian to Triassic	43
2.6.2.	Early Jurassic.....	51
2.6.3.	Middle Jurassic	57
2.6.4.	Late Jurassic.....	59
2.7.	Cretaceous to Cenozoic - Megasequence 3	66
2.8.	Paleogene to Recent - Megasequence 4	70
2.9.	Summary of Palaeogeography and Tectonostratigraphic Framework.....	74
Chapter 3	75
3.	Regional Drilling History Summary	76
3.1.	Introduction.....	76
3.1.1.	Celtic Sea.....	77
3.1.2.	Western Approaches	80
3.1.3.	French Sector.....	82
3.2.	Dragon Discovery.....	84
3.2.1.	Discussion	88

3.3.	Conclusions	90
Chapter 4		91
4.	Methods.....	92
4.1.	Introduction	92
4.1.1.	Petroleum Generation and Expulsion.....	92
4.1.2.	Source Rock Richness, Quality and Maturity	93
4.2.	Geochemical and Visual Analyses.....	93
4.2.1.	Pyrolysis (Rock-Eval)	93
4.2.2.	Kerogen Types.....	96
4.2.3.	Total Organic Carbon (TOC)	98
4.2.4.	Vitrinite Reflectance (VR).....	98
4.2.5.	Visual Analysis of Kerogen	101
4.3.	Wireline Data	102
4.4.	KinEx – Modelling Software	106
4.5.	Discussion	107
4.6.	Conclusions	109
Chapter 5		111
5.	Source Rock Analysis.....	112
5.1.	Introduction	112
5.1.1.	Aim	112
5.1.2.	Objectives	113
5.2.	Data Availability	114
5.2.1.	HI & OI - Rock-Eval and TOC.....	117
5.2.2.	Thermal Maturity Indicators.....	119
5.2.3.	Summary	120
5.3.	Maturity	121
5.3.1.	Indicators of Thermal Maturity.....	121
5.3.2.	Summary of Basin History Models.....	132
5.3.3.	Summary of Thermal Maturity	141

5.4.	Source Rock Richness	142
5.4.1.	Total Organic Carbon	142
5.4.2.	Summary of Source Rock Richness	149
5.5.	Source Rock Quality.....	150
5.5.1.	Celtic Sea.....	151
5.5.2.	Western Approaches	152
5.5.3.	Summary of Source Rock Quality	153
5.6.	Kerogen Type.....	154
5.6.1.	Summary of Kerogen Type	157
5.7.	Source Rock Potential from key well analysis	158
5.7.1.	North Celtic Sea Basin.....	158
5.7.2.	South Celtic Sea Basin.....	165
5.7.3.	Western Approaches – Melville Basin	167
5.7.4.	Summary of Source Rock Potential	172
5.8.	Discussion	174
5.8.1.	Sinemurian to Pliensbachian	174
5.8.2.	Toarcian	175
5.8.3.	Middle Jurassic	176
5.8.4.	Late Jurassic.....	177
5.9.	Conclusions.....	179
Chapter 6	181
6.	Discussion	182
6.1.	Introduction.....	182
6.1.1.	Aim.....	182
6.1.2.	Objectives	182
6.2.	Jurassic Palaeoenvironments	183
6.2.1.	Early Jurassic.....	183
6.2.2.	Middle Jurassic	184
6.2.3.	Late Jurassic.....	184

6.3.	Top M2 Unconformity “Cimmerian”	186
6.3.1.	Introduction	186
6.3.2.	Mechanisms for Uplift	187
6.3.3.	Hypotheses for Uplift Generation.....	189
6.4.	Maturity	195
6.4.1.	Effect of Top M2 Unconformity and Uplift periods	195
6.4.1.	Implications for Petroleum Generation and Expulsion.....	196
6.5.	Implications for the Petroleum System	198
6.5.1.	Sea Surface Slicks (Browning-Stamp, 2017).....	198
6.5.2.	Summary of Work	200
6.6.	Recommendations/Future Work	201
6.6.1.	Rhenium-Osmium Geochronology	201
6.6.2.	Resampling.....	201
6.6.3.	2D Burial History Analysis	202
6.6.4.	Backstripping and Regional Structural Analysis	202
6.6.5.	Further Petroleum System Analysis	203
6.6.6.	Additional Source Rock Potential.....	203
6.6.7.	Seismic Interpretation	204
Chapter 7	209
7.	Conclusions	210
References	212

Acknowledgements

My sincere thanks to my family and friends for their support and encouragement.

Jonny Imber, Ken McCaffrey and Stuart Jones will always have my gratitude for their patience and guidance even as the document kept getting longer and longer.

Stephan Stricker deserves an honourable mention for always giving me a succinct explanation of what I had left to do.

Iain Scotchman, Tony Doré, Julian Moore and Andy Aplin all gave up their time to share their knowledge with me for which I will be eternally grateful.

Eddie Dempsey always challenged me to be bolder.

George Lodwick and Phil Davies shared my pain with Masters' theses of their own.

Pavlos Farangitakis and the Elvet Striders kept me sane and going out for runs.

Thanks to everyone in the Durham University Department of Earth Sciences without whom I would have gone mad months ago.

Thanks to everyone who humoured me at coffee and those who kept me company on the long working weekends (Jordan, Matt, Adam, Kate and Alex).

A special mention to Miles, Sarah and Chris without whom I never would have known when it was time for tea.

Figure List

Chapter 1

Fig 1.1. Map of the region of interest off the south west coast of Britain. The basins distribution and nomenclature as laid out in Section 1.2 are shown (modified after Ziegler, 1987b and Chapman, 1989). The green shading outlines the Celtic Sea Basins with the Western Approaches Basins shaded in blue. Black lines represent tectonic fabrics or faults from Ziegler (1987b) and the magenta outline of the region marks the limits of the UK Sector of the Western Approaches and Celtic Sea.

Fig 1.2. Stratigraphic column for the Wessex Basin with analysis focussed on the Early Jurassic Lower Lias Clays to Upper Lias.

Fig 1.3. Map of the Celtic Sea with fault trends based on Readman *et al.* (1995) superimposed on the map.

Chapter 2

Fig 2.1. Map of the French and UK Western Approaches with the wells included in this chapter from the French and UK Sector shown. Black lines represent tectonic fabrics or faults from Ziegler (1987b) and the magenta outline of the region marks the limits of the UK Sector of the Western Approaches and Celtic Sea.

Fig 2.2. Palaeocontinental reconstructions from the Neoproterozoic. (a) The Rodinia Supercontinent is shown at prior to break-up. (b) The Vendian Supercontinent is shown prior to rifting of Laurentia away from the margin of West Gondwana. S – Southern Britain (region of interest), N – Northern Britain.

Fig 2.3. Tectonic reconstruction for the Cambrian (Woodcock & Strachan, 2012). The south of Britain (Avalonia) is shown on the northern margin of Gondwana with the north of Britain on the margin of Laurentia.

Fig 2.4. Schematic diagram demonstrating the Silurian closure of the Iapetus (Soper *et al.*, 1992a). (a) is a time-slice at the Ordovician-Silurian boundary (440 Ma) showing the position of Laurentia, Avalonia and Baltica during the end Ordovician with Laurentia situated on the equator and separated from Baltica by the Northern Iapetus and from Avalonia by the Tornquist Sea. (b) Silurian-Devonian boundary (420 Ma) with arrows showing plate movements in relation to Laurentia and (c) Early Devonian (400 Ma) showing convergence directions of the Acadian Orogeny with convergence in SW England. Figure 2.4

(c) now includes the newly assembled Laurussia in the Early Devonian (~400 Ma) with Late Silurian to Early Devonian orogenic collapse occurring at the same time as the Acadian Orogeny.

Fig 2.5. Palaeographic reconstruction from Torsvik & Cocks (2017) showing the setting of Britain post-Caledonian Orogeny. D – Dniester River, FJL – Franz Josef Land, G – Gotland, TP – Timan-Pechora.

Fig 2.6. Palaeogeographic reconstructions from the Ordovician through to the Carboniferous showing closure of the Iapetus Ocean and subsequent opening and closing of the Rheic Ocean (Torsvik & Cocks, 2017). Ar - Armorica; B - Bohemia; F - Franconian; IB - Iberia; RO - NW arm of Rheic Ocean; SP - South Pole; S-T - Saxothuringia; STO - Saxothuringian Ocean; T (large) - Saxothuringian Terrane; T (small) - Tisia Terrane.

Fig 2.7. Tectonic map for the Western Approaches region and NW France showing the Bristol Channel-Bray Fault (Shail & Leveridge, 2009). The location of the Permian Cornubian Ridge and Haig Fras granites are also shown. BCBF – Bristol Channel-Bray Fault; EA (Orange) – Eastern Avalonia; LD – Léon Domain; NA (Green) – North Armorica; NT (Pink) – Normannian Terrane; SA (Blue) – South Armorica; SWE (Yellow) SW England; VF – Variscan Front.

Fig 2.8. Tectonic map of SW Europe showing the Variscan tectonic zonation with the Rhenohercynian Zone and Variscan Foreland labelled (Leveridge and Hartley, 2006).

Fig 2.9. A map showing the location of the Haig Fras and Cornubian Granites in the SW of England and offshore (Jones *et al.*, 1988).

Fig 2.10. Tectonic map of the Celtic Sea and Western Approaches region (modified from Ziegler, 1987b) with the Western Approaches Basins, South Celtic Sea Basin and North Celtic Sea Basin. The WNW-ESE trend of the Variscan Front is shown along with the NW-SE trend of basin cutting strike-slip faults.

Fig 2.11. Interpretation of fault structures of onshore Ireland and the Celtic Sea based on bouger gravity anomalies (modified after Readman *et al.*, 1995). The change in structural style between the North Celtic Sea Basin (NCSB) and St George's Channel Basin can be clearly seen along with the apparent NW-SW Caledonian trend of these basins and the South Celtic Sea Basin. ENE-WSW to NE-SW fault trends are blue, ENE-WSW "Variscan" fault trends are red and NW-SE fault trends are green. Granite bodies are shaded light grey.

Fig 2.12. Interpreted diagrams from BIRPS seismic reflection surveys (Klemperer & Hobbs, 1991). The North Celtic Sea Basin is shown as underlain by the Variscan Front which soles into a large scale detachment.

Fig 2.13. Schematic diagram based on interpretation of the BIRPS seismic reflection surveys (Klemperer & Hobbs, 1991). The Variscan Front (VF) is shown as separating the graben style basin of the North Celtic Sea Basin (NCSB) from the half graben style basin of the St George's Channel to the East. SCSB – South Celtic Sea Basin; BFS – Bala Fault System; SISL – South Irish Sea Lineament.

Fig 2.14. Tectonostratigraphy of the Celtic Sea region modified after O'Reilly et al. (1998). R1 and R2 represent rift phases while C1 to C3 represent phases of compressional tectonics.

Fig 2.15. Stratigraphy of Britoil Well 72/10-1A in the Melville Basin in the Western Approaches (modified after Bennet et al, 1985).

Fig 2.16. Simplified map of the geology of Cornwall and Devon showing the extent of the Devonian and Carboniferous basins with the Permo-Triassic coloured orange and granite batholiths coloured red (Shail & Leveridge, 2009). Granite bodies are coloured red, Lizard Complex – Purple, Gramscatho Basin – Light Yellow, Looe Basin – Dark Red, South Devon Basin – Light Red, St Mellion Klippe – Green, Tavy Basin – Blue, Culm Basin – Light Green, North Devon Basin – Brown, Permian-Triassic – Orange.

Fig 2.17. Schematic section based on interpretations from the SWAT 9 section suggesting underlying of the Plymouth Bay Basin by the Carrick and Lizard Nappes (Harvey *et al.*, 1994). A-D represent seismically defined megasequence packages for the Plymouth Bay Basin discussed further in Harvey *et al.* (1994).

Fig 2.18. Geological map of SW England showing the locations and extents of the Culm and South West Basin (Hartley and Warr, 1990). It is likely that the Culm Basin continues offshore and could underlie the South Celtic Sea Basin. CCD - Carreg Cennan Disturbance, SVD - Swansea Valley Disturbance, VND - Neath Disturbance, PA - Pontypridd Anticline, SLFZ - Sticklepath Lustleigh Fault Zone, MGF - Moel Gilau Faul, JT - Johnston Thrust, BF - Benton Fault, RT - Ritec Thrust, CaBT - Caswell Bay Thrust, RFZ - Rusey Fault Zone. CHS - Coalpit Heath Syncline, MA - Mendip Axis, MaA - Maesteg Anticline, GS - Gelligaer Syncline, CS - Caerphilly Syncline, CCF - Cardiff Cowbridge Anticline, UA - Usk Axis, FDS - Forest of Dean Syncline, SEFZ - Severn Estuary Fault Zone. BCFZ - Bristol Channel Fault Zone.

Fig 2.19. Palaeogeographic reconstructions for the Carboniferous of Britain (Waters *et al.*, 2009) with a systematic change in the Celtic Sea and Western Approaches from Platform carbonate and hemipelagic deposition in the Early Carboniferous to Coal Measure deposition and uplands by the Westphalian. AIB – Alston Block, AsB – Askrigg block, CB – Craven Basin, CH – Cheviot High, CuB – Culm Basin, DB – Dublin Basin, LH - Leinster High, ML-D – Manx-Lake District High, MV – Midland Valley, NT – Northumberland Trough, RB – Rossendale Block, SB – Shannon Basin, SUH – Southern Uplands High.

Fig 2.20. Map of the Celtic Sea, Western Approaches and Wytch Farm with the wells discussed in Section 2.5.4 highlighted in orange.

Fig 2.21. Tectonic reconstructions for the Early Permian and Middle Triassic (Woodcock and Strachan, 2012) with Pangaea assembled.

Fig 2.22. Summary of the key events for the Permian and Triassic of the UK with an indication of the tectonics, sediments yields, climate, sea level, biosphere and UK stratigraphy (Woodcock and Strachan, 2012).

Fig 2.23. Schematic map showing the location of the main Triassic rifts with suggested extensional directions (Coward, 1995).

Fig 2.24. Summary of climatic settings in the Triassic with indications of playa lake and halite deposition in the Celtic Sea and Western Approaches region (McKie, 2017).

Fig 2.25. Palaeogeographic reconstructions for the Triassic showing the eventual rift development and predominance of an interpreted sabkha setting in the Celtic Sea and Western Approaches (McKie, 2017).

Fig 2.26. Well correlation panel following a roughly E-W transect along the Western Approaches demonstrating the style of Permian and Triassic sediments (Chapman, 1989).

Fig 2.27. Schematic diagrams for the Melville Basin (modified after Chapman, 1989) showing the salt thickness and extent (pink) and preservation of the Jurassic sequence in the North and South of the basin (light blue).

Fig 2.28. Geological cross-section for the North Celtic Sea and South Celtic Sea Basins (van Hoorn, 1987) with the Permian-Triassic strata of the South Celtic Sea Basin highlighted in pink. Permian to Triassic strata have not been penetrated in the North Celtic Sea Basin due to the deep depth of burial.

Fig 2.29. Map of the current North Atlantic margin of Europe for the Early Jurassic showing the areas of source rock deposition and Mesozoic rift basins (Scotchman, 2016). The Central Atlantic shown is the location of the Hispanic Corridor which starts to open into the Central Atlantic during the Sinemurian.

Fig 2.30. Chronostratigraphic division and radiometric dating for the Early Jurassic (Simms et al., 2004).

Fig 2.31. Schematic diagram of the zones of preservation of Lower Jurassic in the Melville Basin (after Chapman, 1989).

Fig 2.32. Early Palaeogeography based on the Mochras Borehole (Cardigan Bay Basin) and Staithe (Cleveland Basin) that are located with red stars (Ruhl et al. 2016).

Fig 2.33. Cartoon summarising the change in relative sea level and $\delta^{13}C$ through the Pliensbachian and Toarcian (Korte & Hesselbo, 2014). OAE – Oceanic Anoxic Event, S-P Event – Sinemurian to Pliensbachian Event.

Fig 2.34. Palaeogeographic reconstruction for the Middle Jurassic of the British Isles (Baron et al., 2012).

Fig 2.35. Schematic geological map (A) and cross-section (B) showing the North Pyrenean Fault (NPF) with a blue indicating the location of an ECORS seismic section. NPZ - North Pyrenean Zone; NPF - North Pyrenean Fault; SPZ - Southern Pyrenean Zone; B – Boixols thrust.

Fig 2.36. A chronostratigraphic correlation diagram from McMahon & Turner (1998) showing a correlative Berriasian age for the Top M2 Unconformity.

Fig 2.37. Map of maturity for the North Celtic Sea Basin for the top Jurassic with highest maturity indicated in the basin centres (Armstrong, 1988).

Fig 2.38. Map of source rock quality and potential yield for the North Celtic Sea Basin for the top Jurassic with (Armstrong, 1988).

Fig 2.39. Palaeogeographic reconstruction of the present-day North Atlantic margins during the Early Cretaceous with much of the SW of Britain indicated to be in a continental setting (Torsvik & Cocks, 2017). JMM – Jan Meyen Microcontinent, NFL – Newfoundland, P – Porcupine Bank.

Fig 2.40. Schematic diagram demonstrating the likely deposition environment of the Early Cretaceous Greensand in the North Celtic Sea Basin (Melvin, 2005).

Fig 2.41. Palaeogeographic reconstruction for the Cenomanian (Torsvik & Cocks, 2017) with the Celtic Sea and Western Approaches located in a shallow shelf environment which leads to the widespread deposition of limestones/chalk. P – Porcupine Bank.

Fig 2.42. Late Cretaceous Chalk regional isopach map (Tucker & Arter, 1987) with the basin inversion axis shown and truncation of the chalk towards the basin margins.

Fig 2.43. Maps of apparent exhumation: (a) the Upper Cretaceous Chalk, (b) Lower Cretaceous Gault/Greensand with the contours labelled in kilometres (Menpes & Hillis, 1995).

Chapter 3

Fig 3.1. Map of gas and oil shows in the Celtic Sea and Western Approaches.

Fig 3.2. Histogram showing the targets for the wells drilled in the French Sector of the Western Approaches with the majority of exploration focused on the Jurassic and Triassic intervals.

Fig 3.3. Correlation plot of well stratigraphy penetrated in the UK Sector of the Melville Basin with indications of hydrocarbon shows (DECC, 2014).

Fig 3.4. Correlation plot of well stratigraphy penetrated in the UK Sector of the Melville Basin with indications of hydrocarbon shows (DECC, 2014).

Fig 3.5. Map showing the distribution of wells in the French Sector of the Western Approaches.

Fig 3.6. Map of the location of the Dragon Discovery with the major surrounding faults shown (Marathon P804 Relinquishment Report).

Fig 3.7. Wireline data from the Upper Jurassic section of 103/01-1 with a lithology based on the composite well log (Marathon Oil 1994). GR is the gamma ray tool in API, V-Shale is a volume shale log interpreted from the gamma ray log, the Density track contains the bulk density (g/cc) in red and the neutron log (v/v) in black, Vp (ft/sec) is the compressional velocity and Resis is the resistivity in ohms of the formation. A sequence of interbedded shales, sandstones and limestones is present at the base Late Jurassic and Middle Jurassic (2050-2700m TVDs) with high resistivity suggesting the limestones and sandstones to be gas-bearing.

Fig 3.8. Seismic line for the Dragon Discovery which has been interpreted by Marathon (Marathon P804 Relinquishment Report).

Fig 3.9. Map of the Melville Basin with a schematic layout in blue of the location of preserved Jurassic (based on Chapman, 1989) below the Top M2 Unconformity "Cimmerian".

Chapter 4

Fig 4.1. Schematic example of the recording of S1-S3 peaks from Rock-Eval pyrolysis (modified after Espitalie et al, 1977).

Fig 4.2. Schematic pseudo-van Krevelen plot with HI and OI used instead of H/C and O/C atomic ratios. Type I and Type IIS plot with this highest HI relative to OI with decreasing hydrocarbon generative ability towards Type II and Type III. Type IV is indicated as having no hydrocarbon generative potential (Dembicki Jr, 2009).

Fig 4.3. Hydrogen Index (HI) vs Rock-Eval Tmax trends for kerogen types demonstrating the control of maturity on both parameters i.e. increased Tmax and reduced HI (Cornford *et al.*, 1998).

Fig 4.4. R_o profiles from offshore Ireland based on Vitrinite Reflectance data. Data from the Cretaceous of the Celtic Sea are plotted as green squares and offset to the right of the other basins suggesting post-Cretaceous uplift (Corcoran & Clayton, 2001).

Fig 4.5. Wireline logs for an Oligocene sequence in Indonesia with cyclic lacustrine deposition of source rocks indicated in the depth column (Meyer & Nerderlof, 1984). The organic matter-rich zones have low density and low sonic couple with high resistivity but no response from GR due to the lacustrine environment of deposition causing a lack of radioactivity.

Fig 4.6. Wireline logs for the Late Devonian Duvernay source rock interval in Alberta, Canada (Meyer & Nerderlof, 1984). The source rock interval at 8360-8400 ft (2548-2560 m) shows increased GR along with low sonic and density. An increased resistivity response suggests that the interval is mature.

Chapter 5

Fig 5.1. Map of the offshore basins of interest off the south west coast of Britain. Basin outlines and nomenclature modified after Ziegler (1987b). A quadrant is an area enclosed by one degree of longitude and latitude with an assigned number.

Fig 5.2. Map of the region offshore the south west of Britain with the 31 wells included for analysis shown. All wells shown have TOC data available. Wells with a green symbol are considered as within the Celtic Sea (South Celtic Sea, North Celtic Sea and St George's Channel Basins), purple is the Western Approaches (Melville, South West Channel and Plymouth Bay Basins) and orange is the Wytch Farm.

Fig 5.3. Map of the region offshore the south west of Britain showing the 18 wells with S2 pyrolysis peaks available that have been used along with TOC to calculate HI values (Section 4.3.1.2).

Fig 5.4. Map of the region offshore the south west of Britain showing the 7 wells with S3 pyrolysis peaks available that have been used along with TOC to calculate OI values (Section 4.3.1.2).

Fig 5.5. Histogram showing the distribution of TOC measurements within the Jurassic interval with samples favouring the Early and Middle Jurassic with 35 samples labelled as only "Jurassic".

Fig 5.6. A histogram of all the Total Organic Carbon (TOC) samples included in the analysis.

Fig 5.7. Map of the region offshore the south west of Britain showing the 23 wells with Vitrinite Reflectance (VR) data (Section 4.3.4).

Fig 5.8. Vitrinite Reflectance versus Depth (MD ft) for 103/01-1 (modified after James Armstrong and Associates, 1995). The Late Jurassic only reaches the oil window below 7500 ft (2286 m) with the entirety of the Middle Jurassic situated in the oil window. The Early Jurassic passes into late mature at approximately 11500 ft (3505 m). Tmax is shown as blue diamonds next to the R_o profile for VR with Tmax initially between 435-440°C (3000-9000 ft or 914-2743 m) and increasing to 440-450°C at depths greater than 10,000 ft (3048 m).

Fig 5.9. Vitrinite Reflectance (Population 1) vs Depth (m) plot from 102/29-1. The Vitrinite Reflectance shows a subtly increasing trend with depth with R_o increasing from 0.45% at 650 m to 0.55% at 1700 m. Maturity boundaries for R_o are shown based on Allen & Allen (2013).

Fig 5.10. Tmax against Depth (m) plot for 93/02-1 with Tmax points indicated by blue diamonds. Tmax measurement are only available in the Jurassic (undifferentiated).

Fig 5.11. SCI against Depth (MD) and VR against Depth plot for well 93/02-1 modified after Robertson Research (1974). Reliable data has been coloured black with data interpreted as

from reworking has been plotted as an X with caved data as open squares with low vitrinite samples a diamond.

Fig 5.12. Plot of the preferred R_o population from the Paleochem (1983) geochemistry report against Depth (m MD). Data are present in from the Early Cretaceous through to the Triassic. A summary of the SCI analysis is included as colour descriptions of the spore samples.

Fig 5.13. Plot of the preferred R_o population from the Paleochem (1983) geochemistry report against Depth (m MD). Data have only been included with 20% vitrinite.

Fig 5.14. Plot of the preferred R_o population from the Robertson Research (1979) geochemistry report against Depth (m MD) with indications of the SCI values from visual kerogen analysis.

Fig 5.15. Plot of indicated autochthonous R_o population (Evans *et al.*, 1977) against Depth with indications of the SCI over the depth.

Fig 5.16. Map of the region of interest with wells with maturity data for the Early Jurassic coloured by interpreted level of maturity from the geochemistry reports. immature – red; immature to early mature – orange; over mature – blue. Interpretations are based on vitrinite reflectance, spore colouration index and T_{max} available in the geochemistry reports. Analysis of 73/07-1 was provided by Scotchman (unpublished work).

Fig 5.17. Subsidence history plot for the southern Melville Basin (Hillis, 1988) taking into account deposition and erosion based on a detailed tectonic history.

Fig 5.18. Time-depth curve for Melville Basin wells 73/12-1 & 73/13-1.

Fig 5.19. Burial History plot for 73/13-1 in the Melville Basin (Ottaviani *et al.*, unpublished work). Maximum burial is indicated in the Late Jurassic (U. Jur) with subsequent rapid exhumation and reburial from the Early Cretaceous to present.

Fig 5.20. Burial history model for well 50/03-1 in the North Celtic Sea Basin which was calibrated to VR and Apatite Fission Track data (AFT). The plot is coloured by maximum experienced maturity from VR; VR reflects maximum maturity experienced and not current maturity of the interval of study.

Fig 5.21. Map of the North Celtic Sea Basin showing the proximity of 50/03-1 to the Dragon Discovery (103/01-1).

Fig 5.22. Burial History Diagram for the South Celtic Sea Basin based on 93/02-1. Predicted maturity of 0.6% Ro correlates well with the interpretation of 93/02-1 in Section 5.3.1. The maturity zones of oil generation are labelled.

Fig 5.23. Schematic diagram showing the influence of a skewed distribution on the median and arithmetic average with the arithmetic average showing higher influence to low frequency high value samples.

Fig 5.24. A histogram of the TOC (%) distribution for the Jurassic with the majority of data located between 0-1% TOC with very good source rocks at 2-15% and isolated samples of >20% TOC.

Fig 5.25. Map for the region of interest displaying histograms of the TOC distributions in the Jurassic with a red 1% TOC reference line.

Fig 5.26. A crossplot of TOC (%) against S2 peak (mg/g) for the Jurassic (log-log axis) with overlays based on (Dembicki Jr, 2009) with data plotted for the Celtic Sea (green triangles), Western Approaches (purple diamonds) and Wytch Farm (orange squares).

Fig 5.27. A crossplot of TOC (%) against S2 peak (mg/g) for the Jurassic (log-log axis) of the Celtic Sea with overlays based on (Dembicki Jr, 2009) with data plotted for Epoch with the Early Jurassic (dark blue circle), Middle Jurassic (green triangle) and Late Jurassic (light blue square).

Fig 5.28. A crossplot of TOC (%) against S2 peak (mg/g) for the Jurassic (log-log axis) of the Western Approaches with overlays based on (Dembicki Jr, 2009) with data plotted for the Early Jurassic (dark blue diamonds) as no Middle Jurassic or Late Jurassic data was available.

Fig 5.29. Pseudo-van Krevelen plot with Hydrogen Index values (mg/g) plotted against Oxygen Index (mg/g) for the Jurassic by region. No Jurassic samples exist for the Western Approaches. Overlays are based on Cornford *et al.* (1998) & Dembicki Jr (2009) and the applicability of the van-Krevelen plot is discussed in Section 4.3.2.

Fig 5.30. Pseudo-van Krevelen plot with Hydrogen Index values (mg/g) plotted against Oxygen Index (mg/g) for the Epochs of the Jurassic. No Jurassic samples exist for the Western Approaches. Overlays are based on Cornford *et al.* (1998) & Dembicki Jr (2009) and the applicability of the van-Krevelen plot is discussed in Section 4.3.2.

Fig 5.31. Pseudo-van Krevelen plot with Hydrogen Index values (mg/g) plotted against Oxygen Index (mg/g) for the Jurassic coloured by source rock richness (Peters, 1986).

Squares represent Celtic Sea data points and diamonds represent Wytch Farm data. No Jurassic samples exist for the Western Approaches. Overlays are based on Cornford *et al.* (1998) & Dembicki Jr (2009) and the applicability of the van-Krevelen plot is discussed in Section 4.3.2.

Fig 5.32. Wireline data from the Upper Jurassic section of 103/01-1 with a lithology based on the composite well log. TOC values are shown as red circles, HI as blue squares and S1 peaks as green triangles. GR is the gamma ray tool in API, V-Shale is a volume shale log interpreted from the gamma ray log, the Density track contains the bulk density (g/cc) in red and the neutron log (vol/vol) in black, Vp (ft/sec) is the compressional velocity and Resis is the deep resistivity in Ohmm of the formation.

Fig 5.33. Wireline data from the Lower Jurassic section of 103/01-1 with a lithology based on the composite well log. TOC values are shown as red circles, HI as blue squares and S1 peaks as green triangles. GR is the gamma ray tool in API, V-Shale is a volume shale log interpreted from the gamma ray log, the Density track contains the bulk density (g/cc) in red and the neutron log (v/v) in black, Vp (ft/sec) is the compressional velocity and Resis is the deep resistivity in ohmm of the formation.

Fig 5.34. A crossplot of TOC (%) against S2 peak (mg/g) for the Jurassic (log-log axis) of the Celtic Sea with overlays based on (Dembicki Jr, 2009) with data plotted for the 103/01-1 from the Lower Jurassic (dark blue circle), Middle Jurassic (green triangle) and Upper Jurassic (light blue square). All other data is greyed out.

Fig 5.35. Plot of hydrocarbon yield against temperature based on the Upper Jurassic source rock section of 103/01-1 indicated using the KinEx software package with calculations based on Pepper & Corvi (1995). Kerogen type was input as algal matter (50% Type C) with high levels of terrestrial input (50% Type D/E) although Type C & Type D/E end-members were also run.

Fig 5.36. Plot of cumulative HC6+ (oil) and HC1-5 (gas) expulsion. Expulsion of oil would occur between 125-150°C with gas between 130-200°C. Early expulsion would be predominantly oil with later gas expulsion with estimates suggesting the Late Jurassic interval would be able to produce ~58 mmstb/km² of oil and ~42 mmboe/km² of gas.

Fig 5.37. Wireline data from the Lower Jurassic section of 103/02-1. TOC values are shown as red circles with HI and S1 information unavailable. GR is the gamma ray tool in API, V-Shale is a volume shale log interpreted from the gamma ray log, Vp (ft/sec) is the compressional velocity and Resis is the resistivity in ohmm of the formation.

Fig 5.38. Plot of cumulative HC6+ (oil) and HC1-5 (gas) expulsion. Expulsion of oil would occur between 135-160°C with gas between 140-200°C. Early expulsion would be predominantly oil with later gas expulsion with estimates suggesting the Upper Jurassic interval would be able to produce ~4.2 mmstb/km² of oil and ~9.5 mboe/km². Kerogen type is presumed to be predominantly Type D/E of terrestrial origin based on Early Jurassic data in the pseudo-van Krevelen diagrams (Fig 5.29. & Fig 5.30).

Fig 5.39. Wireline data from the Lower Jurassic section of 102/29-1. TOC values are shown as red circles with HI and S1 information unavailable. GR is the gamma ray tool in API, V-Shale is a volume shale log interpreted from the gamma ray log, the Density track contains the bulk density (g/cc) in red and the neutron log (v/v) in black, Vp (ft/sec) is the compressional velocity and Resis is the resistivity in ohmm of the formation.

Fig 5.40. Plot of cumulative HC6+ (oil) and HC1-5 (gas) expulsion. Expulsion of oil would occur between 135-160°C with gas between 140-200°C. Early expulsion would be predominantly oil with later gas expulsion with estimates suggesting the Late Jurassic section would be able to produce ~40 mmstb/km² of oil and ~48 mboe/km² of gas. Kerogen type is presumed to be predominantly Type D/E of terrestrial origin based on Early Jurassic data in the pseudo-Van Krevelen diagrams (Fig 5.29 & 5. 30).

Fig 5.41. Wireline data from the Jurassic section of 103/21-1. TOC values are shown as red circles with HI and S1 information unavailable. GR is the gamma ray tool in API, V-Shale is a volume shale log interpreted from the gamma ray log, the Density track contains the bulk density (g/cc) in red and the neutron log (v/v) in black, Vp (ft/sec) is the compressional velocity and Resis is the deep resistivity in ohmm of the formation.

Fig 5.42. Wireline data from the Lower Jurassic section of 73/13-1. TOC values are shown as red circles, HI as blue squares. GR is the gamma ray tool in API, V-Shale is a volume shale log interpreted from the gamma ray log, the Density track contains the bulk density (g/cc) in red and the neutron log (v/v) in black, Vp (ft/sec) is the compressional velocity and Resis is the resistivity in ohmm of the formation.

Fig 5.43. Plot of hydrocarbon yield against temperature based on the Upper Jurassic source rock section indicated in Fig 5.35 using the KinEx software package with calculations based on Pepper & Corvi (1995). Kerogen type was input based on Scotchman (unpublished work) as marine organic matter (50% Type B) with high levels of terrestrial input (50% Type D/E) although Type B & Type D/E end-members were also run.

Fig 5.44. Plot of cumulative HC6+ (oil) and HC1-5 (gas) expulsion. Expulsion of oil would occur between 135-160°C with gas between 140-200°C. Early expulsion would be predominantly oil with later gas expulsion with estimates suggesting the Upper Jurassic section would be able to produce ~15.5 mmstb/km² of oil and ~15 mmboe/km² of gas. Kerogen type is presumed to be composed of Type B & Type D/E.

Fig 5.45. Wireline data from the Lower Jurassic interval of 88/02-1. TOC values are shown as red circles with HI and S1 information unavailable. GR is the gamma ray tool in API, V-Shale is a volume shale log interpreted from the gamma ray log, the Density track contains the bulk density (g/cc) in red and the neutron log (v/v) in black and Resis is the resistivity in ohmm of the formation. Wireline data is not available until 50 m into the Pliensbachian.

Fig 5.46. Wireline data from the Lower Jurassic section of 98/16-1. TOC values are shown as red circles, HI as blue squares. GR is the gamma ray tool in API, the Density track contains the bulk density (g/cc) in red, Vp (ft/sec) is the compressional velocity and Resis is the resistivity in ohmm of the formation. The Uran track is also included which is the uranium count from SGR in ppm as described in Section 4.4.

Fig 5.47. TOC (red circles) and HI (blue squares) data from Wytch Farm well 98/23-1 showing similar profiles of high TOC in the Pliensbachian to Sinemurian-Hettangian. In addition good source rock potential exists in the Middle Jurassic.

Fig 5.48. Wireline data from the Jurassic section of 98/13-1. TOC values are shown as red circles, HI as blue squares and S1 peaks as green triangles. GR is the gamma ray tool in API, Vp (ft/sec) is the compressional velocity and Resis is the resistivity in ohmm of the formation. Substantial Upper Jurassic potential exists with only minor potential in the Early Jurassic.

Chapter 6

Fig 6.1. Map of the current North Atlantic margin of Europe for the Late Jurassic showing the areas of source rock deposition and Mesozoic rift basins (Scotchman *et al.*, 2016).

Fig 6.2. A seismic section (bottom) and an interpreted seismic profile (top) from A-A' (Chapman, 1988). The Jurassic reflectors are truncated by the Top M2 Unconformity with preservation in a syncline between salt walls.

Fig 6.3. Map of the region of interest showing the lines of the correlation panels in Fig 6.4 (red) and Fig 6.5 (green).

Fig 6.4. Chronostratigraphic correlation panel for the Western Approaches with oil (green) and gas (red) shows and cored sections indicated (Stricker *et al.*, unpublished work). The uncertainty range on any given interval is shown by the red bars. Where no uncertainty is stated the bar is absent.

Fig 6.5. Chronostratigraphic correlation panel for the Celtic Sea with oil (green) and gas (red) shows and cored sections indicated (Stricker *et al.*, unpublished work). The uncertainty range on any given interval is shown by the red bars. Where no uncertainty is stated the bar is absent.

Fig 6.6. A is a map of North Spain showing the uppermost age of the stratigraphy underlying the Wealden. B. shows the overlapping relationship of the Wealden with the underlying Permian to Jurassic sediments with progressively older subcropping sediments to the West.

Fig 6.7. Schematic tectonic reconstruction modified from Lundin & Dore (In Press). Pink indicates highs, light green extension, darker green is hyperextension and blue indicates seafloor spreading.

Fig 6.8. Map of maturity for the North Celtic Sea Basin for the top Late Jurassic with highest maturity indicated in the basin centres (Armstrong, 1988).

Fig 6.9. Map of observed sea surface slicks identified from landsat (Browning-Stamp, 2017).

Fig 6.10. Map of the available seismic lines in the Western Approaches for future analysis and interpretation. The locations of Fig 6.11 & 6.12 are shown in red.

Fig 6.11. Strike-line seismic profile from the southern section of the Melville Basin with stratigraphic tops and wireline gamma ray (green) and compression sonic (red) shown for wells 73/13-1 & 73/13-1. The green marker is interpreted to represent the Top M2 Unconformity with underlying synclinal Jurassic strata truncated. The Lower Jurassic (Lias) is considered to be represented by a high reflective seismic facies which might represent an interbedded sand and shale sequence as discussed in Section 2.6.2.

Fig 6.12. Dip-line seismic profile from the southern section of the Melville Basin with stratigraphic tops and wireline gamma ray (green) and compression sonic (red) shown for well 73/13-1. The green marker is interpreted to represent the Top M2 Unconformity with underlying synclinal Jurassic strata truncated. The Lower Jurassic (Lias) is considered to be represented by a high reflective seismic facies which might represent an interbedded sand and shale sequence as discussed in Section 2.6.2.

Fig 6.13. Isostatic residual gravity map for Ireland, southern Britain and western Europe. The map has been corrected to remove the influence of crustal thickness by making an assumption of the depth to the Moho based on Airy's isostasy (Getech, 2017).

Table List

Chapter 3

Table 3.1. Well information from composite logs and well reports for the North and South Celtic Sea Basins including a summary of hydrocarbon shows, primary and secondary objectives.

Table 3.2. Well information from composite logs and well reports for the Melville, St Mary's, South West Channel and Plymouth Bay Basins in the Western Approaches including a summary of hydrocarbon shows, primary and secondary objectives.

Table 3.3. Well information for the French Sector of the Western Approaches including a shows, target reservoirs and reason for failure from (GTO, accessed 2017).

Chapter 4

Table 4.1. A comparison of the 3 main colour scales for visual kerogen and spore analysis (modified after Smith, 1987).

Table 4.2. Definition of the five classification of organofacies utilised by KinEx with information of deposition environment and stratigraphic age association (Pepper & Corvi, 1994). The possible correlations between the organofacies and the kerogen types described earlier (Section 4.3.2) are also included.

Chapter 5

Table 5.1. Database of the wells analysed in this thesis including regional information, geographical coordinates, total drilling depths, drilling dates, operators and geochemical contractors and the source file for geochemical data.

Table 5.2. Database of geochemical and wireline data utilised including VR, Visual Kerogen Analysis, TOC, Pyrolysis and wireline logs.

Table 5.3. Summary of the number of samples available for TOC, HI and OI divided by region.

Table 5.4. Summary of the indicator of thermal maturity utilised in this project.

Table 5.5. Guidelines for defining source rock richness based on weight percent TOC (Peters, 1986).

Table 5.6 illustrating the number of TOC samples within each time period and the statistical parameters of that data.

Table 5.7 illustrating the number of TOC samples within each epoch of the Jurassic and the statistical parameters of that data.

Table 5.8 statistical parameters and number of samples for TOC in the epochs of the Jurassic split up into the separate regions.

Chapter 1

Introduction

1. Introduction

The presence of regional source rocks that have generated and expelled hydrocarbons are the basis of a working petroleum system (Allen & Allen, 2013). The Jurassic source rock potential of the Western Approaches and Celtic Sea Basins are still poorly understood even though drilling in the UK Sector started in the 1970s (Section 3.1). This Master's thesis uses an approach combining regional palaeogeographic and tectonostratigraphic analysis based on literature with detailed analysis of geochemical measurements run on well cuttings and core mined from unpublished reports as a method for regional source rock analysis. An analysis of thermal maturity, source rock potential and the preservation limits of source rocks for the Western Approaches and Celtic Sea is developed to understand the controls on a functioning Jurassic source rock based petroleum system.

1.1. Aims

The aim of this project is to analyse the source rock potential of the Jurassic of the Celtic Sea and Western Approaches (Fig 1.1) based on review, analysis and synthesis of existing data extracted from literature and existing unpublished reports in order to determine the likely feasibility of a working petroleum system.

1.1.1. Objectives and Project Layout

1. To analyse the palaeogeographic and tectonostratigraphic history of the Western Approaches to pinpoint intervals of source rock deposition and understand how the palaeoenvironment at these times affected the quality of these potential source rocks (Chapter 2).
2. To provide an overview of the wells drilled and their potential reasons for failure followed by a discussion of the Dragon Discovery, which is the only regional prospect to have appraised hydrocarbon shows. (Chapter 3).
3. To describe the key techniques and methods used to measure the data used in this project and the potential pitfalls with using these data (Chapter 4).
4. To investigate the spatial and stratigraphical variation in source rock potential throughout the Jurassic of the region of interest (Chapter 5).

5. To identify the primary intervals of source rock potential and discuss the major controls on hydrocarbon generation and expulsion with a view to predicting whether a working petroleum system is viable in each of the basins of interest (Chapter 6).

1.2. Project Structure and Layout

Chapter 1 provides an initial introduction to the project discussing the aims, objectives and region of interest while laying out the structure of the entire project.

Chapter 2 is focussed on laying out palaeogeographic and tectonostratigraphic framework for the project. The chapter constructs a foundation based on the available literature for further analyses to build into a comprehensive study of the source rock potential of the region of interest. The Jurassic is illustrated to be a period of regional and global source rock deposition and forms the main focus of this Master's thesis. The Cretaceous and Carboniferous are also shown to have source rock potential and are analysed as potential additional intervals of source rock development.

Chapter 3 analyses the history of petroleum exploration in the region of interest and the French sector of the Western Approaches with a focus on identifying the key risks for a functioning petroleum system.

Chapter 4 discusses the main methods and data used in this project. The methods used by oil companies to obtain pyrolysis (Rock-Eval), Total Organic Carbon (TOC), Vitrinite Reflectance (VR) and wireline data along with the strengths and pitfalls of each datatype will be discussed.

Chapter 5 is the main results chapter starting with a discussion of data availability. The chapter then utilises data mined from unpublished geochemistry reports to analyse the maturity of organic matter, source rock richness, quality and potential to generate and expel hydrocarbons of the Jurassic interval in the region of interest.

Chapter 6 discusses the results developed focussing on the key controls on source rock potential and maturity. The chapter will also layout the potential topics for future work based on the questions that still need to be answered.

Chapter 7 provides a statement of the conclusions of this project.

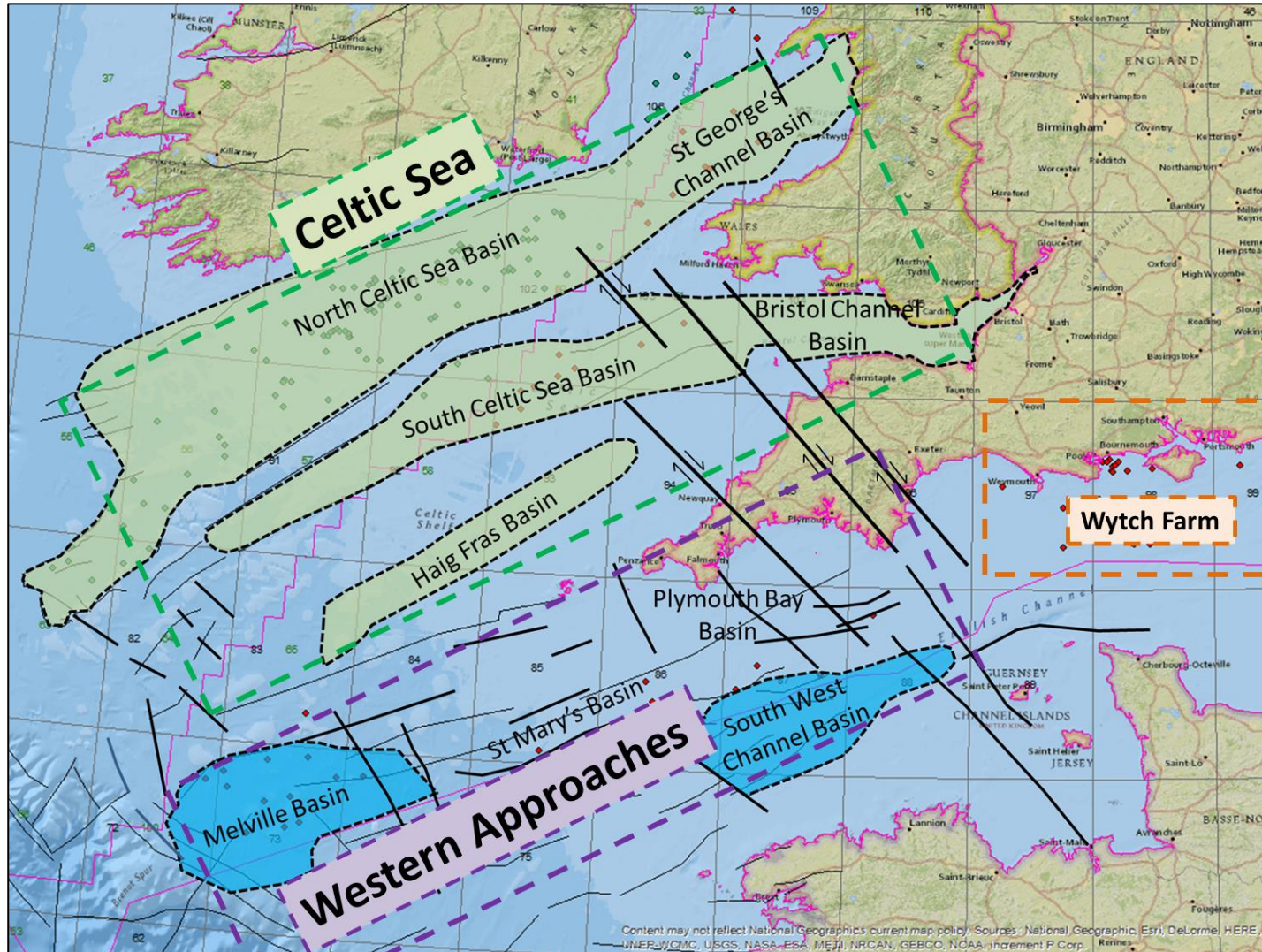


Fig 1.1. Map of the region of interest off the south west coast of Britain. The basins distribution and nomenclature as laid out in Section 1.2 are shown (modified after Ziegler, 1987b and Chapman, 1989). The green shading outlines the Celtic Sea Basins with the Western Approaches Basins shaded in blue. Black lines represent tectonic fabrics or faults from Ziegler (1987b) and the magenta outline of the region marks the limits of the UK Sector of the Western Approaches and Celtic Sea.

1.2.1. Region of Interest and Geological Nomenclature

The region of interest covers the UK offshore Sector off the south west coast of Britain and south coast of Ireland. The principle regions discussed are the Western Approaches and the Celtic Sea. Data from the Wessex Basin are also included in in this thesis as discussed in Section 1.4 (Fig 1.1).

The Western Approaches is referred to by many different terms in the literature but is named after the region here as used by Hillis (1988) and Chapman (1989). The **Western Approaches** (Fig. 1.1) straddles the UK and French dividing line and the basins included here in the UK sector are (from West to East): the **Melville Basin, St Mary's Basin, Plymouth Bay Basin and South West Channel Basin**. The French Sector of the Western Approaches is discussed (Fig 2.1) where appropriate but is not included as a primary focus of this project.

The **Celtic Sea** (Fig. 1.1) lies predominantly on the Irish side of the median line dividing the Irish and UK sectors. The basins in the Celtic Sea focussed on here are (from South to North) the **South Celtic Sea Basin, Bristol Channel Basin, North Celtic Sea Basin**. The **St George's Channel Basin** is also considered here as in the Celtic Sea but is not part of the main focus of this project but rather as a source of additional analogue data for the North Celtic Sea Basin which has limited extent in the UK Sector.

Wytch Farm (Fig 1.1) is considered the offshore extension of the Wessex Basin and while not being within the primary focus of this project has been used as an important analogue for the Western Approaches due to the availability of well data. Similarly due to the proximity and amount of available literature on **onshore Dorset** and the **Wessex Basin** these regions are discussed extensively to provide constraints on the palaeogeographic and tectonic histories of the region of interest.

1.2.1.1. Geochronological Breakdown

Stratigraphy within this thesis is predominantly split up by the specific time interval in which lithological units were formed with subdivisions split into Late, Middle and Early as described in <http://www.stratigraphy.org/upload/bak/chron.htm>. Where a rock unit of a given time is referenced this is termed a Chronostratigraphic Unit and will be labelled Lower, Middle and Upper.

1.3. Source Rocks

Source rocks are organic matter-rich rocks that are capable of expelling petroleum. The main organic components are *kerogen* and *bitumen* (Allen & Allen, 2013). Sedimentary organic matter is predominantly made up of Carbon (C) and Hydrogen (H) with additional heteroatoms of Nitrogen (N), Sulphur (S) and Oxygen (O). The produced oil and gas (*petroleum*) contains the same elements rearranged into hydrocarbons with additional asphaltenes and non-hydrocarbon gases (Pepper & Corvi, 1994). *Kerogen* is the component of organic matter that is insoluble in common organic solvents due to the large size of the molecules (Espitalié *et al.*, 1977; Peters, 1986; Allen & Allen, 2013). *Bitumen* comprises the fraction of organic matter that is extractable with organic solvents (Peters, 1986).

1.4. Analogue Data

In this project the St George's Channel Basin, which is the lateral continuation of the North Celtic Sea Basin and the Wessex Basin (Wytch Farm) are included as analogues (Fig 1.1). The Wessex Basin is considered as a potential additional source of appropriate analogue data for the Western Approaches.

1.4.1. Wessex Basin (Wytch Farm)

The Wessex Basin is an oil and gas producing basin in Southern England with Wytch Farm representing one of Wessex Basin's producing fields that is based on an Early Jurassic petroleum system (DECC, 2014). Data from the Wytch Farm wells in the Wessex Basin are used in this project to supplement the limited data available for the Western Approaches.

The Wessex Basin was formed during Permian-Triassic rifting with Mesozoic sequences developed in extensional graben. Scotchman *et al.* (2016) indicated (Fig 2.30) that in the Early Jurassic a potential connection existed between the Wessex Basin and Western Approaches. This interpretation is supported by $\delta^{13}\text{C}$ measurements from the Sinemurian sediments of 73/13-1 (Paleochem, 1983). The isotopically low $\delta^{13}\text{C}$ values are indicated as isotopically similar to the Wytch Farm. The Carbon isotope similarity suggests that the two regions were linked or influenced by similar depositional processes in the Early Jurassic.

Middle Jurassic and Late Jurassic strata have been eroded from the UK Sector of the Western Approaches. Baron *et al.* (2012) suggested that persistent shallow marine to paralic deposition occurred in the Western Approaches and the Wessex Basin at this time. A comparison of the Middle Jurassic interval suggests a somewhat different facies between the Bristol Channel Basin and the Wessex Basin (Baron *et al.*, 2012) although the similarity to the eroded Middle Jurassic section of the Western Approaches is impossible to know. It is likely that the shallowing discussed in Section 6.2.2 is present in the Western Approaches and could have led to a different palaeoenvironment compared to the shallow marine/paralic palaeoenvironment of the Wessex Basin.

The lack of any preserved Late Jurassic age strata in the Western Approaches means that any comparison to strata of similar age in the Wytch Farm is uncertain but Scotchman *et al.* (2016) does suggest a potential linkage of the basins at this time. In addition the presence of widespread marine deposition (Section 6.2.3) suggests that similar conditions of marine deposition were likely prevalent over the region.

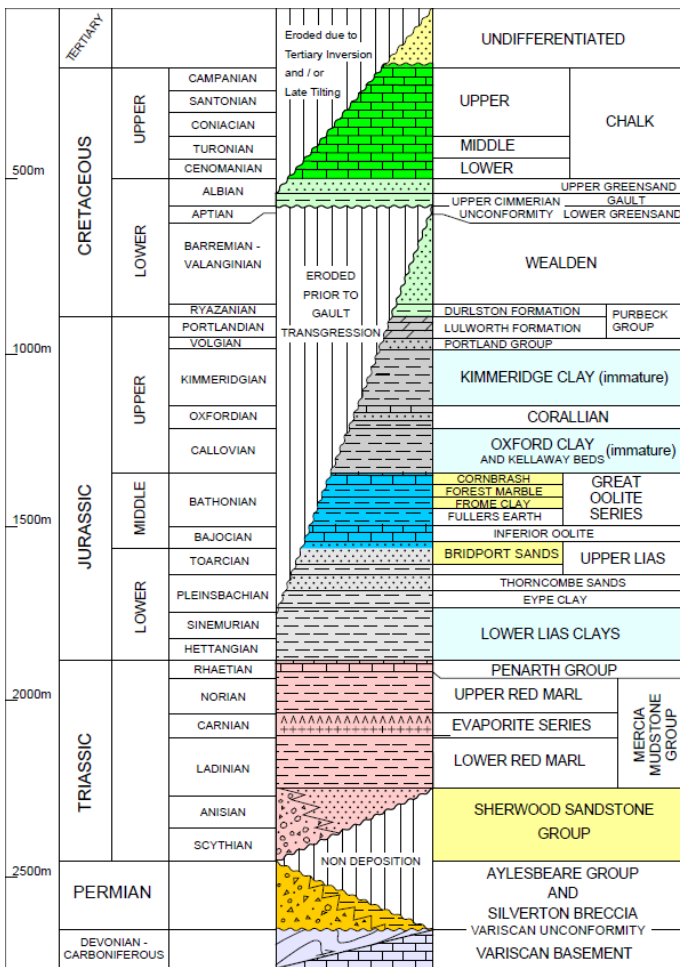


Fig 1.2. Stratigraphic column for the Wessex Basin with analysis focused on the Early Jurassic Lower Lias Clays to Upper Lias.

1.4.2. St George's Channel Basin

The St George's Channel Basin is the northeast continuation of the North Celtic Sea Basin. Section 2.3.5 discusses the change in structural style as interpreted by Klemperer & Hobbs (1991) between the St George's Channel and North Celtic Sea Basins. In addition the St George's Channel Basin follows a NE-SW trend compared to the ENE-WSW trend of the Celtic Sea Basins (Section 2.3.2). The proximity, however, of the St George's Channel Basin to the UK Sector of the North Celtic Sea Basin (Fig 1.3) suggests that it is a suitable analogue. Fig 1.3 indicates that 103/01-1 and the other current North Celtic Sea Basin wells in the UK Sector are also likely to be within the structural regime of the St George's Channel Basin.

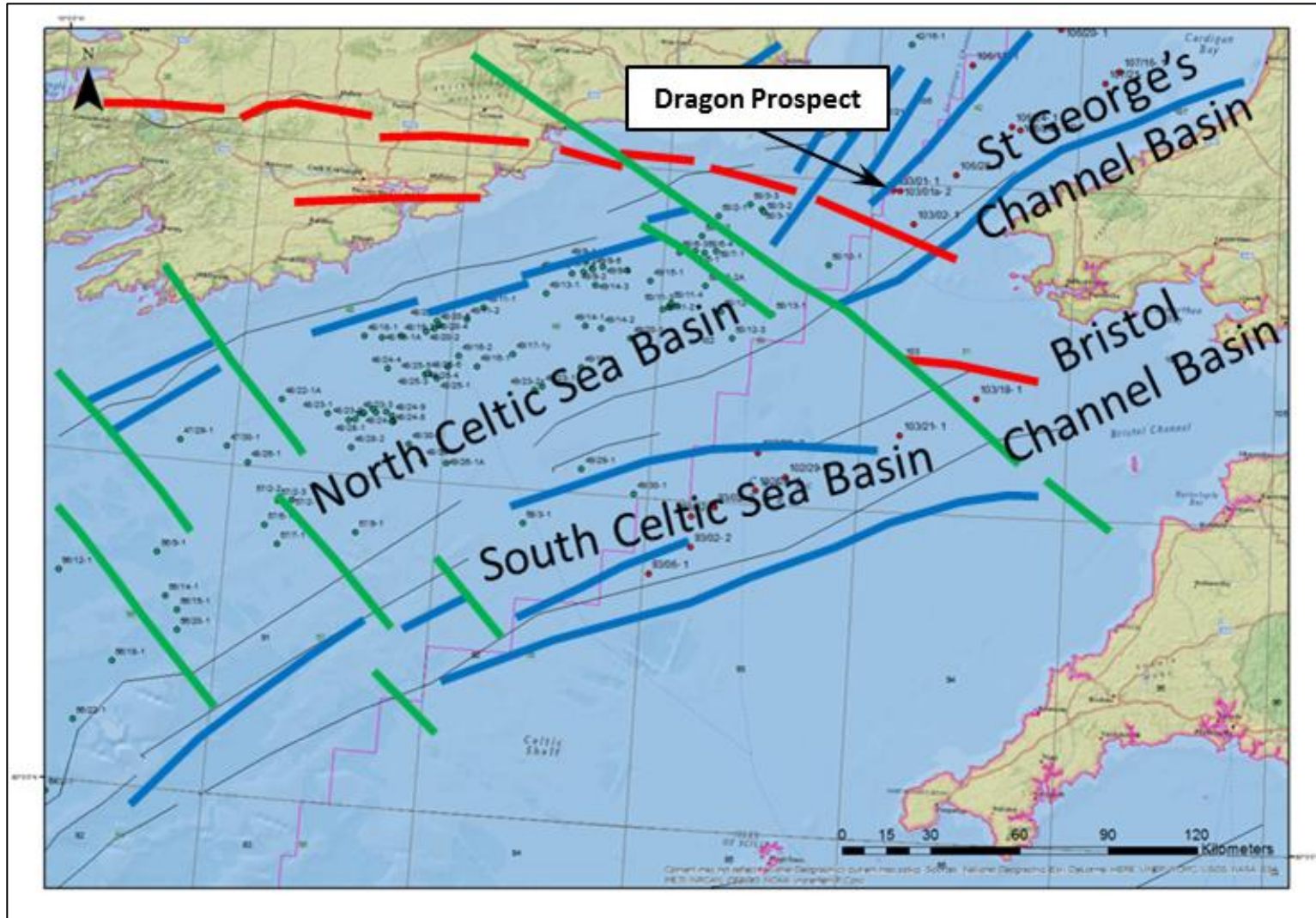


Fig 1.3. Map of the Celtic Sea with fault trends based on Readman *et al.* (1995) superimposed on the map.

1.5. Analysis of new Oil and Gas Authority (OGA) 2D seismic lines

This Master's project initially planned to make use of the new OGA (2016) 2D seismic lines to analyse the Jurassic source rock potential but as these lines arrived late a thorough analysis was not possible within the time scale of the project. The potential Future Work that could be done on the seismic lines is discussed in Section 6.6.7. The OGA 2D seismic lines have had an initial analysis with example images shown for south of the Melville Basin in Section 6.6.7. The 2D seismic lines are shown to demonstrate the style of the Late Jurassic to Early Cretaceous unconformity and the potential preservation of deeper buried Jurassic strata in the south of the Melville Basin. These observations are based on the correlation of a Jurassic seismic facies composed of a series of high amplitude reflectors.

Chapter 2

Palaeogeography and Tectonostratigraphic Framework of the Western Approaches and Celtic Sea Basins

2. Palaeogeography and Tectonostratigraphic Framework of the Western Approaches and Celtic Sea Basins

2.1. Introduction

The Western Approaches and Celtic Sea Basins are Mesozoic basins lying on top of a Palaeozoic basement. This chapter focuses on describing the tectonic, palaeogeographic and stratigraphic history of SW England focusing on the Jurassic interval and discussing the rest of the basin fill and the underlying Palaeozoic basement along with the basin controlling structures and fabrics. The objective is to build the groundwork for future chapters by developing an understanding of the evolution of the Celtic Sea and Western Approaches Mesozoic basins.

In this thesis, an analysis of the tectonic histories of the basins and the processes which formed the basins leads to an ability to predict potential zones of potential source rock because the initial deposition, protection from erosion and later maturation are all controlled by local and regional tectonics, basin scale processes and the palaeoenvironment of deposition. In addition to regional tectonics and palaeoclimate, local processes such as the movement of salt in the Melville Basin could have influenced the deposition, preservation and maturation of potential source rock strata.

2.1.1. Objectives

- Understand the changes in palaeogeography of the Western Approaches and Celtic Sea Basin region through time while linking this to source rock richness and facies deposition and distribution.
- Link basin forming processes and structures to deposition, preservation and the maturation of potential source rock intervals.
- Identify potential intervals of increased source rock potential that will be linked to analyses of Total Organic Carbon (TOC) and Hydrogen Index (HI) (see Chapter 4).
- Understand tectonic and climatic controls on source rock deposition.
- Identify and quantify any local differences in potential source rock depositional environments between basins in the region of interest.

2.1.2. Chapter Layout

Section 2.2

This chapter starts by discussing the key tectonic events of the pre-rift history of the Celtic Sea and Western Approaches in terms of the tectonic context, major structures developed and the evidence from the study area.

Section 2.3

The important basin fabrics and architecture are then described in terms of their effect on the development of the region of interest.

Section 2.4

The Megasequence approach used to define stratigraphic packages that were associated with key phases of basin development.

Section 2.5

The basement and Carboniferous source rock facies are discussed in terms of the additional source rock potential in the pre-rift sediments.

Section 2.6

The Permian to Late Jurassic tectonic and palaeogeographic history is described to identify the main zones of source rock development and the potential controls on source rock deposition and preservation in the Celtic Sea and Western Approaches.

Section 2.7

The post-rift subsidence history and uplift events (Cretaceous to Tertiary) of the region of interest are discussed in terms of the greater tectonic history to analyse the potential burial history of the source rock facies. The deposition of additional source rock potential is also discussed in Section 2.7.

Section 2.8

The Paleogene to recent is discussed to analyse the effect and influence the recent tectonic and subsidence history of the region has on the maturation of source rock facies.

Section 2.9

This section summarises the key points from the chapter in terms of the source rock development of the Jurassic interval.

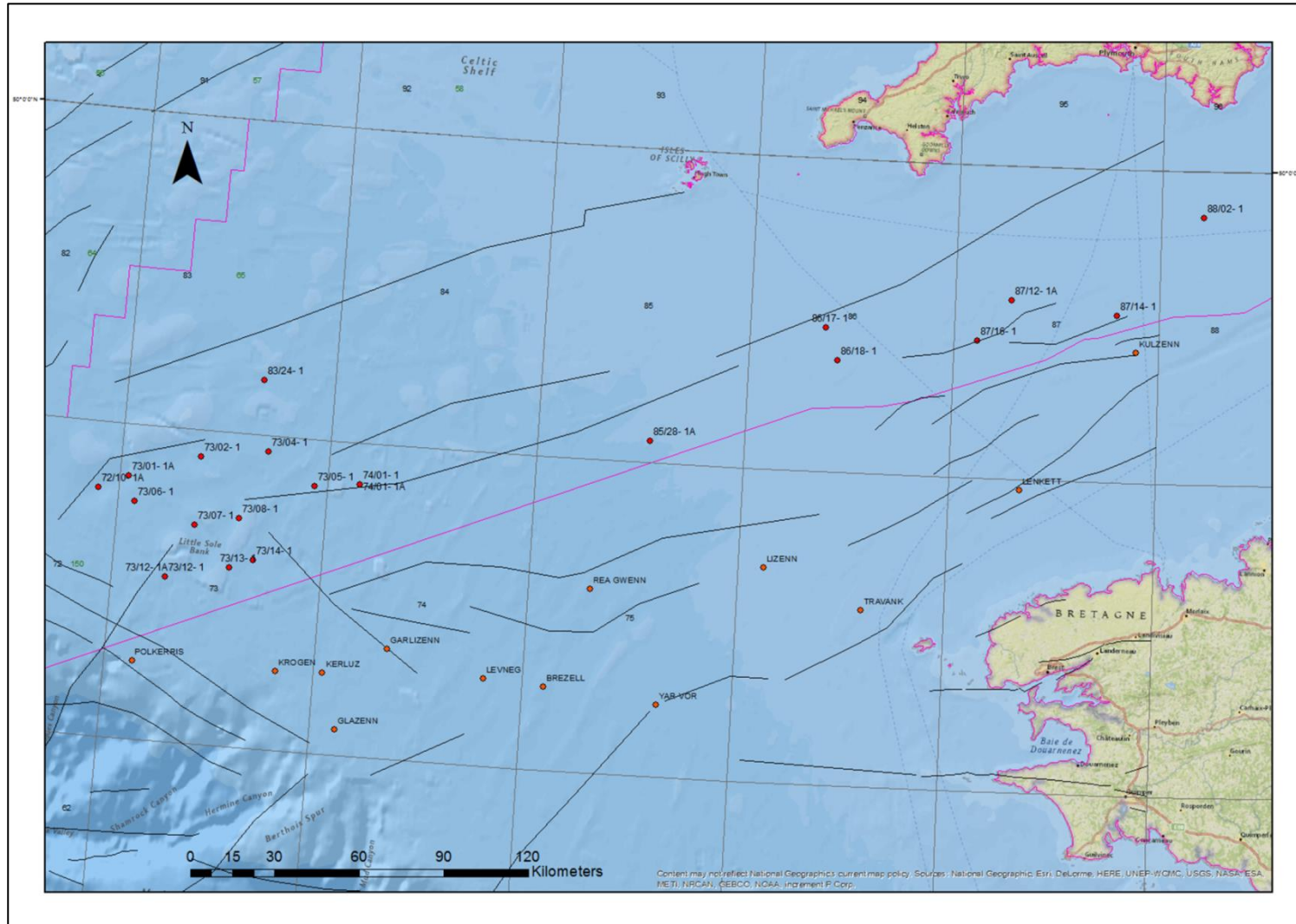


Fig 2.1. Map of the French and UK Western Approaches with the wells included in this chapter from the French and UK Sector shown. Black lines represent tectonic fabrics or faults from Ziegler (1987b) and the magenta outline of the region marks the limits of the UK Sector of the Western Approaches and Celtic Sea.

2.2. Geodynamic and Palaeogeographic Evolution

The main objective for discussing the pre-rift history of the Celtic Sea and Western Approaches region is to develop an understanding of the nature of the basement with a focus on analysing the control the developed trends and structures had on the basin history.

2.2.1. Precambrian to Early Palaeozoic

2.2.1.1. Tectonic Context

Woodcock and Strachan (2012) discuss the two postulated supercontinents during the Neoproterozoic: the Rodinia (~750 Ma) and Vendian (~580 Ma) supercontinents (Fig 2.2). After the break-up of the Rodinia Supercontinent, due to the opening of the Proto-Pacific Ocean with East Gondwana separating from the Laurentian margin, (Torsvik *et al.*, 1996) the African-Baikalian-Brasiliano orogenic events at 620 Ma led to the formation of the Vendian Supercontinent near the South Pole (Fig 2.2). Southern Britain was located on Avalonia at the edge of West Gondwana on the Cadomian Volcanic Arc. Bluck *et al.* (1992) hypothesise that the Devonian and Carboniferous sediments of the southwest Britain conceal an extension of the Avalon Terrane but this concept was not developed any further in their article.

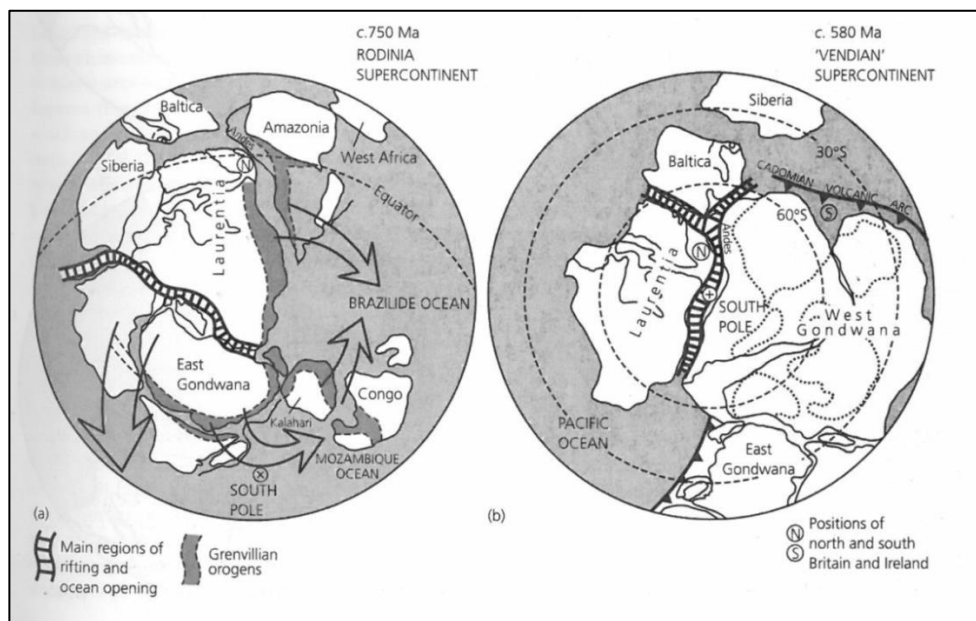


Fig 2.2. Palaeocontinental reconstructions from the Neoproterozoic. (a) The Rodinia Supercontinent is shown at prior to break-up. (b) The Vendian Supercontinent is shown prior to rifting of Laurentia away from the margin of West Gondwana. S – Southern Britain (region of interest), N – Northern Britain.

The Late Neoproterozoic to Cambrian times saw the accretion of old cratons (Fig 2.3) through orogenic events to form Gondwana (Woodcock & Strachan, 2012). Of these events the Cadomian Orogeny (690-550 Ma; Murphy & Nance, 1989) affected southern Britain because southern Britain was situated on the Cadomian Volcanic Arc (Fig 2.2). The Cadomian Orogenic Belt was overprinted and broken up by later post-Cambrian tectonics i.e. Caledonide, Variscan and Alpine orogenies.

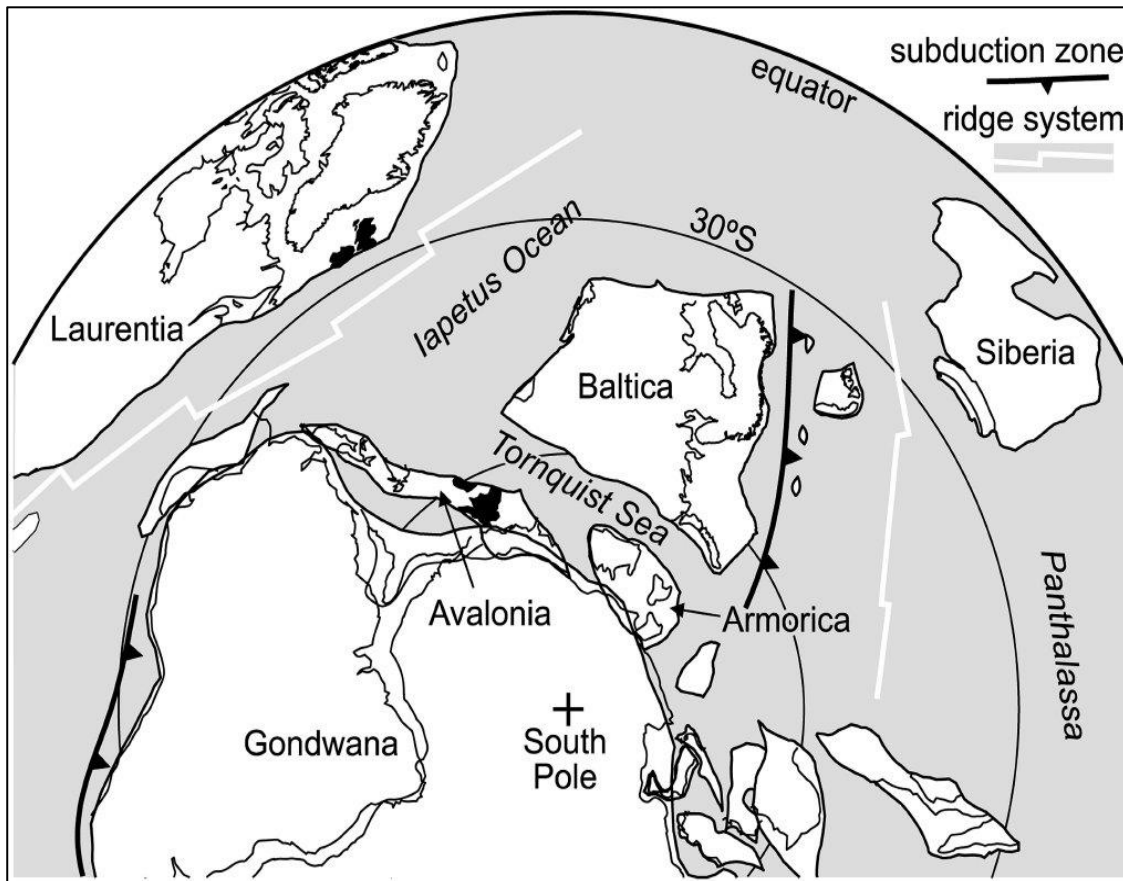


Fig 2.3. Tectonic reconstruction for the Cambrian (Woodcock & Strachan, 2012). The south of Britain (Avalonia) is shown on the northern margin of Gondwana with the north of Britain on the margin of Laurentia.

2.2.1.2. Evidence in Study Area and Adjacent Regions

Chapman (1989) indicates the presence of ultramafic rocks of Cambrian age in the 73/02-1 well in the Melville Basin which he suggests to represent basement consisting of a complex of thrust sheets of Variscan and pre-Variscan rocks similar to the onshore Armorican Massif of NW France. Dewey & Burke (1973) indicate that Cadomian crust underlies the North of Brittany. It is difficult to say for certain the nature of the basement underlying Devonian to Carboniferous basement but it is likely that the pre-Devonian basement is comprised of Cadomian Arc rocks of an Armorican affinity.

2.2.2. Caledonian Orogeny

2.2.2.1. Tectonic Context

McKerrow *et al.* (2000) defined the Caledonian Orogeny as the record of the events that led to the closure of the Iapetus Ocean. This closure took place over a 200 Myr period from the Cambrian to the Devonian times with the closure of different sections of the Iapetus Ocean between Laurentia to the NW and Baltica and Avalonia to the SE and east. The final docking of Baltica, Eastern Avalonia and Western Avalonia on the Laurentian margin during the Silurian led to significant sinistral transpression (Soper *et al.*, 1992).

In the Early Ordovician (c. 480 Ma), northern (Laurentia) and southern British Isles (Avalonia) were still separated by the now closing Iapetus (Torsvik and Cocks, 2017) with Avalonia (southern British Isles) rifting away from margin of Gondwana and migrating northwards towards the Laurentian margin (northern British Isles – Woodcock and Strachan, 2012) closing the Iapetus Ocean while the Rheic Ocean was being opened behind Avalonia (Fig 2.4 (a)).

Soper and Hutton (1984) proposed a triple junction style closure for the Iapetus Ocean with sinistral convergence of terranes in contrast to prior models that had considered a two plate closure (Dewey *et al.*, 1970). Soper *et al.* (1992a) built on this model (Fig 2.4 (b)) illustrating the midpoint of closure during the Middle Silurian (~420 Ma) with Baltica having converged with the Laurentian margin of Greenland. Gravitational collapse occurred in Scandinavia even as convergence continued in the deep lithosphere.

The Acadian Orogeny was initially developed as a term to describe the Appalachians of Northern America but has been expanded to encompass synchronous regional uplift in England (but not in Cornubia) related to the collision of Armorica and Iberia with the Laurussian margin. The Acadian Orogeny represents the change from sinistral regime of the Caledonian (anticlockwise rotation of terranes and continents) to dextral (anticlockwise rotation of terranes and continents) of the Variscan (Soper *et al.*, 1992a).

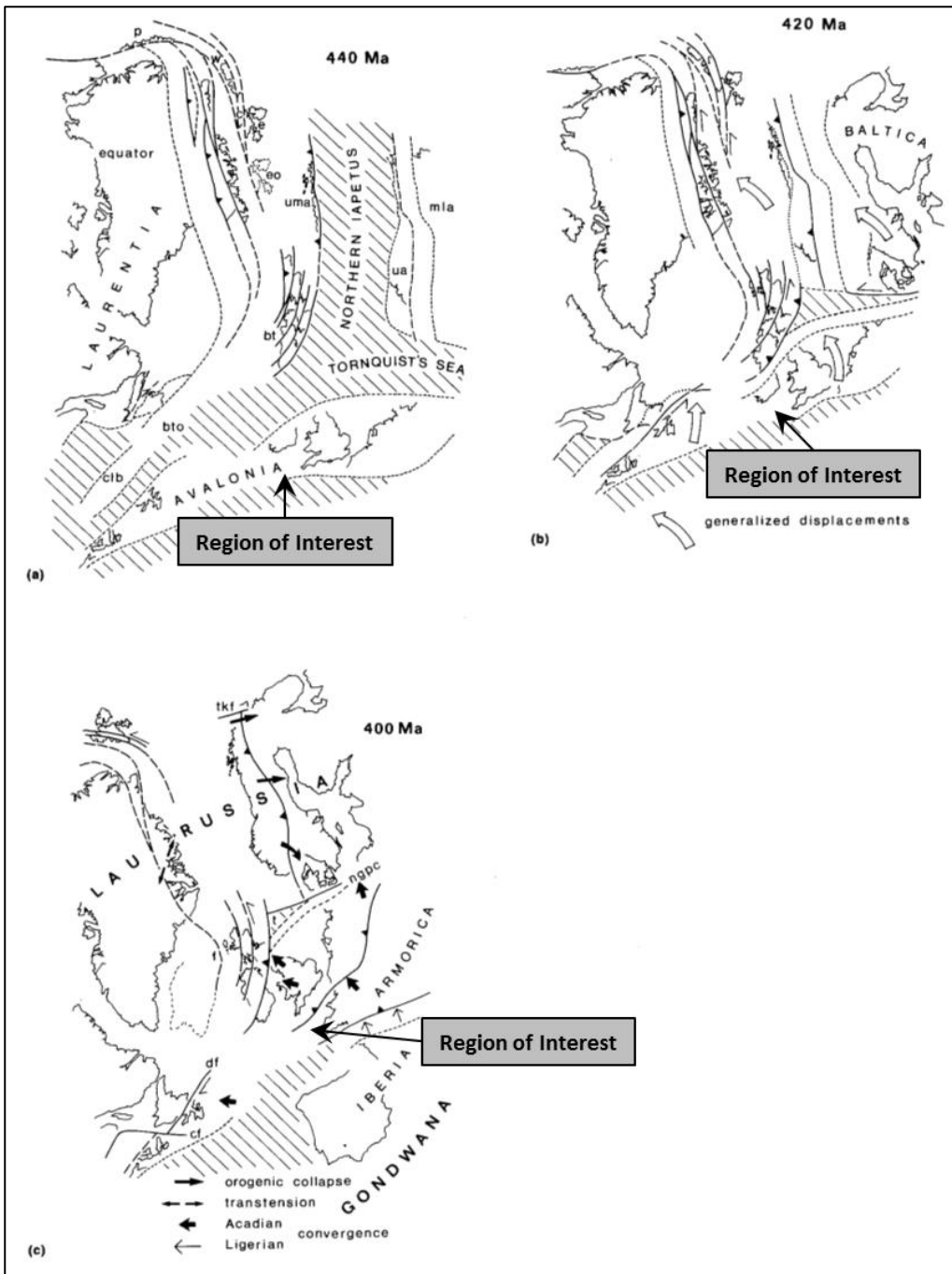


Fig 2.4. Schematic diagram demonstrating the Silurian closure of the Iapetus (Soper *et al.*, 1992a). (a) is a time-slice at the Ordovician-Silurian boundary (440 Ma) showing the position of Laurentia, Avalonia and Baltica during the end Ordovician with Laurentia situated on the equator and separated from Baltica by the Northern Iapetus and from Avalonia by the Tornquist Sea. (b) Silurian-Devonian boundary (420 Ma) with arrows showing plate movements in relation to Laurentia and (c) Early Devonian (400 Ma) showing convergence directions of the Acadian Orogeny with convergence in SW England. Figure 2.4 (c) now includes the newly assembled Laurussia in the Early Devonian (~400 Ma) with Late Silurian to Early Devonian orogenic collapse occurring at the same time as the Acadian Orogeny.

2.2.2.2. Major Structures

SSE shortening in the Welsh Basin ascribed to the docking of East Avalonia with Laurussia in the Silurian to Middle Devonian caused sinistral transpression with NE to NNE trending folds of similar orientation to the Celtic Sea Basins (Woodcock *et al.*, 1988). The onshore continuation of the Bala Fault, however, cross cuts Acadian folds and cleavage in the Welsh Basin indicating that it post-dates the Late Caledonian. The Bala Fault is a major structure underlying the St George's Channel Basin discussed in Section 2.3.5.

2.2.2.1. Implications for Study Area and Adjacent Regions

During the Late Silurian, the region of interest, following the closure of the Iapetus and England and Ireland, sat in a shallow shelf setting (Fig 2.5). The South Celtic Sea Basin, Bristol Channel, Cornwall and Western Approaches are suggested by Torsvik and Cocks (2017) to have been part of the Cornubian Ridge on which volcanic rocks were deposited. The continental interior of the assembled Laurussia (Laurentia and Baltica) would have had the potential to act as a substantial sediment source.



Fig 2.5. Palaeogeographic reconstruction from Torsvik & Cocks (2017) showing the setting of Britain post-Caledonian Orogeny. D – Dniester River, FJL – Franz Josef Land, G – Gotland, TP – Timan-Pechora.

2.2.3. Variscan Orogeny

2.2.3.1. Tectonic Context

The Variscan sediments of Devonian to Carboniferous age comprise the main basement underlying the region of interest. The Variscan Orogeny saw the continuation of continental assemblage leading to the final development of Pangaea (Shail & Leveridge, 2009; Woodcock & Strachan, 2012); previously isolated terranes and continents collided. Torsvik and Cocks (2017) suggest that Variscan orogenic activity peaked in the Late Carboniferous. The events that led to the Variscan Orogeny began with the Rheic Ocean opening as Avalonia moved northwards (Fig 2.6a-b). The Franconian and Saxothuringian terranes moved northward and docked against the assembled Laurussian margin (Fig 2.6c-d).

The final stages of the Variscan Orogeny occurred with the closure of the Rheic and consequent collision of the Amazonia continent and the Iberia, Armorica and Bohemia terranes with the margin of Laurussia (Fig 2.6e-h). Shail and Leveridge (2009) indicated that the Rhenohercynian passive margin was formed on the northern edge of the Rheic Ocean or alternatively as a potential post-Rheic closure successor basin in the Early Devonian to Early Carboniferous (Rhenohercynian Zone – Fig 2.8).

Plate convergence began during the Late Eifelian (Middle Devonian; Ziegler 1987a; Styles, 1997; Shail and Leveridge, 2009) with collision marked by Early Carboniferous (Dodson & Rex, 1971) exhumation of distal continental margin deep marine volcanic and sedimentary sequences. The SW of England and the region of interest saw a change from the Middle Devonian to Early Carboniferous from an extensional regime to a compressional tectonic regime (Hartley and Warr, 1990).

The Variscan Orogeny formed the Variscides, a linear WSW-ENE trending fold-belt which extends today from North America through the Mauritanian belt of North Africa to the Hercynian belt of Western Europe (Dewey & Burke, 1973). Southern Britain was situated on the northern extent of the Variscides with the north of Britain lying within the sub-Variscan foreland. Following the waning of compression in the Stephanian, there was an alteration of the tectonic regime to wrench dominated as Europe went through dextral translation with respect to Africa (Ziegler, 1987a; Styles, 1997).

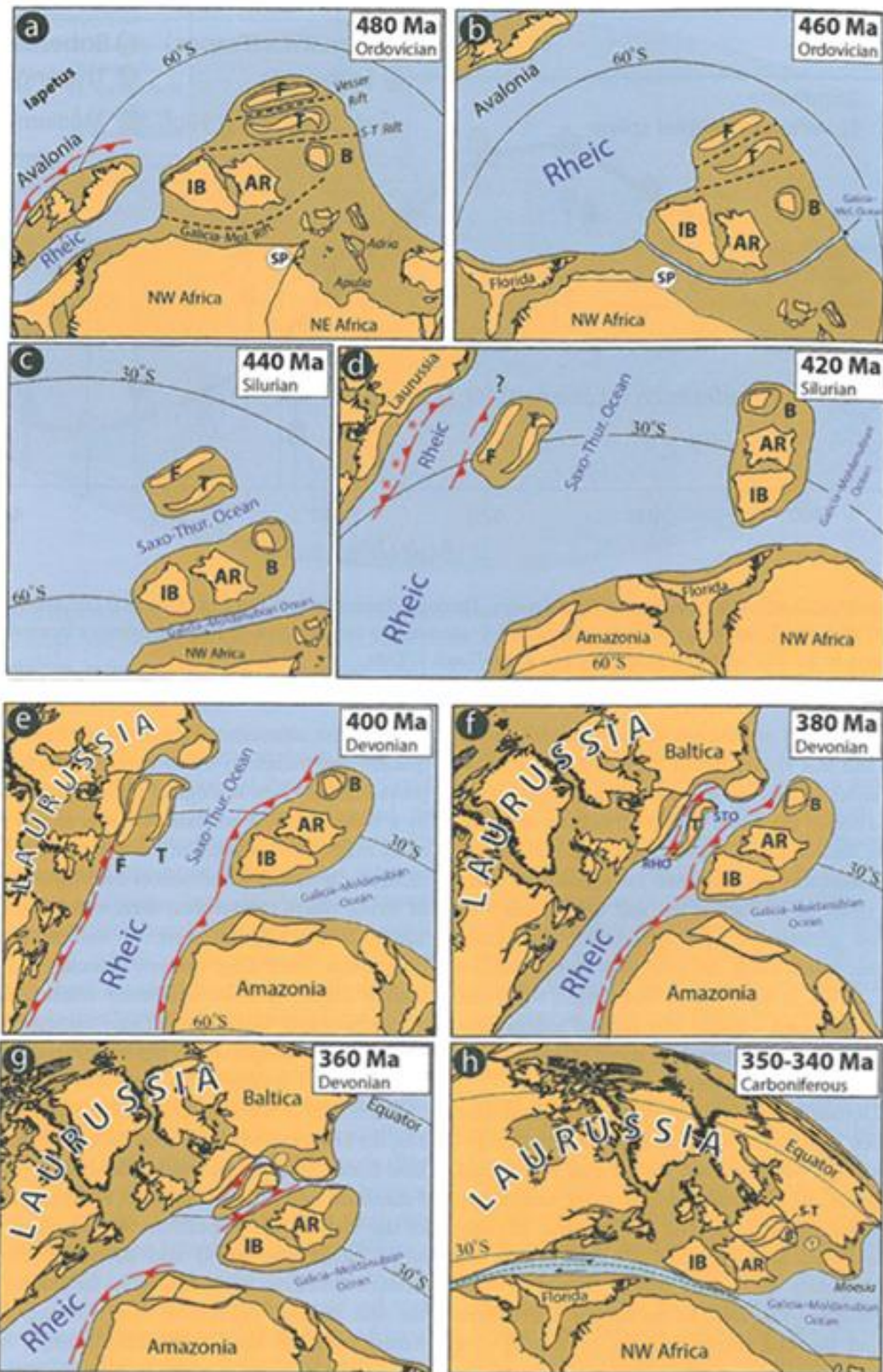


Fig 2.6. Palaeogeographic reconstructions from the Ordovician through to the Carboniferous showing closure of the Iapetus Ocean and subsequent opening and closing of the Rheic Ocean (Torsvik & Cocks, 2017). Ar - Armorica; B - Bohemia; F - Franconian; IB - Iberia; RO - NW arm of Rheic Ocean; SP - South Pole; S-T - Saxothuringia; STO - Saxothuringian Ocean; T (large) - Saxothuringian Terrane; T (small) - Tisia Terrane.

2.2.3.2. Major Structures

Corfield *et al.* (1996) linked variable Late Westphalian inversion in the Variscan foreland north of the region of interest (Fig 2.8) to the pre-existing basin fabrics. Corfield *et al.* (1996) noted that NE-SW striking faults oriented at high angles or perpendicular to the direction of maximum shortening (NNW-SSE or NW-SE) undergo significant inversion compared faults oblique or parallel to shortening (i.e. N-S and NW-SE striking faults). In the Midlands and Staffordshire these N-S striking faults were reactivated as strike-slip with sinistral displacement.

Shail and Leveridge (2009) explain the observed lack of Acadian deformation in SW Britain through dextral displacement on the Bristol Channel - Bray Fault. They suggest a situation of dextral transtension between the Bristol Channel - Bray Fault and the Pyrenean Fault which juxtaposed SW England against southern Britain during Carboniferous convergence (Fig 2.7).

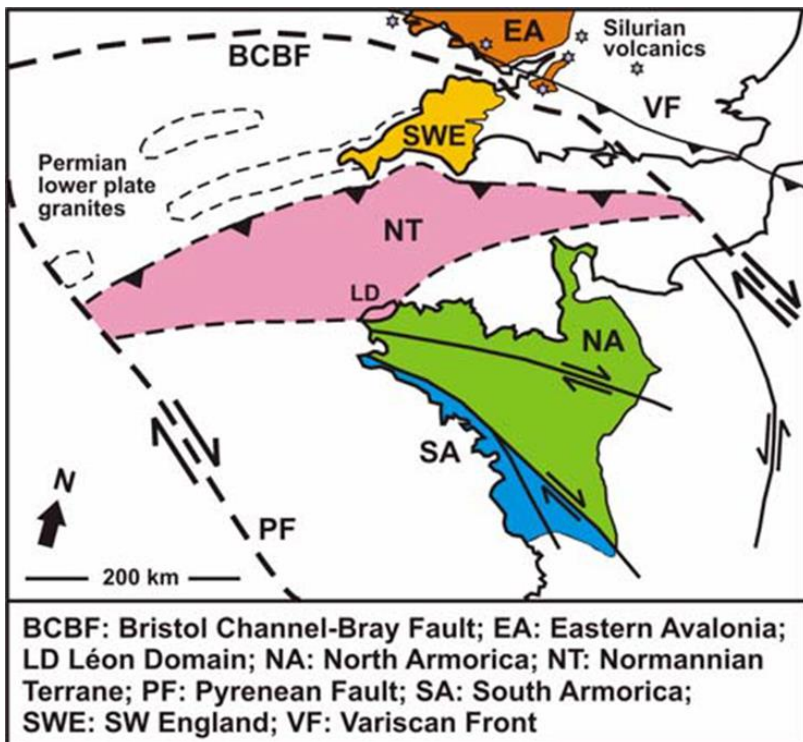


Fig 2.7. Tectonic map for the Western Approaches region and NW France showing the Bristol Channel-Bray Fault (Shail & Leveridge, 2009). The location of the Permian Cornubian Ridge and Haig Fras granites are also shown. BCBF – Bristol Channel - Bray Fault; EA (Orange) – Eastern Avalonia; LD –

Léon Domain; NA (Green) – North Armorica; NT (Pink) – Normannian Terrane; SA (Blue) – South Armorica; SWE (Yellow) SW England; VF – Variscan Front.

2.2.3.3. Orogenic Collapse

Corward (1995) linked the collapse of the Variscan Orogeny during the Late Carboniferous to Early Permian to the formation of the Celtic Sea and Western Approaches Basins indicating that these basins formed along a NE-SW trend perpendicular to Caledonian and Variscan thrust directions. Styles (1997) suggested that the Variscan foldbelt underwent rapid collapse with increased heatflow and steepening of the remnant subduction zone. Increased heatflow combined with extension related to the collapse of the Late Hercynian Foldbelt is suggested by Arche & Lopez-Gomez (1996) as the reason for initiation of basin formation and rifting for the Iberian Basin and its associated basins.

2.2.3.1. Evidence in Study Area and Adjacent Regions

The Variscan Orogeny is an important component to understanding the history of the Western Approaches and Celtic Sea. The basement immediately underlying the Mesozoic rift basin (Hillis, 1988; Style, 1997) are primarily composed of Devonian and Carboniferous sediments and metasediments deposited in rift basins on the Rhenohercynian passive margin and foreland (Fig 2.8). Dewey and Burke (1973) suggested that the main stage of compressional deformation in the region that became the Celtic Sea was during the Serpukhovian-Bashkirian.

The Western Approaches sat within the paratectonic zone (i.e. orogenic belt formed from wedges of sedimentary material during late stage contraction of the ocean basin) along with Iberia and most of southern Europe (Fig 2.8). Shail and Leveridge (2009) indicated that a second phase of post-Namurian deformation can be seen in sediments of the Culm and North Devon Basins. The Culm and North Devon Basins formed as foreland basins between the Rhenohercynian mountain chain and the adjacent craton of SW England. The youngest deformed rocks in the Culm Basin were deposited in the Westphalian C and Shail and Leveridge (2009) suggest that Variscan convergence ended in the Late Carboniferous (~305-300 Ma).

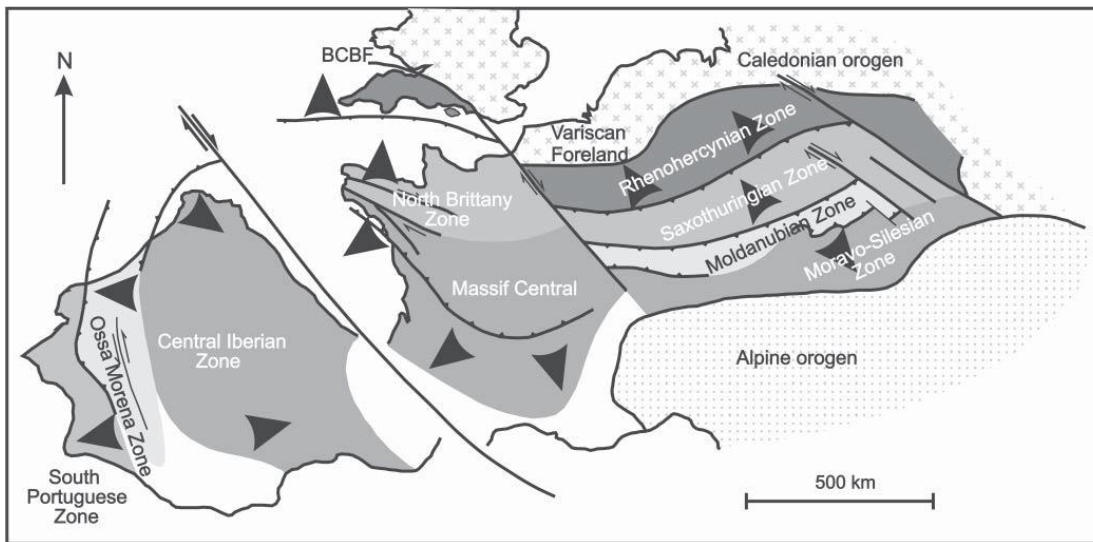


Fig 2.8. Tectonic map of SW Europe showing the Variscan tectonic zonation with the Rhenohercynian Zone and Variscan Foreland labelled (Leveridge and Hartley, 2006).

Offshore the Western Approaches Basins appear to have localised in the hangingwalls of inferred Variscan thrusts with prominent SE dipping reflectors that pass through the crust and mantle picked in the Plymouth Bay Basin (Harvey *et al.*, 1994). Bois *et al.* (1990) and Klemperer and Hobbs (1991) describe similar southward dipping reflectors from the BIRPS seismic surveys which could represent the inferred Variscan thrusts.

The Cornubian Batholiths, which form the Cornubian Ridge offshore, separate the complicated half-graben style rift basins of the Western Approaches from the graben of the Celtic Sea and was emplaced in the Early Permian after convergence was replaced by NNW-SSE extension. The extension was synchronous with substantial crustal thinning through reactivation of earlier structures along with basin development and voluminous magmatism (discussed in Section 2.2.3.1).

2.2.3.1. Permian Igneous Activity

The Cornubian Batholiths are represented by six separate plutons that reflect emplacement of multiple magmatic batches (Fig 2.9 - Taylor, 2007). Alexander and Shail (1996) interpret emplacement as occurring during extensional reactivation of the Variscan thrust faults from the latest Carboniferous to Permian. Gravity modelling of the onshore granites of Dartmoor by Taylor (2007) suggests that granite emplacement exploited pre-existing weaknesses in the Devonian-Carboniferous sedimentary and igneous sequence it was emplaced into. The Haig Fras Granite (Fig 2.9) represents a fine to medium grained granite that was dated at a K-Ar age of 277 ± 10 Mya by Jones *et al.* (1988). Hillis (1988) suggested that the emplacement of the Cornubian Batholith & Haig Fras Granite related to crustal melting during orogenic collapse following the Variscan Orogeny.

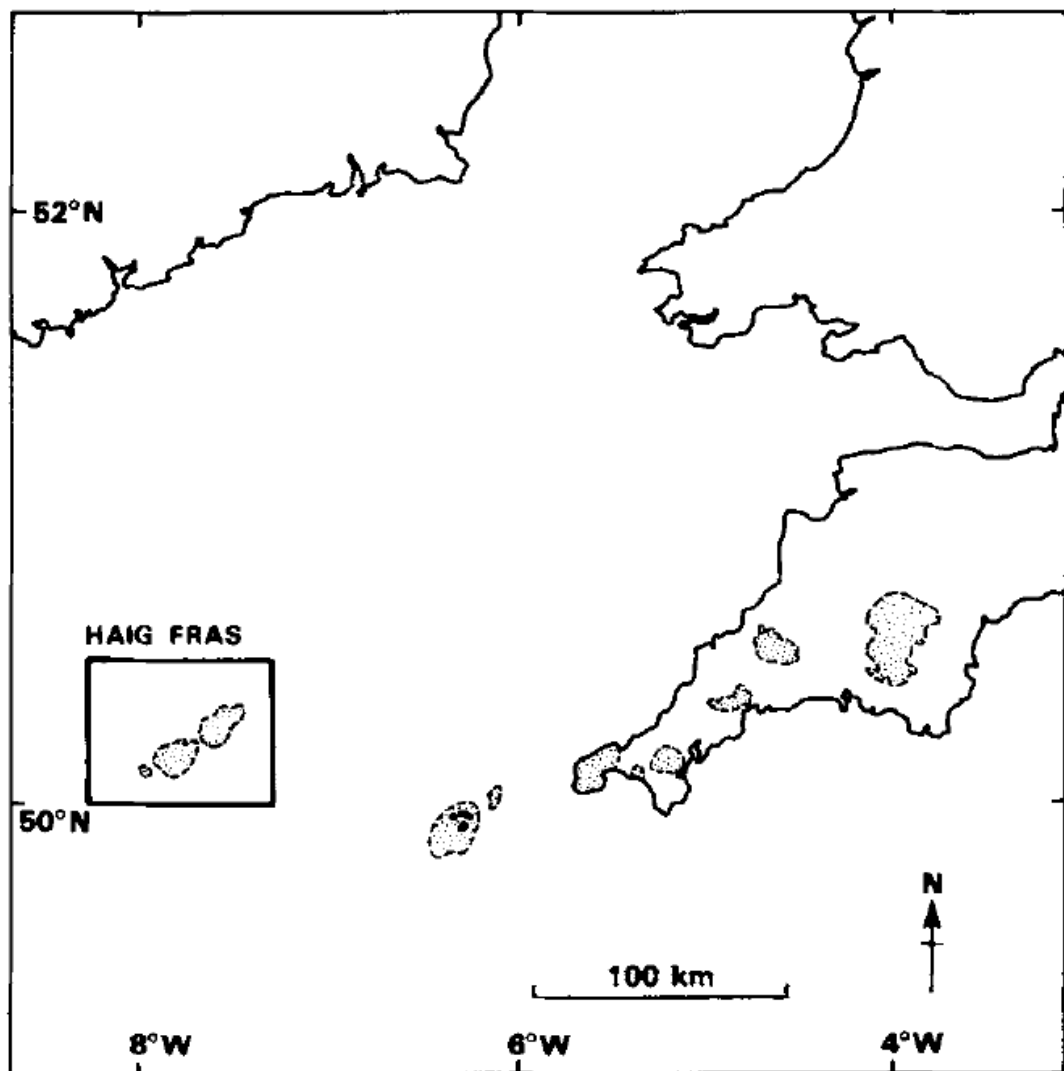


Fig 2.9. A map showing the location of the Haig Fras and Cornubian Granites in the SW of England and offshore (Jones *et al.*, 1988).

2.3. Basin Architecture and Fabrics

A key objective is to utilise analysis of the basin architecture, inherited fabrics and megasequences to understand the deposition, preservation and maturation of the source rock units in the study area. The structural histories of the basins are inherently linked with the deposition of the contained sediments. Holdsworth *et al.* (1997), Butler *et al.* (1997) and Peace *et al.* (2017) discuss the importance that existing tectonic inheritance has on rifting, fault reactivation and reworking in continental deformation: specifically, the influence and control of pre-existing structures on localisation of rifting and controls on the geometry and location of syn-rift deformation.

The principal trends observed within the Western Approaches and Celtic Sea region and discussed in this section are (Fig 1.1; Ziegler 1987b):

- Armorican Trend – **WNW-ESE trend** (Section 2.3.1).
- Caledonian Trends – **ENE-WSW to NE-SW trend** (Section 2.3.2).
- Variscan Trends with the “Variscan Front” bisecting southern England and Ireland – **WNW-ESE to E-W trend** (Section 2.3.3).
- **NW-SE** trending strike-slip faults such as the Sticklepath Fault (Section 2.3.4).

A discussion of each of these trends is followed by a discussion of the 3D architecture of the region of interest (Section 2.3.5).

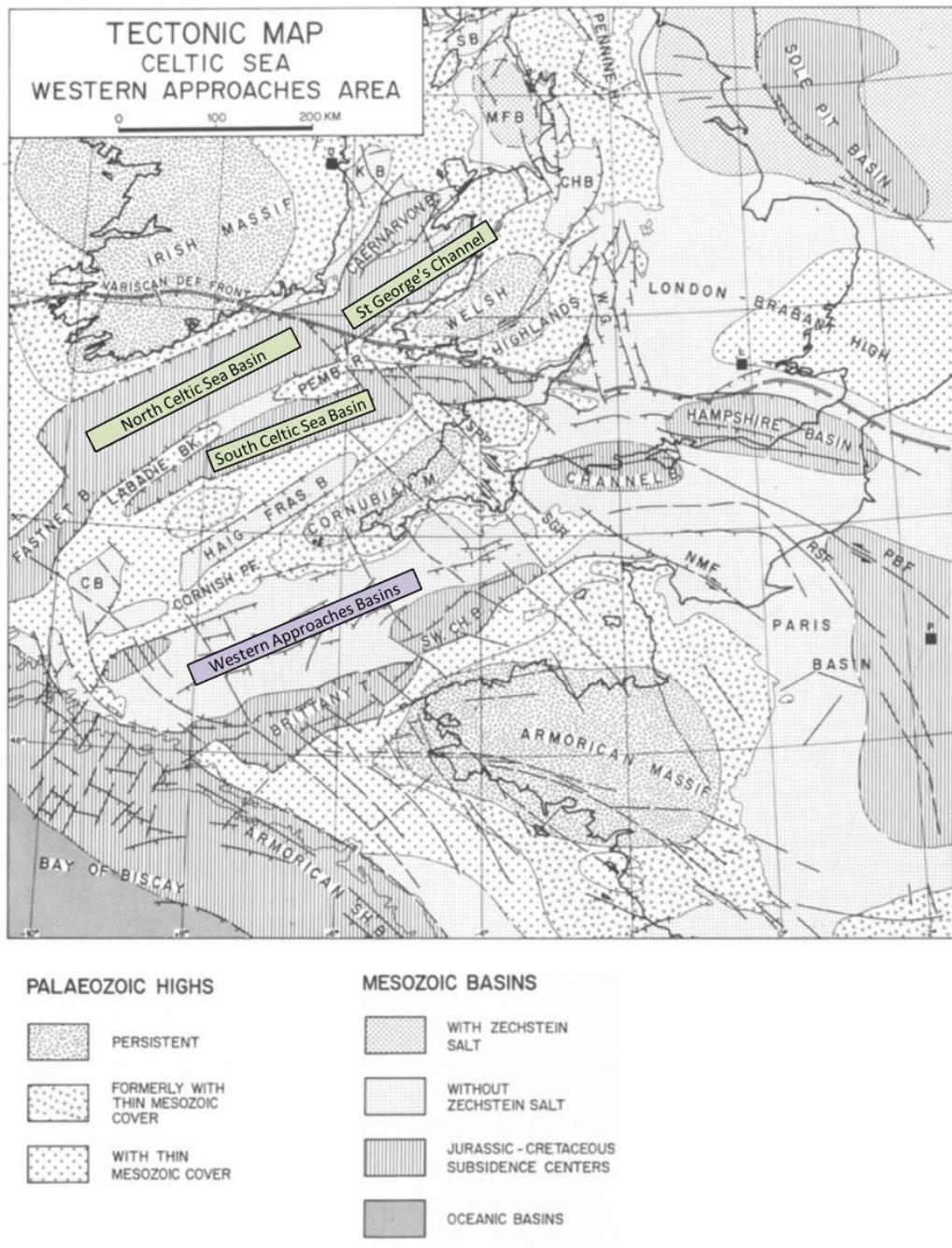


Fig 2.10. Tectonic map of the Celtic Sea and Western Approaches region (modified from Ziegler, 1987b) with the Western Approaches Basins, South Celtic Sea Basin and North Celtic Sea Basin. The WNW-ESE trend of the Variscan Front is shown along with the NW-SE trend of basin cutting strike-slip faults.

2.3.1. Armorican Trends

Hillis (1988) relates the formation of the southern margin of the Western Approaches to the Armorican Massif of Brittany and its offshore extension. The evidence for Armorican Trends in Western Approaches and Celtic Sea, however, is unclear. Gardiner & Sheridan (1981) suggest that there is no evidence for any influence of the WNW-ESE Armorican structural trend on the later faults and basin structure with the conventional line of the Variscan Front cross-cutting basin structures. The WNW-ESE Armorican structural can be seen on the Armorican Massif in Figure 2.10.

2.3.2. Caledonian Trends

The ENE-WSW to NE-SW predominant trend of the Western Approaches (Fig 2.10) and Celtic Sea Basins (Fig 2.11) indicates that the original Caledonian structures undergoing reactivation were the primary control on basin development. Figure 2.11 shows a modified interpretation of fault structures from Readman *et al.* (1995) with the key ENE-WSW to NE-SW (Caledonian) striking faults highlighted in blue.

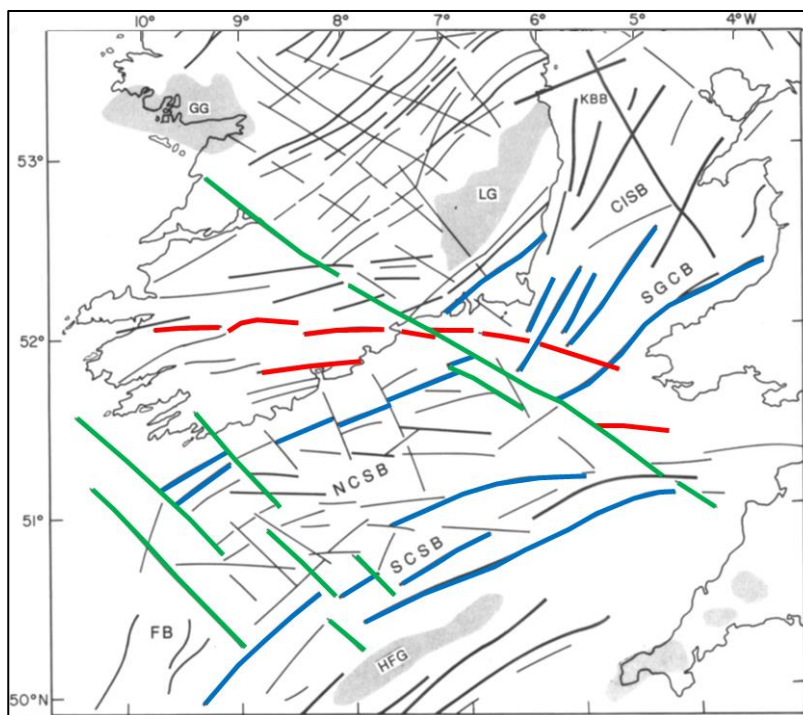


Fig 2.11. Interpretation of fault structures of onshore Ireland and the Celtic Sea based on bouger gravity anomalies (modified after Readman *et al.*, 1995). The change in structural style between the North Celtic Sea Basin (NCSB) and St George's Channel Basin can be clearly seen along with the apparent NW-SW Caledonian trend of these basins and the South Celtic Sea Basin. ENE-WSW to NE-SW fault trends are blue, ENE-WSW "Variscan" fault trends are red and NW-SE fault trends are green. Granite bodies are shaded light grey.

The key faults highlighted constitute the primary basin bounding faults for the North Celtic Sea Basin (NCSB), South Celtic Sea Basin (SCSB) and St George’s Channel Basin (SGCB). The fault trends on Figure 2.11 of the St George’s Channel Basin follow a NE-SW trend. The Celtic Sea Basins are separated from the St George’s Channel Basin by a distinct NW-SE fault structure. The Celtic Sea faults follow an ENE-WSW trend in comparison to the predominantly NE-SW fault trends of the St George’s Channel Basin. The Celtic Sea fault trends are oblique to the onshore Ireland ENE-WSW to E-W trend that is interpreted as Variscan (Section 2.3.3). Gardiner and Sheridan (1981) indicated that regional folds in the Celtic Sea are also aligned along a WSW-ENE trend and were inherited from the Caledonian basement structures.

2.3.3. Variscan Trends

The major WNW-ESE trend identified in Figure 2.11 is shown as bisecting the south of onshore Ireland near the lateral change from the St George’s Channel Basin to the North Celtic Sea Basin. The Variscan Front is shown by Klemperer & Hobbs (1991) to bisect the south of England and pass roughly WNW-ESE through the south of Ireland in a similar location (Fig 2.12). The Variscan Front is defined here as the northern extent of Variscan deformation similar to the Variscan Deformation Front term used by Klemperer and Hobbs (1991). The Variscan Front (Gardiner & Sheridan, 1981) is indicated as the northern boundary of the orthotectonic sequence of the Rheno-Hercynian Zone and describes the northern extent of possible Variscan Granites.

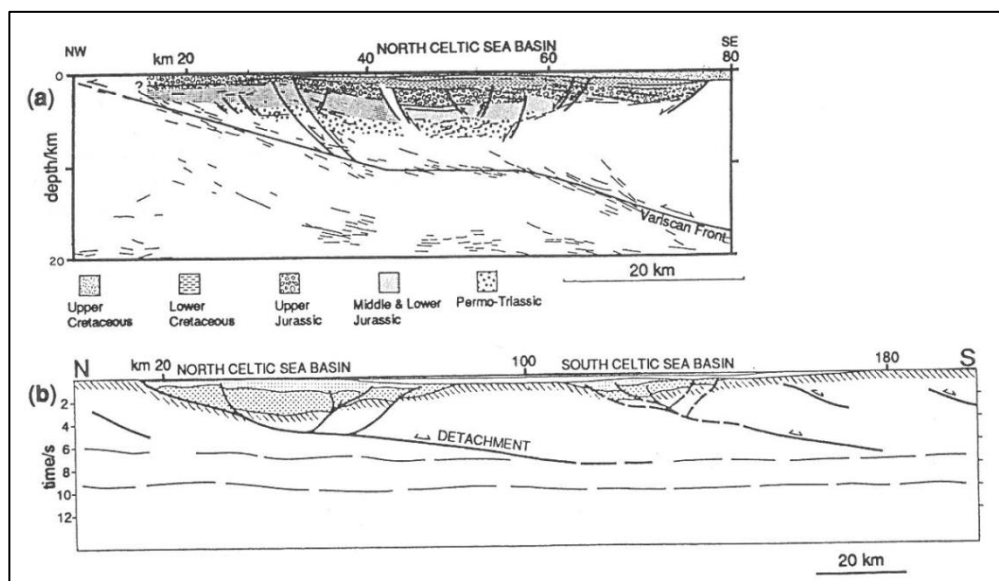


Fig 2.12. Interpreted diagrams from BIRPS seismic reflection surveys (Klemperer & Hobbs, 1991). The North Celtic Sea Basin is shown as underlain by the Variscan Front which soles into a large scale detachment.

Interpretation of the original SWAT seismic reflection profiles by Klemperer & Hobbs (1991) suggested that the North Celtic Sea Basin is underlain by the Variscan Front that has been reactivated as a basin detachment structure and facilitated basin development (Fig 2.12). The Rheno-Hercynian sector of the Variscan fold belt in the Celtic Sea and Southern British Isles is indicated as transecting the earlier Caledonian structural trends, the subsequent Mesozoic break-up and basin development in the offshore is parallel to the ENW-WSW Caledonian trends (Gardiner & Sheridan, 1981; Ziegler 1978b; Tucker & Arter, 1987; Doré *et al.*, 1999).

Onshore Ireland, a similarity in trend of structural fabrics identified from gravity anomaly work by Readman *et al.* (1995) and granite body intrusions (shaded in Fig 2.11) indicates that granites have taken advantage of earlier Caledonian and Variscan orogenic fabrics. Analysing bouger gravity anomalies, Readman *et al.* (1995) concluded that the Variscan and Caledonide structure offshore Ireland controlled basin development not just in the Mesozoic but prior to this in the Carboniferous through reactivation of the fault and fracture networks (Fig 2.11.).

2.3.4. Strike-Slip Faults

A major structural component of these basins is a set of NW-SE trending strike-slip faults that can be seen to cut the Mesozoic basins (coloured green on Figure 2.11). These faults include the Sticklepath Fault (SPF), which in this study forms the boundary between the South Celtic Sea Basin and the Bristol Channel Basin. A set of strike-slip faults and related pull-apart basins also define the termination of the Western Approaches Trough and the Cornubian Massif. Shail and Leveridge (2009) show similar NW-SE trends to those of the Sticklepath Fault and other strike-slip faults in the region of interest to the Pyrenean Fault that facilitated the rotation of Iberia away from the Western Approaches in the Mesozoic. The eventual rotation of Iberia away from the region of interest will be discussed later in this chapter to understand how it potentially affected the local tectonics and therefore the deposition of potential source rock facies. Coward *et al.* (1995) highlights the importance of the NW-SE “tear” strike-slip faults which cross cut and separate the Celtic sea Basins.

2.3.5. 3D Architecture

Rifting in the South Celtic Sea Basin has also been interpreted to have initiated through reactivation of a Variscan thrust linking into a basal detachment (Fig 2.12 & Fig 2.13; Klemperer and Hobbs, 1991). This is in contrast to the apparent NE-SW trend of the basin which implies Caledonian control. The reactivation of Caledonian fabrics during Variscan thrusting with later reactivation of the Variscan thrusts as basin detachment could be one possible explanation. An alternative interpretation would be that the basin detachments are originally Variscan trends but this does not explain why they are oblique to onshore Irish Variscan fault trends. Gibbs (1978) suggests that all steep normal faults sole into the basal detachment fault. Arche & Lopez-Gomez (1996) indicate a similar style of basin formation in the Iberian Basin with Hercynian (Variscan) and older trends controlling asymmetric NE extension in the Early Permian.

The interpretation of the Variscan Front from Klemperer & Hobbs (1991) is displayed in Figure 2.13 and is shown as separating the half graben northward soling faults of the St George's Channel from the graben-style basins of the North Celtic Sea and South Celtic Sea Basins. The interpreted fault trends from bouger gravity anomalies in Figure 2.11 indicate that a major NW-SE trending fault structure separates the zones of structural difference. The Variscan Front (coloured red in Figure 2.11) is shown as passing north of the actual zone of structural change between the North Celtic Sea Basin and St George's Channel Basin.

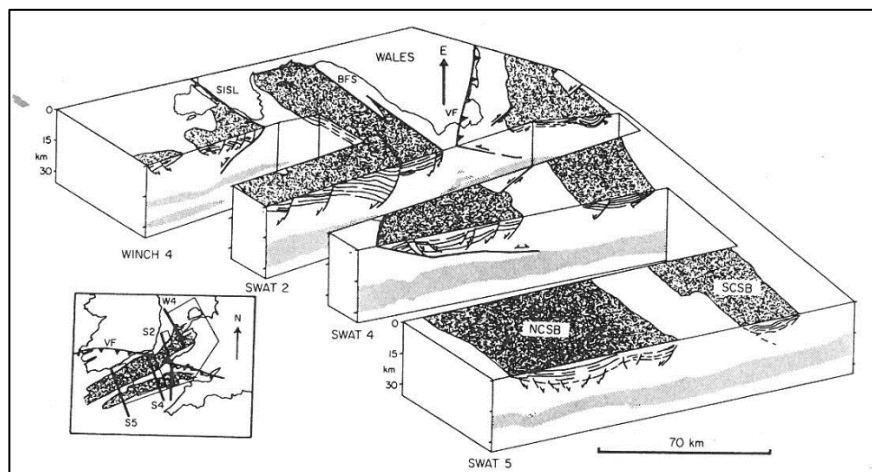


Fig 2.13. Schematic diagram based on interpretation of the BIRPS seismic reflection surveys (Klemperer & Hobbs, 1991). The Variscan Front (VF) is shown as separating the graben style basin of the North Celtic Sea Basin (NCSB) from the half graben style basin of the St George's Channel to the East. SCSB – South Celtic Sea Basin; BFS – Bala Fault System; SISL – South Irish Sea Lineament.

2.4. Megasequences

Megasequences can be assigned to stratigraphy to represent distinct tectonostratigraphic units which can be identified both from well log analysis and seismic (Allen and Allen 2013). In this study, they have been defined in similar terms to Hubbard *et al.* (1985). Four megasequences have been defined which are bounded by major regional scale unconformities and which represent distinct tectonic environments (Fig 2.14 & 2.15). The following sections will focus on providing global and regional tectonic context before describing the lithostratigraphy of the component intervals of each megasequence.

Megasequence 1 (M1) – Culm Basin and Variscan sediments (Devonian to Carboniferous) which are bounded on the top by the basement-cover interface (BCI) unconformity (Section 2.5).

Megasequence 2 (M2) – Syn-rift and post-rift sediments bounded by the BCI at the base, and the Top M2 “Cimmerian” Unconformity at the top (Section 2.6). This megasequence represents Permian-Triassic to Late Jurassic sedimentary rocks and encompasses all the main rift phases in the region of interest. Megasequence 2 has been subdivided into “rift sequences” which represent sediments packages formed by distinct rift events on a basin scale.

The Top M2 Unconformity has been traditionally term the “Cimmerian unconformity” in the literature (Hillis, 1988; Chapman, 1989) but has been termed here as M2 Unconformity as it is unclear whether there is any tectonic link to the Cimmerian Orogeny. The Cimmerian Orogeny involved the building of a mountain chain along the northwest boundary of the Tethys in the latest Jurassic (Woodcock & Strachan, 2013). In addition the age relationships of the unconformity are highly variable with the base of the M3 megasequence varying in age from the Latest Jurassic to Middle Cretaceous and the Top of the M2 megasequence being as old as the Permian-Triassic sequence in some areas due to erosion or non-deposition.

Megasequence 3 (M3) – Post-rift sediments (Section 2.7) between the Top M2 Unconformity and the Alpine Unconformity (Cretaceous to Paleogene).

Megasequence 4 (M4) – Post-Mesozoic inversion sediments (Section 2.8) and cover which are bounded to the base by the Alpine Unconformity and to the top by the seabed (Paleogene to Recent).

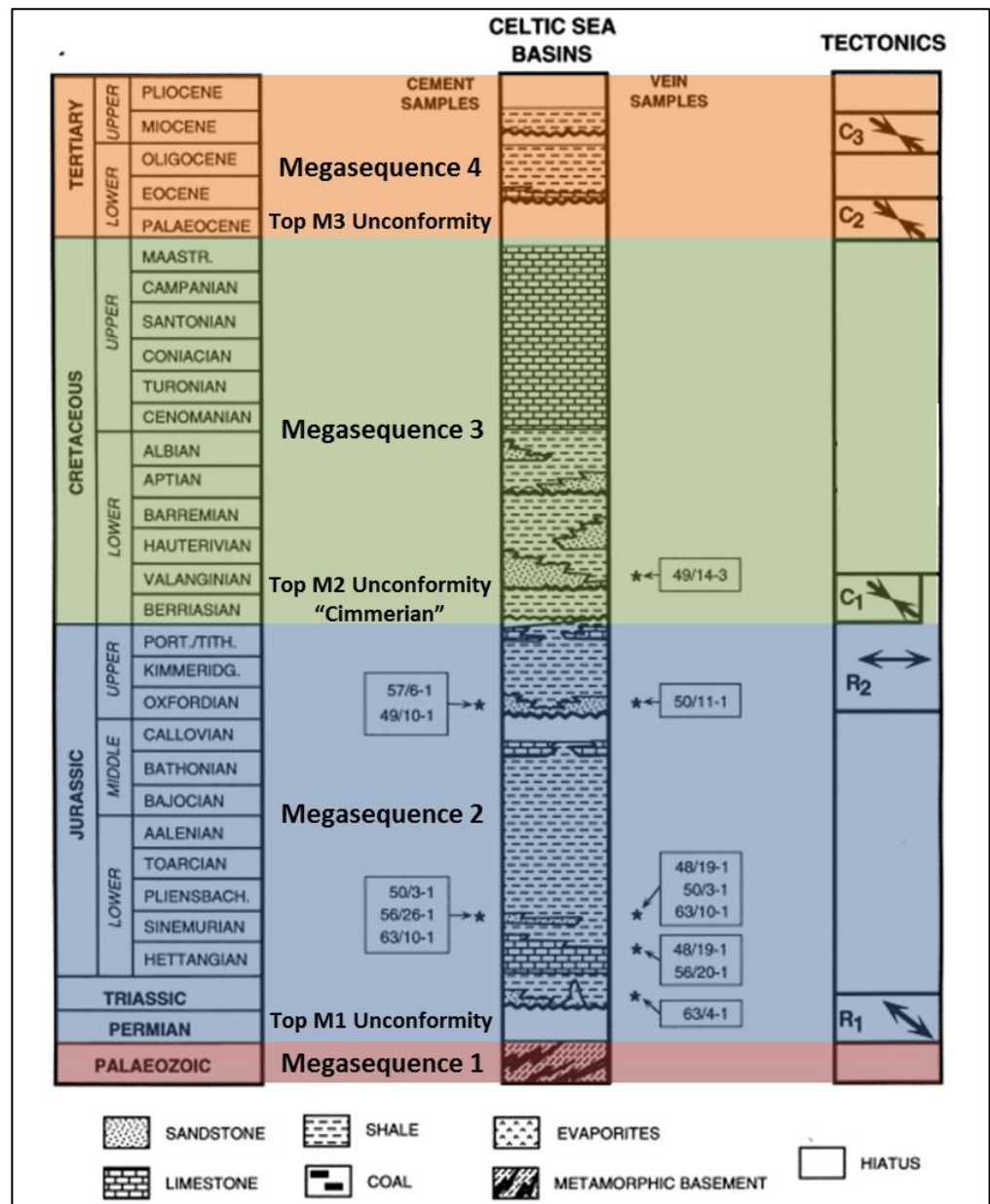


Fig 2.14. Tectonostratigraphy of the Celtic Sea region modified after O'Reilly *et al.* (1998). R1 and R2 represent rift phases while C1 to C3 represent phases of compressional tectonics.

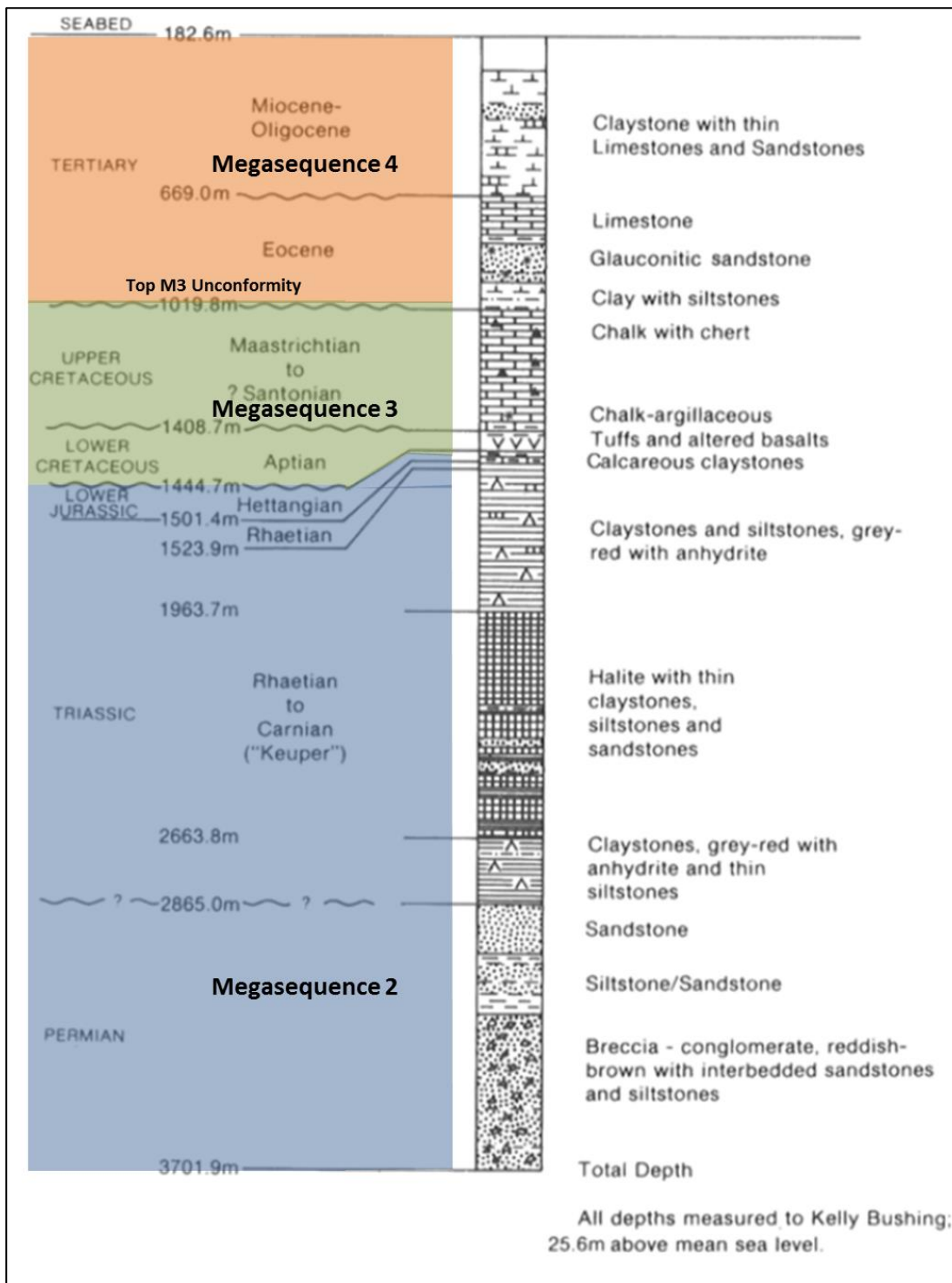


Fig 2.15. Stratigraphy of Britoil Well 72/10-1A in the Melville Basin in the Western Approaches (modified after Bennet et al, 1985).

2.5. Devonian & Carboniferous - Megasequence 1

This section will focus on discussing the lithostratigraphy of the Devonian and Carboniferous as the tectonic context has been previously outlined in Section 2.2.3.

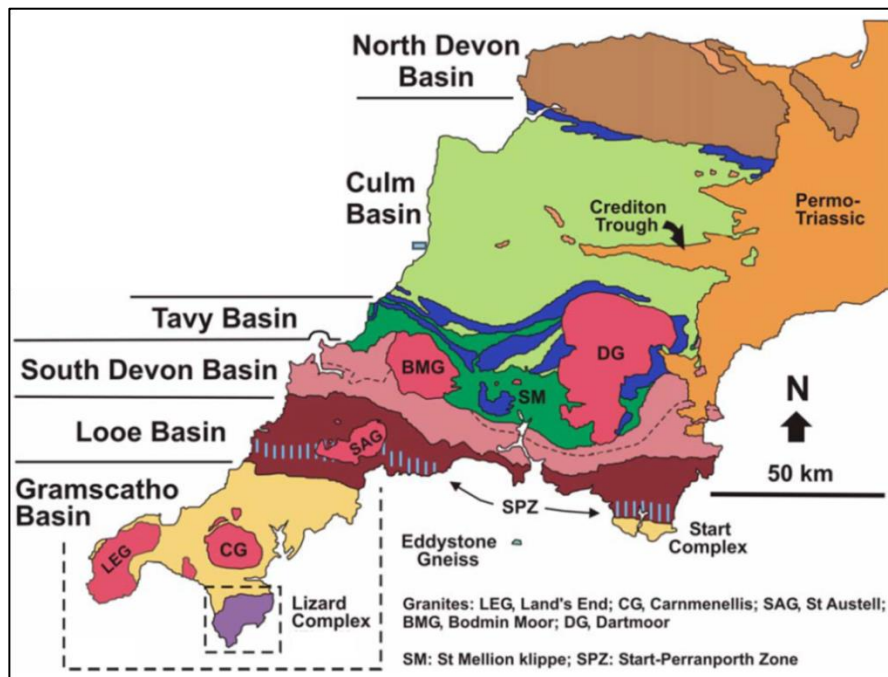


Fig 2.16. Simplified map of the geology of Cornwall and Devon showing the extent of the Devonian and Carboniferous basins with the Permo-Triassic coloured orange and granite batholiths coloured red (Shail & Leveridge, 2009). Granite bodies are coloured red, Lizard Complex – Purple, Gramscatho Basin – Light Yellow, Looe Basin – Dark Red, South Devon Basin – Light Red, St Mellion Klippe – Green, Tavy Basin – Blue, Culm Basin –Light Green, North Devon Basin – Brown, Permian-Triassic – Orange.

2.5.1. Early Devonian

The Early Devonian Looe Basin deposits represent an E-W trending band 15 km wide and 100 km long stretching from Torquay to Newquay containing a sedimentary sequence likely deposited on the Older Red Sandstone Continent (Styles, 1997). The Looe Basin (Fig 2.16.) contains two distinct groups: Dartmouth Group (Early Devonian) and Meadfoot Group (Early to Middle Devonian).

The Dartmouth Group (Early Devonian) was deposited in a continental setting with interspersed marine conditions and suggested active rifting (Styles, 1997). The Meadfoot beds (Early to Middle Devonian) of the Meadfoot Group were deposited in shallow marine conditions before shallowing conditions led to the deposition of the fluvial and delta deposits of the Staddon Grits.

2.5.2. Devonian to Early Carboniferous

N-S extension led to the development of sub-basins being formed in a subsiding shelf region (Styles, 1997). The most southerly Gramscatho Basin (Fig 2.16) is floored by oceanic lithosphere and developed outboard of the shelf in a deep marine rift setting. Thrust faults juxtaposed the allochthonous sequence from the marginal Gramscatho Sea, the Lizard Complex and Dodman Phyllites, placing them on top of the parautochthonous mudstones of the Gramscatho Basin.

The Early Devonian shelf deposits transition into the greywackes of the Gramscatho Group. Middle Devonian Trewogan Sandstones grade upwards into the mud dominated Porthtowan Formation of the Late Devonian (Leveridge & Hartley, 2006). The top of the succession is the Mylor Slate Formation which is mainly made up of grey and grey-green shales with an olistolithic breccia at its top. The sequence represents progressive deepening of the deep marine rift basin (Styles, 1997).

Allochthonous sequences consist of the different thrust bounded Variscan nappes: the Porthscatho Formation of the Carrick Nappe; varying sedimentary sequence of the Veryan Nappe; mafic and ultramafic meta-igneous units of the Lizard Complex; and phyllites and strained sandstones of the Dodman Nappe. Harvey *et al.* (1994) used the BIRPS SWAT 9 line to suggest that the Plymouth Bay Basin is underlain by the thrust Carrick and Lizard Nappes with rifting initiated in relation to granite emplacement or the collapse of the nappe pile (Fig 2.17).

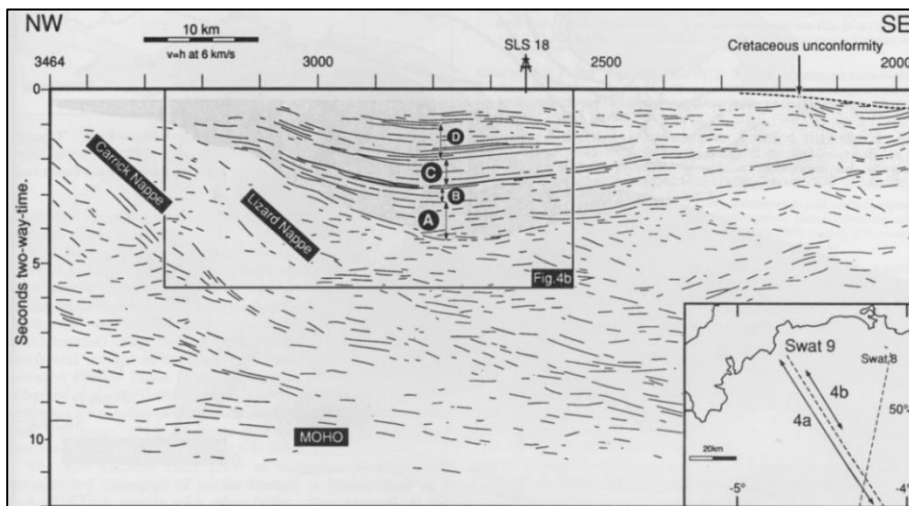


Fig 2.17. Schematic section based on interpretations from the SWAT 9 section suggesting underlying of the Plymouth Bay Basin by the Carrick and Lizard Nappes (Harvey *et al.*, 1994). A-D represent seismically defined megasequence packages for the Plymouth Bay Basin discussed further in Harvey *et al.* (1994).

The South Devon Basin is an E-W trending basin of Middle Devonian to Namurian basinal rocks. The South Devon Basin is made up of sequence of sub-basins and highs which transition from the limestones in the east, thought to have developed on the Liskeard High, to mudstones and volcanics to the west which shallow to the north (sometimes termed the Trevone Basin – Styles, 1997). The western sequence is composed of deep basin deposits of latest Middle Devonian to Early Carboniferous of age. In the east the Dartmouth and Meadfoot groups of the Looe Basin grade upwards into limestone dominated lithologies of Late Devonian to Early Carboniferous age passing into deep-water pelagic shales. Acidic tuffs and lavas common in the Middle Devonian strata of Ashprington and Kingsteignmouth areas indicate active volcanism concurrent with extension. The North Devon Basin is composed of a thick sequence of Devonian to Early Carboniferous shallow marine and alluvial deposits. It is bounded to the south by the Culm Basin and to the north by the Bristol Channel Fault (Styles, 1997).

2.5.3. Culm Basin and South Wales Basin

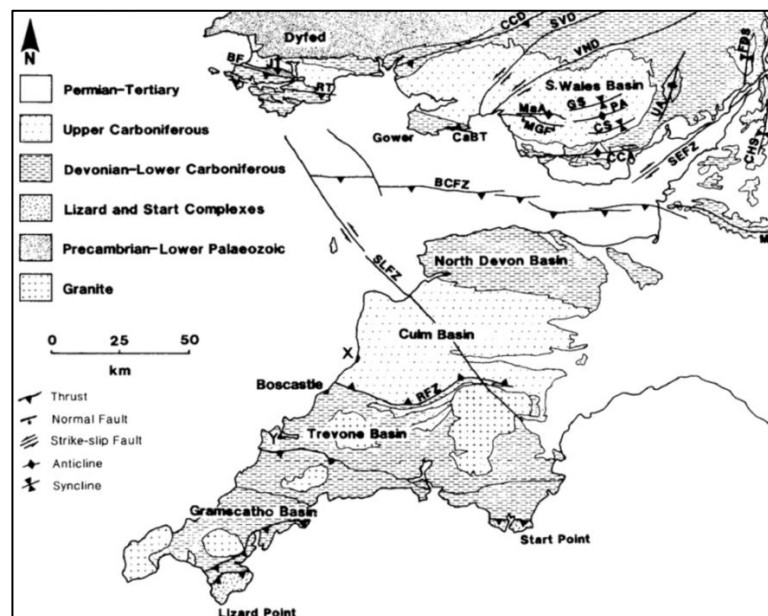


Fig 2.18. Geological map of SW England showing the locations and extents of the Culm and South West Basin (Hartley and Warr, 1990). It is likely that the Culm Basin continues offshore and could underlie the South Celtic Sea Basin. CCD - Carreg Cennan Disturbance, SVD - Swansea Valley Disturbance, VND - Neath Disturbance, PA - Pontypridd Anticline, SLFZ - Sticklepath Lustleigh Fault Zone, MGF - Moel Gilau Faul, JT - Johnston Thrust, BF - Benton Fault, RT - Ritec Thrust, CaBT - Caswell Bay Thrust, RFZ - Rusey Fault Zone. CHS - Coalpit Heath Syncline, MA - Mendip Axis, MaA - Maesteg Anticline, GS - Gelligaer Syncline, CS - Caerphilly Syncline, CCF - Cardiff Cowbridge Anticline, UA - Usk Axis, FDS - Forest of Dean Syncline, SEFZ -Severn Estuary Fault Zone. BCFZ - Bristol Channel Fault Zone.

The Culm Basin and South Wales Basin (Fig 2.18) represent Carboniferous foreland basins situated between the Variscide Mountain Chain and the adjacent Wales-Brabant Massif developed due to flexure in response to an advance of Variscan thrusting in the Carboniferous (Allen *et al.*, 1986; Hillis, 1988; Hartley & Warr, 1990). Hartley & Warr (1990) identified a correlation between the thickness of Middle Devonian and Early Carboniferous syn-rift and the location of subsequent Late Carboniferous sedimentation with thick syn-rift sequences becoming thrust nappes and topographic highs. The areas of thin syn-rift such as Culm Basin and South Wales Basin became the areas of active sedimentation (Fig 2.19).

Namurian sediments in SW England are distal 'Bouma-type' turbidites of the Crackington Formation (Waters *et al.*, 2009) with indications of bimodal palaeocurrents (E-W) suggestive of an axial drainage pattern (Hartley & Warr, 1990). Palaeontological data suggests that the northerly derived Bideford formation may extend down into the Upper Namurian which would indicate that the source to the north was emergent in the Late Namurian times (Hartley & Warr, 1990). Kelling (1988) indicated the Namurian sediments of the South Wales as displaying a fining up sequence with a change from shallow marine, high energy quartzites (Basal Grit) to lagoonal shallow marine mudstones of the Shale Group.

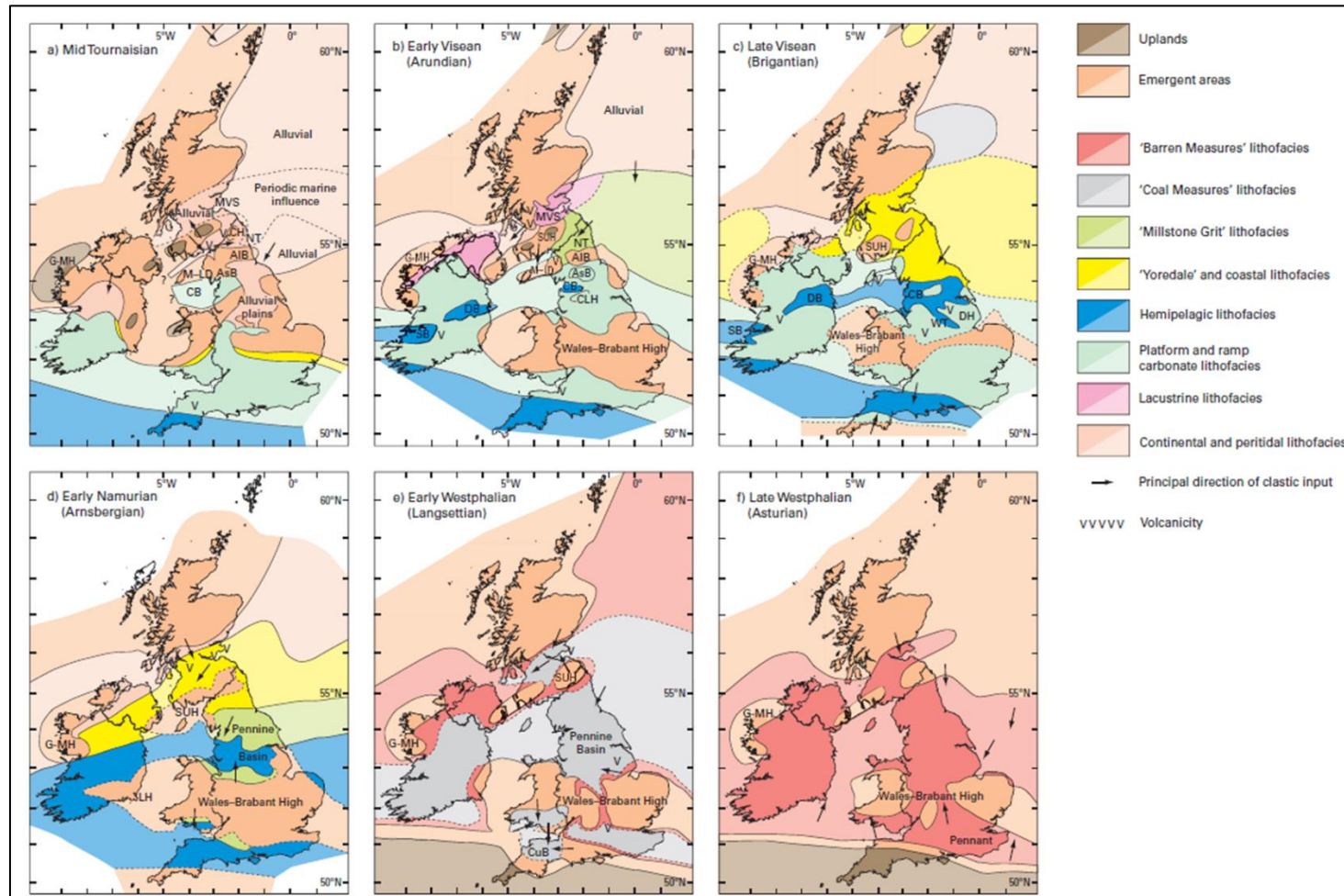


Fig 2.19. Palaeogeographic reconstructions for the Carboniferous of Britain (Waters *et al.*, 2009) with a systematic change in the Celtic Sea and Western Approaches from Platform carbonate and hemipelagic deposition in the Early Carboniferous to Coal Measure deposition and uplands by the Westphalian. AIB – Alston Block, AsB – Askrigg block, CB – Craven Basin, CH – Cheviot High, CuB – Culm Basin, DB – Dublin Basin, LH - Leinster High, ML-D – Manx-Lake District High, MV – Midland Valley, NT – Northumberland Trough, RB – Rossendale Block, SB – Shannon Basin, SUH – Southern Uplands High.

During the Westphalian A (Westphalian chronostratigraphy and biostratigraphy is described in Waters *et al.*, 2009), deposition of distal turbidites (Crackington Formation) and deltaic mudstones with abundant sandstones and siltstones (Bideford Formation) continued with occasional influx of freshwater lake storm and turbidite deposits of the Bude Formation (Waters *et al.*, 2009). Cornford *et al.* (2011) discussed the existence of sheared coals and carbonaceous shales termed the “Bideford Black” which occur within the Bideford Formation. The Bude Formation continues up until the Westphalian C in the Culm Basin (Styles, 1997). In South Wales, Westphalian A to early Westphalian C deposition was primarily dominated by mudstones and coals of the Lower and Middle Coal Measures. These were deposited in a swampy, coastal plain environment prone to marine transgressions (Water and Davies, 2006). Although these coal measures show similar lithologies and environments of deposition to those in the Pennine Basin, the Wales-Brabant Massif segregated these areas of coal deposition (Water and Davies, 2006). Structural features trending E-W were still active controlling facies distribution and sediment thickness.

While no sediments later than the early Westphalian C are preserved in the Culm Basin the sedimentary sequence in South Wales shows a change from the Coal Measures to overlying Pennant Measures which are sandstone-dominated. The Pennant Measures are suggested by Hartley & Warr (1990) to represent a proximal braidplain with large scale alluvial channel systems with limited mudstones deposition on the floodplain. Palaeocurrent and compositional data indicates a southerly source for the coals and immature lithic detritus (Hartley & Warr, 1990). During the latest Westphalian to Stephanian the Culm Basin and South West Wales Basin underwent inversion during regional shortening.

2.5.4. Potential Source Rock Strata in Megasequence 1

Devonian age strata have been penetrated in well 87/12-1A in the Plymouth Bay Basin which Pharaoh *et al.* (2017) interpreted as carbonates containing algae, ostracods, gastropods, rugose corals, stromatoporoids, etc. Other penetrated lithologies in the Variscan Basement of the Western Approaches include slate (83/24-1), pelite, phyllite and quartzite (Pharaoh *et al.*, 2017) all of which can be seen in the onshore Devonian to Carboniferous sequence of Cornwall and Devon. In the Melville Basin the Devonian to Carboniferous sequence is seen to be overlain unconformably by Permian-Triassic syn-rift sediments. Chapman (1989) identified the presence of Late Carboniferous to Early Permian rocks which lie below the basal Permian-Triassic unconformity in the Britoil (86/18-1) well. Figure 2.20 shows the locations of the UK Sector Western Approaches wells referred to in this section.

It is possible that potential Westphalian coal measures extend offshore into the Western Approaches or Celtic Sea Basins. The Corrib Gas Field in the Slyne Basin has been sourced from Westphalian Coals and although these strata are likely overmature in the initial basin centres; Carboniferous coals could represent an additional play type for Permian-Triassic basins (Pharaoh *et al.*, 2017). Cornford *et al.* (2011) indicated that coals of the “Bideford Black” exist with vitrinite reflectance of as low as 1.6% Ro. This observation suggests that there is the potential that Carboniferous strata can be protected from burial and overmaturity in the region of interest.

No shows and only trace background gas was encountered in the metamorphosed Palaeozoic section of wells 93/02-2 and 98/23-1. The Palaeozoic basement sequence drilled in 99/18-1B is interpreted to have been deposited in an oxidative environment and is indicated to have no source rock potential. Similarly in 83/24-1, Rock-Eval analysis suggests no source rock potential within the Palaeozoic sequence (Cooles *et al.*, 1986). While there is potential for coal and kerogen-bearing mudrocks within the Palaeozoic basement in the region of interest it is considered here as unlikely to generate substantial hydrocarbons due to likely overmaturity.

2.6. Permian to Late Jurassic - Megasequence 2

Megasequence 2 represents the syn-rift and post-rift sediments from formation of the Late Paleozoic to Mesozoic in the Permian-Triassic and is bounded to the top by the Top M2 Unconformity, termed in the literature as the “Cimmerian” by Hillis (1988) and Chapman (1989). In the Western Approaches, Permian to Triassic sediments make up the majority of the basin fill (Chapman, 1989). Megasequence 2 encompasses over a 100 million years of strata and includes the Jurassic sequence which is the main focus of this thesis. Therefore understanding the basin forming process, style of syn-rift and post-rift fill in the context of the regional and global plate tectonics and palaeogeographic environment is fundamental to the data analysis in this Masters project. The primary objective is to discuss the key factors that controlled source rock deposition and preservation during the Permian to Jurassic interval.

2.6.1. Permian to Triassic

2.6.1.1. Tectonic Context and Palaeogeographic Framework

In the Early Permian Pangaea had consolidated (Fig 2.21) with Britain and Ireland being situated near to the equator and the Palaeotethys open to the SE of Laurussia (Woodcock & Strachan, 2012). The unconformity that marks the base of Megasequence 2 represents regional uplift of Britain, subsequent to this orogenic collapse led to a period of thermal subsidence and rifting pulses (Woodcock & Strachan, 2012). Subsidence and rifting caused the opening of the Mesozoic basins in the Celtic Sea and Western Approaches (Fig 2.22) with sedimentation restarting by the Early Permian in a monsoonal arid to semi-arid climate. The deposition of widespread evaporites and red-beds occurred at this time across much of Europe (Woodcock & Strachan, 2012).

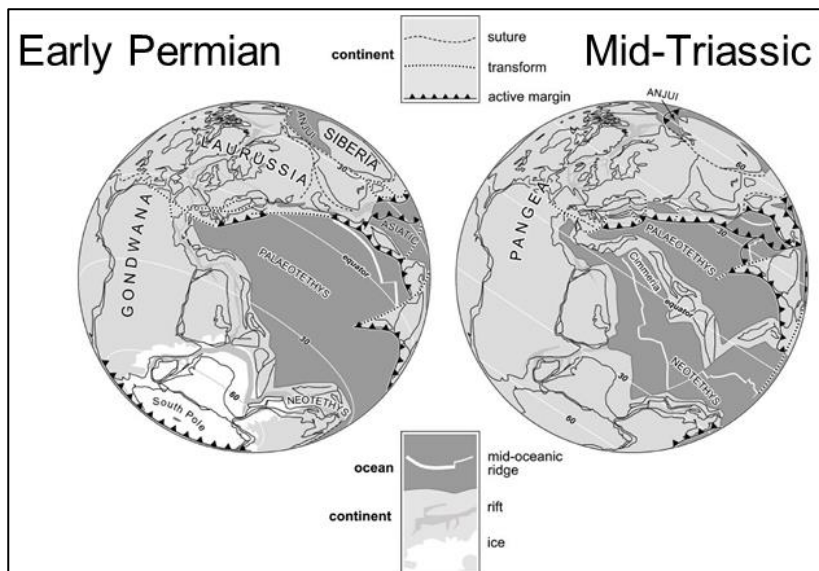


Fig 2.21. Tectonic reconstructions for the Early Permian and Middle Triassic (Woodcock & Strachan, 2012) with Pangaea assembled.

Middle to Upper Permian strata in SW Britain are characterised by desert sandstones and mudstones that pass upwards into limestones and evaporites (Woodcock & Strachan, 2012) such as the marine derived evaporitic sequence of the Zechstein in the North Sea (McKie, 2017). Evaporite deposition was related to evaporation of saline waters in the isolated continental to marginal marine basins of the Late Permian with limestone deposition caused by a Late Permian rise in sea-level (Fig 2.21). Woodcock & Strachan (2012) in contrast suggests a fall in sea-levels during this time (Fig 2.22).

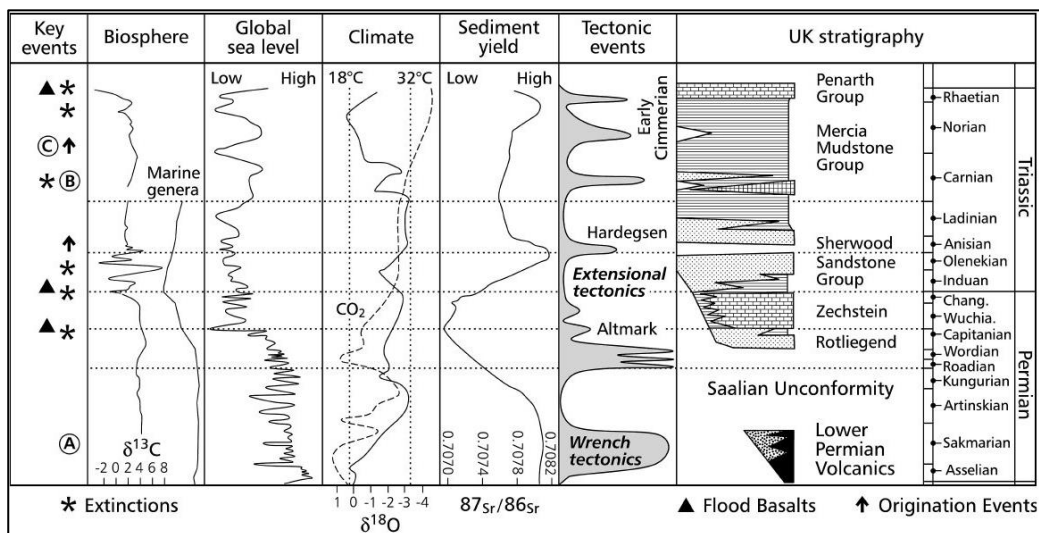


Fig 2.22. Summary of the key events for the Permian and Triassic of the UK with an indication of the tectonics, sediments yields, climate, sea level, biosphere and UK stratigraphy (Woodcock & Strachan, 2012).

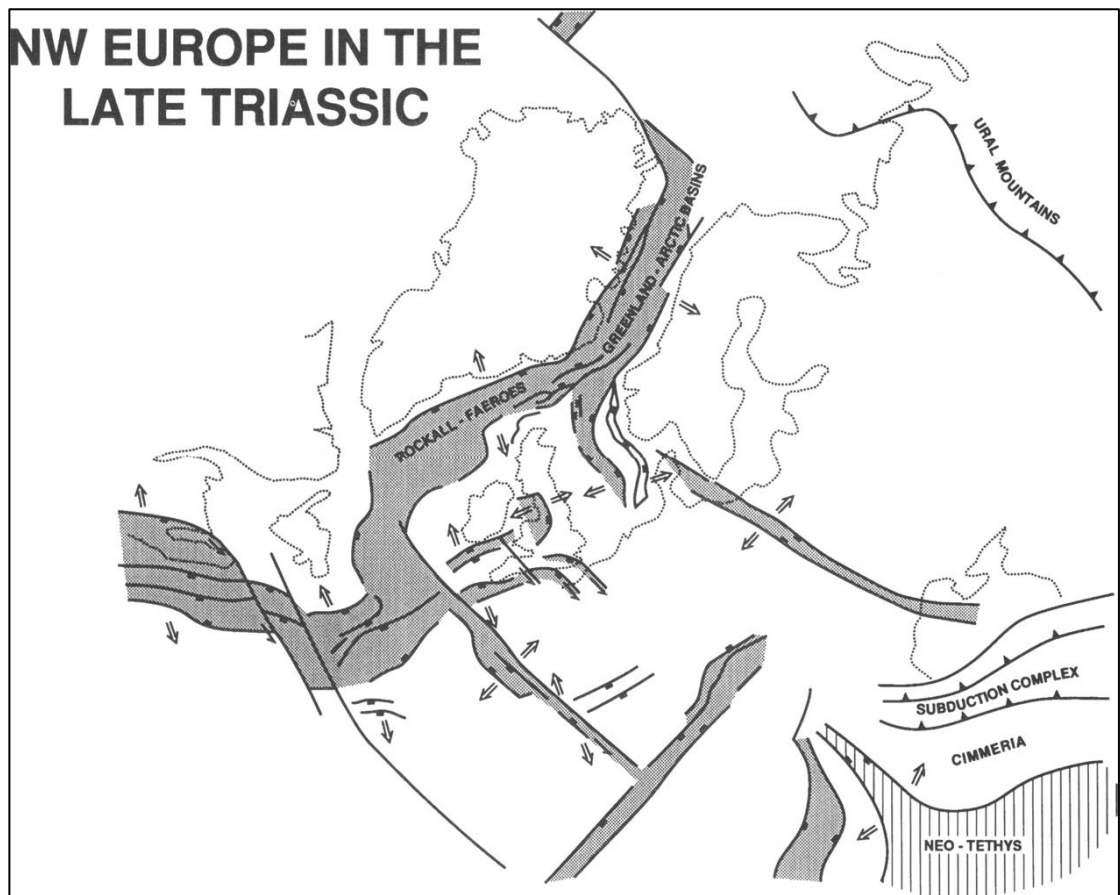


Fig 2.23. Schematic map showing the location of the main Triassic rifts with suggested extensional directions (Coward, 1995).

Torsvik and Cocks (2017) suggest that the main body of Pangaea remained intact through the Triassic. During the Triassic most of Europe underwent extensional tectonics leading to local fluctuations in relative sea level and systems of north-south trending graben that developed and deepened. This north-south rifting is consistent with the formation of the east-west trending rift zones shown in Figure 2.23 (Coward, 1995). Coward (1995) suggested that the Atlantic Rift had developed by the Triassic (Fig 2.23) and was linked into the Western Tethys with the Palaeotethys ocean almost fully closed and the Cimmerian mountain belt formed through Turkey to China.

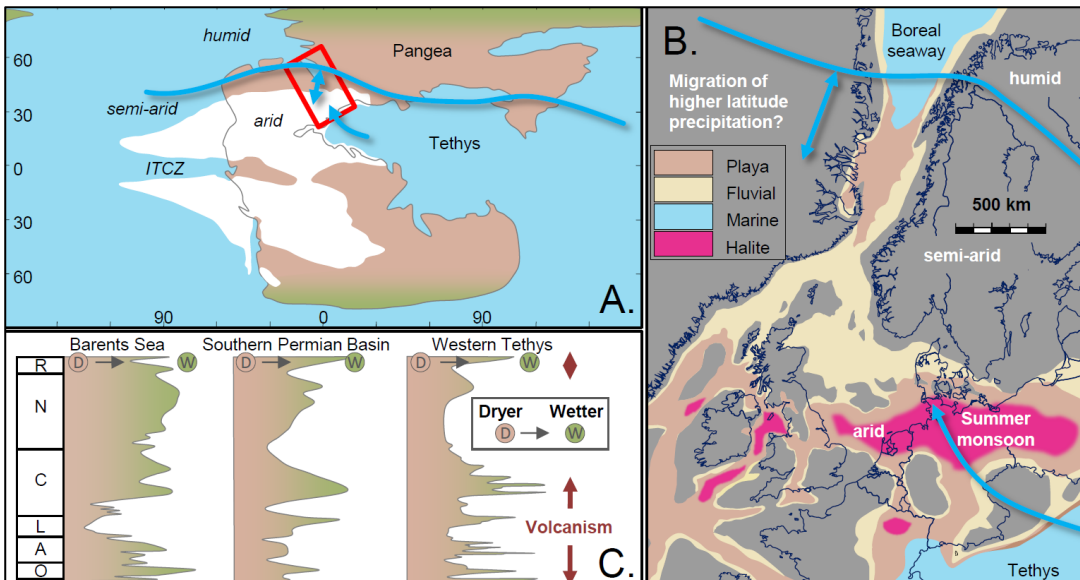


Fig 2.24. Summary of climatic settings in the Triassic with indications of playa lake and halite deposition in the Celtic Sea and Western Approaches region (McKie, 2017).

Torsvik's and Cocks' (2017) palaeogeographic reconstructions suggest that by the Carnian (230 Ma), the Western Approaches and Celtic Sea regions were characterised by a shallow sea shelf environment. McKie (2017), however, indicates that complex topography likely formed due to polyphase rifting along multiple extensional vectors. It was this topography that he suggests limited full marine flooding of the rift basins and but allowed seepage into the arid rift basins (Fig 2.24 & 2.25). The Late Triassic saw widespread transgressions across Britain as sea-levels rose accompanied by a change to a more humid climate as Britain drifted northward (Woodcock & Strachan, 2012).

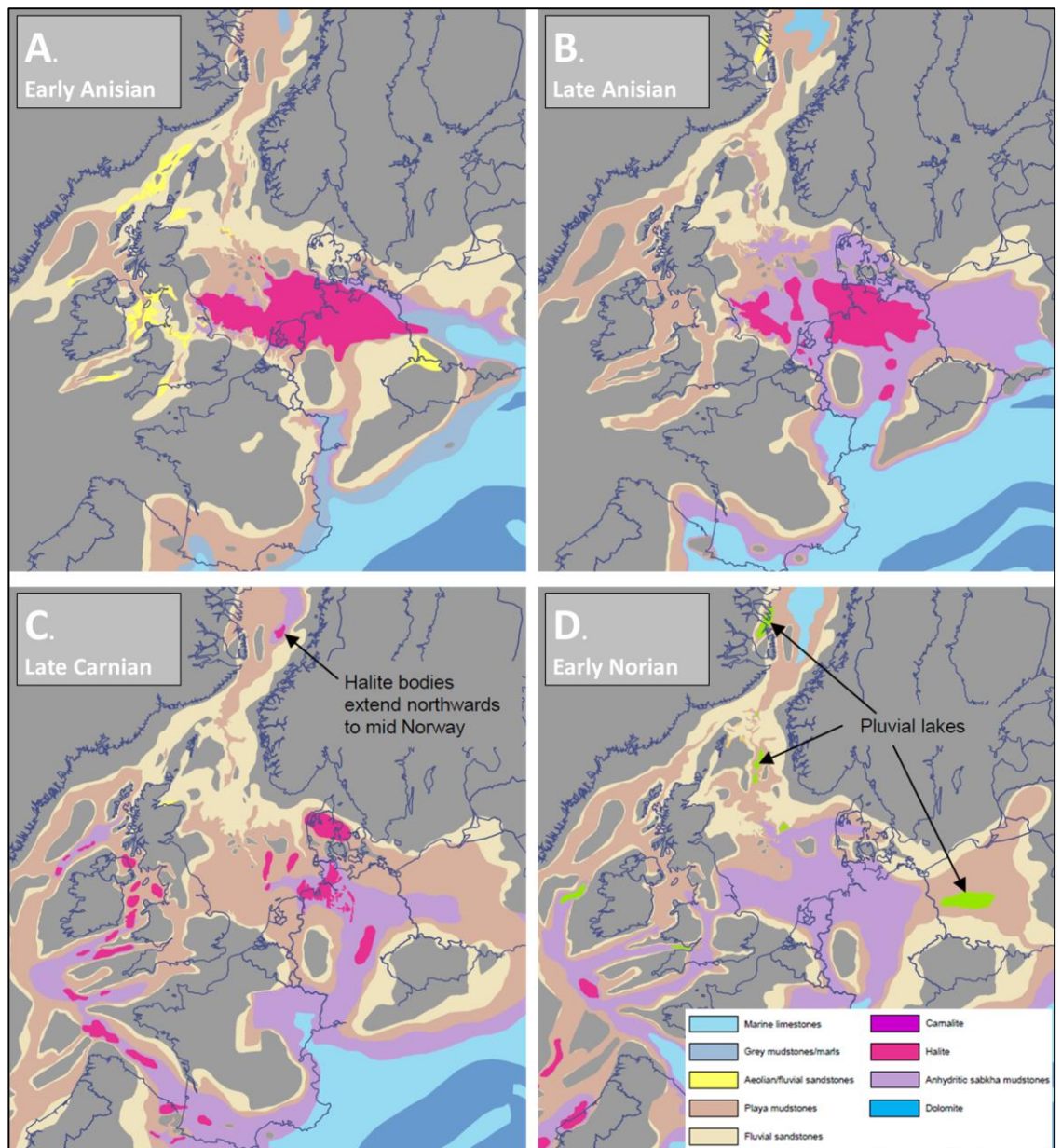


Fig 2.25. Palaeogeographic reconstructions for the Triassic showing the eventual rift development and predominance of an interpreted sabkha setting in the Celtic Sea and Western Approaches (McKie, 2017).

2.6.1.2. Permian to Triassic Lithostratigraphy

The oldest unit in the Melville Basin is comprised of Permian volcanics extruded during earliest rifting in the Western Approaches. Overlying the Permian volcanics is a basal breccia-conglomerate unit similar to that onshore South Devon (Chapman, 1989). The sequence then passes upwards into siltstones with common sandstones in some areas that fine upwards into mudstones (Fig 2.26). The overlying Sherwood Sandstone Group which is comprised of quartzose and arkosic sandstones in an argillaceous matrix with typically fining upward units (Hillis, 1988). Chapman (1989) suggests that the Sherwood Sandstone Group can be taken to represent the base of the Triassic in the Western Approaches.

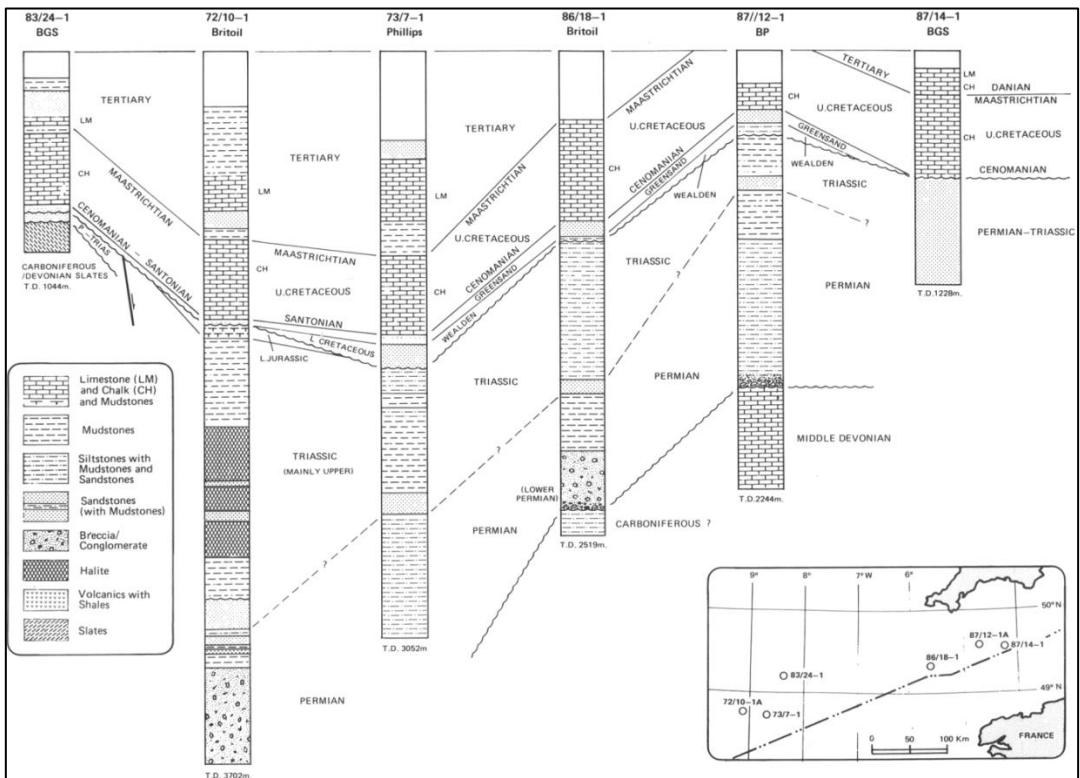


Fig 2.26. Well correlation panel following a roughly E-W transect along the Western Approaches demonstrating the style of Permian and Triassic sediments (Chapman, 1989).

In the North Melville Basin a massive unit of halite exists (Hillis, 1988) that reaches 1700 m thick in well 72/10-1A (Fig 2.27 - Fisher & Jeans, 1982). Flowage has meant that the salt has thickened above NE and ENE trending faults (Chapman, 1989) with the dominant movement of salt being northward during Tertiary and synchronous with the Top M2 unconformity (Hillis, 1988). Upper Triassic red-grey claystones with siltstones with anhydrite of playa lake origin (Hillis, 1988) overly the salt (Mercia Mudstone Group) and pass upwards into grey claystones with thin limestones of the Rhaetic (also termed the Penarth Group).

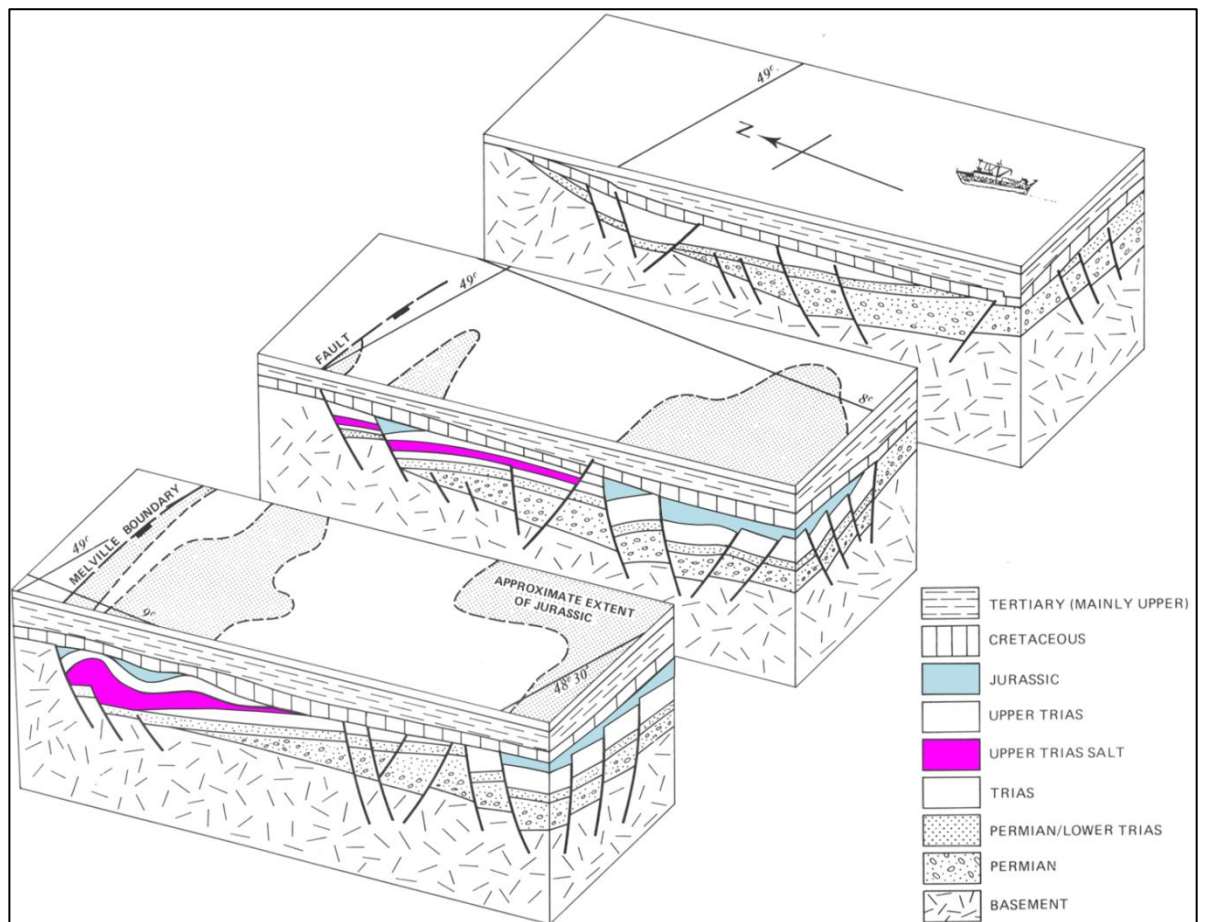


Fig 2.27. Schematic diagrams for the Melville Basin (modified after Chapman, 1989) showing the salt thickness and extent (pink) and preservation of the Jurassic sequence in the North and South of the basin (light blue).

Bulnes & McClay (1998) describe the Permian and Triassic syn-rift sequence of the South Celtic Sea Basin as being represented by similar lithologies to those of the Melville Basin but without the older Permian sediments and volcanics. In the South Celtic Sea Basin the Palaeozoic low-grade metamorphic basement is overlain by Permian to Triassic claystones and siltstones with thin intercalated sandstones (Fig 2.28 - Bulnes & McClay, 1998). These strata are immediately overlain by evaporites that are likely to be similar to the halite seen in the Melville Basin with the evaporites underlying mudstones, sandstones and limestones that mark the top of the Triassic.

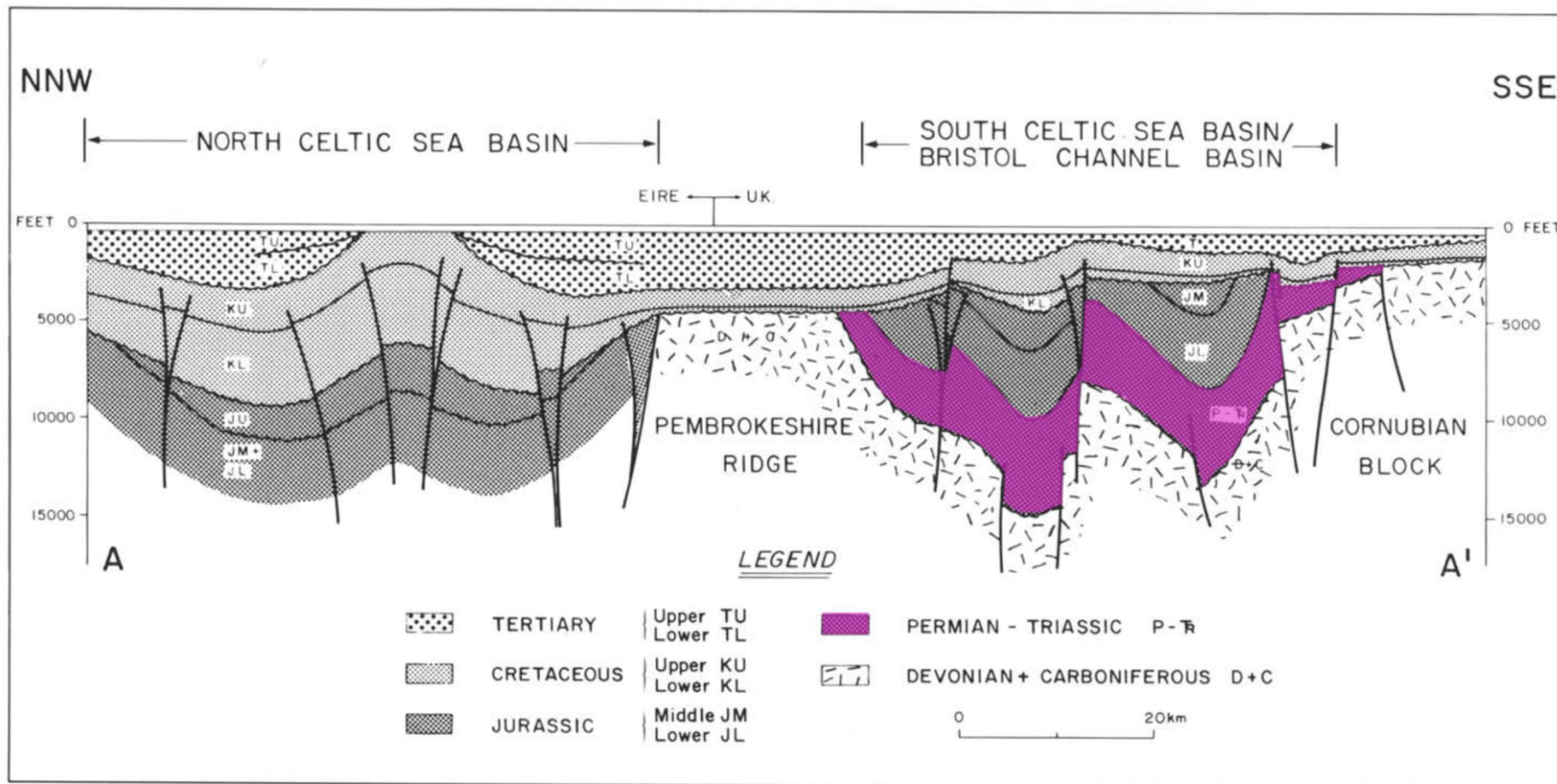


Fig 2.28. Geological cross-section for the North Celtic Sea and South Celtic Sea Basins (van Hoorn, 1987) with the Permian-Triassic strata of the South Celtic Sea Basin highlighted in pink. Permian to Triassic strata have not been penetrated in the North Celtic Sea Basin due to the deep depth of burial.

2.6.2. Early Jurassic

2.6.2.1. Palaeogeographic Framework

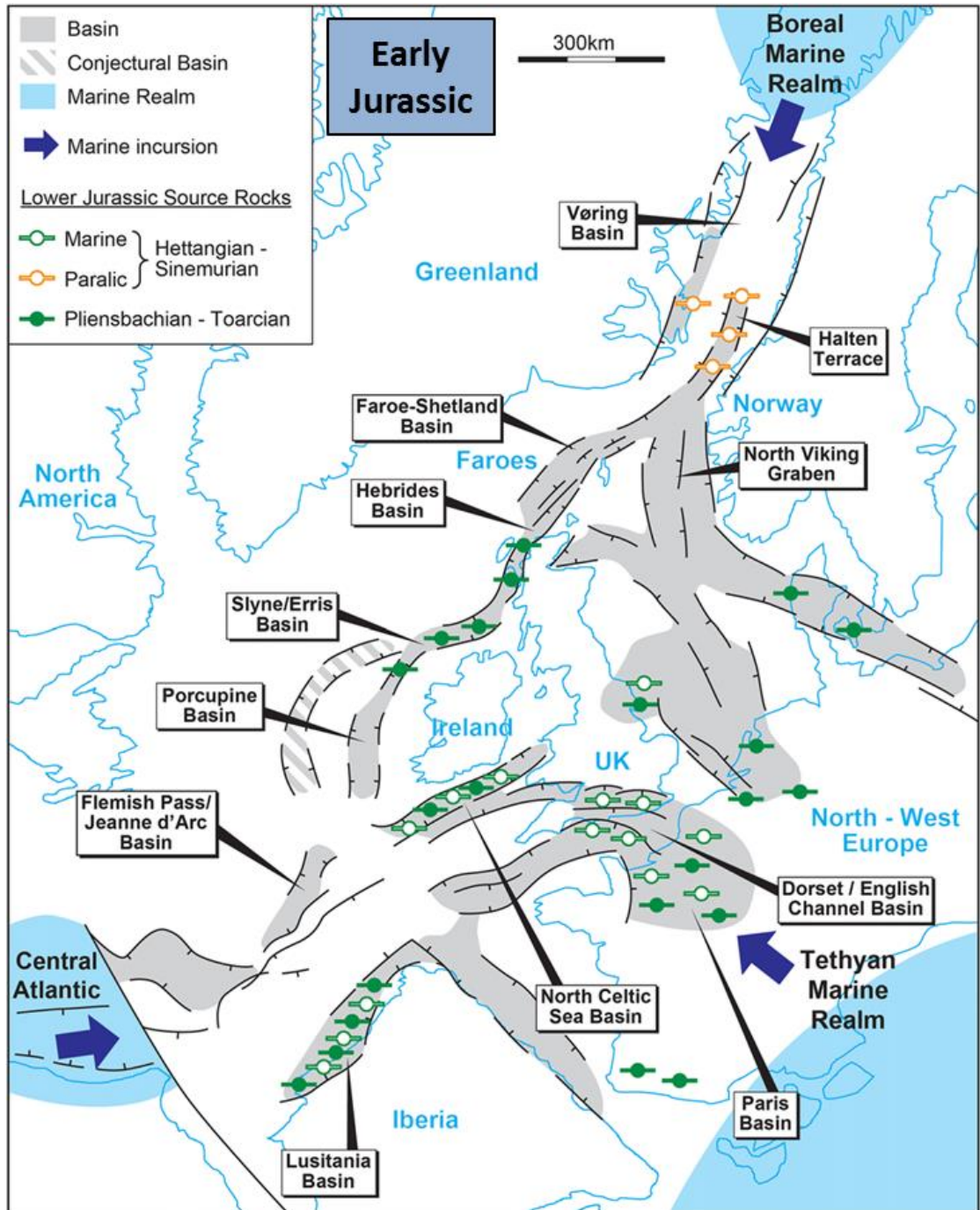


Fig 2.29. Map of the current North Atlantic margin of Europe for the Early Jurassic showing the areas of source rock deposition and Mesozoic rift basins (Scotchman, 2016). The Central Atlantic shown is the location of the Hispanic Corridor which starts to open into the Central Atlantic during the Sinemurian.

The Early Jurassic was characterised by a period of tectonic quiescence in SW Britain (Lundin, 2002) with thermal subsidence related sedimentation occurring (Murphy *et al.*, 1995; Rowell, 1995; Woodcock & Strachan, 2012) along with the possibility of minor rifting in the Celtic Sea and Western Approaches Basins (Bulnes & McClay, 1998; Scotchman, 2016). The period is characterised by the deposition of mudstone dominated marine facies (Hillis, 1988; Murphy *et al.*, 1995) as isolated rift basins underwent marine infiltrations after a Latest Triassic to Earliest Jurassic marine transgression. Southern Britain was dominated by marine waters from the newly opening Central Atlantic and Tethyan Marine Realm while in the North (Fig 2.29) the Boreal Marine Realm influenced deposition in areas such as the Halten Terrace and Viking Graben (Scotchman *et al.*, 2016).

Worldwide enhanced carbon burial occurred related to extreme climate changes with rapid swings between icehouse and greenhouse conditions (Korte & Hesselbo, 2011; Hesselbo *et al.*, 2013) which Dera *et al.* (2011) have linked to repeated volcanic pulses from the Karoo-Ferrar and Camp Large Igneous Provinces (LIPs). Hillis (1988) indicates the deposition of a 1 km sequence of Early Jurassic in Lenkett-1 in the SW Channel Basin (Fig 2.1).

The stratigraphy of the Early Jurassic of the Celtic Sea and Western Approaches is here termed the Lias (Fig 2.30) which is split up as described by Simms *et al.* (2004).

Middle Jurassic	Aalenian			Radiometric dates (Ma)	
				Pálffy <i>et al.</i>	Harland <i>et al.</i>
Lower Jurassic	Toarcian	Upper Lias	Lias Group	178.0 (+1.0/-1.5)	178.0 (+10.5/-10.5)
	Pliensbachian	Middle Lias		183.6 (+1.7/-1.1)	182.0 (+16.0/-14.0)
	Sinemurian	Lower Lias		191.5 (+1.9/-4.7)	189.5 (+7.5/-7.5)
	Hettangian			196.5 (+1.7/-5.7)	203.5 (+7.5/-5.0)
Upper Triassic	Rhaetian			199.6 (+0.3/-0.3)	210.5 (+6.3/-8.8)

Fig 2.30. Chronostratigraphic division and radiometric dating for the Early Jurassic (Simms *et al.*, 2004).

2.6.2.2. Hettangian to Early Sinemurian

Tectonic Context

A rapid rise in sea-level is suggested to have occurred during the Rhaetian by Hillis (1988) and earliest Jurassic by Hallam & Wignall (2004) and led to marine incursions from the Tethyan Marine Realm and Panthalassic Marine Realm, via the Hispanic Corridor (Fig 2.32). The Hispanic Corridor started opening into the Central Atlantic (Fig 2.29) in the Sinemurian (Labails *et al.*, 2010). The marine incursions infiltrated into the isolated rift basins (Ruhl *et al.*, 2016) and led to deposition of marine facies mudrocks.

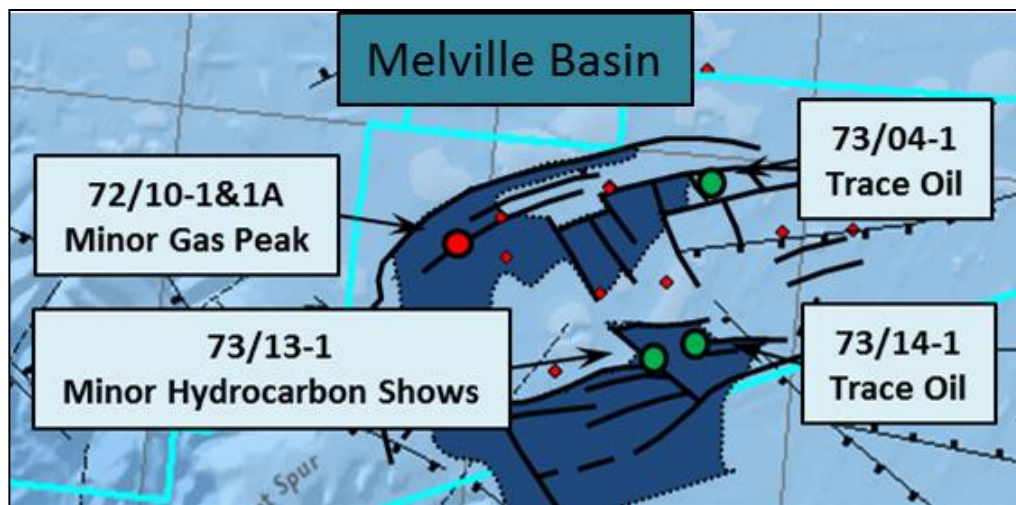


Fig 2.31. Schematic diagram of the zones of preservation of Lower Jurassic in the Melville Basin (after Chapman, 1989).

Lithostratigraphy

Jenkyns *et al.* (2002) suggested oxygen-depleted depositional environments led to local enrichment in organic carbon during the deposition of the Rhaetian to Hettangian sediments of SW Britain. The earliest source rocks of the Hettangian to Sinemurian Blue Lias of Dorset are indicated as containing Tethyan fauna suggesting a direct connection to the Tethyan Marine Realm (Jenkyns *et al.*, 2002). Potential source rocks in Somerset of this age have TOC values up to 10%. This is in contrast to the Hettangian to Sinemurian of the Western Approaches which Hillis (1988) describes as slightly carbonaceous mudstones with interbedded micritic limestones deposited in a sublittoral to near-shore environment. These sediments are similar to those in described in the South Celtic Sea and Bristol Channel Basins (Kamerling, 1979) and in the Brittany and SW Channel Basins (Hillis, 1988). The preservation limit of the UK Western Approaches Lower Jurassic sequence is shown in Figure 2.31. 15 m of Hettangian sands are indicated in well 73/01-1A which have no other

equivalents in the UK sector of the Western Approaches. In the adjacent well 72/10-1A (Fig 2.31) only a thin sliver of Hettangian carbonaceous mudstones are present with no Hettangian sands present (BNOC, 1979).

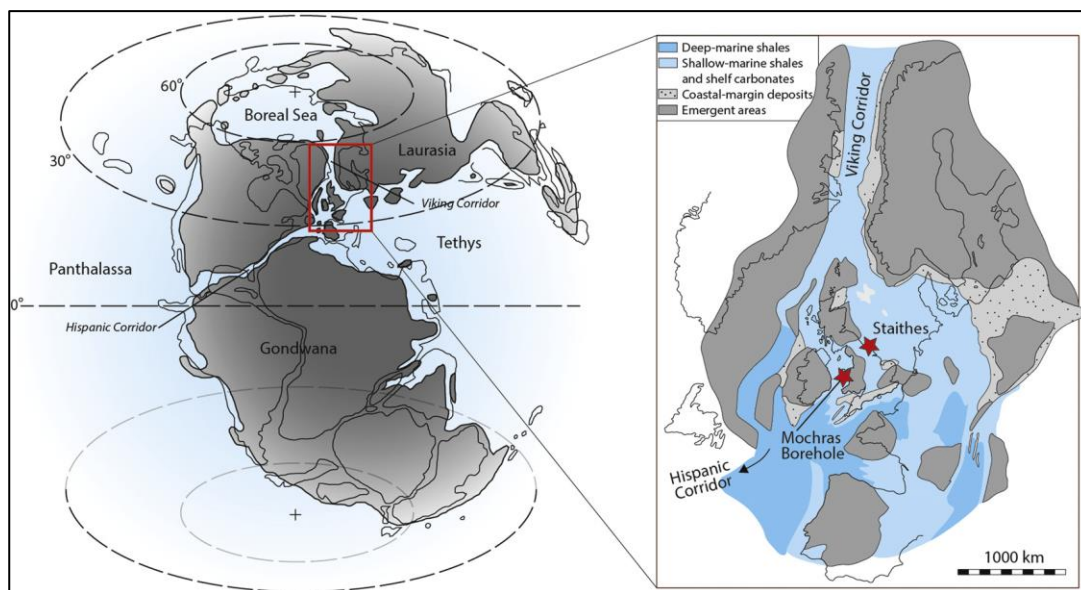


Fig 2.32. Early Palaeogeography based on the Mochras Borehole (Cardigan Bay Basin) and Staithes (Cleveland Basin) that are located with red stars (Ruhl *et al.* 2016).

Scotchman *et al.* (2016) indicated the presence of Hettangian to Sinemurian marine source rocks (Fig 2.29) in the Celtic Sea, Wytch Farm and Lusitania Basins. The absence of indicated source rocks on Figure 2.29 in the Western Approaches might be due to a lack of data, however. The presence of potential source rocks in the Lower Jurassic of the Western Approaches is a key focus of analysis in this thesis (Chapter 5). Scotchman (2001) also suggested that the Hettangian to Early Sinemurian age strata represent a potential Atlantic Margin source rock zone. Onshore in Dorset, the lower part of the Shales-With-Beef unit (*semicostatum* Zone – Early Sinemurian) is described as shaly and locally dark and has been shown to be TOC-rich (Hallam & Wignall, 2004).

2.6.2.3. Sinemurian to Pliensbachian

Tectonic Context

Korte & Hesselbo (2011) link the Early Jurassic with the deposition of deep water organic shales with an initial negative carbon isotope excursion (-2 ‰) in the Sinemurian to Pliensbachian. This negative carbon isotope excursion was followed by a later Late Pliensbachian positive excursion of (+2 ‰) with synchronous Late Pliensbachian cooling (Fig 2.33) indicated by Ruhl *et al.* (2016).

Lithostratigraphy

Scotchman (2001) and Scotchman *et al.* (2016) suggested the Sinemurian to Pliensbachian to represent another potential source rock interval of rich oil prone source rocks on the Atlantic Margin. Onshore in Dorset, Jenkyns *et al.* (2012) described Middle Sinemurian (*turneri* to *obtusum* Zone) black shales with some intercalated coarser clastics. Similarly in the Wessex Basin black shales (Lower Lias) of up to 100 m in thickness are described by Jenkyns *et al.* (2012), these are indicated as being composed of Type II kerogen composed of predominantly algal matter. Murphy *et al.* (1995) indicated that marine Sinemurian to Toarcian strata in the Celtic Sea have an average of 1% TOC which is lower than the overlying Toarcian strata. The kerogen type and TOC enrichment of the Sinemurian to Pliensbachian interval is analysed in the Chapter 5.

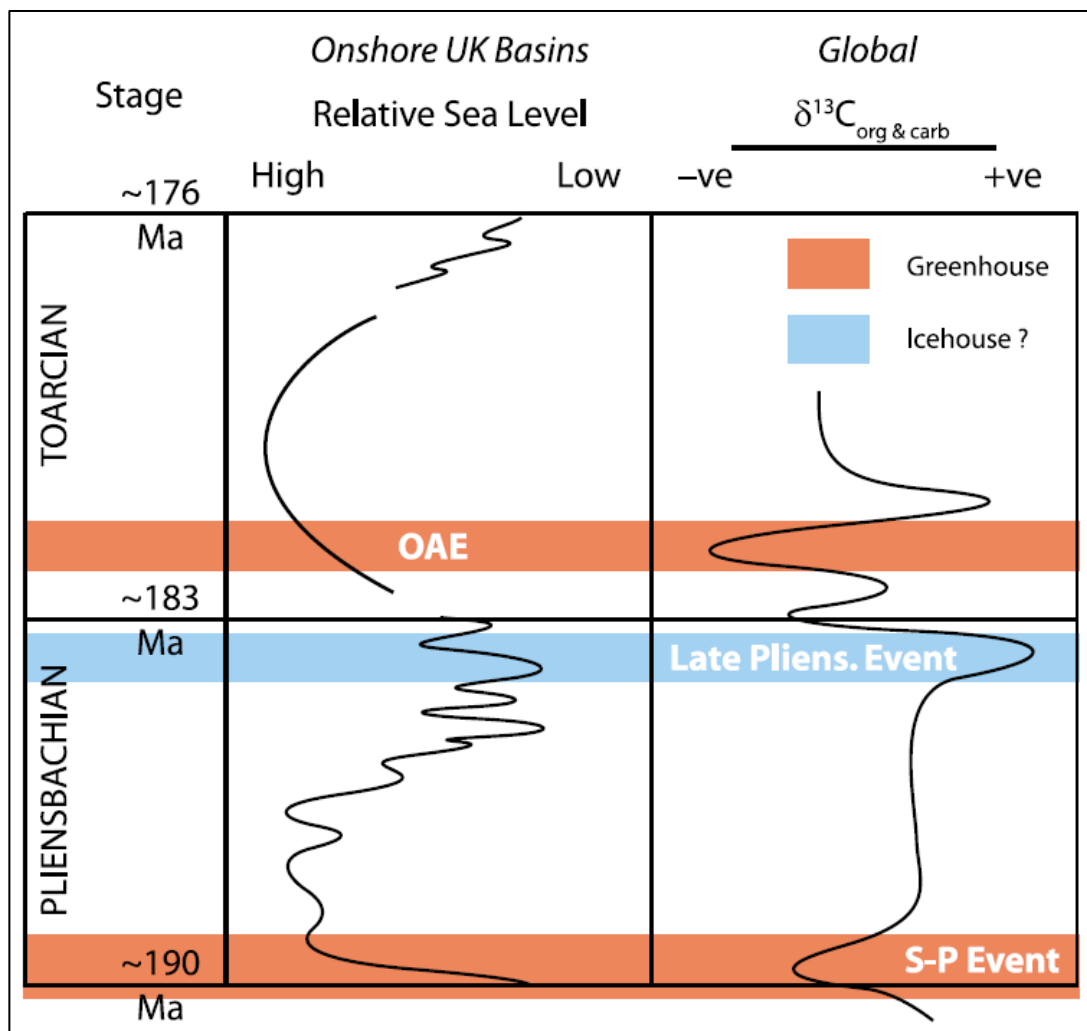


Fig 2.33. Cartoon summarising the change in relative sea level and $\delta^{13}C$ through the Pliensbachian and Toarcian (Korte & Hesselbo, 2014). OAE – Oceanic Anoxic Event, S-P Event – Sinemurian to Pliensbachian Event.

2.6.2.4. Toarcian

Tectonic Context

Scotchman (2001) has interpreted the Toarcian sequence to represent a rich, transgressive oil-prone source rock interval (Scotchman, 2001) deposited on a broad marine shelf (Murphy *et al.*, 1995). The Toarcian saw a change from the cooling of the Pliensbachian to greenhouse conditions (Fig 2.33 - Ruhl *et al.*, 2016).

Lithostratigraphy

Favourable conditions in the Toarcian led to global development of Lower Toarcian organic matter enriched shales with such facies indicated as well developed in the North Celtic Sea Basin (Murphy *et al.*, 1995). Similar Toarcian source rocks were deposited across NW Europe with organic matter-rich shales described within the *falciferum* Zone in Italy (Jenkyns & Clayton, 1986). In contrast to Figure 2.33., Murphy *et al.* (1995) indicates an overall relative rise in sea-level throughout the Early Jurassic reaching its maximum in the Toarcian with important deepening in the Celtic Sea and a change from argillaceous siliclastic or limestone deposition in the Pliensbachian to Earliest Toarcian to mudrock facies of the Lower Toarcian.

Summary

- The Early Jurassic was a time of predominantly thermal subsidence (Murphy *et al.*, 1995; Rowell, 1995; Woodcock & Strachan, 2012). In contrast Bulnes & McClay (1998) suggest Early Jurassic rifting in Celtic Sea Basins.
 - Early Jurassic rifting also occurred in the Lusitania Basin (Lundin, 2002).
- A potential Rhaetian to Earliest Hettangian sea-level rise might have occurred (Hillis, 1988; Hallam *et al.*, 2004).
- The Early Jurassic was a time of extreme climate change from glacial to greenhouse conditions (Korte & Hesselbo, 2011; Hesselbo *et al.*, 2013) has been linked to volcanic pulses from Large Igneous Provinces (Dera *et al.*, 2011).
- Deposition of widespread marine facies occurred offshore UK (Hillis, 1988; Murphy *et al.*, 1995) and was a key period of source rock deposition in Celtic Sea and Western Approaches (Howell & Griffiths, 1995).

- The marine penetration of rift basins took place in the Western Approaches from Tethyan and Central Atlantic Oceans in the South and Boreal Marine Realm in the North (Jenkyns & Clayton, 1986; Scotchman *et al.*, 2016; Ruhl *et al.*, 2016).

2.6.3. Middle Jurassic

Tectonic Context

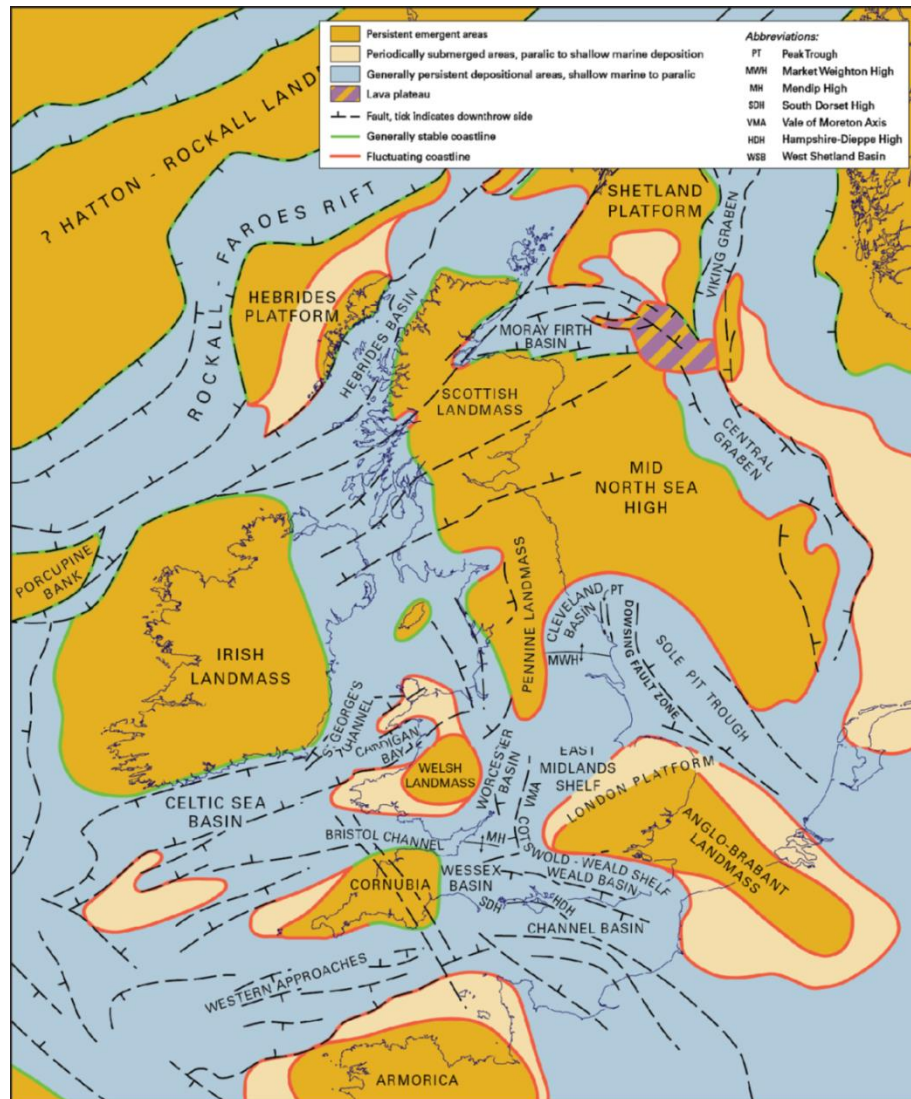


Fig 2.34. Palaeogeographic reconstruction for the Middle Jurassic of the British Isles (Baron *et al.*, 2012).

The Middle Jurassic strata of SW Britain record an early Aalenian to Bathonian fall in sea-levels with the potential for increased siliclastic input on a shallow marine shelf (Fig 2.34). This regression was followed by a marine transgression from the Bathonian to the Callovian (Scotchman, 2016), represented by widespread deposition of limestones (Baron *et al.*, 2012). Underhill and Partington (1993) related terrestrial conditions in the Central North Sea to regional updoming. The extent of doming is suggested to be limited to the North Sea

(Fig 2.34 – Baron *et al.*, 2012) and therefore unlikely to have affected the SW of England. Scotchman *et al.* (2016) suggested that there was widespread marine withdrawal from the Atlantic Margin rift basins with restriction between the Tethyan and Boreal Marine Realms. The Middle Jurassic was also associated with an increase in spreading rates for the Central Atlantic (Labails *et al.*, 2010), which could have affected sea-levels offshore Britain as a better connection was established between the Central Atlantic and Neotethys.

Lithostratigraphy

In the UK Sector of the Western Approaches, the Middle Jurassic has been removed by the Top M2 Unconformity (Hillis, 1988; Chapman, 1989). Hillis (1988) described Middle Jurassic sediments preserved in the French sector of the Western Approaches. 187 m of dolomite is present in Lenkett-1 (Fig 2.1) compared to calcareous mudstones of the Brittany Basin from the early Middle Jurassic that were deposited in a tranquil shelf environment (Hillis, 1988) similar to that suggested in Figure 2.26. Regressive sequences have been described in other wells in the Western Approaches with Lizenn-1 (Fig 2.1) showing increased layers of sandstone interbedded in the mudstones (Hillis, 1988).

Similar shallowing has been seen in the Celtic Sea (Van Hoorn, 1987) with a Bathonian to Bajocian unconformity present onshore in the Wessex Basin (Tucker & Arter, 1987). Onshore Dorset, the Oxford Clay of the Middle Callovian to Early Oxfordian in the *athleta*, *coronatum* and *jason* Zones is suggested to be organic matter-rich (Jenkyns *et al.*, 2002). Kamerling (1979) describes Early and Middle Jurassic sediments as being predominantly grey, calcareous marine shales with interbedded limestones and sandstones to the East in the UK Sector.

Summary

- A major marine regression from the Aalenian to Bathonian occurred in the SW of Britain (Baron *et al.*, 2012; Scotchman, 2016) with Underhill and Partington (1993) proposing updoming of the Central North Sea.
- This was followed by marine transgression and deposition of limestones in the Bathonian and Callovian (Baron *et al.*, 2012) and formed reservoir rocks in the Dragon Discovery.

- While the Central Atlantic began to open during the Sinemurian stage spreading rates were initially slow and it was not until the Early Bajocian that the speed of opening increased (Labails *et al.*, 2010).

2.6.4. Late Jurassic

Tectonic Context

The key tectonic events in the Late Jurassic for the SW of Britain and the region of interest are the renewal of rifting in Western Approaches and Celtic Sea, regional uplift and exhumation, and the initiation of rifting of Iberia away from the Brittany and the southern Western Approaches which led to the opening of the Bay of Biscay. Deepening of the Mesozoic basins continued in the Late Jurassic with active rifting in the region of interest (Rowell, 1995; McMahon & Turner, 1998). Chapman (1989) suggested that rifting due to sinistral transtension led to the Late Jurassic basin margins in the Melville Basin extending beyond the original Permian-Triassic basin extents.

Synchronous with rifting and regional uplift in the region of interest, sinistral transtensional rifting began in the future Bay of Biscay (Tugend *et al.*, 2014) with rifting utilising the Hercynian North Pyrenean Fault (Visser *et al.*, 2016; Lundin & Dore, in press) to allow Iberia to move as a microcontinent with respect to Eurasia (Jammes *et al.*, 2009). It seems likely that rifting in the UK Sector was related to the strain imparted on the continental crust by the movement of this Iberian microcontinent (Fig 2.36). Hillis (1988) suggested that the Western Approaches underwent a competition between active rifting and regional uplift. Sediment deposition occurred in the deepening rift basins with erosion of the basin margins.

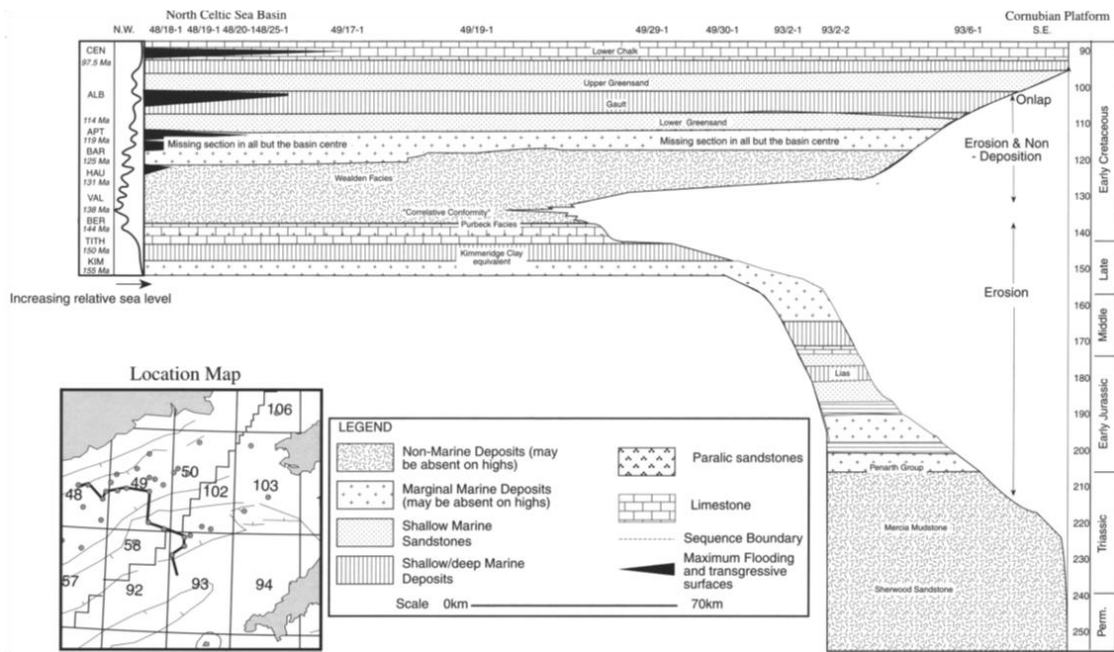


Fig 2.35. A chronostratigraphic correlation diagram from McMahon & Turner (1998) showing a correlative Berriasian age for the Top M2 Unconformity.

Top M2 Unconformity

The Top M2 unconformity, often termed the “Cimmerian” in the literature led to the absence by removal or non-deposition of most of the Jurassic sequence in the Melville Basin (Hillis, 1988; Chapman, 1989) and the South Celtic Sea Basin (Kamerling, 1979; McMahon & Turner, 1998). The distribution of the Lower Jurassic preserved is shown in Figure 2.31. The unconformity is well developed in the Fastnet, South Celtic Sea, Melville, Plymouth Bay and Bristol Channel basin but absent in the Brittany Trough and South West Channel Basin and only poorly developed in the North Celtic Sea Basin (Hillis, 1988). Figure 2.31 shows the Top M2 Unconformity truncating the underlying Early Jurassic, Triassic and Permian sequence in the Melville Basin. Hillis (1988) and Ruffell (1995) indicated uplift of ~0.7 km in the location of well 73/13-1 suggesting that a similar thickness of Middle to Upper Jurassic strata have been eroded (Section 5.3.2). In contrast Ottaviani *et al.* (unpublished work) suggested that up to 2.8 km of uplift occurred in the Melville Basin which would suggest the removal of a significant sequence of Jurassic strata (Section 5.3.2).

It is the Top M2 Unconformity event that controls the preservation of the Lower Jurassic in the Melville Basin with the Lower Jurassic preserved only in the north and south of the basin (Fig 2.31). Chapman (1989) suggested that the unconformity occurred between the Early Jurassic and Berriasian while Hillis (1989) believes the unconformity to vary in age

regionally. McMahon & Turner (1998) utilised chronostratigraphic data for the Celtic Sea Basins and the Western Approaches and suggest a correlative age of the Berriasian for the Top M2 Unconformity (Fig 2.35). The Top M2 Unconformity and its control on the removal of potential Jurassic strata will be discussed further in Section 6.3.

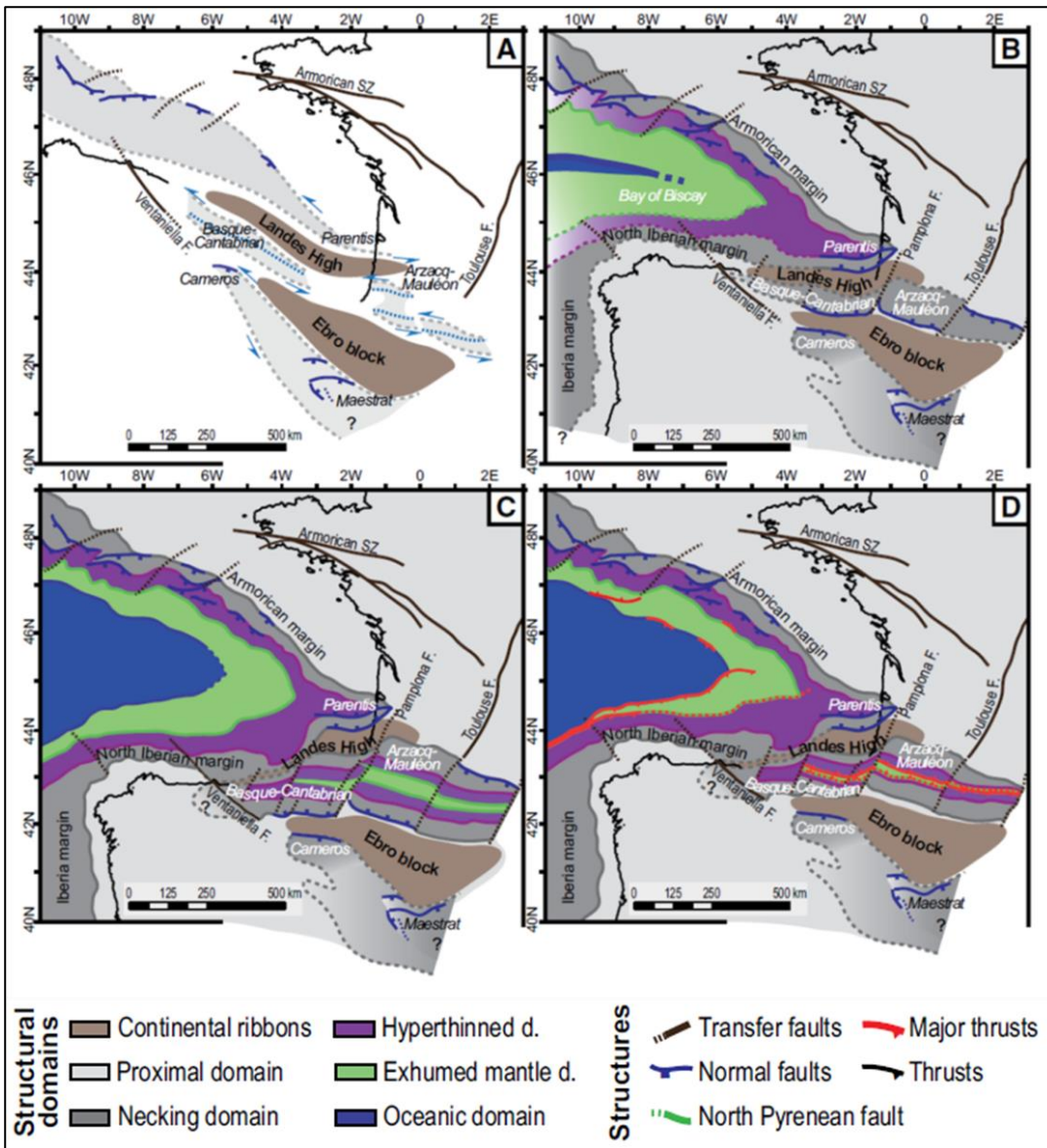


Fig 2.36. Restoration demonstrating the development of the Iberian-European Plate Boundary (Tugend *et al.*, 2014). A: Initial stage of transtensional rifting in the Late Jurassic. B: Start of sea floor spreading in the Aptian to Albian. C: Failed localisation of the plate boundary prior to the Santonian. D: Start of subduction in the Late Cretaceous.

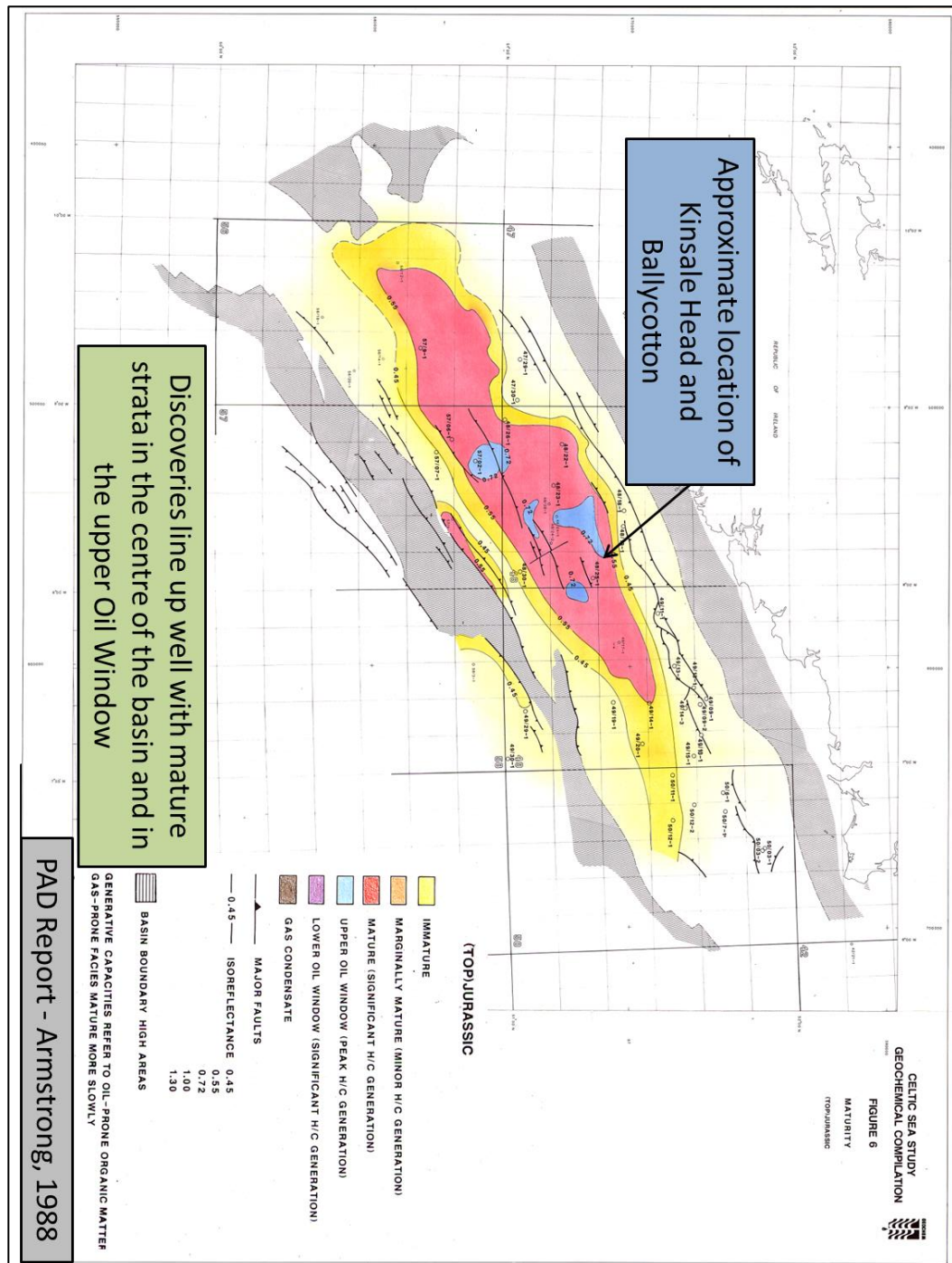


Fig 2.37. Map of maturity for the North Celtic Sea Basin for the top Jurassic with highest maturity indicated in the basin centres (Armstrong, 1988).

Lithostratigraphy

In the SW Channel Basin, Tithonian calcareous sandstones and shales with interbedded anhydrite are preserved. Similar Upper Jurassic sedimentary rocks are preserved in the Brittany Basin and in areas of the South Celtic Sea, Bristol Channel Basin and Fastnet Basin (Hillis 1988). These sediments were deposited in a shallow marine to brackish and freshwater environment with the layers of anhydrite indicating periodic emergence and

evaporation (Hillis 1988). Only on the current continental shelf are open marine sediments present with reefal and peri-reefal limestones from the Tithonian and Kimmeridgian.

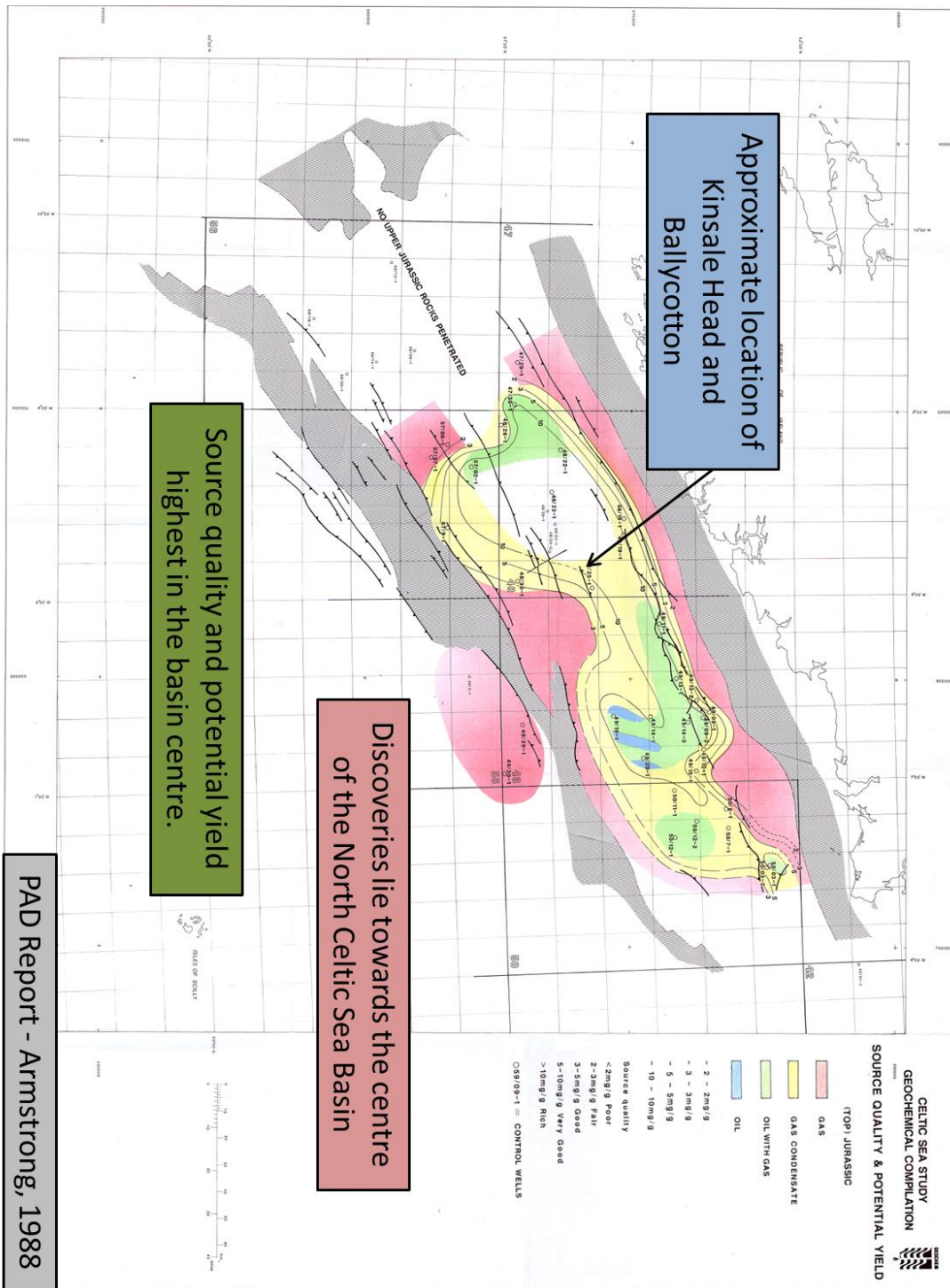


Fig 2.38. Map of source rock quality and potential yield for the North Celtic Sea Basin for the top Jurassic with (Armstrong, 1988).

In the Irish Sector of the North Celtic Sea Basin, Murphy *et al.* (1995) inferred the deposition of organic matter-rich lacustrine to estuarine claystones (Caston, 1995) from the Kimmeridgian to the Berriasian. Armstrong (1988) suggested there was limited erosion

during the Late Jurassic to Early Cretaceous in the North Celtic Sea Basin with a shallow marine depositional environment characterised by sandstones, shales and limestones. Overall, the Late Jurassic appears to have been associated with deposition in a widespread anoxic environment (“Purbeck facies”). These sediments show a wide range of source facies and demonstrate both increasing maturity and source rock quality to the axial regions of the basin (Fig 2.37 & 2.38).

Greenhalgh (2016) described the Upper Jurassic sediments of the Wessex Basin in detail. Here, the Oxford Clay is comprised of a dark, fossiliferous and fissile shale, which was deposited in a dysoxic environment (Peterborough Member) and lean, grey calcareous shales (Stewartby and Weymouth Members). The Corallian is a sequence of cyclic shallow marine sandstones, mudstones and limestones suggested by Greenhalgh (2016) as having been deposited on a ramp style margin. The Kimmeridge Clay is interpreted as having been deposited in an anoxic environment with four mudstone zones with minor siltstones and limestones. The environment is suggested to be epicontinental shelfal.

Jenkyns *et al.* (2002) described equivalent lithologies onshore in Dorset, with the Blackstone Band having TOCs in excess of 50% in parts. Tyson (2004) identified a symmetrical pattern of TOC enrichment within Upper Jurassic sediments in Dorset with TOCs of 1-2% at the base and top of the Kimmeridge Clay Formation and 8-9% in the centre. Tyson (2004), however, does not state the thickness over which this variation occurred. Tyson (2004) describes a direct correlation between the source rock richness and terrestrial input suggesting dilution was the main control on source rock quality.

Summary

- Late Jurassic strata were truncated by the top Megasequence 2 unconformity in the Western Approaches and South Celtic Sea Basin (Kamerling, 1979; Hillis, 1988; Chapman, 1989).
- Initiation of Bay of Biscay rifting occurred in the Late Jurassic to Early Cretaceous (Tugend *et al.*, 2014; Lundin & Dore, in press).
- Decrease in $\delta^{18}\text{O}$ was likely due to increased intensive magmatism in the Karoo-Ferrar LIP & NE Asian Igneous Provinces (Dera *et al.*, 2011).
- Peak marine high stand sea levels occurred in the Kimmeridgian stage (Scotchman *et al.*, 2016).

- High levels of CO₂ (four times current levels) with plant productivity concentrated at mid-latitudes and coals and evaporites are common at lower latitudes (Selwood & Valdes, 2006).
- The deposition of potential source rock facies occurred in SW Britain with Middle to Upper Jurassic lacustrine to estuarine source rocks present in the Irish Sector of the North Celtic Sea Basin (Jenkyns *et al.*, 2012; Tyson, 2014; Scotchman *et al.*, 2016; Greenhalgh, 2016).
- Late Jurassic to Early Cretaceous rifting, potential doming and regional uplift occurred in the Western Approaches and Celtic Sea (Van Hoorn, 1979; Hillis, 1988; Chapman, 1989; Murphy *et al.*, 1995).

2.7. Cretaceous to Cenozoic - Megasequence 3

Tectonic Context

Opening of the Central Atlantic started during the Jurassic (Section 2.6) but it was not until the Cretaceous that the Atlantic opened in the form recognisable today with the initial opening of the South Atlantic and Late Cretaceous separation of Greenland and Eurasia (Woodcock and Strachan, 2012). The rotation of Iberia away from southern Britain continued (Scotese, 2001; Tugend *et al.*, 2014; Lundin & Dore, In Press) with the eventual development of a deep shelf in the Bay of Biscay and sea floor spreading (Fig 2.36 & 2.39). Sibuet *et al.* (2017) estimated the extension between Iberia and Eurasia from the Late Jurassic to Early Aptian to be 350 km and proposed the existence of a marine connection between the region of interest and the Neo-Tethys to the southeast. Ziegler (1987a) suggested that crustal separation in the Bay of Biscay was associated with a major, Middle Aptian phase of wrench deformation evident in the Celtic Sea and Western Approaches. Lundin & Dore (In Press), however, argued that Late Cretaceous inversion of the rift system between Eurasia and Iberia occurred as subduction initiated subsequent to Iberia locking onto the African Plate (Tugend *et al.*, 2014).

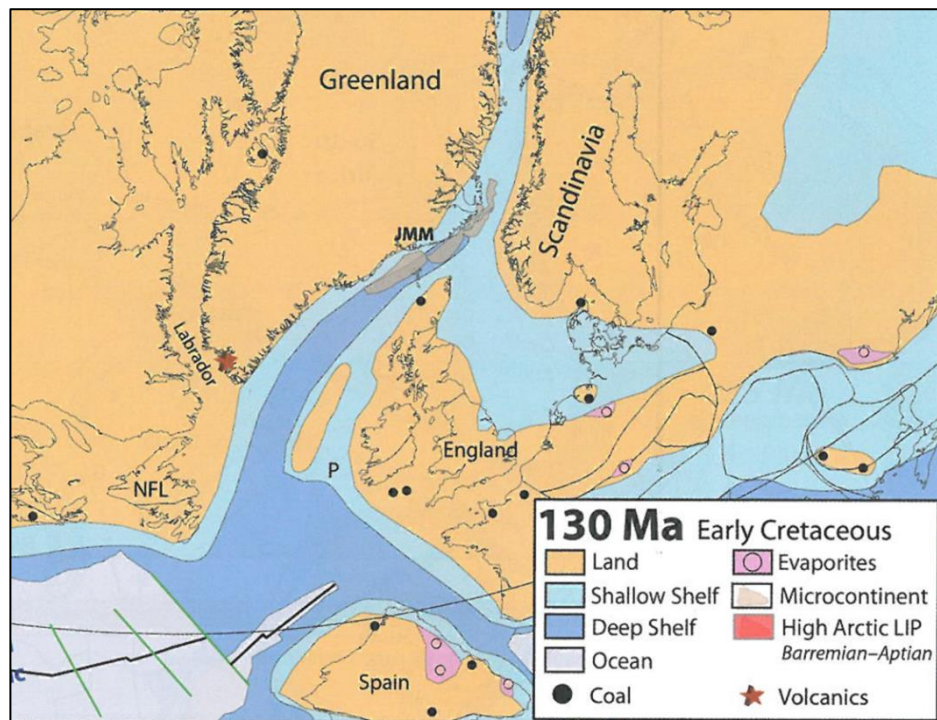


Fig 2.39. Palaeogeographic reconstruction of the present-day North Atlantic margins during the Early Cretaceous with much of the SW of Britain indicated to be in a continental setting (Torsvik & Cocks, 2017). JMM – Jan Meyen Microcontinent, NFL – Newfoundland, P – Porcupine Bank.

Lithostratigraphy

Following the end of Early Cretaceous rifting, the Celtic Sea and Western Approaches underwent a period of relative stability during which time the basins experienced thermal subsidence (Rowell, 1995). The deposition of clastics occurred in the South Celtic Sea Basin in a continental setting which changed into a marine setting as sea-levels rose (Bulnes & McClay, 1998). Wealden sediments (Valangian to Barremian) are present in the Western Approaches as a thin section overlying the Top M2 unconformity (Chapman, 1989).

In the North Celtic Sea Basin, Wealden sediments represent an argillaceous section with occasional coals (Armstrong, 1988). Armstrong (1988) indicates the Lower Cretaceous coals to have low Hydrogen Index values but are rich if immature sources for gas. The Wealden of the North Celtic Sea sediments are overlain by the Aptian to Albian Greensands/Gault. The Lower Cretaceous Greensand Formation comprises the primary producing reservoir of the North Celtic Sea Basin and is made up of marine glauconitic sandstones and mudstones which vary in thickness from 35-100 m (Melvin, 2005). The formation passes into distal marine shales to the south west and is overlain by the marine Gault shales (Fig 2.40).

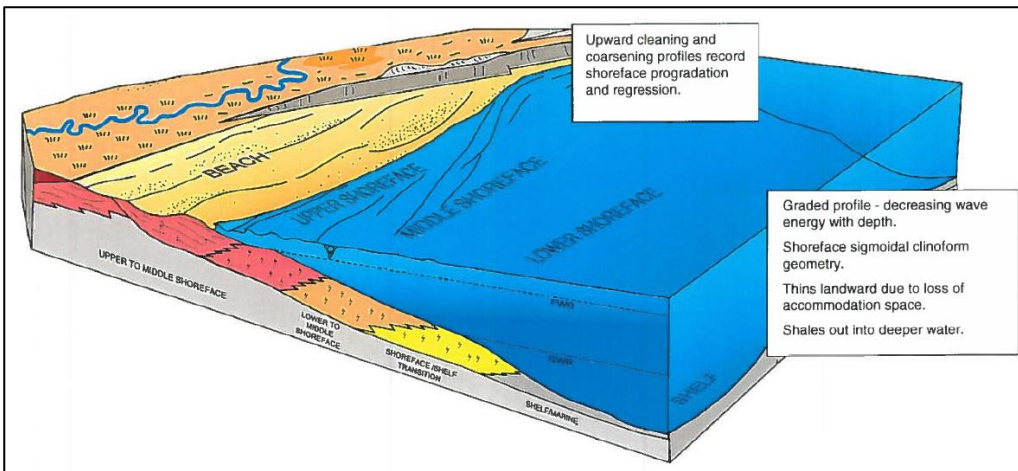


Fig 2.40. Schematic diagram demonstrating the likely deposition environment of the Early Cretaceous Greensand in the North Celtic Sea Basin (Melvin, 2005).

The Upper Cretaceous succession is characterised by the presence of thick marine limestones/chalk of the Celtic Sea (Rowell, 1995) that are truncated to the top by the Alpine Unconformity. Bulnes & McClay (1998) indicate the thickness of the Upper Cretaceous chalk in the South Celtic Sea Basin to be latitudinally variable (300 in the south to 800 in the north m) due to erosion with no change along NNW-SSE strike. The Western Approaches similarly to the Celtic Sea Basins underwent the widespread deposition of chalk/limestone sediments in the Late Cretaceous with pelagic facies deposited off the continental shelf (Hillis, 1988).

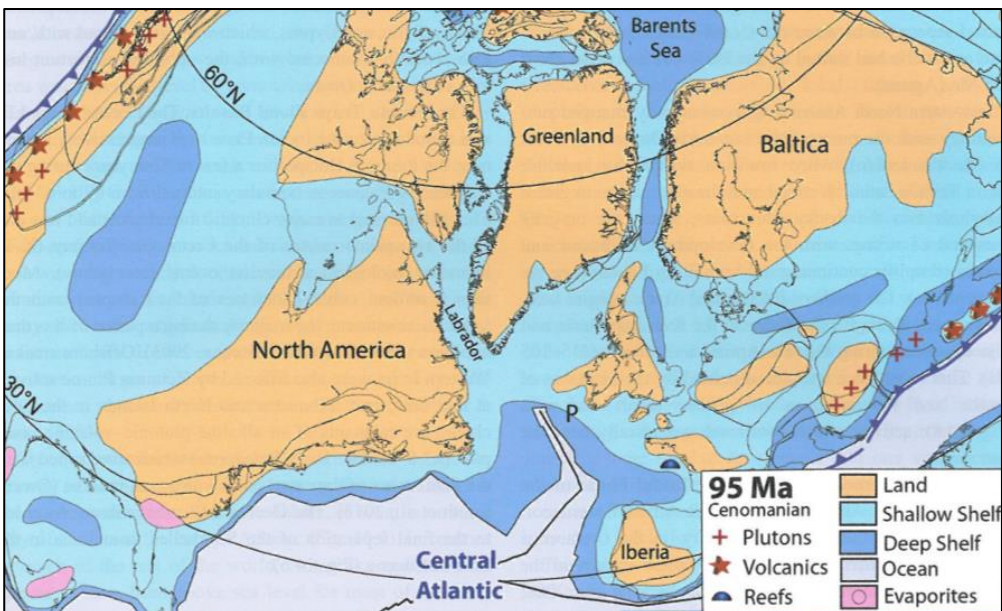


Fig 2.41. Palaeogeographic reconstruction for the Cenomanian (Torsvik & Cocks, 2017) with the Celtic Sea and Western Approaches located in a shallow shelf environment which leads to the widespread deposition of limestones/chalk. P – Porcupine Bank.

The climate of the Cretaceous was variable as it spanned such a long period of time. Most of the Cretaceous was warmer than average Phanerozoic temperature with a peak of temperatures in the Turonian (90 Ma). It was not until 70 Ma that the Earth became much cooler (Torsvik and Cocks, 2017) with the highest sea levels in the Phanerozoic during the Late Cenomanian (95 Ma). Torsvik and Cocks (2017) suggested that large parts of the continents were submerged and characterised by shallow shelf environments at this time, giving rise to the deposition of the Upper Cretaceous chalk/limestone sequence (Fig 2.41).

Armstrong (1988) discussed the source rock potential of the Cretaceous sequence in the Celtic Sea region with the potential for rich gas source rocks in the coals of the Wealden. The Wealden coals have low HI values but are highly enriched in TOC (>50 %). The Wealden argillaceous sediments have TOC values of 0.95-4.2 % TOC which indicate fair to very good source rock richness. The Cretaceous sequence is indicated by Armstrong (1988) based on VR analysis (0.33% R_o) as being immature for hydrocarbon generation.

Summary

- The Bay of Biscay continued to open with seafloor spreading initiated by the Aptian-Albian (Tugend *et al.*, 2014; Lundin & Dore, in press).
- Rifting in the Celtic Sea and Western Approaches had terminated by the end of the Early Cretaceous with deepening of the basins by thermal subsidence (Hillis, 1988; Chapman, 1989; Rowell, 1995).
- Deposition of continental argillaceous sediments and coals of the Wealden took place in the Celtic Sea with widespread deposition of Upper Cretaceous limestone/chalk (Hillis, 1988; Rowell, 1995).

2.8. Paleogene to Recent - Megasequence 4

Tectonic Context

The collision of the African and Eurasian plates initiated the Alpine Orogeny during the Paleogene. The eruption of the North Atlantic Igneous Province (linked to the potential Iceland plume) also started in the Paleogene from 63 Ma. Global temperatures increased in the Late Paleogene and peaked during the Palaeocene-Eocene Thermal Maximum (PETM). The PETM resulted in a sharp negative excursion in oxygen, nitrogen and carbon isotopes (Torsvik & Cocks, 2017). The Eocene saw cooling with Antarctic glaciation in the Late Eocene (Torsvik & Cocks, 2017). The Neogene and Quaternary periods were dominated by tectonic events such as the Alps, Himalayan and western American orogenic events. The climate during this interval was dramatically changed by the Pliocene to Pleistocene glaciation which has yet to terminate (Torsvik & Cocks, 2017).

Cenozoic Uplift and Inversion

The story of the Cenozoic in the Western Approaches and Celtic Sea is predominantly one of uplift, erosion and basin inversion related to Alpine and Pyrenean compression (Blundell, 2002; Anell *et al.*, 2009) with some sedimentation due to variations in eustatic sea level and regional subsidence (Hillis, 1988). Holford *et al.* (2005) has used apatite fission track analysis in combination with vitrinite reflectance data from the Irish Sea to describe two periods of regional uplift in the Early Palaeogene and Late Palaeogene-Neogene. In the South Celtic Sea Basin and Bristol Channel Basin inversion produced WNW trending folds and reactivation of extensional faults is described by Glen *et al.*, 2005.

Figure 2.43 demonstrates the amount of Cenozoic uplift estimated by Menpes and Hillis (1995) with the Meville Basin undergoing only 0.2-0.6 km uplift in contrast to 0.6-1.2 km in the North and South Celtic Sea Basins. In addition uplift in the eastern Western Approaches is estimated to be between 0.6-1.0 km.

In the North Celtic Sea Basin and South Celtic Sea Basin, widespread Palaeocene to Eocene inversion has been proposed by Tucker & Arter (1987) and Bulnes & McClay (1998). The presence of undeformed Middle-Upper Eocene and Oligocene sediments suggests termination of inversion before the Middle Eocene. Inversion occurred with the pre-existing normal faults being reactivated with reverse movement (Tucker & Arter, 1987; Bulnes & McClay, 1998; Blundell, 2002; Glen *et al.*, 2005). The North Celtic Sea Basin saw the upwarping of the main Cretaceous depocentre (Fig 2.42 - Tucker & Arter, 1987) with the development of anticlines and flower structures (Byrne, 2014).

Cenozoic inversion and uplift is significant as the removal of strata will lead to a lower degree of maturity relative to the similar strata that have undergone continuous burial. Burial history models demonstrating the implications of Cenozoic uplift are described and discussed in Section 5.3.2. The erosion of potential source rocks strata during the Cenozoic could also have a significant impact on the source rock potential of the region of interest.

Lithostratigraphy

The Western Approaches has a relatively thick Cenozoic sequence (up to 1500 m thick) of mudstone, limestones and sandstones punctuated by multiple hiatuses in deposition that vary in time period and lateral extent (Hillis, 1988). This succession is in contrast to the Tertiary strata of the Bristol Channel Basin and South Celtic Sea Basin, which are only thinly developed (Van Hoorn, 1986), with a clastic succession that thins from 300 m thickness in the north to 75 m in the south with onlap onto the Cretaceous unconformity (Bulnes & McClay, 1998).

In the North Celtic Sea Basin, an intra-Tertiary unconformity separates Middle-Late Eocene sediments from overlying undeformed Oligocene sediments. The Bristol Channel Basin only has Quaternary sediments of uneven thickness which lie on shallowly dipping Early Jurassic sediments in the central part of the basin (Evans & Thompson, 1979). These sediments are interpreted to be Holocene silts deposited in a marine setting.

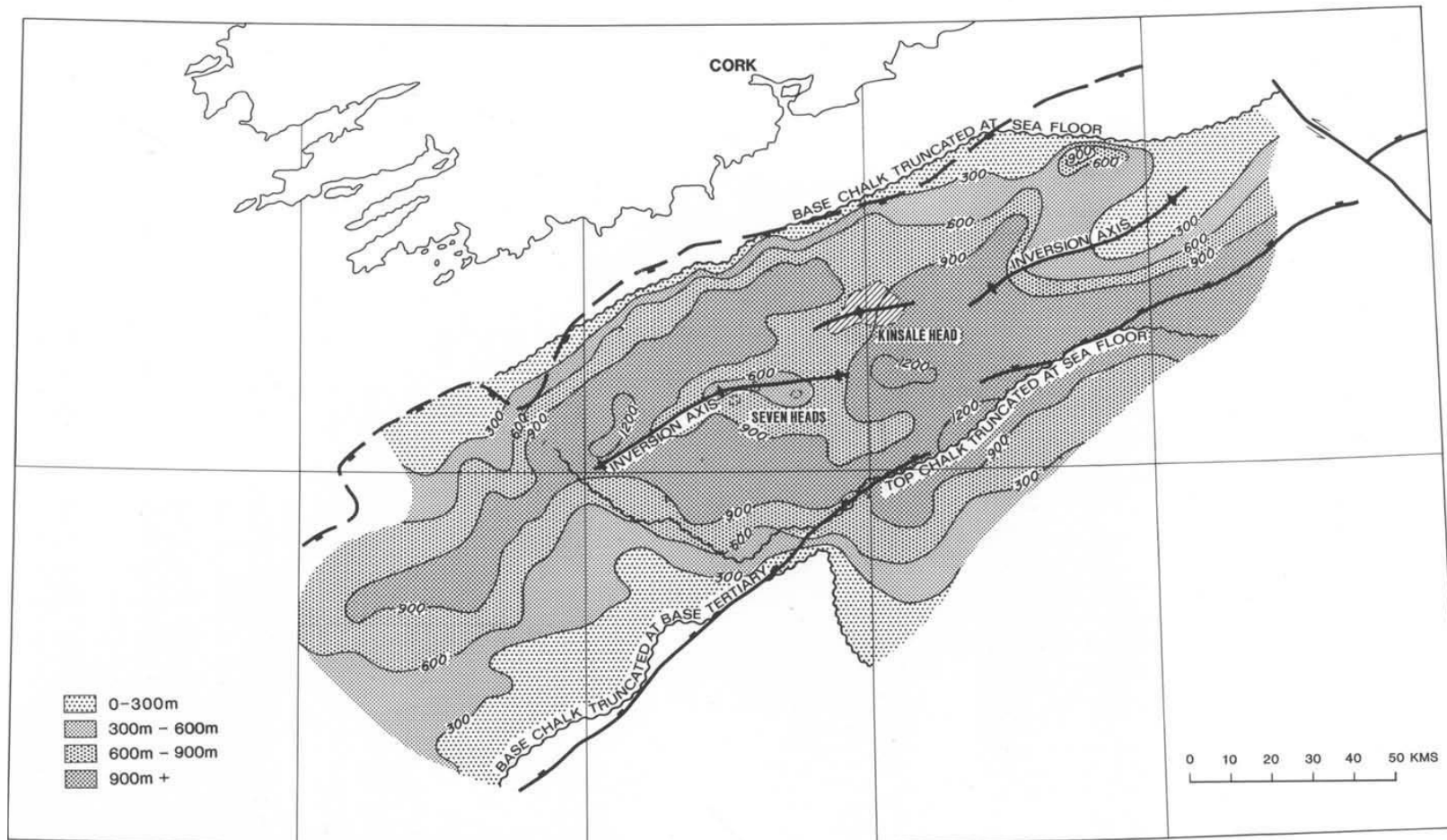


Fig 2.42. Late Cretaceous Chalk regional isopach map (Tucker & Arter, 1987) with the basin inversion axis shown and truncation of the chalk towards the basin margins.

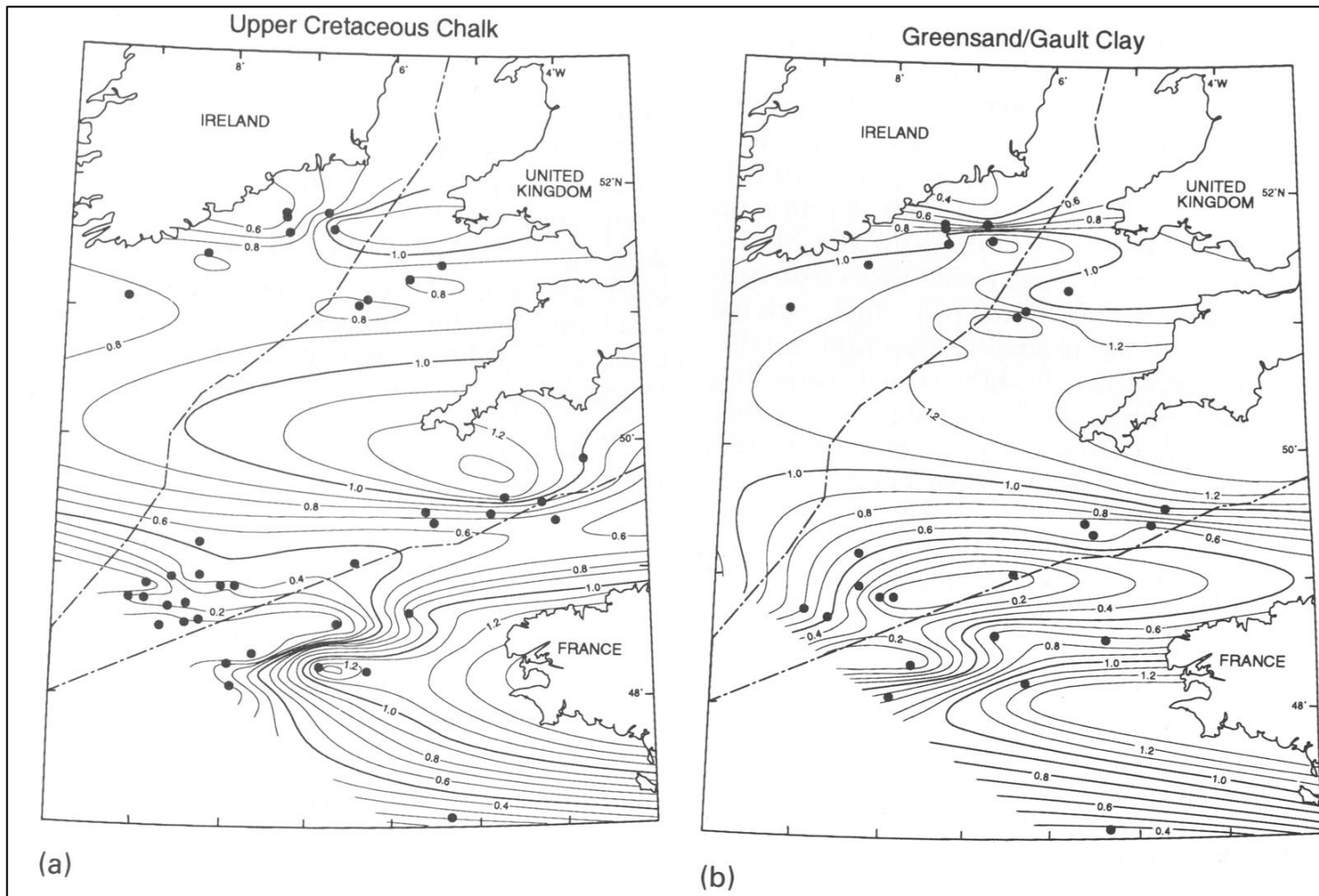


Fig 2.43. Maps of apparent exhumation: (a) the Upper Cretaceous Chalk, (b) Lower Cretaceous Gault/Greensand with the contours labelled in kilometres (Menpes & Hillis, 1995).

Summary

- The initiation of the Alpine Orogeny occurred during the Paleogene with uplift and hiatuses in the Celtic Sea and Western Approaches Basins (Van Hoorn, 1986; Hillis, 1988; Murdoch *et al.*, 1995) followed by minor thermal subsidence (Rowell, 1995).
- Large scale inversion of pre-existing structures occurred in the North Celtic Sea Basin (Van Hoorn, 1986; Tucker & Arter, 1987; Rowell, 1995; Bulnes & McClay, 1998; Glen *et al.*, 2005; Byrne, 2014).

2.9. Summary of Palaeogeography and Tectonostratigraphic Framework

- The Mesozoic basins of the Western Approaches and Celtic Sea were formed due to rifting in the Permian to the Triassic which utilised pre-existing Caledonian and Variscan fabrics.
- There is source rock potential in the Culm Coal Measures where they underlie the rift basins and were protected from overmaturity.
- Thermal subsidence in the Early Jurassic led to the development of multiple zones of source rock that are potentially preserved in the isolated deep rift basins.
- Upper Jurassic source rocks of predominantly lacustrine or lagoonal facies developed in the Irish Sector of the North Celtic Sea Basin but maturity is a potential issue.
- Removal of large sections of the Jurassic sequence in the Western Approaches and South Celtic Sea Basin due to uplift and erosion occurred during the Late Jurassic to Early Cretaceous (Top M2 Unconformity).
- Some source rock potential in the Lower Cretaceous with argillaceous shales and gas-prone coals but unlikely to have reached maturity in any basin.
- Widespread uplift in the Western Approaches and Celtic Sea region and inversion in the Celtic Sea Basins took place in the Early Cenozoic.

Chapter 3

Regional Drilling History Summary

3. Regional Drilling History Summary

The aim of this chapter is to provide an overview of the drilling history for the region of interest followed by a discussion of 103/01-1 which is the only well to have appraised hydrocarbon shows.

3.1. Introduction

The primary reason for drilling an exploration well is to find economic quantities of hydrocarbons in producible reservoirs with appraisal wells drilled later to identify the extents and properties of a discovery. In true frontier regions exploration wells can also be drilled to research the biostratigraphy and geology of a region such as well 93/02-1 which was drilled in 1974 (Table 3.1). The Western Approaches (UK Sector) and the Celtic Sea went through its peak of exploration in the 1970s and early 1980s with 30 of the 37 wells drilled (including respudded wells) in the region in the ten year period between 1973 and 1983. Drilling rates decreased after this peak with five wells drilled in the South Celtic Sea Basin and the Melville Basin between 1986 and 1991. In 1994 the Dragon Discovery was drilled by 103/01-1 as a gas discovery and then appraised in 2005 by the final well drilled in the region (103/01a-2).

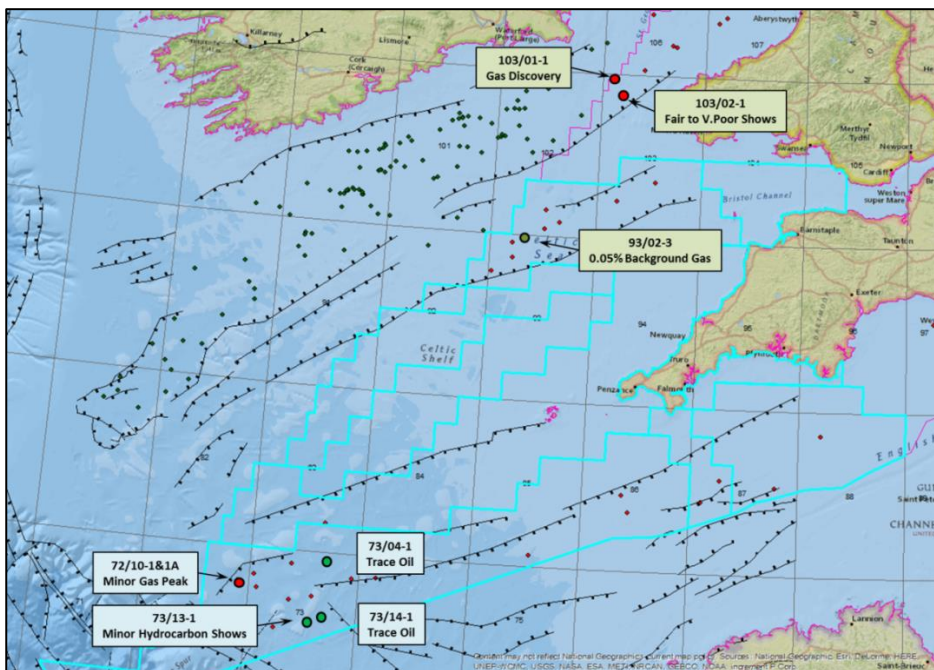


Fig 3.1. Map of gas and oil shows in the Celtic Sea and Western Approaches.

GTO published a flyer (GTO, accessed 2017) on the French Sector which indicates that French exploration started earlier in 1975 and peaked between then and 1981 with 10 exploration wells drilled in the region abutting the UK Sector (Fig 3.2). Only two more are

indicated as having been drilled later (1985 and 2003). Hydrocarbon shows are indicated in many of the wells in the French Sector. There have been no hydrocarbon shows reported in the Irish Sector of the South Celtic Sea Basin (Celtex S Report).

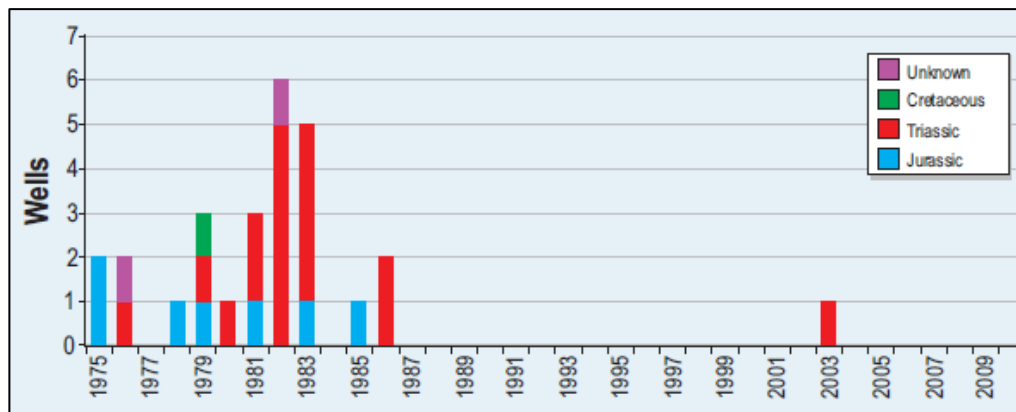


Fig 3.2. Histogram showing the targets for the wells drilled in the French Sector of the Western Approaches with the majority of exploration focused on the Jurassic and Triassic intervals (GTO, accessed 2017).

3.1.1. Celtic Sea

The North Celtic Sea Basin (NCSB) lies predominantly in the Irish Sector and only three wells have been drilled in the UK Sector (Table 3.1). The Dragon Discovery represents the only discovery in the region of interest. In 1976, 103/02-1 was to test Triassic Bunter sandstones with a secondary objective of the Middle Jurassic sandstones but all intervals of interest were water wet (Allen, 1977). In 1994, Marathon Oil Plc drilled 103/01-1 to test the Jurassic Dragon Discovery and encountered gas-bearing Middle Jurassic sandstones (Marathon P804 Relinquishment Report). In 2005, 103/01a-2 was drilled to appraise the continuity of the gas-bearing sandstones but discovered the prospective reservoirs to be water bearing (Marathon P804 Relinquishment Report).

The South Celtic Sea Basin (SCSB), in contrast to the North Celtic Sea Basin (NCSB), extends a significant distance into the UK Sector with nine wells (Table 3.1) drilled in three prospective blocks (93, 102 & 103). While limited information is available on the primary and secondary objectives for all of these wells; objectives indicated range from the Early Cretaceous to the Triassic Sherwood Sandstone but were all discovered to be water wet. 93/02-3 (Houchen *et al.*, 1991) indicated background gas values of 0.05% over an interval of 4650 ft (1417 m) but aside from this potential show no indications of hydrocarbons have been noted in any of the drilled wells. In addition the background gas in 93/02-3 could be sourced from one location in the openhole rather than the entire section.

Well Name	Spud Date	Well Type	Well Class	Hydrocarbon Shows	Primary Objective	Secondary Objective(s)
North Celtic Sea Basin						
103/01-1	19/07/1994	Exploration	Gas Well	Number of gas bearing Middle Jurassic Ssts	Middle Jurassic (Bajocian)	Triassic Sherwood Sst
103/01a-2	17/09/2005	Appraisal	Dry Hole	Middle Jurassic Water wet	Middle Jurassic	
103/02-1	12/11/1976	Exploration	Dry Hole	Fair to V.Poor (2210-2660 ft) - All zones Water wet	Triassic Bunter Ssts	Middle Jurassic Ssts
South Celtic Sea Basin						
93/02-1	24/03/1974	Exploration	Dry Hole	No Hydrocarbon Shows	Stratigraphic Test Well	
93/02-2	06/04/1986	Exploration	Dry Hole	No Hydrocarbon Shows Indicated		
93/02-3	31/07/1989	Exploration	Dry Hole	0.05% background gas (2600-7250ft) - Water wet	Triassic Sherwood Sst	
93/06-1	30/07/1977	Exploration	Dry Hole	No Hydrocarbon Shows Indicated		
102/28-1	21/06/1973	Exploration	Dry Hole	No Hydrocarbon Shows Indicated		
102/28-2	02/02/1991	Exploration	Dry Hole	No Hydrocarbon Shows	Lower Triassic Sherwood Sst & Lower Cretaceous Wealden Ssts	
102/29-1	10/07/1977	Exploration	Dry Hole	No Hydrocarbon Shows - Water wet	Lower Jurassic	Lower Cretaceous Wealden/Greensand
103/18-1	08/11/1976	Exploration	Dry Hole	No Hydrocarbon Shows	Middle-Lower Jurassic Limestones	Triassic
103/21-1	13/06/1976	Exploration	Dry Hole	No Hydrocarbon Shows Indicated		

Table 3.1. Well information from composite logs and well reports for the North and South Celtic Sea Basins including a summary of hydrocarbon shows, primary and secondary objectives.

Well Name	Spud Date	Well Type	Well Class	Hydrocarbon Shows	Primary Objective	Secondary Objective(s)
Melville Basin						
72/10-1A	08/01/1979	Respod	Dry Hole	No Hydrocarbon Shows - Water wet	Jurassic Ssts (absent)	Permian-Triassic
73/01-1A	29/05/1982	Respod	Dry Hole	No Hydrocarbon Shows - Water wet	Lower Jurassic Ssts	
73/02-1	15/07/1983	Exploration	Dry Hole	No Hydrocarbon Shows - Water wet	Lower Intra Triassic Ssts	Upper Intra Triassic Ssts and Lower Cretaceous Ssts
73/04-1	28/05/1986	Exploration	Dry Hole	No Hydrocarbon Shows	Lower Cretaceous Ssts	Middle Eocene Sst
73/05-1	09/10/1983	Exploration	Dry Hole	No Hydrocarbon Shows		
73/06-1	27/05/1983	Exploration	Dry Hole	No Hydrocarbon Shows	Lower Cretaceous Ssts	Pre-salt Section
73/07-1	23/07/1981	Exploration	Dry Hole			
73/08-1	29/05/1982	Exploration	Dry Hole	No Hydrocarbon Shows	Triassic	Permian
73/12-1A	15/08/1982	Respod	Dry Hole	No Hydrocarbon Shows	Permian-Triassic Sst	
73/13-1	04/05/1983	Exploration	Dry Hole	Minor Hydrocarbon Shows	Lower Jurassic	Lower Cretaceous Ssts and Eocene
73/14-1	21/06/1986	Exploration	Dry Hole	No Hydrocarbon Shows Indicated		
74/01-1A	27/06/1982	Respod	Dry Hole	No Hydrocarbon Indications	Lower Triassic Bunter Sst	Lower Cretaceous & Permian-Triassic Ssts
83/24-1	29/08/1977	Exploration	Dry Hole	No Hydrocarbon Shows Indicated		
St Mary's Basin						
85/28-1A	20/03/1982	Exploration	Dry Hole	Water bearing	Lower Triassic Sst	Permian
86/17-1	23/06/1983	Exploration	Dry Hole	No Hydrocarbon Shows		
86/18-1	06/04/1979	Exploration	Dry Hole	No Hydrocarbon Indications - Water wet	Lower Triassic sandstones (absent)	Permian Ssts & Conglomerates
South West Channel Basin and Plymouth Bay Basin						
87/12-1A	21/03/1979	Exploration	Dry Hole	No Significant Hydrocarbon Shows	Permian Ssts	Triassic & Carboniferous Ssts
87/14-1	09/08/1977	Exploration	Dry Hole	No Hydrocarbon Shows Indicated		
87/16-1	09/10/1977	Exploration	Dry Hole	No Hydrocarbon Shows Indicated		
88/02-1	11/07/1977	Exploration	Dry Hole	No Hydrocarbon Shows Indicated		

Table 3.2. Well information from composite logs and well reports for the Melville, St Mary's, South West Channel and Plymouth Bay Basins in the Western Approaches including a summary of hydrocarbon shows, primary and secondary objectives.

3.1.2. Western Approaches

All the exploration in the Western Approaches Basins took place between 1977 and 1986 with the focus of this exploration being the Melville Basin with limited exploration in the St Mary's, Plymouth Bay and South West Channel Basins in the UK sector (Table 3.2). Primary objectives ranged from Lower Cretaceous sandstones to Permian sandstones with secondary objectives ranging from the Eocene to the Carboniferous sections. Unconformities encountered meant that the primary objective sections Jurassic (sandstones in 72/10-1A and Lower Triassic sandstones in 74/01-1A) were absent due to erosional truncation by the Top M2 Unconformity (Fig 3.3 & 3.4).

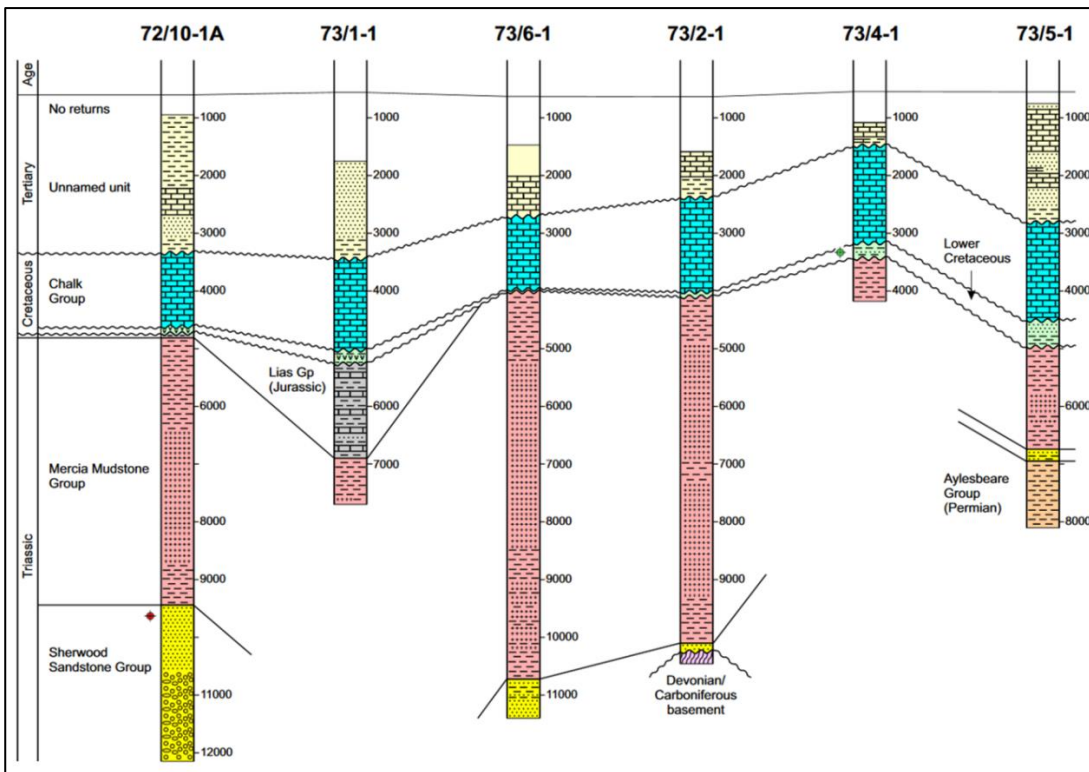


Fig 3.3. Correlation plot of well stratigraphy penetrated in the UK Sector of the Melville Basin with indications of hydrocarbon shows (DECC, 2014).

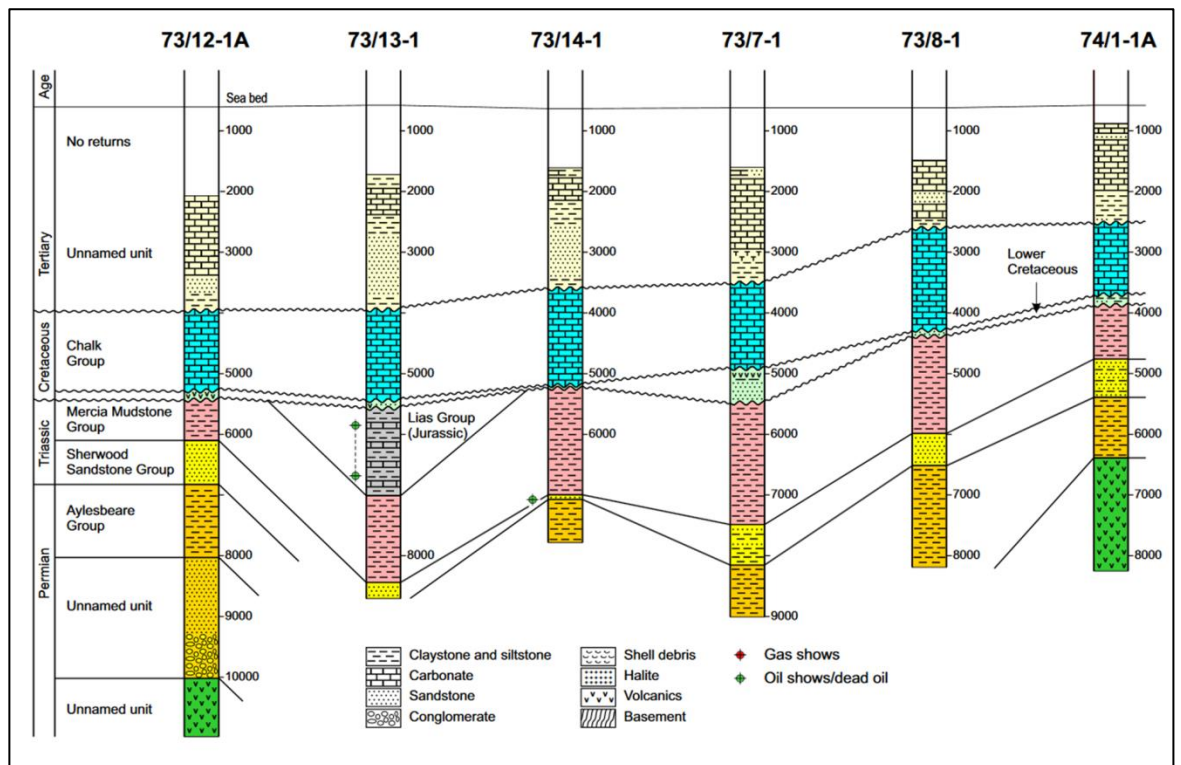


Fig 3.4. Correlation plot of well stratigraphy penetrated in the UK Sector of the Melville Basin with indications of hydrocarbon shows (DECC, 2014).

The DECC (2015) indicates the presence of trace oil in 73/04-1 and 73/14-1 with a gas show in the Sherwood Sandstone of 72/10-1A (Fig 3.3 & 3.4). The gas show in the 72/10-1A seems to result from a minor gas peak of 0.15% observed at 10020 ft MD (3054 m). In 73/04-1 the well report suggests that no hydrocarbon shows were observed during drilling and no reports were available to test the trace oil in 73/14-1 but work by Stricker (per comms) indicates the presence of residual oil present in the pore space of the Sherwood Sandstone. 73/14-1 is in close proximity to the 73/13-1 which suggests that communication from the Early Jurassic could be possible and 72/10-1A includes a small section of penetrated Early Jurassic (Fig 3.4).

3.1.3. French Sector

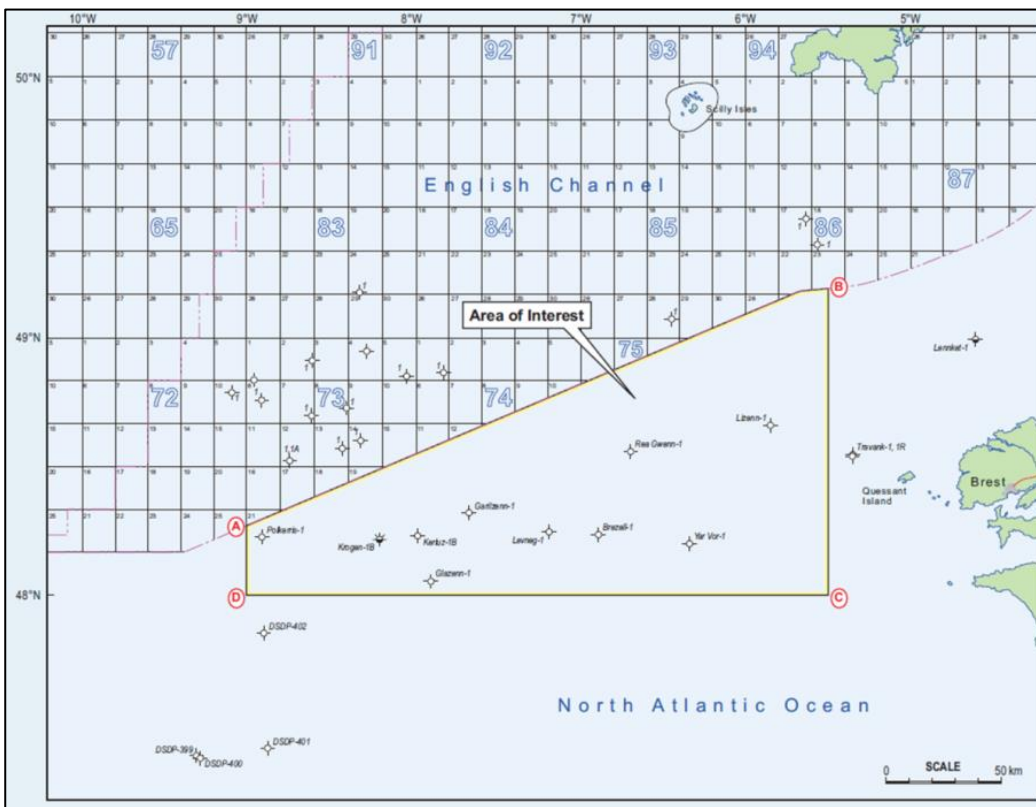


Fig 3.5. Map showing the distribution of wells in the French Sector of the Western Approaches.

The reasons wells failed in the French Sector are highly variable (Table 3.3) with issues in all aspects of the petroleum system indicated throughout the area of interest. The lack of quality reservoir rocks and traps seem to be the most common problem with eight out of ten wells indicating reservoir quality issues and seven wells having a lack of valid trap (GTO, accessed 2017 – Table 3.3). Polkerris, which is situated close to the median line, is suggested to have petroleum generated prior to the Top M2 Unconformity with later leakage indicated (GTO, accessed 2017). The targeting of Tertiary inversion structures has been suggested as a reason for the lack of success on the French side of the Western Approaches and that these structures post-date the earlier hydrocarbon charge (GTO, accessed 2017).

Well	Date	TD (m)	Reservoir	Show	Reason for Failure
French Sector					
Krogen-1B	1983	4200 (Lower Jurassic)	Middle Jurassic Sst, Lower Jurassic	Oil + Gas	Lack of valid trap. Quality of reservoir rocks.
Garlizenn-1	1981	2526, (Palaeozoic)	Middle Jurassic, Lower Jurassic		Quality of reservoir rocks. Lack of valid trap.
Kerluz-1B	1985	1950, (Upper Jurassic)	Jurassic		Lack of source, migration, reservoir quality.
Glazenn-1	1979	3104, (Valanginian)	Cretaceous		Did not reach Jurassic. Lack of good quality Cretaceous reservoir. Lack of hydrocarbon charge.
Levneg-1	1978	3525 (Basement)	Lower Jurassic	Gas	Lack of trap. Quality of reservoir.
Brezell-1	1976	3337 (Permian/Triassic)	Middle Jurassic, Lower Jurassic, Triassic		Lack of trap. Access to source/charge.
Rea Gwenn-1	1981	2526 (Norian)	Triassic MMG	Gas	Good source, lack of valid trap. Quality of reservoir rocks.
Yar Vor-1	1979	3543, (Hettangian/Basement)	Jurassic		Lack of trap. Quality of reservoir. Access to source/charge.
Lizenn-1	1975	4552, (Hettanginian/Sinemurian)	Jurassic		Lack of trap. Quality of reservoir.
Polkerris-1	2003	2131	Triassic		Albian erosional unconformity: All oil generated beforehand escaped

Table 3.3. Well information for the French Sector of the Western Approaches including a shows, target reservoirs and reason for failure from (GTO, accessed 2017).

3.2. Dragon Discovery

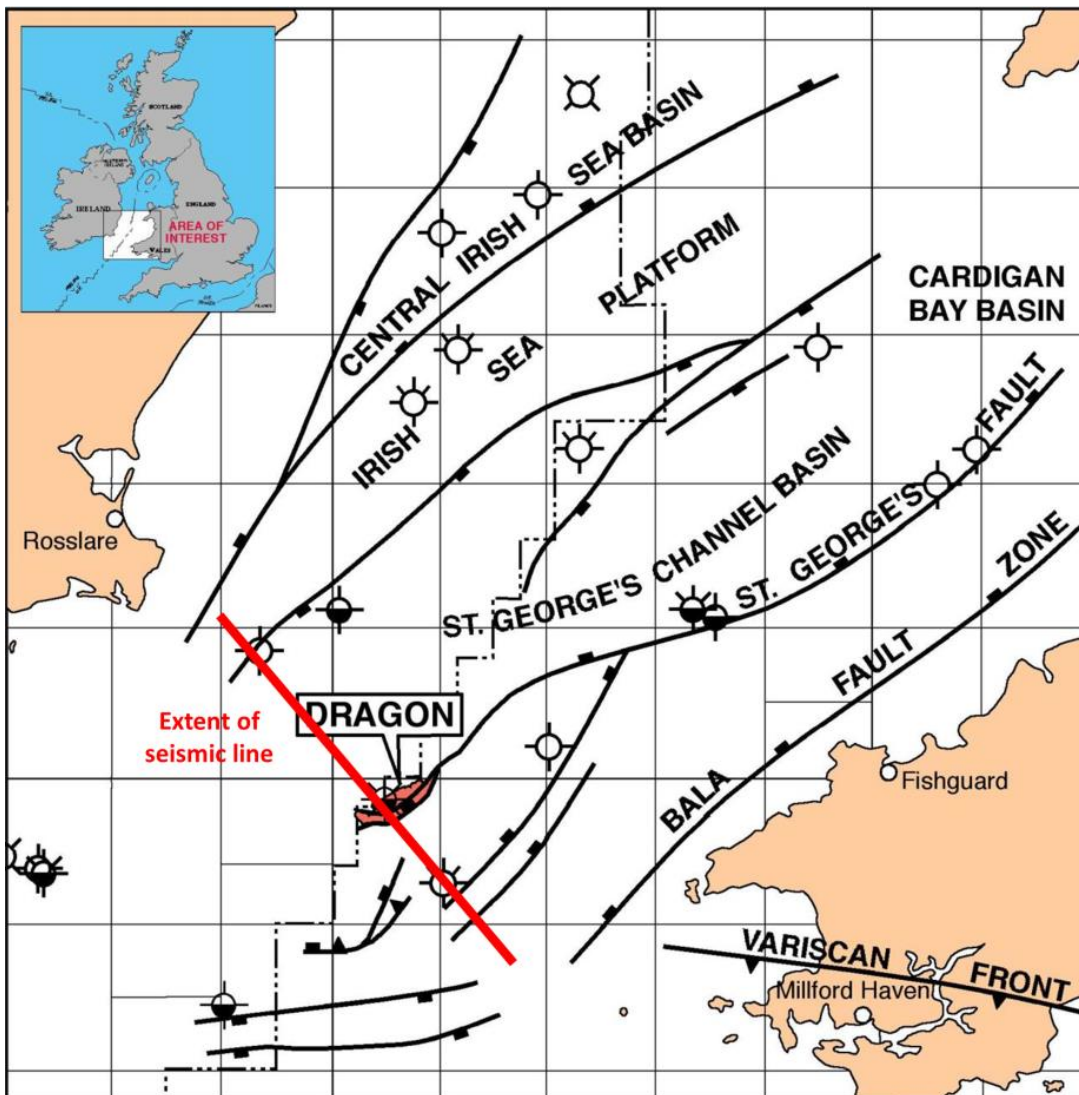


Fig 3.6. Map of the location of the Dragon Discovery with the major surrounding faults shown (Marathon P804 Relinquishment Report).

In 1993, Marathon Oil won License P804 which included all of block 103/01a. Two wells (one exploration and one appraisal well) were drilled and a 3D seismic survey was acquired. License P804 is in the St George's Channel, lying between the boundaries of Ireland and the UK. Marathon drilled their first well (103/1-1) in 1994 to test the Jurassic "Dragon" prospect. The Dragon Discovery is located some 40km off the southeast coast of Ireland and 35km off the coast of Wales (Fig 3.6).

The Dragon Discovery was initially identified as a three-way closure from 2D seismic data in the Middle Jurassic on a NE-SW trending fault system (Marathon P804 Relinquishment Report). The drilling of 103/1-1 proved the prospectivity of this closure but also demonstrated its limited size. 103/1-1 was identified as having two zones of potential

prospectivity to test: a Jurassic Bajocian target in the hanging wall of the fault system and a deeper Triassic Sherwood Sandstone prospect located in the footwall. Gas was encountered in Middle Jurassic age sandstone reservoirs within the footwall to a fault (Fig 3.8). In 2005, 103/1-2 was drilled as an appraisal well to test the continuity of the gas-bearing sandstone reservoirs across the mapped fault block. The appraisal well succeeded in finding reservoirs of equivalent age but failed to encounter any gas. The resource calculation made meant that the Dragon Discovery was considered to be non-commercial. Marathon Oil and partners Summit Petroleum then relinquished the license in 2010 (Providence Relinquishment Report, 2016).

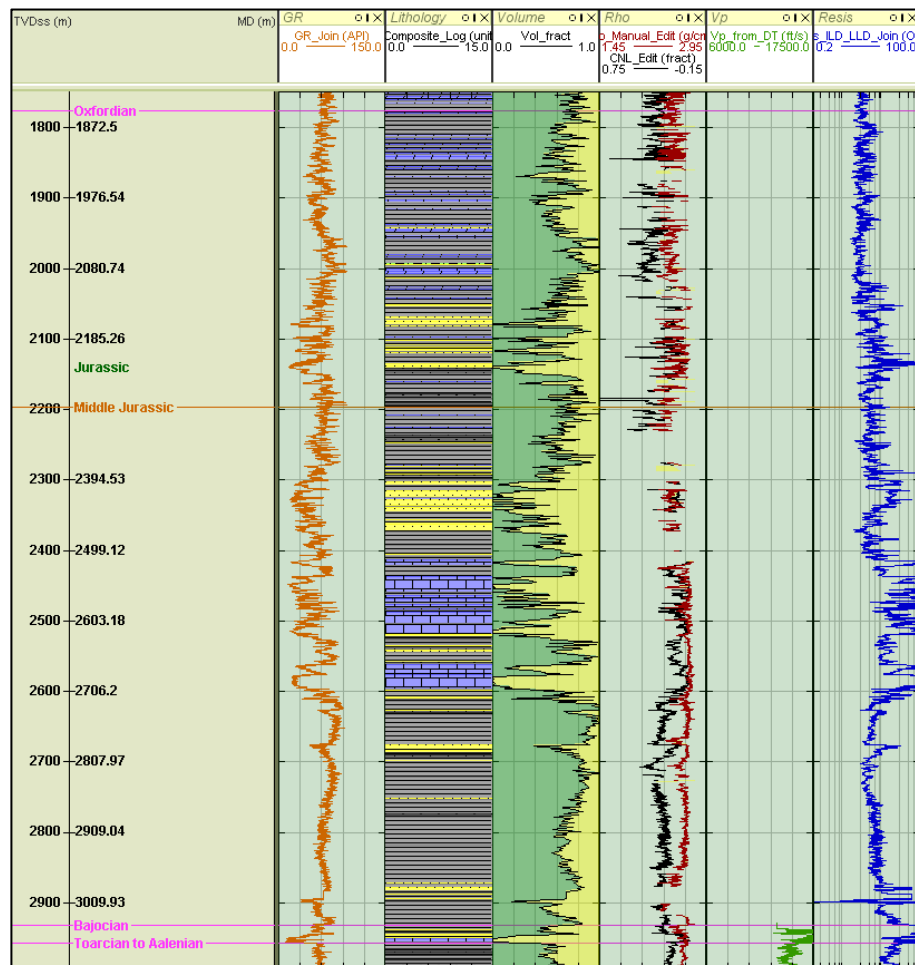


Fig 3.7. Wireline data from the Upper Jurassic section of 103/01-1 with a lithology based on the composite well log (Marathon Oil 1994). GR is the gamma ray tool in API, V-Shale is a volume shale log interpreted from the gamma ray log, the Density track contains the bulk density (g/cc) in red and the neutron log (vol/vol) in black, Vp (ft/sec) is the compressional velocity and Resis is the resistivity in ohms of the formation. A sequence of interbedded shales, sandstones and limestones is present at the base Late Jurassic and Middle Jurassic (2050-2700m TVDss) with high resistivity suggesting the limestones and sandstones to be gas-bearing.

The license for the Dragon Discovery (P1930) was acquired by Providence Resources and partner Star Energy Oil and Gas in 2012. Marathon had produced probabilistic volumetrics for the fault block drilled by 103/1-1 of 100BCF GIIP (Providence Relinquishment Report, 2016). An Extended Elastic Impedance anomaly identified by Providence Resources from 3D seismic data suggested extension of the discovery into the down-dip fault blocks.

The outcome of the technical analysis of the P1930 license by Providence Resource suggests that currently the Dragon Gas Field is volumetrically non-commercial Providence's volumetric estimates for the Upper Callovian and Lower Reservoir units were between 24-53 BCF (Providence Relinquishment Report, 2016). In addition there are no other commercially viable targets within the license to benefit the commercial viability of the prospect. The license was not progressed to second term.

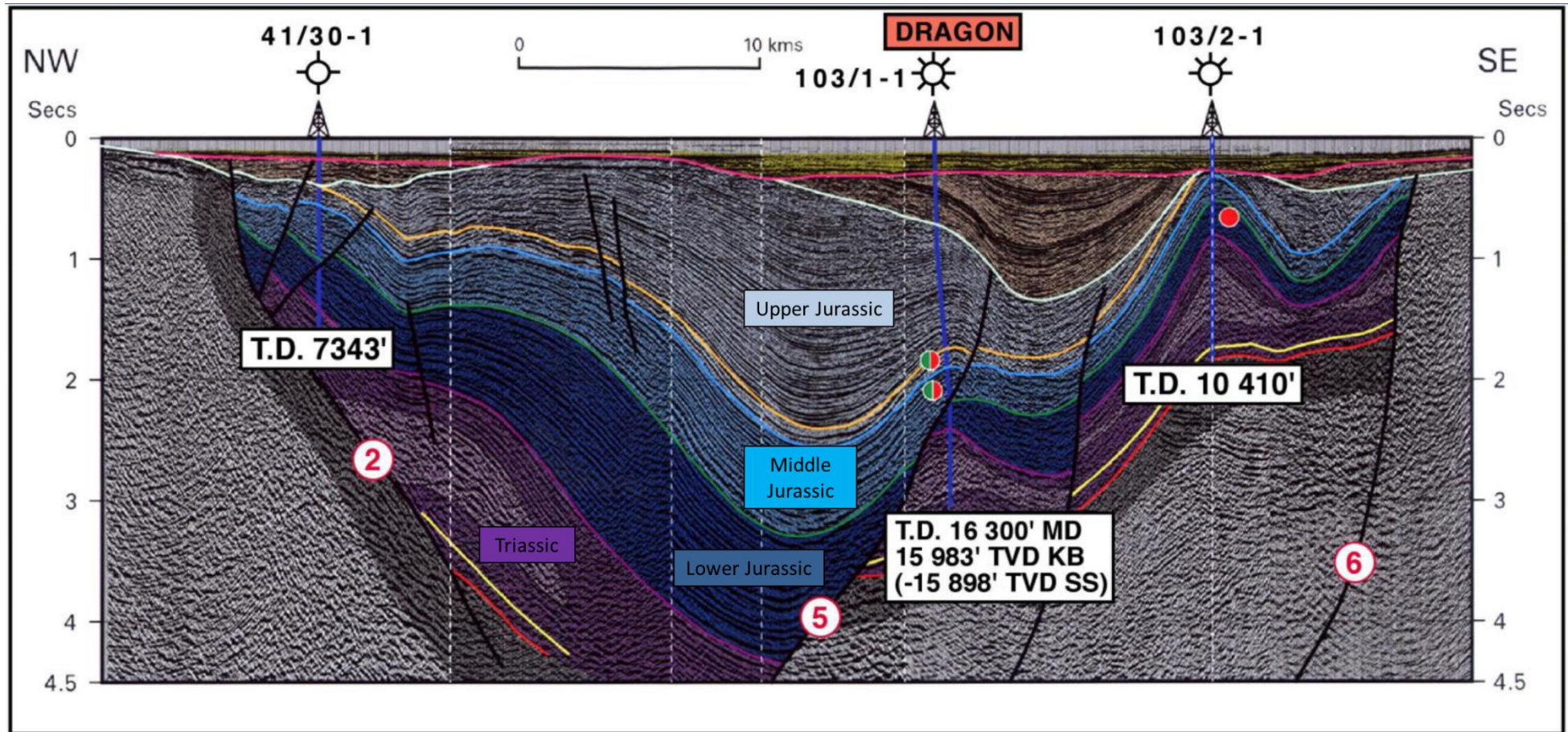


Fig 3.8. Seismic line for the Dragon Discovery which has been interpreted by Marathon (Marathon P804 Relinquishment Report).

3.2.1. Discussion

Only one sub-economic discovery (Dragon Discovery) has been made in the region of interest compared to the multiple economic finds in the Irish North Celtic Sea Basin (Ballycotton Gas Field and Kinsale Head Gas Field – Caston, 1995). There is also a distinct lack of hydrocarbon shows with the most significant observed in the 103/01-1 where a petroleum system is known to function with hydrocarbons sourced from Jurassic strata buried in the basin centre. Other potential shows, minor shows in 73/13-1 and 0.05% background in 93/02-3 generally occur in wells in close proximity to penetrations of Lower Jurassic strata.

There is a good correlation between the limited hydrocarbon shows and minor gas peaks and the presence of Lower Jurassic in close proximity (Fig 3.9). Although well reports are only available for 87/12-1A in the South West Channel Basin and Plymouth Bay Basin there are no indications of hydrocarbons in Western Approaches Basins in the UK sector other than in the Melville Basin. This corresponds with the areas of preserved Lower Jurassic (Chapman, 1989) and further enforces the importance of Jurassic deposition and preservation to the existence of a working petroleum system in the region of interest.

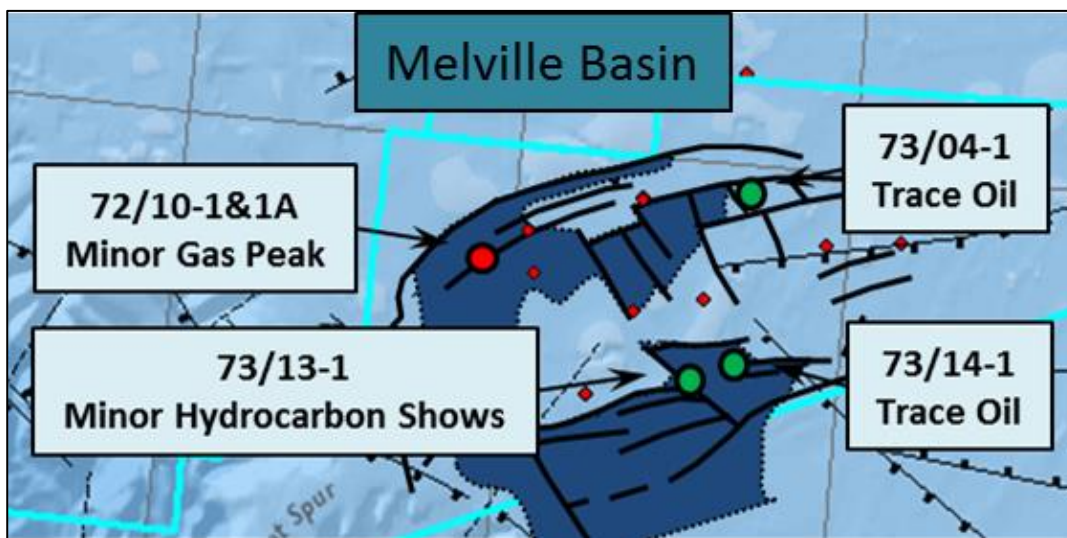


Fig 3.9. Map of the Melville Basin with a schematic layout in blue of the location of preserved Jurassic (based on Chapman, 1989) below the Top M2 Unconformity "Cimmerian".

The Dragon Discovery represents the only discovery in the UK Sector of the Celtic Sea and the Western Approaches. Gas-bearing Middle Jurassic zones of reservoir quality are present within a thick Jurassic section (3000 m) with Jurassic strata thickening basinwards to the northwest. Marathon (1995) indicates that oil sampled is of higher maturity (likely Jurassic)

than the strata penetrated in the well. It is likely that Jurassic strata in the deeper section of the basin, to the northwest of the Dragon Discovery (Fig 3.8), provided the hydrocarbon charge for discovery tested in 103/01-1 but future basin modelling would be required to test this hypothesis. The Dragon Discovery demonstrates that where a thick section of deeply buried Jurassic is present (Fig 3.8) then a working petroleum system is possible. The lack of other finds within the region of interest and rarity of hydrocarbon shows suggests that the source rock in the Celtic Sea and Western Approaches is a serious risk to the probability of an active petroleum system in most areas.

The potential continuation of Jurassic strata into the French sector of the Western Approaches (Chapman, 1989; GTO, accessed 2017 – Fig 3.3) means that a migration pathway could exist from deeper, thicker sections of Jurassic source rocks. The potential for a migration pathway from deeper, mature Jurassic strata in the French Sector could help to de-risk the source rock in the UK Sector. The timing of maturation and peak oil generation could be an issue if the hydrocarbon charge has been able to leak to surface. Future work could focus on working up the French well data and testing the hypothesis proposed above.

Analysis done by GTO (GTO, accessed 2017) suggests that migration of hydrocarbons in the French Sector will have occurred prior to the formation of Cenozoic traps which could be an issue in the Western Approaches. Burial history models available for the region of interest are discussed in more detail in Section 5.3.2.

Chapter 5 builds on the work discussed here with a detailed discussion of source rock maturity, richness, quality and potential after a discussion of method in Chapter 4. The discussion in Chapter 6 is then designed to bring together the material discussed here and in Chapter 2 with the main results in Chapter 5 to discuss the main controls on a Jurassic source rock as the basis of a petroleum system in the region of interest.

3.3. Conclusions

- Hydrocarbon shows are rare in wells drilled in the UK Sector of the Celtic Sea and Western Approaches.
- Hydrocarbon shows in the Melville Basin occur in proximity to areas of preserved Jurassic.
- Reservoir rocks have been targeted at every interval in each of the regions but if there has been no hydrocarbon charge then the presence of reservoir rocks are inconsequential.
- The Dragon Discovery represents the only discovery in the region of interest although it has been classified as sub-economic.
 - A thick deeply buried section (up to 4 seconds) of Early Jurassic strata is present to the NW of the Dragon Discovery (Fig 3.8).
- The source rock preservation is the main risk on the presence of a working petroleum system in the region of interest.
- The preservation, maturity and distribution of the Jurassic is the key to the feasibility of a working petroleum system in the Western Approaches.
- Future work could focus on analysis of the French Sector of the Western Approaches to understand how this could impact the UK sector.
 - Future work could use French seismic and well data to test the potential for hydrocarbon sourcing from deeper buried French Sector Jurassic source rocks.

Chapter 4

Methods

4. Methods

4.1. Introduction

The aim of this chapter is to introduce and describe the geochemical methods by which the data used in Chapter 5 (Source Rock Analysis) were attained and discuss the methods by which these data were analysed as indicators of source rock quality and richness.

Initially this chapter focuses on defining the basic properties and components of source rocks. Subsequently the key measurement techniques, utilised in Chapter 5, for source rocks are described and evaluated in context of their likely strengths and pitfalls. Finally the KinEx software used in this thesis to evaluate petroleum generation and expulsion from identified source rock zones will be described and discussed (Pepper & Corvi, 1994; Pepper & Corvi, 1995).

4.1.1. Petroleum Generation and Expulsion

Petroleum *generation* is the process by which kerogen is broken down to form hydrocarbons as a function of time and temperature (Allen & Allen, 2013). Petroleum expulsion, however, relates to the movement of these generated hydrocarbons out of the source rock probably by microfractures due to overpressure build up during petroleum generation (Allen & Allen, 2013).

4.1.2. Source Rock Richness, Quality and Maturity

The *richness* of a source rock will be considered within this thesis to represent the quantity of organic matter within a rock as reflected by the Total Organic Carbon (TOC) in weight percent. The TOC of a rock or sample is a measure of the organic carbon present in the form of bitumen or kerogen.

Source rock *quality* reflects the proportions of petroleum generating kerogen within a rock or sample and the measure of the ability of that rock or sample to produce petroleum in the form of gas (C1-5) or oil (C6+). To produce hydrocarbons carbon has to be associated with hydrogen so not all kerogen or source rocks are created equally (Dembicki Jr, 2009). Therefore the richness of a source rock in TOC is not always a good indicator of its ability to generate hydrocarbons.

The *maturity* is a measure of heat energy as a function of time and temperature with the degree of degradation of kerogen in a rock or sample modelled as a function of thermal maturity. TOC and kerogen will decrease with increasing temperature as organic matter as the reactive kerogen is consumed (Dembicki Jr, 2009) with a corresponding increasing in bitumen.

4.2. Geochemical and Visual Analyses

This section will discuss the key measurements in determining source rock quality, richness and maturity utilised in this thesis with particular focus on Pyrolysis (Rock-Eval), Vitrinite Reflectance, spore analyses and TOC measurement.

4.2.1. Pyrolysis (Rock-Eval)

Pyrolysis involves the degradation of organic matter in the absence of oxygen to produce organic compounds (Peters, 1986). *Rock-Eval* is a standard pyrolysis procedure that was developed by Espitalié *et al.* (1977) in which hydrocarbon products generated are measured using a flame ionisation detector as a function of time as a sample is brought to 550°C (Allen & Allen, 2013). Pulverised samples of 100g pyrolysed in a helium atmosphere at 300°C for 3-4min followed by stepped increase of the temperature by 25°C/min to 550°C (Peters, 1986). Three peaks are measured (Espitalié *et al.*, 1977; Peters, 1986): S1, S2 & S3 or P1, P2 & P3.

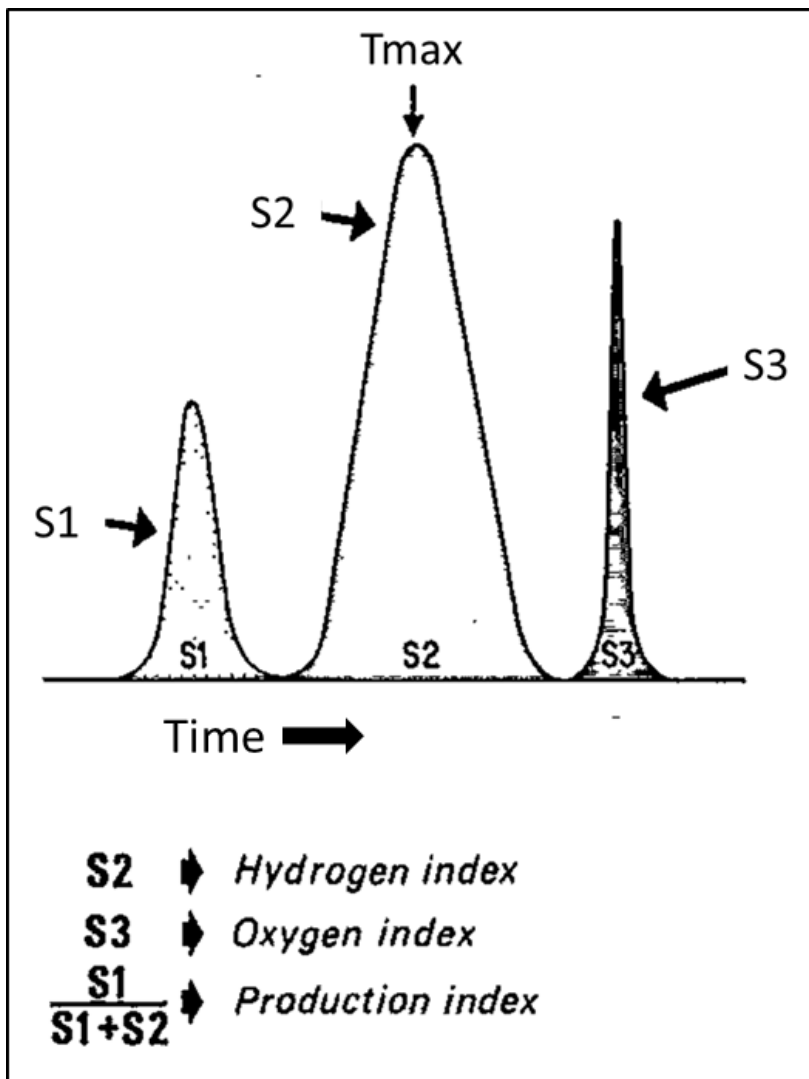


Fig 4.1. Schematic example of the recording of S1-S3 peaks from Rock-Eval pyrolysis (modified after Espitalié et al, 1977).

4.2.1.1. Outputs

S1 – the free hydrocarbons present in the rock sample which are volatilised below 300°C in mg of hydrocarbon per g rock (Fig 4.1 - Espitalié *et al.*, 1977).

S2 – the hydrocarbons evolved due to degradation of the kerogen up to 550°C in mg of hydrocarbon per g rock (Fig 4.1 - Espitalié *et al.*, 1977; Peters, 1986; Allen & Allen, 2013).

S3 – Carbon Dioxide (CO₂) formed during pyrolysis of the organic matter in the rock in mg of CO₂ per g rock (Fig 4.1 - Espitalié *et al.*, 1977).

Tmax – The temperature at which the maximum amount of hydrocarbons are evolved (Peters, 1986; Tissot *et al.*, 1987; Allen & Allen, 2013). The Tmax is a rough measurement of thermal maturity and other factors with Tmax increasing with increased maturity of the rock sample. Poor quality of organic material (degradating and oxidisation of kerogen) can

cause anomalously high Tmax that do not reflect maturity (Moore per comms). Espitalié *et al.* (1977) suggests that Tmax values of 400°C -435°C correspond to immature organic matter with values between 435°C-460°C characterising the Oil Window or Mature Zone. Values of 460°C or greater are indicated as representing organic matter in the Gas Window or the Metamorphosed Zone.

Peters (1986) indicates that immature sediments give anomalous S1 peaks due to poor separation of the S1 & S2 peaks.

4.2.1.2. Calculable Factors

Hydrogen Index (HI) – an expression of the pyrolysable fraction of the organic matter (Allen & Allen, 2013). HI is a measure of the hydrogen richness of the S2 peak organic matter.

$HI = (S2 / TOC) \times 100$ in mg Hydrocarbon/g Organic carbon

Oxygen Index (OI) – Quantity of CO₂ from the S3 peak relative to the TOC. HI is a measure of the oxygen richness of the organic matter.

$OI = (S3 / TOC) \times 100$ in mg CO₂/g Organic Carbon

The HI and OI show a good correlation with H/C and O/C atomic ratios obtained from elementary analysis (Espitalié *et al.*, 1977).

Production Index (PI) – is the ratio of S1 / S1 + S2 which shows an increasing trend with temperature (Espitalié *et al.*, 1977) as with increasing maturity the S1 peak increases as free hydrocarbons are evolved and the S2 peak decreases as kerogen is consumed. PI will increase in the during oil generation due to incomplete expulsion before declining in the gas window.

Petroleum Potential is considered to be S1 + S2 as S1 represents the currently generated hydrocarbons in the rock and S2 the quantity of hydrocarbons that could be produced (Espitalié *et al.*, 1977).

4.2.2. Kerogen Types

The most common used method for classifying kerogen type is the van Krevelen plot (or a pseudo-van Krevelen plot – Fig 4.2) or atomic H/C vs O/C diagram (Tissot *et al.*, 1974). Five types of kerogen are discriminated (Fig 4.2):

Type I – Predominantly derived from algal material and deposited in a lacustrine environment with high initial H/C and low O/C atomic ratios. Type I kerogen typically produces waxy oils (Dembicki Jr, 2009).

Type II – Autochthonous organic matter deposited in a marine or lacustrine environment with moderate H/C and O/C atomic ratios which produces naphthenic oil (Dembicki Jr, 2009).

Type III – Terrestrial plant matter or organic matter with low initial H/C and high initial O/C atomic ratios that is traditionally considered to produce mainly gas (Dembicki Jr, 2009). Pepper & Corvi (1994) suggest, however, that only sediments with very low H/C ratios or (HIs) produce more gas than oil.

Type IV – Inert kerogen with no hydrocarbon generating potential due to alteration and/or oxidisation.

Type IIS – Kerogen which is enriched in sulphur. Type IIS is deposited in highly reducing conditions in a marine environment with initially high H/C and low O/C ratios with early generation of high sulphur naphthenic oil (Dembicki Jr, 2009). Sulphur can also be incorporated during early diagenesis.

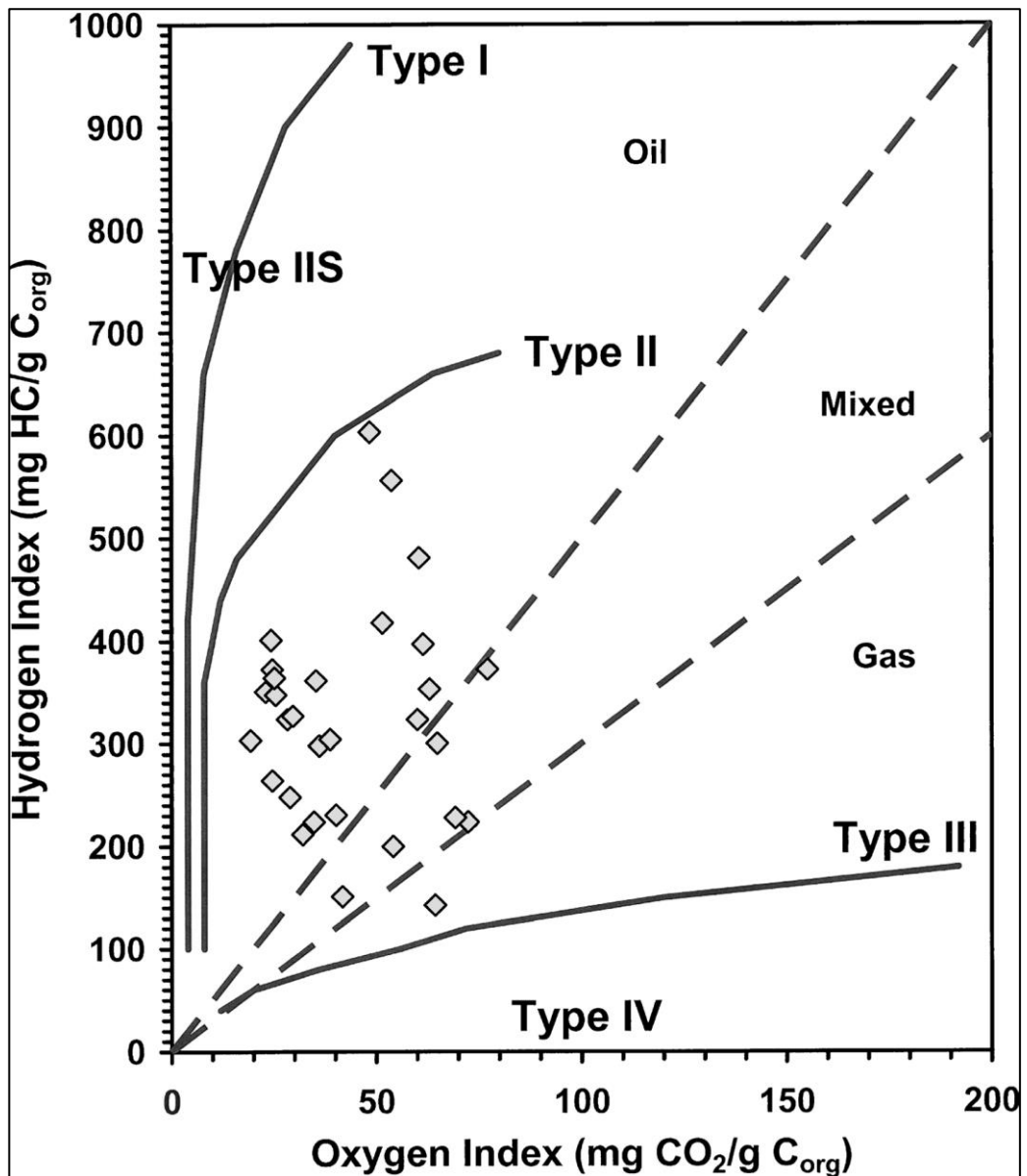


Fig 4.2. Schematic pseudo-van Krevelen plot with HI and OI used instead of H/C and O/C atomic ratios. Type I and Type IIS plot with this highest HI relative to OI with decreasing hydrocarbon generative ability towards Type II and Type III. Type IV is indicated as having no hydrocarbon generative potential (Dembicki Jr, 2009).

Dembicki Jr (2009) describes the effects of mixed kerogen types on the pseudo-van Krevelen plot with kerogen types or dilution by Type IV inert kerogen causing results to plot in an intermediate zone relative to the abundance of each kerogen type. Cornford *et al.* (1998) discuss the use of HI vs Rock-Eval T_{max} for identification and discrimination of kerogen types (Fig 4.3). Note the effect of maturation (increasing R_o) on the kerogen type distribution. HI (and OI) change with increasing maturity so that it can be difficult to assess the kerogen type in mature/overmature rocks.

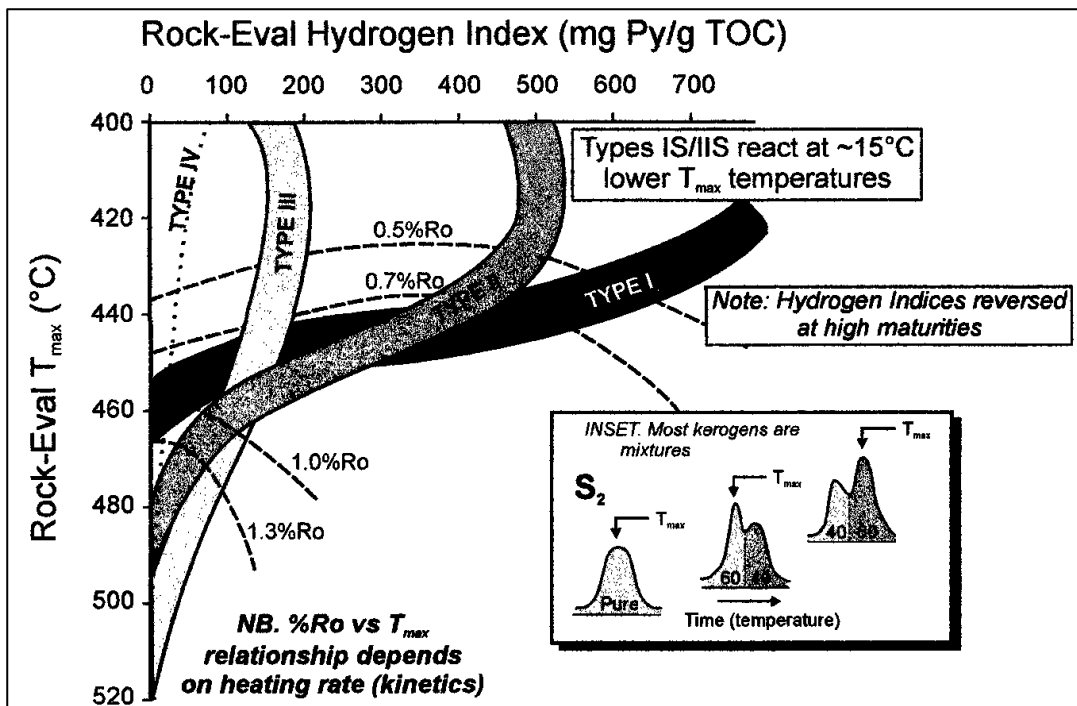


Fig 4.3. Hydrogen Index (HI) vs Rock-Eval Tmax trends for kerogen types demonstrating the control of maturity on both parameters i.e. increased Tmax and reduced HI (Cornford *et al.*, 1998).

4.2.3. Total Organic Carbon (TOC)

Peters (1986) discusses the different methods for the determination of Total Organic Carbon from rock samples. TOC can be determined by the direct combustion method by which crushed samples are initially treated with acid in a filtering crucible to remove carbonate before being combusted at 1000°C and analysed as CO₂. Comparable results are obtainable by a modification of the direct method with non-filtering crucibles and an indirect method. The indirect method involves summing the total carbon and then subtracting the amount of carbon related to carbonate. The method of TOC measurement is rarely indicated in the geochemistry reports assessed in this thesis.

4.2.4. Vitrinite Reflectance (VR)

Vitrinite Reflectance (VR) is one of the most common methods in the Petroleum Industry to analysis maturity (Tissot *et al.*, 1987) and has long since been associated with increasing maturity in coals with time and temperature (Burnham & Sweeney, 1989). Vitrinite Reflectance is considered as R_o, where R_o is the percentage of light reflected from a particle in oil immersion (Burnham & Sweeney, 1989). What is considered the VR scale is the result of calibration to field studies of oil and gas provinces and other maturity parameters so that

R_o can be correlated with the main thresholds of petroleum generation (Allen & Allen, 2013).

$R_o < 0.55\%$	Immature to Early Mature
$0.55\% < R_o < 0.80\%$	Oil and Gas generation
$0.80\% < R_o < 1.00\%$	Cracking of Oil to Gas (gas condensate zone)
$1.00\% < R_o < 2.50\%$	Dry Gas generation

Vitrinite Reflectance is suggested to be a very good indicator of maturity above $\sim 0.7-0.8\%$ R_o (Allen & Allen, 2013). Vitrinite Reflectance data is commonly reported as a set of populations based on the analysis companies interpretations with good data points typically having >30 reproduced particles of a given $\%R_o$ (Moore per comms). Rare geochemical reports analysed for this thesis contain the histogram distributions for each data point although in contrast to this data exist in some reports without any indications of sampling populations.

Vitrinite Reflectance measurements can be plotted as a function of depth to give R_o profiles. The slope of the VR curve is an indicator of the geothermal gradient in the history of the basin. In regions unaffected by unconformities, young dip-slip faulting and igneous activity $\log R_o$ should have a linear relationship with depth (Allen & Allen, 2013) due to the exponential evolution of organic matter with time. In basins of significant uplift R_o profiles will be offset from the usual seabed intercept of $0.2-0.4\%$ R_o (Fig 4.4 – Corcoran & Clayton, 2001). Figure 4.4 also demonstrates the scatter commonly associated with VR measurements which can lead to general trends in the data being misleading.

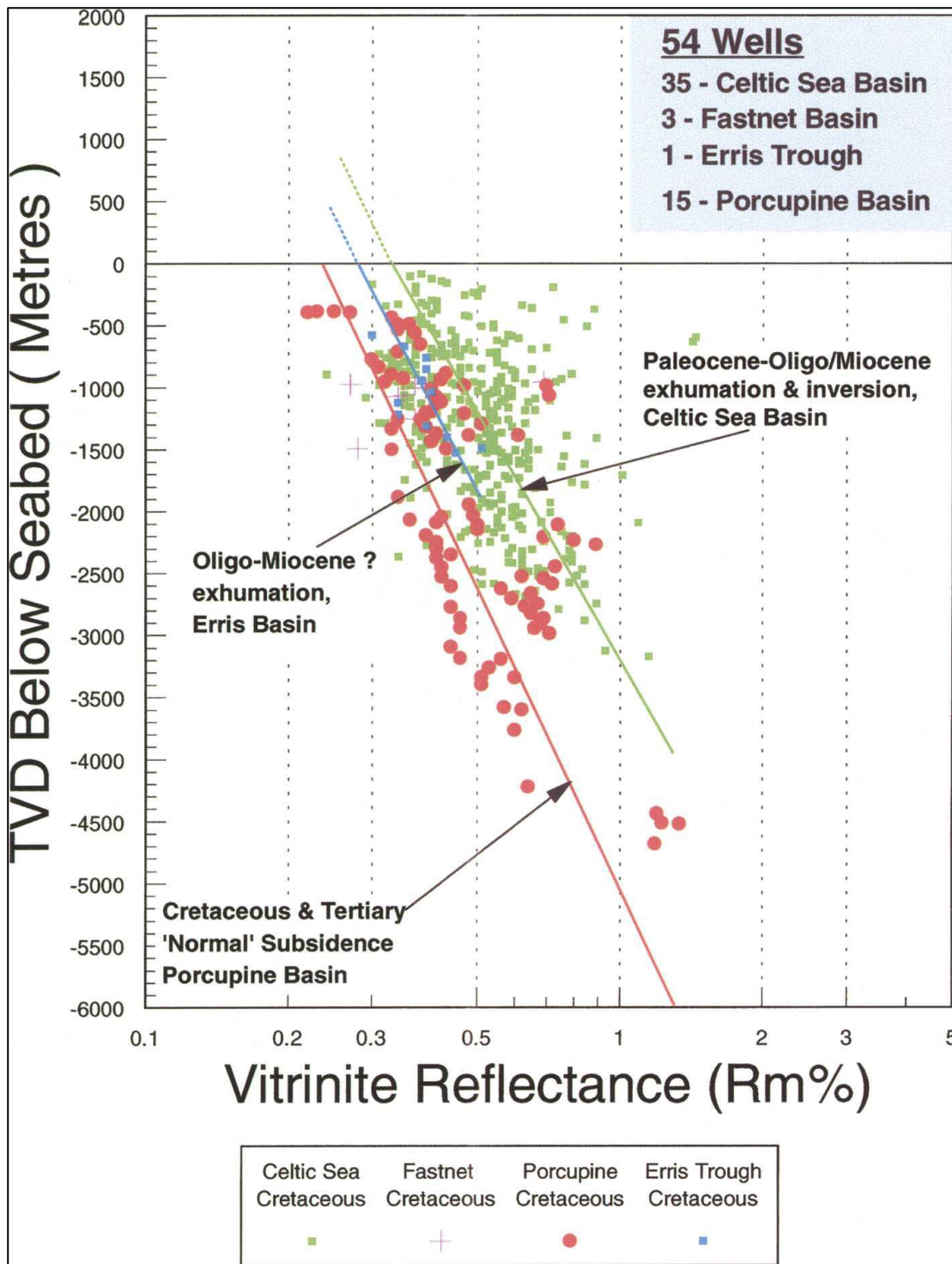


Fig 4.4. R_o profiles from offshore Ireland based on Vitrinite Reflectance data. Data from the Cretaceous of the Celtic Sea are plotted as green squares and offset to the right of the other basins suggesting post-Cretaceous uplift (Corcoran & Clayton, 2001).

4.2.5. Visual Analysis of Kerogen

Optical examination of kerogen under transmitted light has demonstrated an irreversible and progressive colour change of spores, pollen and microfossils with increasing maturity (Smith, 1983; Allen & Allen, 2013). Three main colour index scales are discussed in the literature. Smith (1983) managed to create spectra from all standard materials for each method that produced a reliable correlation between the three sets of standards (Table 4.1).

1. Staplin's Thermal Alteration Index (TAI)

Staplin's (1969, 1977) Thermal Alteration Index is a 1-5 scale based on the analysis of spores, cuticle and amorphous sapropelic debris. Smith (1983) indicates that the basing of TAI on sapropels can lead to apparent higher maturity than shown in spores.

2. Robertson Research's Spore Colouration Index (SCI)

Robertson Research International developed the Spore Colouration Index (Barnard et al, 1976) 1-10 scale based on spore colour. Smith's (1983) analysis of the SCI methodology suggests that a skilled operator should be capable of producing accurate and consistent interpretations. Spore colouration displays a progressive change from yellow through orange then brown to black (Allen & Allen, 2013).

3. Batten's Colour Index

Batten (1980) produced a 1-7 colour scale based on spores. This will not be dealt with in detail as it was not referenced in geochemistry reports in the region of interest.

Visual assessment of palynomorph colour against a set of standards is a quick and cheap method of estimating maturity in organic material. Differences between the interpretations of separate operators are suggested as a weakness of this type of analysis. In addition, estimates performed on different organic material in one slide to another may produce varying assessments of maturity (Smith, 1987).

Batten (1976)		Robertson (1976)		Staplin (1969)	
Palynomorph	Maturation	Palynomorph colour	Maturation stage	Organic matter	Associated hydrocarbons
1 Colourless pale yellow	Immature	1 Colourless pale yellow	Immature	1 Fresh yellow	Wet or dry
2 Yellow	Immature	2 Pale yellow – lemon yellow	Immature	2 Brownish yellow	Wet or dry
3 Light brownish yellow, yellowish-orange	Marginally mature	3 Lemon yellow	Transition to maturity	3 Brown	Wet or dry
4 Light-medium brown	Mature oil generation	4 Golden yellow	Transition to maturity	4 Black	Dry gas
5 Dark brown	Mature, gas condensate	5 Yellow orange	Fully mature	5 Black, with additional evidence of rock metamorphism	Dry gas to barren
6 Very dark brown-black	Over-mature dry gas	6 Orange	Optimum oil generation		
7 Black (opaque)	Trace of dry gas	7 Orange brown	Optimum oil generation		
		8 Dark brown	Mature, gas condensate		
		9 Dark brown-black	Post mature, dry gas		
		10 Black	Post mature, trace of dry gas		

Table 4.1. A comparison of the 3 main colour scales for visual kerogen and spore analysis (modified after Smith, 1987).

4.3. Wireline Data

In order to better characterise zones and extents of source rock potential the geochemical data previously discussed in this chapter have been considered along with wireline well logs where available. Wireline logs are recorded when drilling tools are no longer in the hole and represent the measurement of mechanical, spontaneous or induced measurements of the rock surrounding the wellbore using specialised equipment (Rider, 1996). The primary logs considered here are:

1. Gamma Ray (GR API)

A gamma ray detector measures the natural radioactivity of the rock surrounding the wellbore (Rider, 1996) and is typically used to discriminate different lithological units. Sandstones and limestones usually show low radioactivity while shales typically have higher natural radioactivity. The GR and SGR tools can be used to localise zones of source rock potential due to the relationship between uranium and organic matter (discussed below under the spectral gamma ray).

Spectral Gamma Ray (SGR)

The spectral gamma ray tool works on a similar principle to standard GR but is able to assign gamma radiation into several energy windows which discriminate the distinctive energy peaks of Uranium (U ppm), Thorium (ppm) and Potassium (K %). Of these Uranium can be enriched in sediments through adsorption to organic matter or during precipitation in acidic or reducing environments and is therefore a very good indicator of source rock potential (Rider, 1996). The relationship between uranium and organic matter, however is not always evident as coals and lacustrine source rocks are indicated by Rider (1996) as being typified by low natural radioactivity (low GR – Fig 4.5).

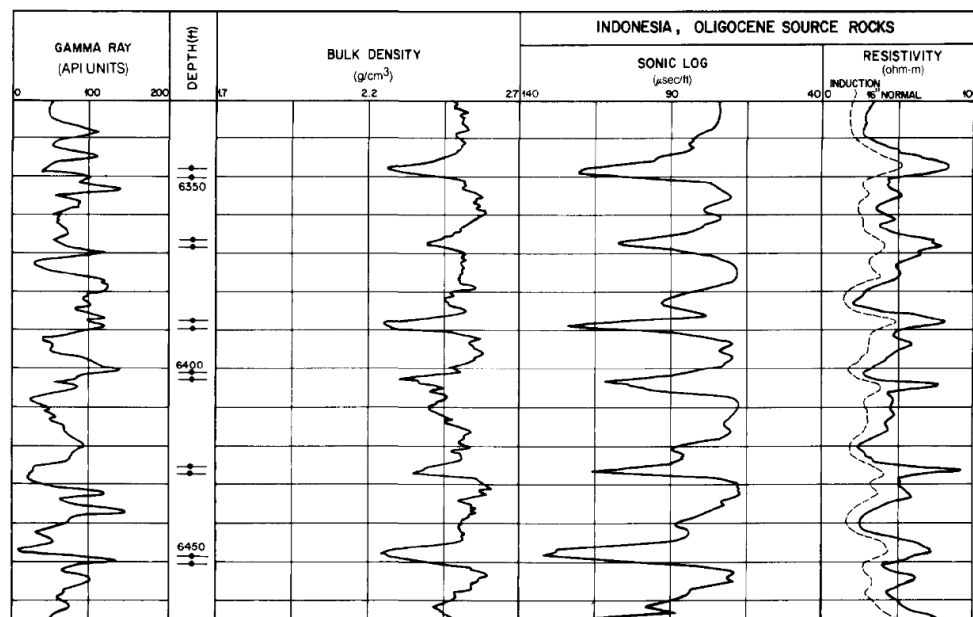


Fig 4.5. Wireline logs for an Oligocene sequence in Indonesia with cyclic lacustrine deposition of source rocks indicated in the depth column (Meyer & Nerderlof, 1984). The organic matter-rich zones have low density and low sonic couple with high resistivity but no response from GR due to the lacustrine environment of deposition causing a lack of radioactivity.

2. Sonic log (DT)

The time taken for a compressional sound wave to travel through ~0.25 cm (1 ft) of rock from a sonic sonde to a receiver. Velocity is a rock property considered in this thesis which is the inverse of the sonic travel time and is a function of porosity and lithology (Allen & Allen, 2013). The sonic log cannot be used to indicate source rock potential (Rider, 1996) but the presence of organic matter lowers the sonic velocity in direct relation to the abundance of organic matter (Fig 4.5 & 4.6). A zone of high source rock richness will demonstrate a slower sonic velocity (Passey *et al.*, 1990).

3. Density (Rho g/cc)

The density tool actually measures the electron density of the rock by emitting gamma rays from a radioactivity source. The gamma rays then collide with electrons in the formation and are scattered or lose energy. The electron density is measured by a detector that records the number of scattered gamma rays. The electron density is almost identical to the bulk density for most minerals except in the case of evaporitic minerals and coals which show anomalously low density values (Allen & Allen, 2013). Coals show an electron density of 1.2-1.8 g/cc. In addition Rho can be used to qualitatively discriminate zones of source rock richness as organic matter has densities between 0.5-1.8 g/cc in contrast to a normal matrix density of 2.7 g/cc for clay minerals in a shale (Rider, 1996). Increased percentage of organic matter in the rock matrix has a significant effect on the density log (low Rho response; Fig 4.5 & 4.6; Passey *et al.*, 1990).

4. Compensated Neutron log (CNL v/v)

The neutron tool works on the principle that neutrons are emitted from a radioactive source and collide with nuclei in the rock surrounding the wellbore and are captured. A detector measures the returning neutrons. Since neutrons lose the most energy when colliding with hydrogen nuclei the neutron log gives a measure of all the hydrogen present in the formation including pore fluid and hydrogen bound in clays and kerogen. CNL is calibrated to read the true porosity of limestones so provides limestone porosity units (Allen & Allen, 2013). Coal and organic matter contains hydrogen so will demonstrate an increased neutron response (Rider, 1996). Passey *et al.* (1990) suggests that the neutron tool is sensitive to small amounts of organic matter therefore making it very useful in source rock discrimination. The neutron log is typically used in combination with the density log to qualitatively characterise lithological variation.

5. Resistivity (Resis Ohmm)

The resistivity log is a measurement of a formation's resistivity i.e. resistance to the movement of an electric current in ohms/m²/m (simplified here to Ohmm). Most rock materials are insulators with enclosed fluids being conductive except in the case of hydrocarbons which are infinitely resistive (Rider, 1996). A lithology with a saline water pore fluid will have a low resistivity in contrast to the same lithology bearing gas which would show a much higher response. Resistivity is typically used to identify porous hydrocarbon bearing zones (Rider, 1996). Rider (1996) indicates that at low maturities the resistivity log does show a large response to organic matter but at high maturities (Fig 4.6) where hydrocarbon has been liberated into the pore space the resistivity shows high values (Passey *et al.*, 1990). Coals are indicated as having typically high resistivity responses.

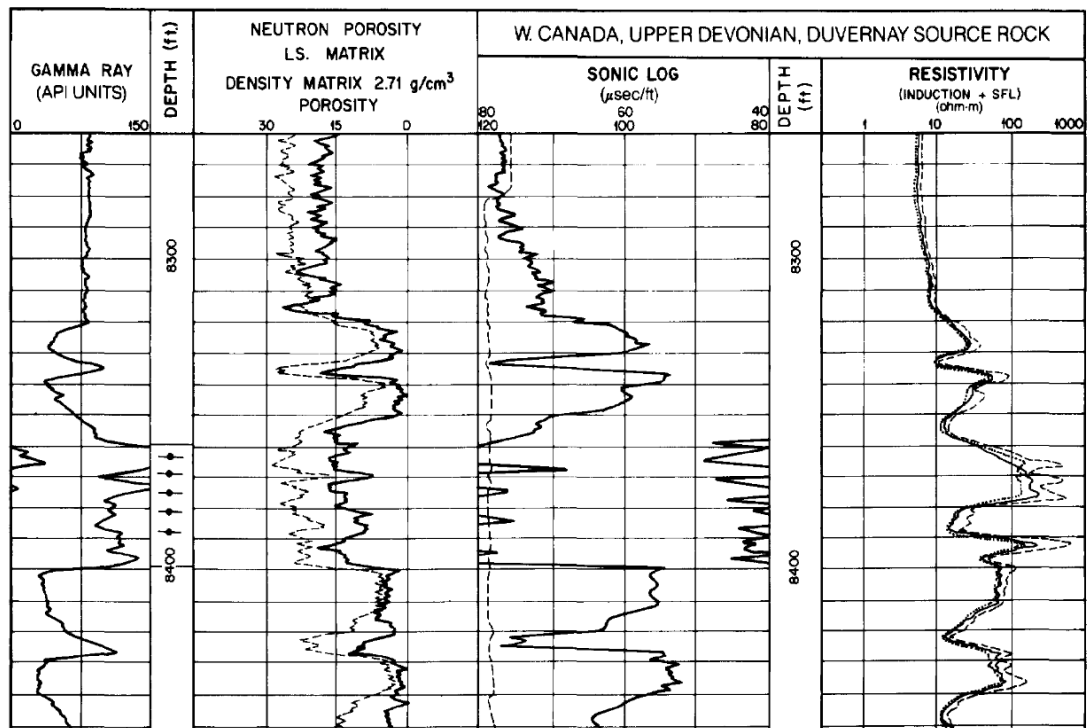


Fig 4.6. Wireline logs for the Late Devonian Duvernay source rock interval in Alberta, Canada (Meyer & Nerderlof, 1984). The source rock interval at 8360-8400 ft (2548-2560 m) shows increased GR along with low sonic and density. An increased resistivity response suggests that the interval is mature.

4.3.1.1. Issues with wireline data

Wireline logs are designed to provide to give repeatable and reliable readings of subsurface formations, however these ideals are never met (Rider, 1996). One reason for this is that drilling of a well causes a disturbance of the rock with varying degrees of mud invasion (inducement of mud into the rock formation), deviation of the wellbore from a spherical profile and the propagation of cracks into the formation. A caliper log is typically taken to measure the variations in the borehole diameter with depth.

A second issue is that the perfect conditions for measurement are never met with a tool moved up or down the wellbore. The tools such as GR can show shoulder effects at lithological boundaries due to averaging of the values if the tool is moved too quickly (Rider, 1996).

4.4. KinEx – Modelling Software

KinEx is propriety software developed by Zetaware, Inc and aims at providing a source rock maturation modelling tool for estimating the expelled products from a source rock based on a set of organofacies based on the kinetic models outlined in Pepper & Corvi (1994). The use of five organofacies (Table 4.2) is designed to make the model appropriate for use in areas of low geochemical knowledge. In contrast to the kerogen types defined earlier (Section 4.2.2) the organofacies are based on combined parameters of gross depositional environment and stratigraphic age. An additional key factor of the software is the use of a heating rate which elevates or depresses the temperature range of generation for a given organofacies by $\sim 15^{\circ}\text{C}$ with an order of magnitude variation. The KinEx software also models the movement of petroleum from the source rock beds simultaneously concurrently considering oil and gas generation, oil-gas cracking (Pepper & Dodd, 1994), hydrocarbon storage capacity of kerogen and the expulsion of hydrocarbons after saturation of the kerogen sponge (Pepper & Corvi, 1995). KinEx models a sorption capacity for C1-5 and C6+ with C1-5 and C6+ only expelled after that capacity is met.

Organofacies	Descriptor	Principal biomass	Sulphur incorporation	Environmental/ age association	Possible IFP classification
A	Aquatic, marine, siliceous or carbonate/evaporite	Marine algae, bacteria	High	Marine, upwelling zones, clastic-starved basins (any age)	Type II'S'
B	Aquatic, marine, siliciclastic	Marine algae, bacteria	Moderate	Marine, clastic basins (any age)	Type II
C	Aquatic, non-marine, lacustrine	Freshwater algae, bacteria	Low	'Tectonic' non-marine basins; minor on coastal plains (Phanerozoic)	Type I
D	Terrigenous, non-marine, waxy	Higher plant cuticle, resin, lignin; bacteria	Low	Some (Mesozoic and younger) 'ever-wet' coastal plains	Type III'H'
E					
F	Terrigenous, non-marine, wax-poor	Lignin	Low	Coastal plains (Late Palaeozoic and younger)	Type III/IV

Table 4.2. Definition of the five classification of organofacies utilised by KinEx with information of deposition environment and stratigraphic age association (Pepper & Corvi, 1994). The possible correlations between the organofacies and the kerogen types described earlier (Section 4.2.2) are also included.

4.5. Discussion

Geochemical and visual analysis measurements are reliant on rock samples from the zones of interest, usually from core or bit cuttings. A full discussion of the working of wellbore complexity is beyond the scope of this thesis but the conditions of the wellbore and method of sampling along with human error have a large effect on the quality of the samples especially cuttings. Cuttings from the drill bit are preferentially preserved based on competence so will be skewed away from the typically softer organic matter-rich shales typically underestimating the bulk TOC and pyrolysis results for a section (Scotchman, per comms). Integration of geochemical data with wireline logs will be used to better characterise the shale zones and represent the extent of zones of high source rock potential. While resampling and measuring of data would lead to better representation of softer lithologies such work is not feasible within the timescale of this project.

Increasing maturity has a large effect on the results of Rock-Eval pyrolysis and TOC due to the generation and expulsion of hydrocarbons (Dembicki Jr, 2009). S₂, HI and TOC have a decreasing trend with increasing maturity as generative kerogen is consumed (Allen & Allen, 1986). Analysis of the thermal maturity of samples will be utilised along with the S₁ peak (free hydrocarbons) to understand whether petroleum generation has diminished generative potential and to estimate expelled volumes. Section 5.3 demonstrates a general trend of immaturity/early maturity throughout the region (with the exception of 103/01-1) therefore maturity of samples is not considered to be an important source of error within the data population.

Vitrinite Reflectance is the most commonly used method of assessing the thermal maturity of organic matter (Tissot *et al.*, 1987) and represents the main method of analysis in Section 5.4. Data quality issues are present with large separation of results that could be due to vitrinite lean samples, human error, allochthonous material and variability within samples. Pitfalls exist within other methods such as those discussed earlier for Tmax (Section 4.2.1) and in visual kerogen analysis Section 4.2.5. These measurements have been used to check and interpret R_o populations where ambiguity exists. Tmax data in the sample population is considered anomalously high due to very poor quality of the organic matter within the samples caused by degradation and oxidisation of the kerogen and is not considered to be a reliable measurement of maturity within the region of interest (Moore per comms).

The use of wireline data in this Master's thesis has been focussed on qualitative analysis of zones of source rock richness as in Section 5.7. Initially a calibrated Passey's Method was attempted (Passey *et al.*, 1990) but wireline log responses were not found to be correlateable between different wells. The result did not respond well enough to known source rock intervals due to lithological variation. The caliper log and density correction log (measures the correction applied to the density log by the tool) have been used to understand zones of irregular borehole shape. The wireline logs, where possible, have been calibrated using TOC and pyrolysis data. The calibrated response has then been extrapolated across the source rock interval to provide an understanding of the intervals thickness.

The KinEx software has been utilised in this project to model oil and gas generation and expulsion as the kinetic principles and assumption used are outlined in a series of three papers published by Pepper (Pepper & Corvi, 1994; Pepper & Dodds, 1994; Pepper & Corvi, 1995). The input parameters can be simply defined such as the organofacies (Table 4.2) which can be assigned based on depositional environment and stratigraphic age. The proportion of each of these organofacies can be described as a set of thicknesses over a defined interval. A heating rate is also required but as described in Section 4.4 is an insensitive parameter and the standard value $2^{\circ}\text{C}/\text{Ma}^{-1}$. Pepper & Corvi (1994) suggest that most petroliferous sedimentary basins sit between a heating rate $1\text{-}5^{\circ}\text{C}/\text{Ma}^{-1}$ therefore a value of $2^{\circ}\text{C}/\text{Ma}^{-1}$ is likely to cause minimal error.

4.6. Conclusions

1. The majority of geochemical and visual data utilised in this thesis have been measured using common consistent and reproducible petroleum industry methods.
2. Geochemical data produced can be related to source rock quality, richness and the thermal maturity.
3. General reliance on well samples leads to uncertainties in each method due to the sampling, human error and allochthonous material.
4. Vitrinite Reflectance is best used in combination with other factors such as Tmax and visual analysis of kerogen to understand thermal maturity.
5. Reporting of geochemical and visual data is often poor leading to a lack of clarity of data quality.
6. The KinEx software has been used to model petroleum generation and expulsion due to its applicability in areas of low geochemical information and the availability of information regarding to the underlying kinetic models.

Chapter 5

Source Rock Analysis

5. Source Rock Analysis

5.1. Introduction

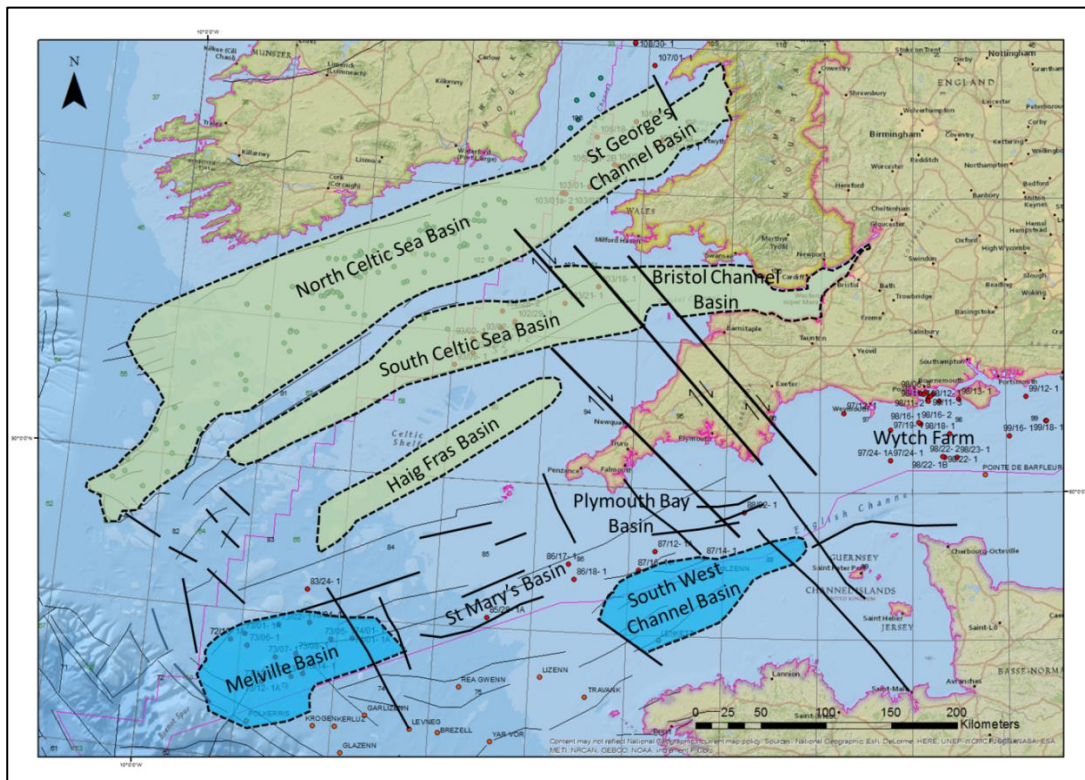


Fig 5.1. Map of the offshore basins of interest off the south west coast of Britain. Basin outlines and nomenclature modified after Ziegler (1987b). A quadrant is an area enclosed by one degree of longitude and latitude with an assigned number.

5.1.1. Aim

The aim of this chapter is to investigate the spatial and stratigraphical variation in source rock potential throughout the Jurassic within the Western Approaches and Celtic Sea regions (Fig 5.1).

The focus of this chapter will be on the Jurassic interval of the Western Approaches and Celtic Sea area (region of interest) with additional wells from the St George's Channel Basin and Wytch Farm used to increase the population of statistical data. In addition wells 98/13-1, 98/16-1 and 98/23-1 have been included in the discussion where they provide additional evidence to support or contradict the arguments provided. The applicability of using data from the Western Approaches and St George's Channel is discussed in Section 1.2.

The layout of this chapter is designed to allow increasing levels of complexity to be dealt with while showing the initial data, hypotheses and assumptions at each stage. The chapter

starts with a discussion of the data used and then considers the maturity of the Jurassic to understand the potential effects on the Rock-Eval and TOC data. Source rock richness as a factor of TOC is then discussed, before moving on to source rock quality which is dealt with as a factor of TOC and S₂ yield. Kerogen type is then described and discussed before focus is brought to key wells and estimating their potential for petroleum generation and expulsion.

5.1.2. Objectives

- 1) To evaluate the availability and quality of geochemical and wireline well data in the region of interest (Section 5.2).
- 2) To analyse the thermal maturity of the Jurassic interval within the region of interest (Section 5.3) utilising Vitrinite Reflectance (Section 4.2.4) and other indicators of thermal maturity (discussed in Section 4.2.1.1 & Section 4.2.5).
- 3) To identify periods of geological time associated with increased source rock richness, using statistical methods such as arithmetic average and median combined with the use of measures of central tendency and standard deviation to evaluate the homogeneity of source rock rich intervals (Section 5.4).
- 4) To analyse source rock quality through the use of pyrolysis and TOC data (Section 5.5)
- 5) To perform kerogen type analysis utilising the pseudo-van Krevelen plot method combined with other indications of kerogen type (Section 5.6).
- 6) To plot pyrolysis Rock-Eval geochemical data (HI, S₁...etc.) and TOC against wireline data over the Jurassic interval for Key Wells, in order to further discriminate and analyse zones of enriched source rock potential (Section 5.7).
- 7) To quantify potential hydrocarbon volumes that could be generated and expelled if the zones identified were taken to high thermal maturity for oil and gas (~200°C), using KinEx software (Section 4.4).

Well	Region	Basin	Latitude	Longitude	Total Depth (MD ft)	Total Depth (MD m)	Spud Date	Completion Date	Operator	Geochemical Contractors	Source of Data
72/10-1	Western Approaches	Melville Basin	48°47'22.9"N	09°06'1.4"W	2613	796.4	19/12/1978	05/01/1979	BP (BNO)	Robertson Research	Geochemistry Report
72/10-1A	Western Approaches	Melville Basin	48°47'23.4"N	09°06'01.9"W	12146	3702.1	08/01/1979	02/04/1979	BP (BNO)	Geochem Laboratories	Geochemistry Report
73/02-1	Western Approaches	Melville Basin	48°54'59.2"N	08°37'01.2"W	10454	3186.4	15/07/1983	16/08/1983	Monsanto Oil	Petra-Chem Ltd	Geochemistry Report
73/07-1	Western Approaches	Melville Basin	48°31'49.1"N	08°37'18.0"W	10013	3052.0	24/07/1981	30/09/1981	Phillips Petroleum	Geochem Laboratories	Geochemistry Report
73/13-1	Western Approaches	Melville Basin	48°34'18.7"N	08°26'22.8"W	8703	2652.7	04/05/1983	30/05/1983	Murphy Petroleum	Paleochem Ltd	Geochemistry Report
73/14-1	Western Approaches	Melville Basin	48°36'03.1"N	08°19'36.6"W	7782	2372.0	Unknown	Unknown	Murphy Petroleum	Palaeoservices	Geochemistry Report
83/24-1	Western Approaches	Melville Basin	49°10'35.1"N	08°20'34.3"W	3424	1043.6	29/08/1977	16/09/1977	Department of Energy, UK	BP (Geochemistry Branch)	Zephyr Report
87/14-1	Western Approaches	South West Channel Basin	49°32'02.3"N	04°12'25.6"W	4029	1228.0	09/08/1977	22/08/1977	Department of Energy, UK	BP (Geochemistry Branch)	Zephyr Report
87/16-1	Western Approaches	South West Channel Basin	49°26'21.7"N	04°53'17.4"W	3049	929.3	09/10/1977	20/10/1977	Department of Energy, UK	BP (Geochemistry Branch)	Zephyr Report
88/02-1	Western Approaches	Plymouth Bay Basin	49°51'13.9"N	03°47'21.2"W	2863	872.6	11/07/1977	04/08/1977	Department of Energy, UK	BP (Geochemistry Branch)	Zephyr Report
93/02-1	Celtic Sea	South Celtic Sea Basin	50°57'09.8"N	06°46'56.5"W		0.0	25/03/1974	04/06/1974	BP	Phillips/Robertson Research	Geochemistry Reports
102/29-1	Celtic Sea	South Celtic Sea Basin	51°05'22.0"N	06°20'38.4"W	5638	1718.5	10/07/1977	27/07/1977	Conocophillips	Robertson Research	End of Well Report
103/21-1	Celtic Sea	South Celtic Sea Basin	51°14'02.0"N	05°48'13.1"W	6466	1970.8	17/07/1976	21/07/1976	BP (AMOCO)	Geochem Laboratories	Geochemistry Report
103/01-1	Celtic Sea	North Celtic Sea Basin	51°58'46.5"N	05°53'51.2"W	16300	4968.2	19/05/1994	29/09/1994	Marathon	Armstrong and Associates/Marathon	Geochemistry Reports
103/02-1	Celtic Sea	North Celtic Sea Basin	51°52'42"N	05°47'30"W	10410	3173.0	09/10/1976	12/02/1977	Chevron	Texaco/Robertson Research	Geochemistry Reports
106/18-1	Celtic Sea	St George's Channel Basin	52°22'14"N	05°32'23.9"W	8569	2611.8	18/09/1995	07/10/1995	Marathon	Armstrong and Associates	Geochemistry Report
106/24-1	Celtic Sea	St George's Channel Basin	52°11'17.0"N	05°19'54.5"W	9136	2784.7	17/02/1974	07/05/1974	BP (ARCO)	Robertson Research	Geochemistry Report
106/28-1	Celtic Sea	St George's Channel Basin	52°01'57.6"N	05°35'44.6"W	10010	3051.0	16/08/1976	04/11/1976	Shell (British Gas)	ESSO/Robertson Research	Geochemistry Reports
107/16-1	Celtic Sea	St George's Channel Basin	52°22'09.5"N	04°48'35"W	6440	1962.9	06/11/1984	28/12/1984	Shell (British Gas)	Petra-Chem Ltd	Geochemistry Report
107/21-1	Celtic Sea	St George's Channel Basin	52°19'50"N	04°52'45.4"W	7131	2173.5	13/10/1978	25/11/1978	Shell (British Gas)	ESSO/Geochem Laboratories/Merlin	Geochemistry Reports
98/11-1	Wytch Farm	Wessex Basin	50°39'13.3"N	01°49'55.2"W	7167	2184.5	12/03/1983	28/04/1983	Shell (British Gas)	Paleochem Ltd	Geochemistry Report
98/11-2	Wytch Farm	Wessex Basin	50°37'49.7"N	01°50'28.6"W	11391	3472.0	06/06/1984	23/08/1984	Shell (British Gas)	Geochem Laboratories	Geochemistry Report
98/11-3	Wytch Farm	Wessex Basin	50°39'37.0"N	01°48'43.1"W	6915	2107.7	07/08/1986	07/10/1986	Shell (British Gas)	Petra-Chem Ltd	Geochemistry Reports
98/11-4	Wytch Farm	Wessex Basin	50°37'35.7"N	01°49'55.5"W	6798	2072.0	12/02/1987	20/03/1987	Shell (British Gas)	Petra-Chem Ltd	Geochemistry Report
98/13-1	Wytch Farm	Wessex Basin	50°38'35.3"N	01°30'27.1"W	7960	2426.2	24/03/1991	03/05/1991	ELF Enterprise	Robertson Research	End of Well Report
98/16-1	Wytch Farm	Wessex Basin	50°28'22.3"N	01°54'42.6"W	8150	2484.1	25/08/1988	25/10/1988	Occidental Petroleum	Geochem Laboratories	End of Well Report
98/16-2A	Wytch Farm	Wessex Basin	50°28'53.7"N	01°56'18.9"W	8638	2632.9	20/01/1991	14/03/1991	ELF Enterprise	Palaeoservices/Robertson Group	End of Well Report
98/22-1B	Wytch Farm	Wessex Basin	50°14'39.0"N	01°39'22.3"W	2489	758.6	06/02/1979	30/03/1979	Shell (British Gas)	Geochem Laboratories	Geochemistry Report
98/22-2	Wytch Farm	Wessex Basin	50°14'51.2"N	01°40'30.7"W	4813	1467.0	06/10/1979	13/11/1979	Shell (British Gas)	British Gas	Geochemistry Reports
98/23-1	Wytch Farm	Wessex Basin	50°14'35.9"N	01°31'16"W	5059	1542.0	26/03/1983	01/06/1983	Conocophillips	Paleochem Ltd	Geochemistry Report
99/12-1	Wytch Farm	Wessex Basin	50°39'22.6"N	00°46'30"W	4000	1219.2	22/06/1984	16/07/1984	ESSO	Hartman-Stroup	Geochemistry Report

Table 5.1. Database of the wells analysed in this thesis including regional information, geographical coordinates, total drilling depths, drilling dates, operators and geochemical contractors and the source file for geochemical data.

Well	Region	Basin	Key Well	VR				Visual Analysis				TOC	Pyrolysis (Rock-Eval)				Wireline						Other		
				Data	Populations	Histograms/Raw Data	Data Extents	SCI	TAI	Kerogen Comp	Other		Data Extents	S1	S2*	S3**	Tmax	GR	SGR	Rho	CNL	DT		Resis	Other Loaded
72/10-1	Western Approaches	Melville Basin	x	✓	✓	x	E Cret, E Jur & Tr	✓	x	✓	x	E Cret, L Cret, E Jur & Tr	✓	✓	✓	✓	x	x	x	x	x	x		No lis, dils or las files available	
72/10-1A	Western Approaches	Melville Basin	x	✓	✓	x	E Jur-Tr	x	x	✓	✓	E Cret, E Jur & Tr	x	x	x	x	✓	x	✓	✓	✓	x			
73/02-1	Western Approaches	Melville Basin	x	✓	✓	x	Paleogene, E Cret & Tr	✓	x	✓	x	Paleogene, E Cret & Tr	x	x	x	x	✓	x	✓	✓	✓	x			
73/07-1	Western Approaches	Melville Basin	x	✓	✓	✓	L Cret & Tr	x	x	x	✓	Paleogene, E Cret & Tr	x	x	x	✓	✓	x	x	✓	✓	✓			
73/13-1	Western Approaches	Melville Basin	✓	✓	✓	x	E Cret, E Jur & Tr	✓	✓	x	x	E Jur-Tr	✓	✓	x	✓	✓	x	✓	✓	✓	✓			
73/14-1	Western Approaches	Melville Basin	x	x	x	x	x	x	x	x	x	Tr	✓	✓	x	✓	✓	x	✓	✓	✓	✓			
83/24-1	Western Approaches	Melville Basin	x	x	x	x	x	x	x	x	x	Neogene, L Cret & Carb/Dev	x	x	x	x	x	x	x	x	x	x		No lis, dils or las files available	
87/14-1	Western Approaches	South West Channel Basin	x	x	x	x	x	x	x	x	x	Paleogene, L Cret & Perm/Tr	x	x	x	x	x	x	x	x	x	x		No lis, dils or las files available	
87/16-1	Western Approaches	South West Channel Basin	x	x	x	x	x	x	x	x	x	Paleogene-L Cret	x	x	x	x	x	x	x	x	x	x		No lis, dils or las files available	
88/02-1	Western Approaches	Plymouth Bay Basin	✓	✓	✓	x	E Jur-Tr	✓	x	✓	x	L Cret, E Jur & L Tr	x	x	x	x	✓	x	✓	✓	✓	x			
93/02-1	Celtic Sea	South Celtic Sea Basin	✓	✓	✓	x	Paleogene, E Cret & Jur	✓	✓	✓	x	E Cret & Undiff Jur	✓	✓	✓	✓	x	x	x	x	x	x		No lis, dils or las files available	
102/29-1	Celtic Sea	South Celtic Sea Basin	✓	✓	x	x	E Jur	✓	x	✓	x	E Cret & E Jur	x	x	x	x	✓	x	✓	✓	✓	✓			
103/21-1	Celtic Sea	South Celtic Sea Basin	✓	x	x	x	x	x	✓	✓	x	M Jur-Tr & Dev	x	x	x	x	✓	x	✓	✓	✓	✓			
103/01-1	Celtic Sea	North Celtic Sea Basin	✓	✓	✓	x	L Jur-E Jur	x	x	x	x	L Jur-E Jur	✓	✓	x	✓	✓	✓	✓	✓	✓	✓		Lith from Comp Log	Gas Chromatography & Biomarker Analysis
103/02-1	Celtic Sea	North Celtic Sea Basin	✓	x	x	x	x	x	✓	x	x	M Jur-Tr	x	x	x	x	✓	x	x	x	x	x			
106/18-1	Celtic Sea	St George's Channel Basin	x	✓	✓	x	E Jur-Tr	x	x	✓	x	E Jur-Tr & Carb	✓	✓	x	✓	✓	x	✓	✓	✓	✓		Limited Data Extents	
106/24-1	Celtic Sea	St George's Channel Basin	x	x	x	x	x	x	x	x	x	Cret-M Jur	x	x	x	✓	x	x	x	x	x	x		No lis, dils or las files available	Palaeotemp & Light HC analysis
106/28-1	Celtic Sea	St George's Channel Basin	x	✓	✓	x	Paleogene, E Jur & Tr	✓	✓	✓	x	M Jur-Tr	✓	✓	✓	✓	✓	x	x	x	x	x			
107/16-1	Celtic Sea	St George's Channel Basin	x	✓	✓	x	L Jur-M Jur	✓	x	✓	x	L Jur-M Jur	x	x	x	x	✓	x	✓	✓	✓	✓			
107/21-1	Celtic Sea	St George's Channel Basin	x	✓	✓	x	L Jur-M Jur	✓	x	✓	x	Paleogene & L Jur-E Jur	✓	✓	✓	✓	✓	✓	✓	✓	✓	✓			
98/11-1	Wythch Farm	Wessex Basin	x	✓	✓	✓	L Jur-Tr	✓	x	✓	x	E Cret-Tr	✓	✓	x	x	Wells included to increase geochemical database							Error with lis conversion	Gas Chromatography
98/11-2	Wythch Farm	Wessex Basin	x	✓	✓	✓	L Jur-Tr	✓	x	✓	x	E Cret-L Tr	✓	✓	x	x	Wells included to increase geochemical database								
98/11-3	Wythch Farm	Wessex Basin	x	✓	✓	x	E Cret-E Jur	✓	x	✓	x	E Cret-L Tr	✓	✓	x	✓	Wells included to increase geochemical database								
98/11-4	Wythch Farm	Wessex Basin	x	✓	✓	x	L Jur & E Jur	✓	x	✓	x	L Jur-E Jur	✓	✓	x	✓	Wells included to increase geochemical database								
98/13-1	Wythch Farm	Wessex Basin	✓	✓	✓	x	M Jur-Perm	✓	x	✓	x	L Jur-E Jur	✓	✓	✓	✓	Wells included to increase geochemical database								
98/16-1	Wythch Farm	Wessex Basin	x	✓	✓	x	M Jur-L Jur	x	✓	✓	x	E Cret-Tr	✓	✓	x	✓	Wells included to increase geochemical database								
98/16-2A	Wythch Farm	Wessex Basin	x	✓	✓	x	E Cret-Perm/Tr	x	✓	✓	x	E Cret-L Tr	✓	✓	x	✓	Wells included to increase geochemical database								
98/22-1B	Wythch Farm	Wessex Basin	x	x	x	x	x	x	✓	✓	x	M Jur-L Tr	x	x	x	✓	Wells included to increase geochemical database								
98/22-2	Wythch Farm	Wessex Basin	x	✓	✓	x	M Jur-Tr	x	✓	✓	x	M Jur-L Tr	✓	✓	x	✓	Wells included to increase geochemical database								
98/23-1	Wythch Farm	Wessex Basin	✓	✓	✓	x	M Jur-E Jur	✓	x	✓	x	L Jur-L Tr	✓	✓	x	✓	Wells included to increase geochemical database								
99/12-1	Wythch Farm	Wessex Basin	x	x	x	x	x	x	✓	✓	x	Paleogene-M Jur & Basement	✓	✓	✓	✓	Wells included to increase geochemical database							No wireline data included in lis	Gas Chromatography & Carbon Isotopes Gas Chromatography Biomarker Analysis

Table 5.2. Database of geochemical and wireline data utilised including VR, Visual Kerogen Analysis, TOC, Pyrolysis and wireline logs.

5.2.1. HI & OI - Rock-Eval and TOC

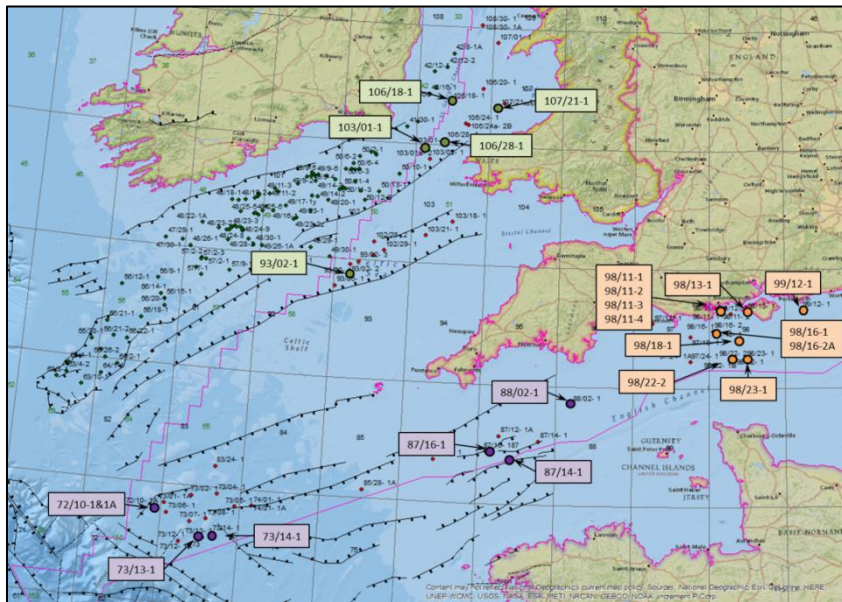


Fig 5.3. Map of the region offshore the south west of Britain showing the 18 wells with S2 pyrolysis peaks available that have been used along with TOC to calculate HI values (Section 4.2.1.2).

Table 5.2 summarises the range of geochemical data and wireline data included in this study with additional data from Wytch Farm and the St George's Channel Basin added in to make up for the lack of pyrolysis data (Fig 5.3-5.6); primarily S2 peaks & S3 peaks (Table 5.3) which can be used to calculate OI and HI when combined with TOC - Section 4.2.1.2. While inclusion of Wytch Farm and St George's Channel Basin wells has increased the amount of S2 data available to 18 wells (Fig 5.3) there are still only seven wells with S3 peaks data available (Fig 5.4). The applicability of using Wytch Farm and St George's Channel Basin data as analogues for the Western Approaches and Celtic Sea Basins is discussed in detail in the Discussion (Section 6.5).

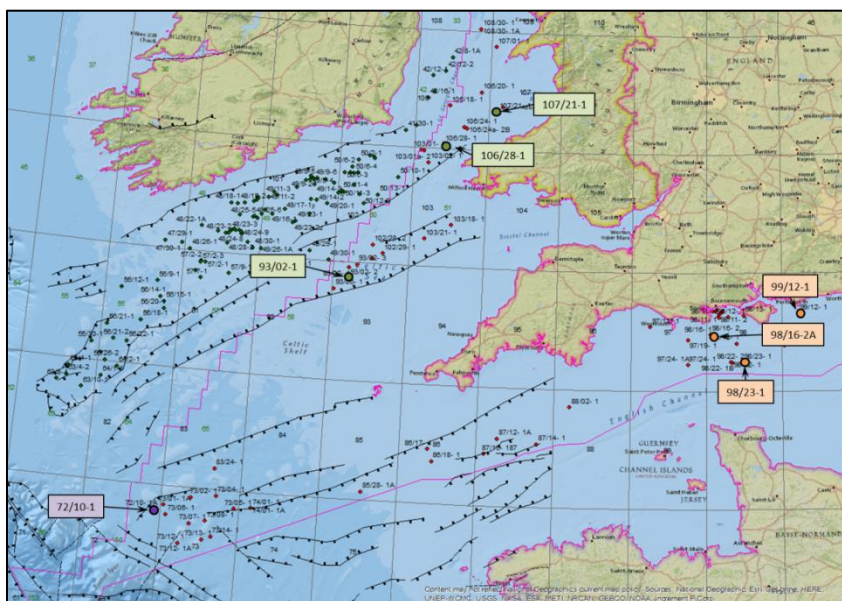


Fig 5.4. Map of the region offshore the south west of Britain showing the 7 wells with S3 pyrolysis peaks available that have been used along with TOC to calculate OI values (Section 4.2.1.2).

Region	TOC	Hydrogen Index	Oxygen Index
	No. Samples (N)	No. Samples (N)	No. Samples (N)
All	2364	568	215
Western Approaches	447	104	31
Wytch Farm	1068	291	78
Celtic Sea	849	173	106

Table 5.3. Summary of the number of samples available for TOC, HI and OI divided by region.

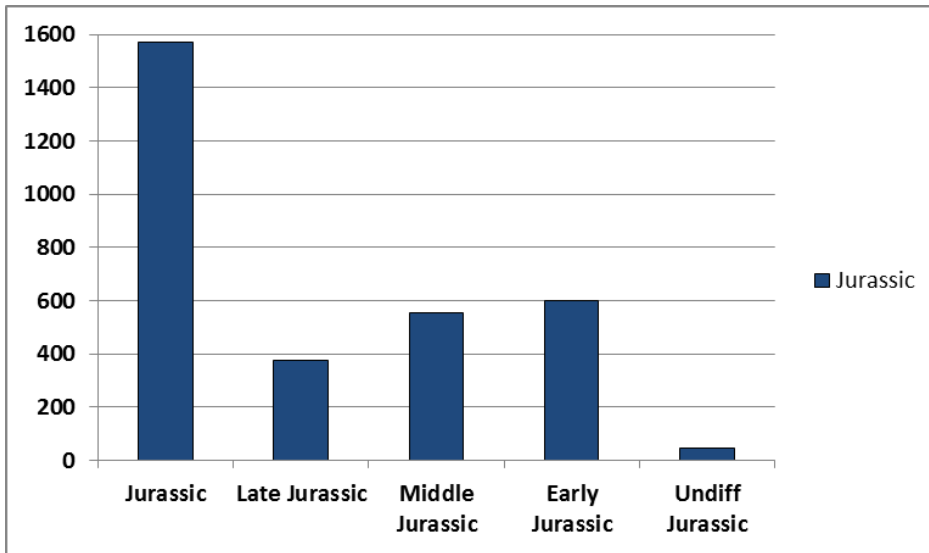


Fig 5.5. Histogram showing the distribution of TOC measurements within the Jurassic interval with samples favouring the Early and Middle Jurassic with 35 samples labelled as only "Jurassic".

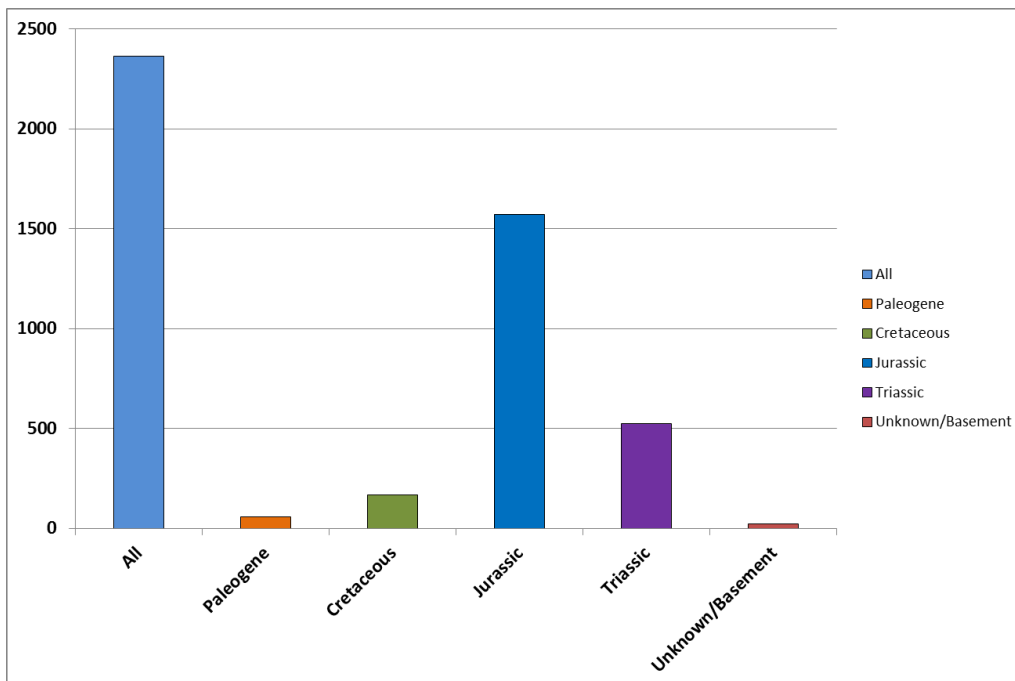


Fig 5.6. A histogram of all the Total Organic Carbon (TOC) samples included in the analysis.

5.2.2. Thermal Maturity Indicators

Vitrinite Reflectance (VR) data has been run on over two-thirds of the wells analysed with 23 wells including VR data (Table 5.4). The majority of VR measurements (22 wells) include the population of samples i.e. how many vitrinite samples were measured for a single VR data point. An additional four wells include a summary of the raw data or a histogram of these sample populations allowing the integrity of each point to be analysed. The inclusion of sampling population values and raw data/histograms is integral as each factor enables further interrogation of the data quality. The larger the sample population of each measurement the better and lower standard deviation and greater central tendency increases confidence in each data point.

Well	Region	Basin	VR				Visual Analysis				Pyrolysis
			Data	Populations	Histograms/Raw Data	Data Extents	SCI	TAI	Kerogen Comp	Other	Tmax
72/10-1	Western Approaches	Melville Basin	✓	✓	x	E Cret, E Jur & Tr	✓	x	✓	x	✓
72/10-1A	Western Approaches	Melville Basin	✓	✓	x	E Jur-Tr	x	x	✓	✓	x
73/02-1	Western Approaches	Melville Basin	✓	✓	x	Paleogene, E Cret & Tr	✓	x	✓	x	x
73/07-1	Western Approaches	Melville Basin	✓	✓	✓	L Cret & Tr	x	x	x	✓	✓
73/13-1	Western Approaches	Melville Basin	✓	✓	x	E Cret, E Jur & Tr	✓	✓	x	x	x
73/14-1	Western Approaches	Melville Basin	x	x	x	x	x	x	x	x	✓
83/24-1	Western Approaches	Melville Basin	x	x	x	x	x	x	x	x	x
87/14-1	Western Approaches	South West Channel Basin	x	x	x	x	x	x	x	x	x
87/16-1	Western Approaches	South West Channel Basin	x	x	x	x	x	x	x	x	x
88/02-1	Western Approaches	Plymouth Bay Basin	✓	✓	x	E Jur-Tr	✓	x	✓	x	x
93/02-1	Celtic Sea	South Celtic Sea Basin	✓	✓	x	Paleogene, E Cret & Jur	✓	✓	✓	x	✓
102/29-1	Celtic Sea	South Celtic Sea Basin	✓	x	x	E Jur	✓	x	✓	x	x
103/21-1	Celtic Sea	South Celtic Sea Basin	x	x	x	x	x	x	✓	✓	x
103/01-1	Celtic Sea	North Celtic Sea Basin	✓	✓	x	L Jur-E Jur	x	x	x	x	✓
103/02-1	Celtic Sea	North Celtic Sea Basin	x	x	x	x	x	✓	x	x	x
106/18-1	Celtic Sea	St George's Channel Basin	✓	✓	x	E Jur-Tr	x	x	✓	x	✓
106/24-1	Celtic Sea	St George's Channel Basin	x	x	x	x	x	x	x	x	✓
106/28-1	Celtic Sea	St George's Channel Basin	✓	✓	x	Paleogene, E Jur & Tr	✓	✓	✓	x	✓
107/16-1	Celtic Sea	St George's Channel Basin	✓	✓	x	L Jur-M Jur	✓	x	✓	x	x
107/21-1	Celtic Sea	St George's Channel Basin	✓	✓	✓	L Jur-M Jur	✓	x	✓	x	✓
98/11-1	Wythch Farm	Wessex Basin	✓	✓	✓	L Jur-Tr	✓	x	✓	x	x
98/11-2	Wythch Farm	Wessex Basin	✓	✓	✓	L Jur-Tr	✓	x	✓	x	x
98/11-3	Wythch Farm	Wessex Basin	✓	✓	x	E Cret-E Jur	✓	x	✓	x	✓
98/11-4	Wythch Farm	Wessex Basin	✓	✓	x	L Jur & E Jur	✓	x	✓	x	✓
98/13-1	Wythch Farm	Wessex Basin	✓	✓	x	M Jur-Perm	✓	x	✓	x	✓
98/16-1	Wythch Farm	Wessex Basin	✓	✓	x	M Jur-L Jur	x	✓	✓	x	✓
98/16-2A	Wythch Farm	Wessex Basin	✓	✓	x	E Cret-Perm/Tr	x	✓	✓	x	✓
98/22-1B	Wythch Farm	Wessex Basin	x	x	x	x	x	✓	✓	x	x
98/22-2	Wythch Farm	Wessex Basin	✓	✓	x	M Jur-Tr	x	✓	✓	x	x
98/23-1	Wythch Farm	Wessex Basin	✓	✓	x	M Jur-E Jur	✓	x	✓	x	x
99/12-1	Wythch Farm	Wessex Basin	x	x	x	x	x	✓	✓	x	x

Table 5.4. Summary of the indicator of thermal maturity utilised in this project.

The geographical distribution of wells with VR measurements is shown in Fig 5.7. Wells are present in every basin with geochemical sampling except the South West Channel Basin with each region including five or more wells with VR populations. The VR data have been cross checked against additional maturity indicators such as spore colouration information from visual analysis (Section 4.2.5) and Tmax (Section 4.2.1.1); the extents of these data are summarised in Table 5.4 with 24 wells providing data on maturity from visual analysis which is quite often backed up kerogen composition information. 15 wells include information from Rock-Eval pyrolysis on Tmax. The strengths and pitfalls of both of these data are discussed in Chapter 4 and the data have been included to provide a better constraint on the thermal maturity of the region of interest.

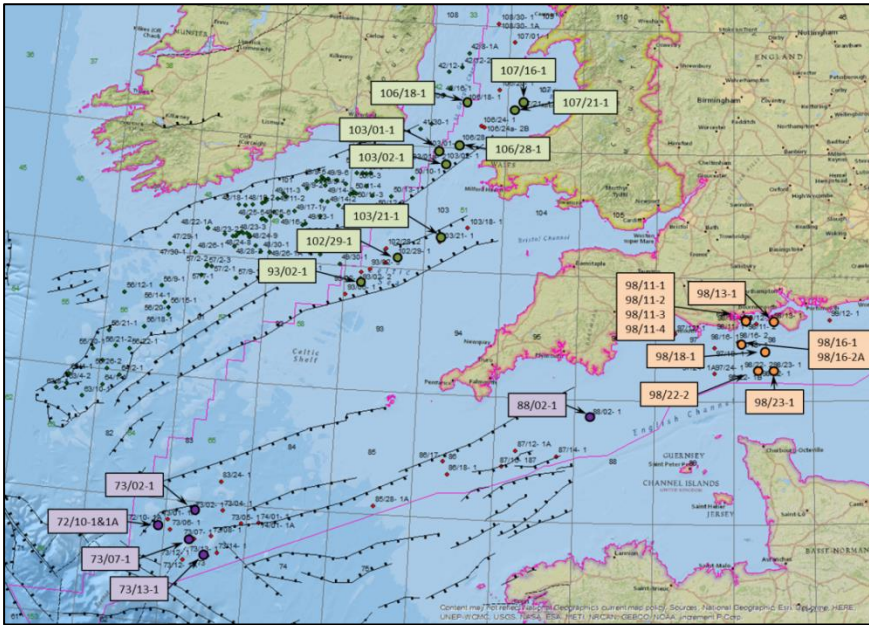


Fig 5.7. Map of the region offshore the south west of Britain showing the 23 wells with Vitrinite Reflectance (VR) data (Section 4.2.4).

5.2.3. Summary

- Geochemical data have been mined and analysed from 31 wells from the Celtic Sea, Western Approaches, St George's Channel and Wytch farm.
- No geochemical information was available from the St Mary's Basin.
 - Only 88/02-1 available in the Plymouth Bay basin
 - 87/16-1 & 87/14-1 have TOC data in the South West Channel Basin but no Rock-Eval or VR data.
- TOC and Rock-Eval data are skewed to the Jurassic.
- The size of the region of interest and the low density of some data types such as Oxygen Index and Vitrinite Reflectance will affect the ability to draw robust conclusions.
- Data from the St George's Channel and Wytch Farm have been added to the project to increase the amount of geochemical measurements for analysis.

5.3. Maturity

The maturity of the Jurassic interval in the region of interest is discussed first in this chapter due to the effect thermal maturity has on pyrolysis and TOC data. TOC and the S2 and S3 yield decrease with increasing maturity as the organic matter is converted into hydrocarbons and expelled (Section 4.5).

Analysis of the wells in blocks 106 & 107 and Wytch Farm was carried out similarly to that described in this section but are not discussed here as the wells lie outside the region of interest but nonetheless provide useful correlation information.

5.3.1. Indicators of Thermal Maturity

5.3.1.1. Celtic Sea

103/01-1

Two geochemical analyses done in parallel by James Armstrong and Associates (1995) and Dembicki Jr (1995) on behalf of Marathon Oil with data based on sidewell cores (7 used by Armstrong and Associates) and cuttings (40 cuttings used by Armstrong and Associates and 36 cutting samples used by Dembicki Jr 1995). The Vitrinite Reflectance data for well 103/01-1 (Dragon Discovery) are shown in Figure 5.8 (from James Armstrong and Associates, 1995). Armstrong and Associates have described four populations of VR data based on their experience with a preferred population (pink) and populations 1-3 (orange, green and blue) which they interpret, respectively to represent bitumen, caved material, reworked organic matter and inertinite. Tmax (Fig 5.8) shows an increasing trend from 435°C at 3000 ft (914 m) to ~445°C by 11,000 ft (3352 m).

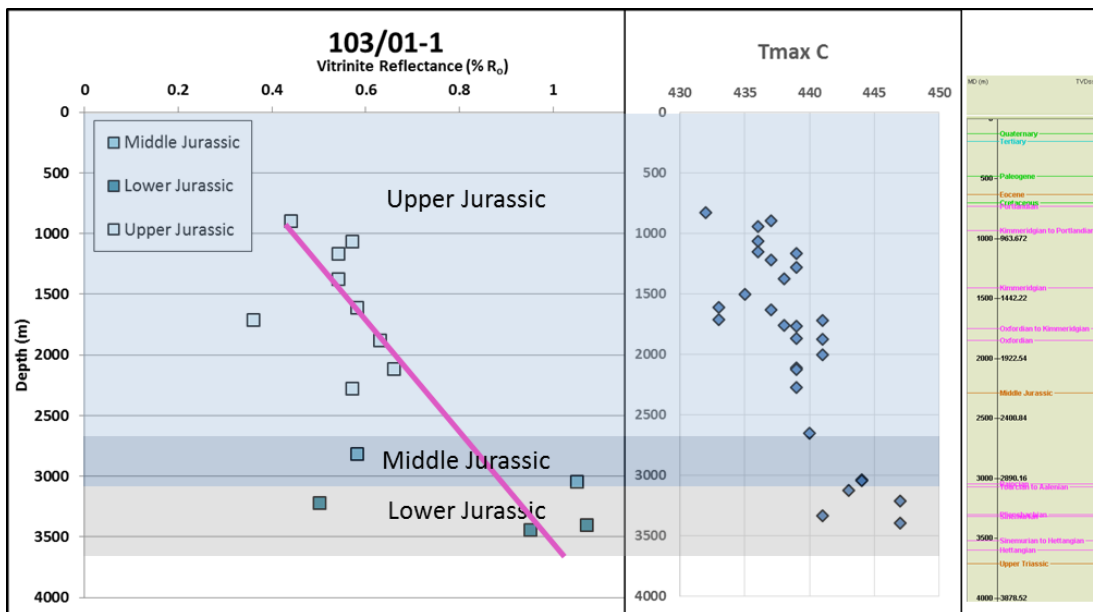


Fig 5.8. Vitrinite Reflectance versus Depth (MD ft) for 103/01-1. The Upper Jurassic only reaches the oil window below 7500 ft (2286 m) with the entirety of the Middle Jurassic situated in the oil window. The Lower Jurassic passes into late mature at approximately 11500 ft (3505 m). Tmax is shown as blue diamonds next to the R_o profile for VR with Tmax initially between 435-440°C (3000-9000 ft or 914-2743 m) and increasing to 440-450°C at depths greater than 10,000 ft (3048 m).

Armstrong and Associates (1995) have included an interpreted R_o profile that increases from immaturity (<4000 ft or <1219 m) to early maturity (4000-7500 ft or 1219-2286 m) to the oil window (7500-11500 ft) and through to late maturity (>11500 ft or >3505 m). This is in contrast to the Tmax population which suggests the sediments to be within the oil window (435-460°C - Section 4.2.1.1). The filtering of the R_o population by Armstrong and Associates (1995) in combination with the potential pitfalls with Tmax data discussed in Section 4.5 lead to the interpretation from the VR population to be preferred here. Visual kerogen analysis, if it was available, would potentially have provided an extra evidence to support or contradict this interpretation.

102/29-1

VR increases from 0.45% at 650 m to 0.55% at 1700 m (Fig 5.9) with some variation but along a marginally increasing trend. Visual analysis of plentiful spore and pollen present in samples was carried out using the Spore Colouration Index by Robertson Research (1977). SCI values vary from 2.5 at 2000 ft (610 m) to 3.5 at 4000 ft (1219 m) through to 5.0 at 5500 ft (1677 m). 3.0-3.5 represents the narrow zone between Immaturity and Early Maturity (Robertson Research, 1977). Robertson Research (1977) recorded that palaeo-temperature samples were measured but indicate these suggest maturity from 2000 ft (610 m) and are likely erroneous. Tmax data were not available for analysis in this case.

Jurassic sediments in 102/29-1 are interpreted to be Immature to Early Mature based on VR and visual analysis of spores and pollen.

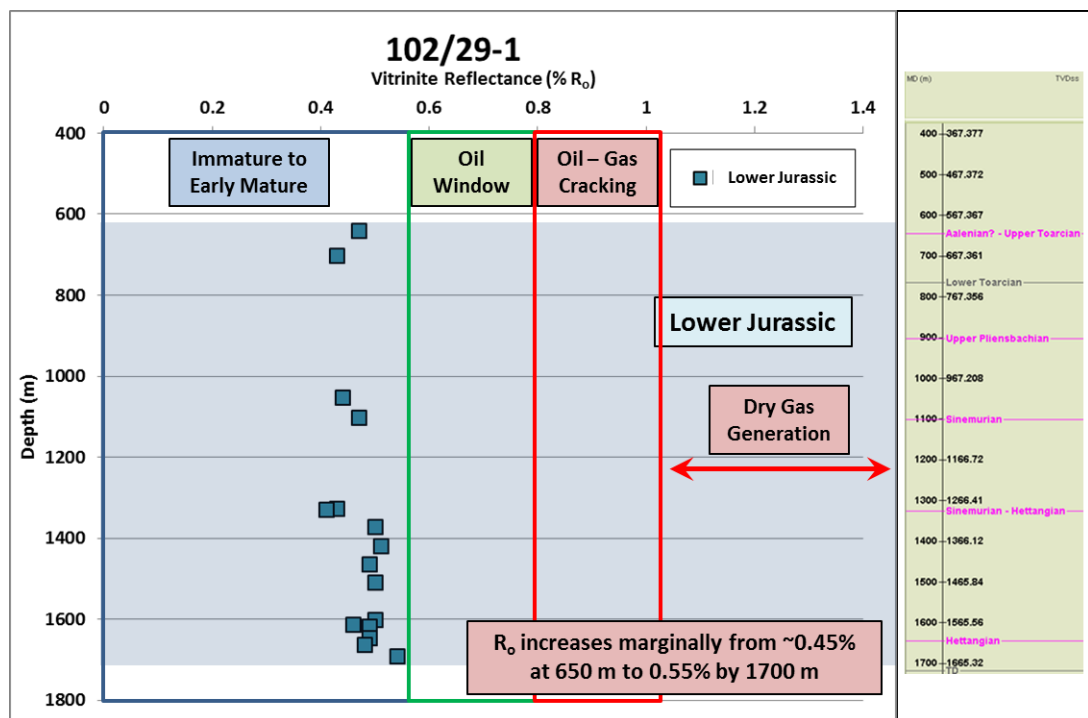


Fig 5.9. Vitrinite Reflectance (Population 1) vs Depth (m) plot from 102/29-1. The Vitrinite Reflectance shows a subtly increasing trend with depth with R_o increasing from 0.45% at 650 m to 0.55% at 1700 m. Maturity boundaries for R_o are shown based on Allen & Allen (2013).

Vitrinite Reflectance, Tmax and visual maturity indications data (Fig 5.10 & 5.11) were measured from samples in the Tertiary, Lower Cretaceous and the Jurassic (undifferentiated). Two R_o and one SCI measurement were taken in the Tertiary with seven R_o measurements and two SCI measurements in the Lower Cretaceous. In the Jurassic interval 13 R_o and seven SCI measurements were taken. A large degree of scatter can be seen in the VR data from the Jurassic and Lower Cretaceous which is interpreted by Robertson Research (1974) as relating to the presence of caved and low vitrinite samples. The SCI samples seem to be more constrained except for a stained palynomorph sample in the Lower Cretaceous. Tmax samples lie between 1500 and 2100 m and vary between 435°C and 445°C with substantial scatter.

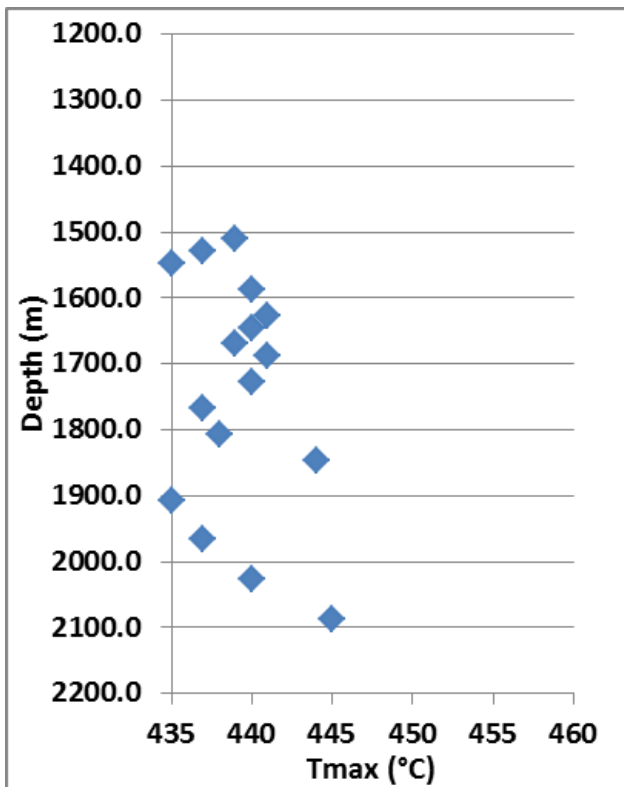


Fig 5.10. Tmax against Depth (m) plot for 93/02-1 with Tmax points indicated by blue diamonds. Tmax measurement are only available in the Jurassic (undifferentiated).

Increasing profiles of Vitrinite Reflectance and spore colouration (Fig 5.11) have been interpreted by Robertson Research (1994). Vitrinite Reflectance suggests that the sediments are likely immature to early mature with the SCI measurements indicating the organic matter as early mature. Tmax (Fig 5.10) indicates that rocks lie within the oil window, similar to 103/01-1. The interpretation favoured in this thesis is that the organic matter is at an early mature stage of maturity as indicated by both the VR and spore colouration analyses (Fig 5.11). The VR population in Figure 5.11 shows no significant jump is evident across the Top M2 Unconformity which suggests that the Jurassic interval is close to or at maximum burial at the current day.

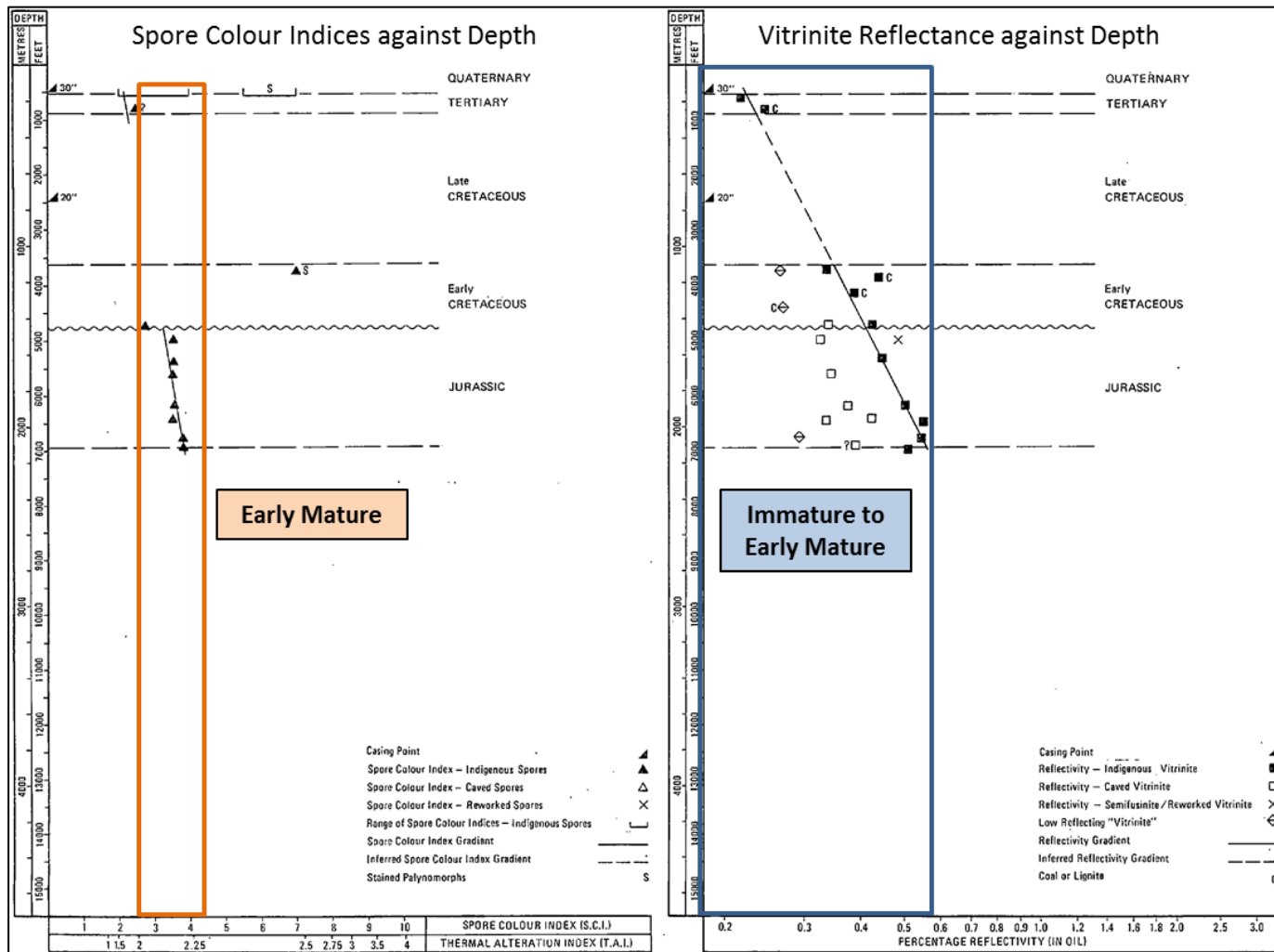


Fig 5.11. SCI against Depth (MD) and VR against Depth plot for well 93/02-1 modified after Robertson Research (1974). Reliable data has been coloured black with data interpreted as from reworking has been plotted as an X with caved data as open squares with low vitrinite samples a diamond.

5.3.1.2. Western Approaches

73/13-1

Geochemical analysis provided by Paleochem (1983) over the Cretaceous, Early Jurassic and Triassic section (5500-8700 ft or 1676-2652 m) using 94 cutting samples. Vitrinite Reflectance samples are available from 1650 m to 2200 m and show a large degree of variation (Fig 5.12) with the majority of data sitting between 0.30-0.65% R_o and only three data points sitting between 1.0-1.15% R_o (2050-2200 m). Figure 5.13 shows the same data with only samples with greater than 20% vitrinite plotted. The VR data sits between 0.45-0.60% R_o and sits at the edge of the oil window. SCI analysis run by Paleochem (1983) on spore samples found that samples from 5500-6000 ft (1676-1829 m) were predominantly yellow to medium orange increasing from 6000 ft (1829 m) to medium orange/yellow to dark orange down to 7100 ft (2164 m) where samples are indicated as dark orange to red. Tmax measurements were not available for 73/13-1.

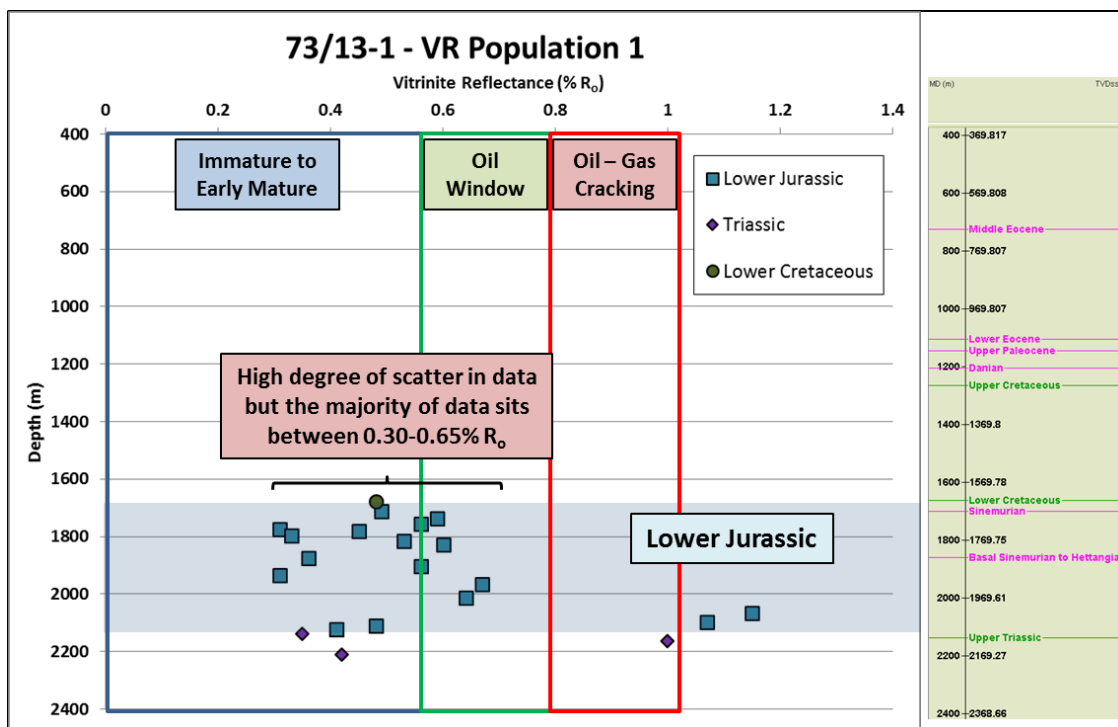


Fig 5.12. Plot of the preferred R_o population from the Paleochem (1983) geochemistry report against Depth (m MD). Data are present in from the Lower Cretaceous through to the Triassic. A summary of the SCI analysis is included as colour descriptions of the spore samples. The high degree of scatter within this plot could be due to issues with the data which are discussed in Section 4.5.

Indications from the filtered VR population in Figure 5.13 suggest that the Lower Jurassic is early mature to mature for oil generation. SCI measurements indicate that the Jurassic

section from 1675 to 1830 m is potentially early mature to mature with organic matter in peak oil generation from 1830-2164 m. The interpretation here is that the top Jurassic is early mature to mature with the sediments in the oil window from ~1830 m using VR data supported by visual kerogen measurements (Paleochem, 1983).

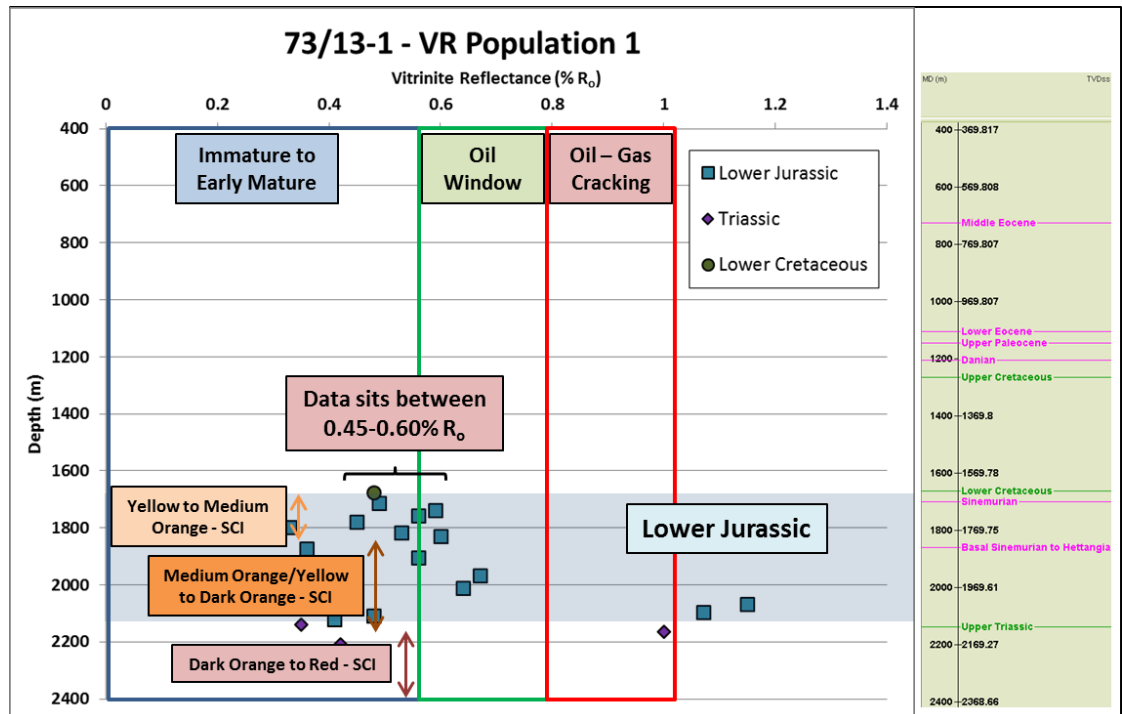


Fig 5.13. Plot of the preferred R_o population from the Paleochem (1983) geochemistry report against Depth (m MD). Data have only been included with 20% vitrinite to remove the effect of vitrinite lean samples.

72/10-1

Maturity analysis of 72/10-1 was carried out by Cooper & Collins (1979) with 20 samples analysed for Vitrinite Reflectance (Fig 5.14) and 27 for spore colouration (SCI methodology) and kerogen typing with an additional 12 samples used for Rock-Eval pyrolysis with Tmax information available. The analyses were produced on sidewall core and ditch cuttings samples provided by BNO.

Kerogen abundances were found to be low, with minimal amounts of vitrinite for VR analysis, producing small and scattered histogram populations (Cooper & Collins, 1979). A value of 0.31% R_o coupled with a SCI measurement of 3-3.5 is selected by Cooper & Collins (1979) as reliable. SCI values from 4630-5005 ft (1411-1526 m) are suggested as reliable with uniform spore colouration down to 5680 ft (1731 m). Tmax values are between 427-429°C from 4817-4973 ft (1468-1516 m). The interval from 8737-9288 ft (2663-2831 m) has a VR measurement of 1.16% R_o and an assigned SCI value of 8 (Fig 5.14) by Cooper & Collins (1979).

The VR data present for 72/10-1 suggests the section to be Immature to Mature for oil generation. The VR quality issues mentioned earlier are worth noting, however. The SCI values of 3-4 and Tmax values of 427-429°C indicate the section is more likely immature to early mature for hydrocarbon generation.

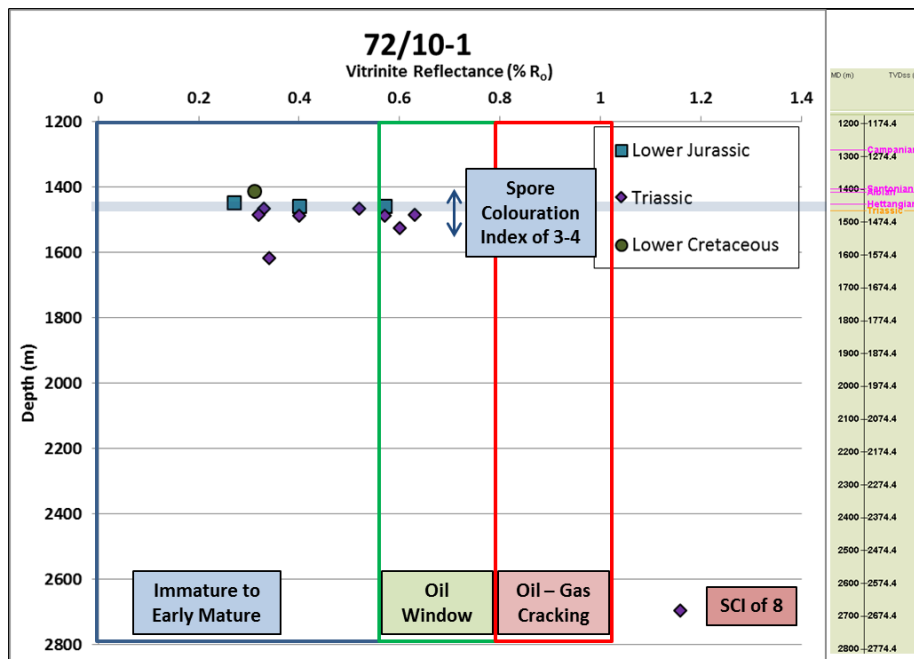


Fig 5.14. Plot of the preferred R_o population from the Robertson Research (1979) geochemistry report against Depth (m MD) with indications of the SCI values from visual kerogen analysis.

Cooper & Collins (1979) indicate that the section from 4630-6442 ft (1411-1964 m) is immature to early mature with interpreted increased maturity due to volcanic activity. An alternative hypothesis is that the zones of higher maturity are related to poor measurement quality as Cooper & Collins (1979) mention the low abundance of vitrinite for examination. The key interpretation is that indicators in the Early Jurassic section suggest that the section is immature to early mature. Whether late maturity occurs in the deepest section is debateable with high VR (1.16% R_o) and SCI value of 8 in the interval from 2663-2831 m (Triassic) being attributed to higher maturity by Cooper & Collins (1979). In contrast, Scotchman (unpublished work) suggests these indications of high maturity are more likely related to the presence of reworked material.

88/02-1

88/02-1 was drilled as a stratigraphic test well to determine sub-Chalk geology in the SW Approaches. Geochemical evaluation was done by BP Research, Sunbury with the data based on short cores and drill cuttings. Vitrinite Reflectance and visual analysis measurements are available for well 88/02-1 in the Plymouth Bay Basin (Evans *et al.*, 1977). The R_o population (Fig 5.15) demonstrates no determinable trend with variation between 0.30-0.55% R_o over the interval 420-750 m. Scotchman (unpublished work) links the variability in the VR data to bitumen staining of the vitrinitic material due to the presence of oil-prone kerogen in the samples.

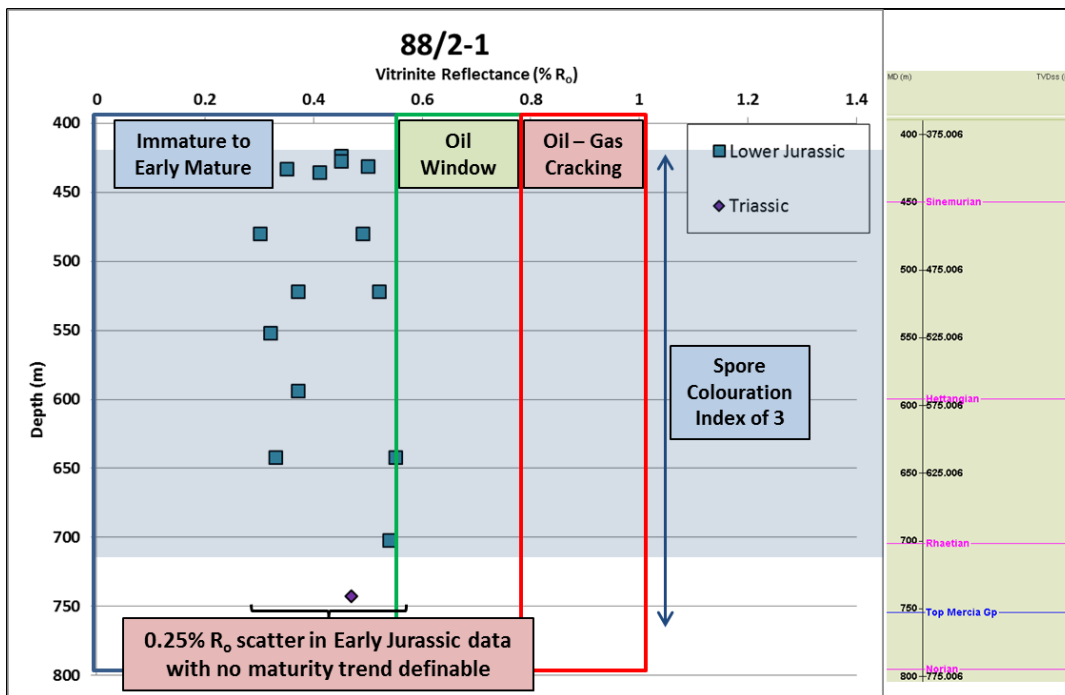


Fig 5.15. Plot of indicated autochthonous R_0 population (Evans *et al.*, 1977) against Depth with indications of the SCI over the depth.

SCI measurements of vitrinite bearing samples (Evans *et al.*, 1977) are consistently assigned a value of 3. No T_{max} data were available for 88/02-1. Scotchman (unpublished work) suggests that maturity indicators from gas chromatography (GC) indicate an immature Lower Jurassic section. Despite the variation in the R_0 population all measurements sit within the immature to early mature zone. SCI values and GC indicators indicate that the Lower Jurassic section is immature on-structure. The shallow depth of burial combined with VR and SCI indicates that it is likely that the Jurassic section in 88/02-1 is likely immature for hydrocarbon generation.

5.3.1.3. Discussion of Thermal Maturity from Geochemical Indicators

A summary figure of the interpreted thermal maturity for geochemical analyses is shown in Figure 5.16. The Jurassic sections in the wells analysed are generally considered to be immature to early mature for hydrocarbon generation. The only wells that have reached maturity for oil generation are 103/01-1, which is interpreted to be mature to late mature and 73/13-1 which is interpreted to reach the oil window at ~1830m (1654m TVDml). Armstrong and Associates interpret 103/01-1 to have reached the oil window from a depth of 7500 ft (2286 m MD – 2100 m TVDml). There is ~450 m difference between the two depths of top oil window. Hypotheses could be that the difference is due to the varying burial histories and tectonic histories of the basins (discussed in Chapter 2 & Section 6.3) or that there are errors in the measurements. More data are required to investigate the relationship between maturity and depth and map zones of similar maturity within the Western Approaches and Celtic Sea. Addition VR data in the St Mary' Channel, South West Channel and Plymouth Bay Basins would be the most useful as this area has the least wells with maturity indicators but extra data would be necessary in each basin. The general trend of immaturity to early maturity in the region means that there is unlikely to be a substantial on the Rock-Eval and TOC data outside isolated examples such as 103/01-1. In the case of 103/01-1 the S1 peak has been analysed to understand the effect of generation on the Rock-Eval and TOC measurements.

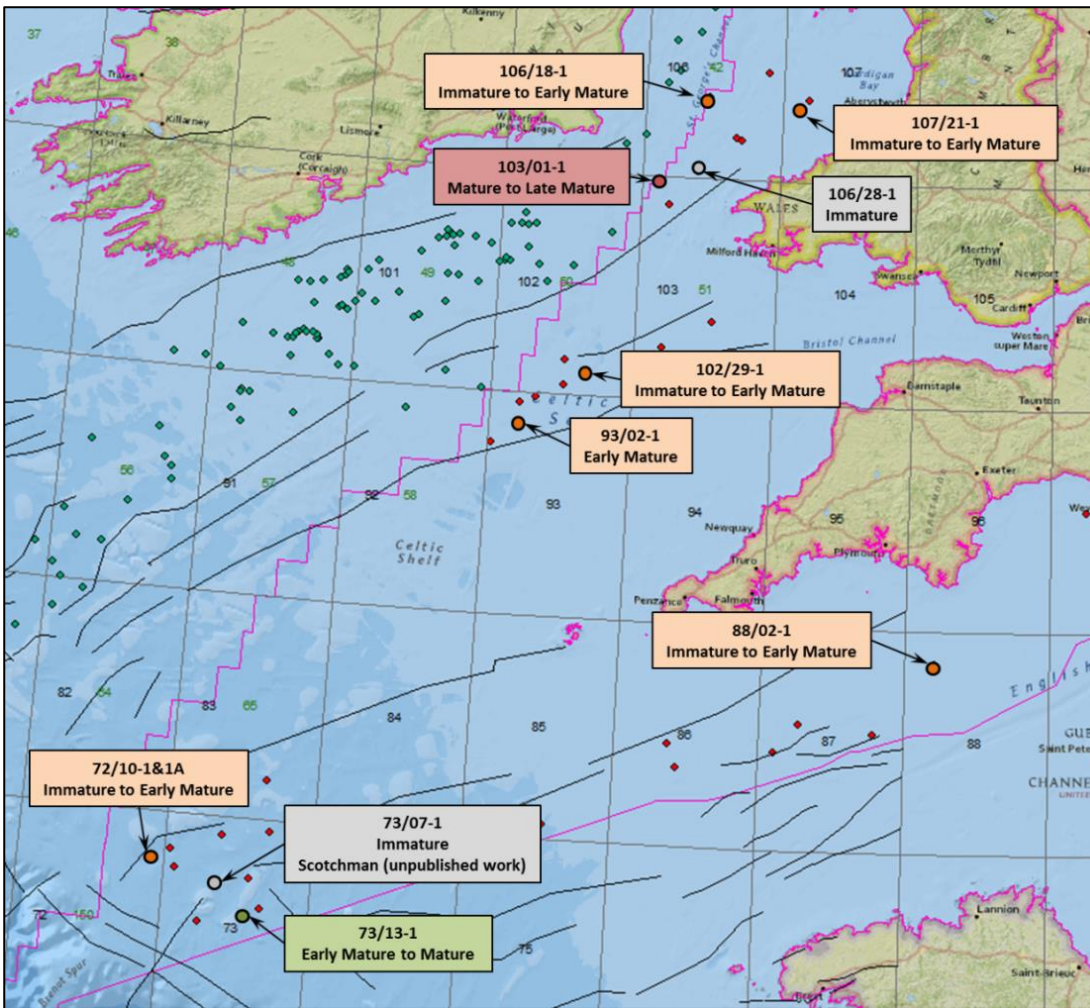


Fig 5.16. Map of the region of interest with wells with maturity data for the Early Jurassic coloured by interpreted level of maturity from the geochemistry reports. Immature – red; immature to early mature – orange; over mature – blue. Interpretations are based on vitrinite reflectance, spore colouration index and Tmax available in the geochemistry reports. Analysis of 73/07-1 was provided by Scotchman (unpublished work).

5.3.2. Summary of Basin History Models

In this section burial history models and time-depth plots will be presented for the Western Approaches from Hillis (1988), Ruffell (1995) and Ottaviani *et al.* (unpublished work) and Murdoch (1995) for the North Celtic Sea Basin. The burial history models available are discussed here to further analyse the thermal maturity for the region of interest, with a focus on how the tectonic history (i.e. rift phases, uplift...etc.) may have affected the maturity and timing of maturity in the separate basins.

5.3.2.1. Western Approaches

Hillis (1988)

Hillis (1988) presented curves of tectonic subsidence normalised for water loading for the southern Melville Basin (Fig 5.17), northern Melville Basin and Brittany Basin. The plots are based on quantifications of subsidence and erosion based on a detailed tectonic history compiled from well information and seismic reflection profiles. Backstripping techniques (Steckler & Watts, 1978) and sonic log compaction trends are discussed earlier in Hillis's PhD thesis.

The subsidence history plot for the southern Melville Basin (Fig 5.17) shows initial tectonic subsidence (~1.8 km) related to the thermal collapse of the Variscan Massif in the Permian with later Triassic fault controlled rifting. This phase is followed by Jurassic thermal subsidence with a potential Late Jurassic rift phase with ~1.0 km subsidence. The Top M2 Unconformity (Section 2.6.4) is quantified as ~0.7 km of thermal uplift in the Late Jurassic to Early Cretaceous which is followed by Late Cretaceous subsidence (~0.5 km). The Tertiary is characterised by inferred subsidence and uplift/erosion with (~0.1 km) net burial (Hillis, 1988).

Ruffell (1995)

Ruffell (1995) has developed simplified time-depth curves based on stratigraphic data obtained from wells from the Brittany, St Mary's and Melville Basins (Fig 5.18) with an indicated 10 Ma error bar on dates of stratigraphic horizons. The exact type of plots the time-depth curves represent or the assumptions made in their production are not stated in Ruffell (1995). These plots were developed as part of a kinematic analysis of basin extension and inversion with Ruffell (1995) indicating the development of a structural and stratigraphic model. The tectonic events used to develop the time-depth curve and calibration data are unknown, however, visually the plot for the southern Melville Basin (73/13-1 & 73/12-1 - Fig 5.18) is very similar to the tectonic subsidence history curves presented by Hillis (1988). The major difference between the curves is the absence of Cenozoic Alpine uplift and erosion meaning present day burial below 3 km.

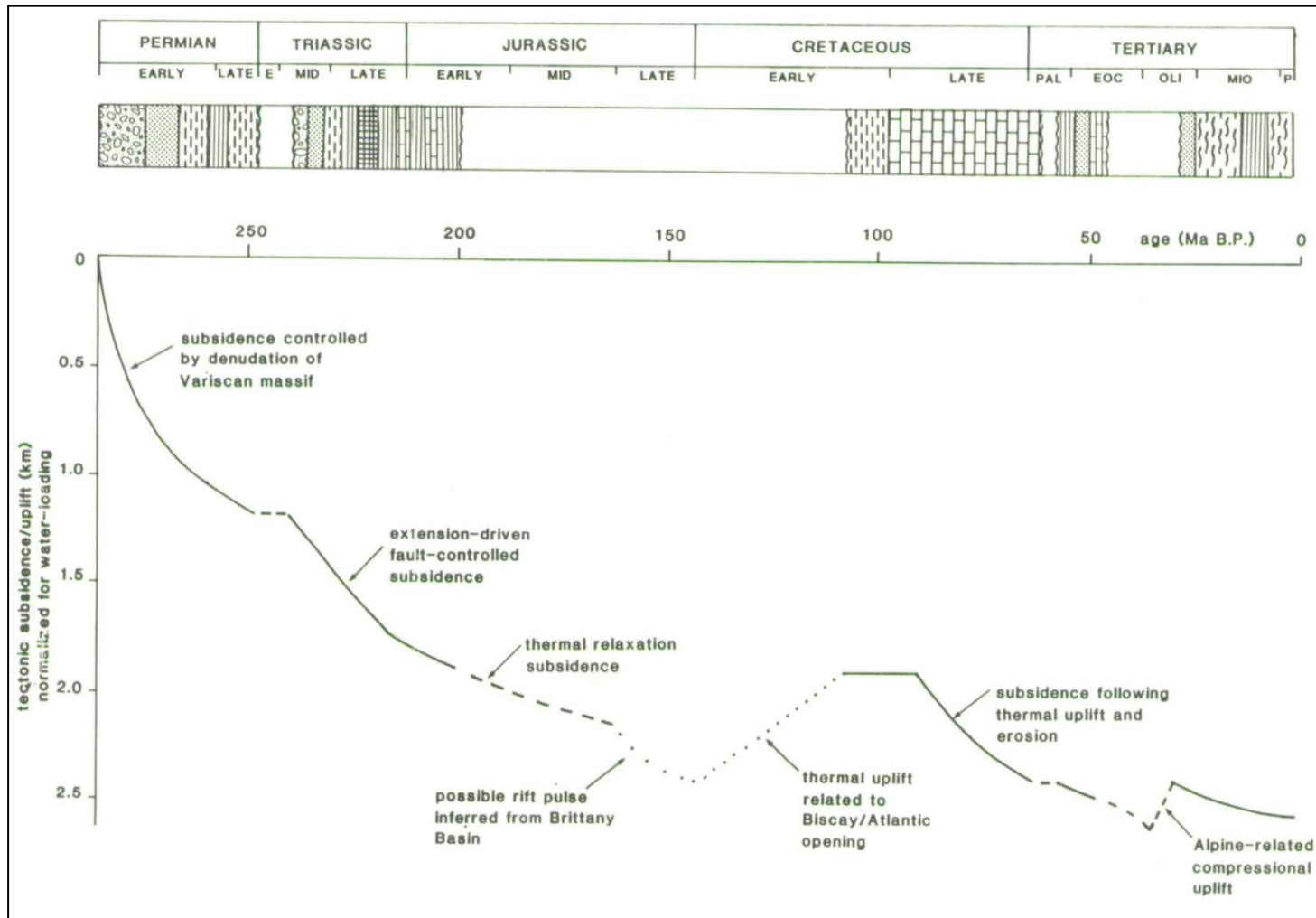


Fig 5.17. Subsidence history plot for the southern Melville Basin (Hillis, 1988) taking into account deposition and erosion based on a detailed tectonic history.

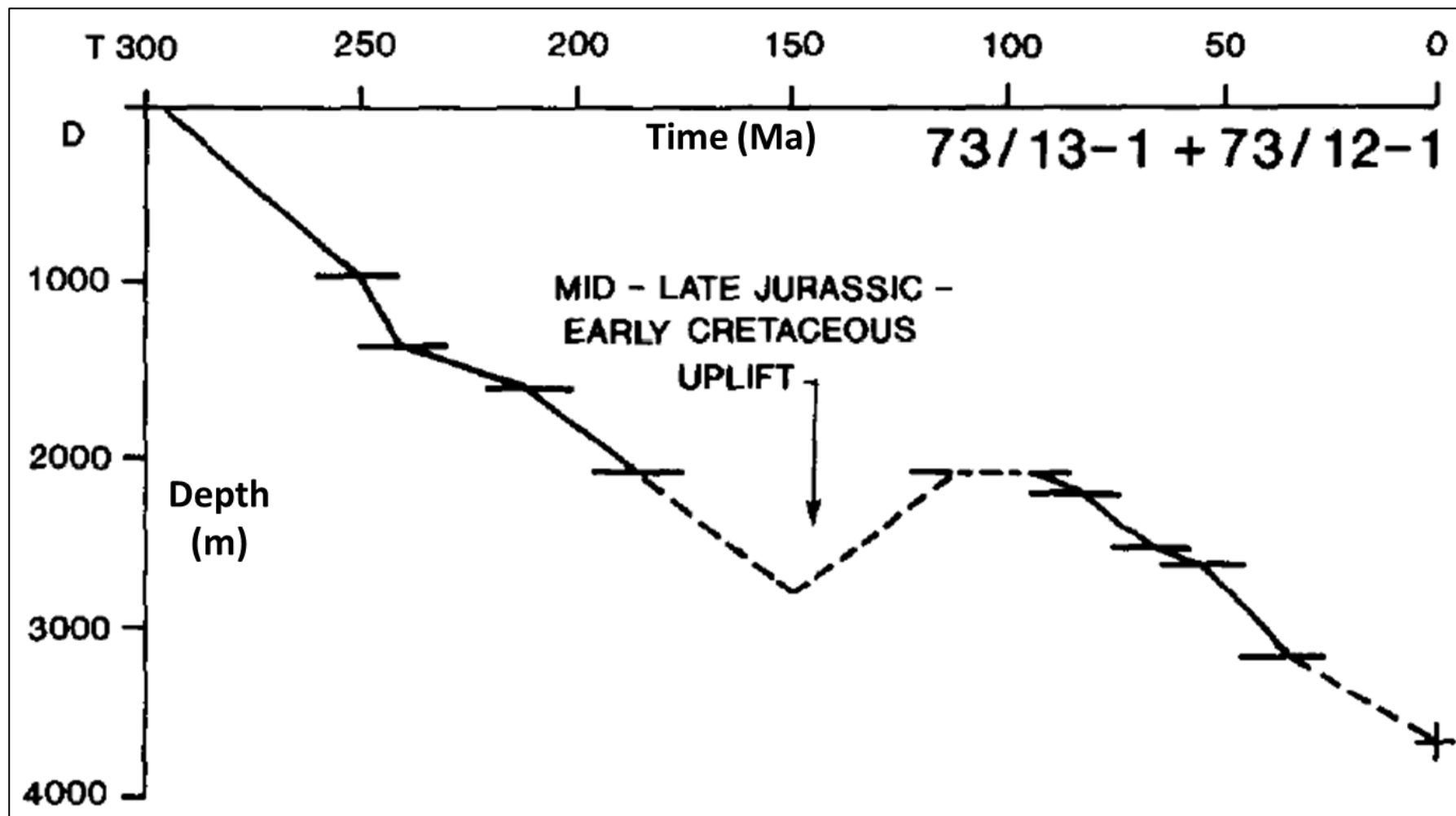


Fig 5.18. Time-depth curve for Melville Basin wells 73/12-1 & 73/13-1.

Ottaviani *et al.* (unpublished work)

One dimensional burial history models and evaluations of thermal maturity are presented for wells in the Melville Basin (Fig 5.19), St Mary's Basin and Plymouth Bay Basin. The models were calibrated through the use of wireline data, well summary logs, micropalaeontological information and well reports. This study relies heavily on the work of Hillis (1988) to quantify the burial history of the Western Approaches, with modelling facilitated by Schlumberger propriety software Petromod™. Heatflow and thermal conductivity are both discussed in detail with calibration to well bottomhole temperatures (BHTs) and cross-checking against VR measurements (Ottaviani *et al.*, unpublished).

The main points of contrast to the curves produced by Hillis (1988) and Ruffell (1995) are that:

1. The models are highly detailed with 36 intervals of deposition, non-deposition (hiatus) or erosion/uplift included in the Melville Basin models (Fig 5.19).
2. Subsidence initiates at the start of the Triassic (250 Ma) with both other papers indicating Permian subsidence.
3. The Top M2 unconformity is associated with a much higher magnitude of uplift (up to 2.8km).
4. Ottaviani *et al.* (unpublished work) produced burial history model with evaluation of thermal maturity in comparison to the subsidence curves (Hillis, 1988) and time-depth curves (Ruffell, 1995).
5. Ottaviani *et al.* (unpublished work) and Hillis (1988) include multiple Cenozoic uplift events compared to the net Cenozoic burial of ~0.7 km proposed by Ruffell (1995).

Murdoch *et al.* (1995)

Murdoch *et al.* (1995) performed burial history and maturity modelling for the North Celtic Sea Basin (Fig 5.20). These authors focussed on modelling the effect of Tertiary uplift on source rock maturity, using Basin Mod™ Software. The magnitude of Cenozoic uplift was calculated by comparison of seismic interval velocities from the Upper Cretaceous Chalk to a linear compaction curve with calibration to sonic logs (Section 4.3). This method assumes only mechanical compaction in the chalk interval and that compaction is described by a linear compaction profile. Another assumption in the model is the geothermal gradient of 32°C/km which is an average current day temperature but does not necessarily correspond to palaeotemperatures.

The model for well 50/03-1 importantly shows that the Top M2 Unconformity is not developed, with continuous subsidence from the Jurassic to the Paleocene (4 km). The Cenozoic is characterised by two uplift events ~0.5 km in the Paleocene and ~1.2 km from the Oligocene to end of the Miocene. Murdoch *et al.* (1995) indicates that the Lower Jurassic section has reached maturity for oil generation (Fig 5.20). The model for 49/09-1 includes 0.7 km of uplift at the Jurassic-Cretaceous boundary. In this case the maximum burial could be prior to Top M2 Unconformity, Paleocene or Oligocene uplift events (Murdoch *et al.*, 1995). The location of 50/03-1 relative to 103/01-1 (Dragon Discovery) is shown in Figure 5.21.

A burial history model, obtained from the Irish Petroleum Affairs Division but of unknown authorship, for the South Celtic Sea Basin is shown in Figure 5.22. The top of peak oil generation is indicated at a depth of ~9000 ft (2750 m). The lack of the full report means that the assumptions and modelling parameters are not known except that the model is based on well 93/02-1 and seismic SP 3050 line MP 84CR 19₂19/1₂ which was not available for this study.

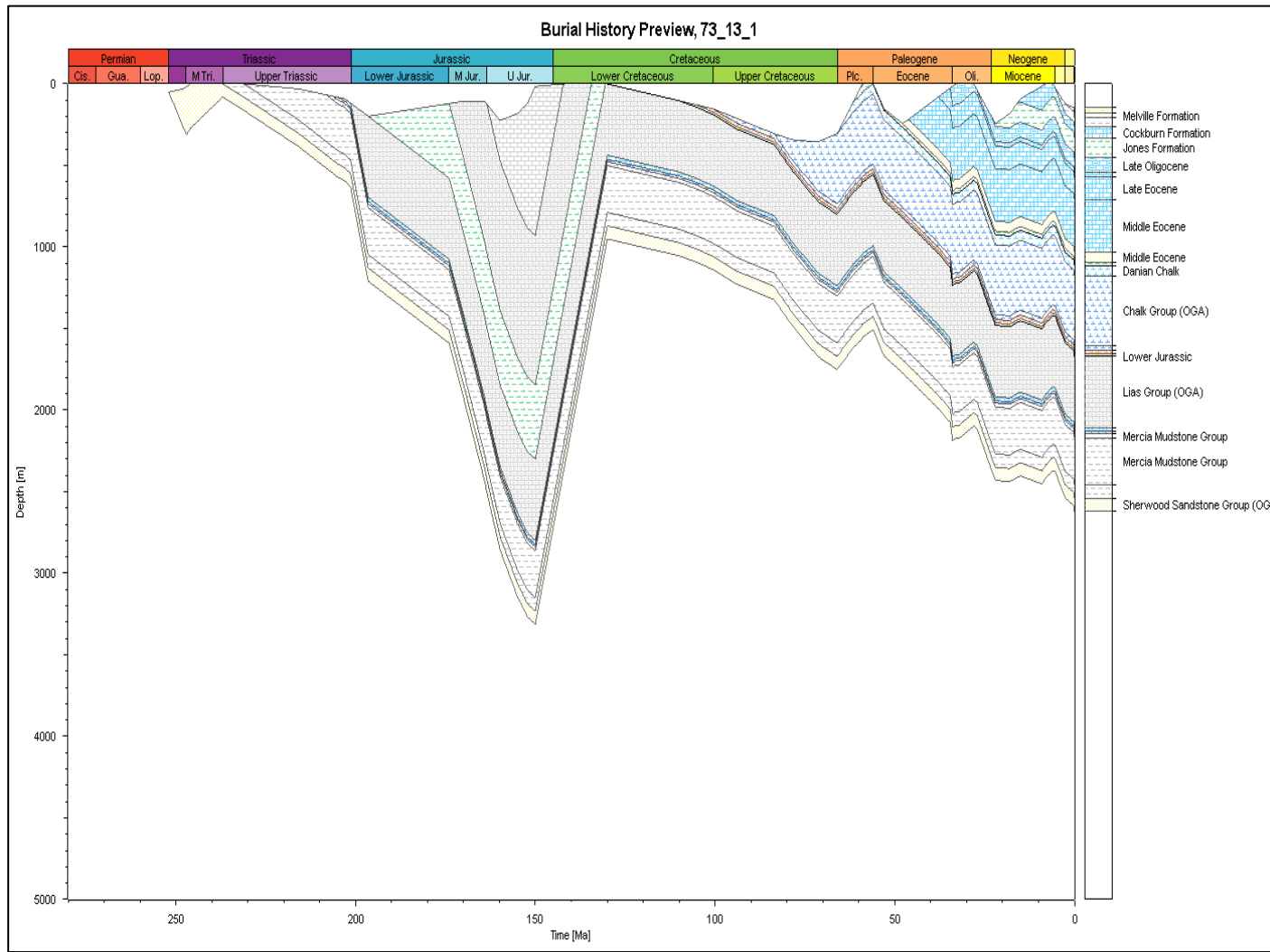


Fig 5.19. Burial History plot for 73/13-1 in the Melville Basin (Ottaviani *et al.*, unpublished work). Maximum burial is indicated in the Late Jurassic (U. Jur) with subsequent rapid exhumation and reburial from the Early Cretaceous to present.

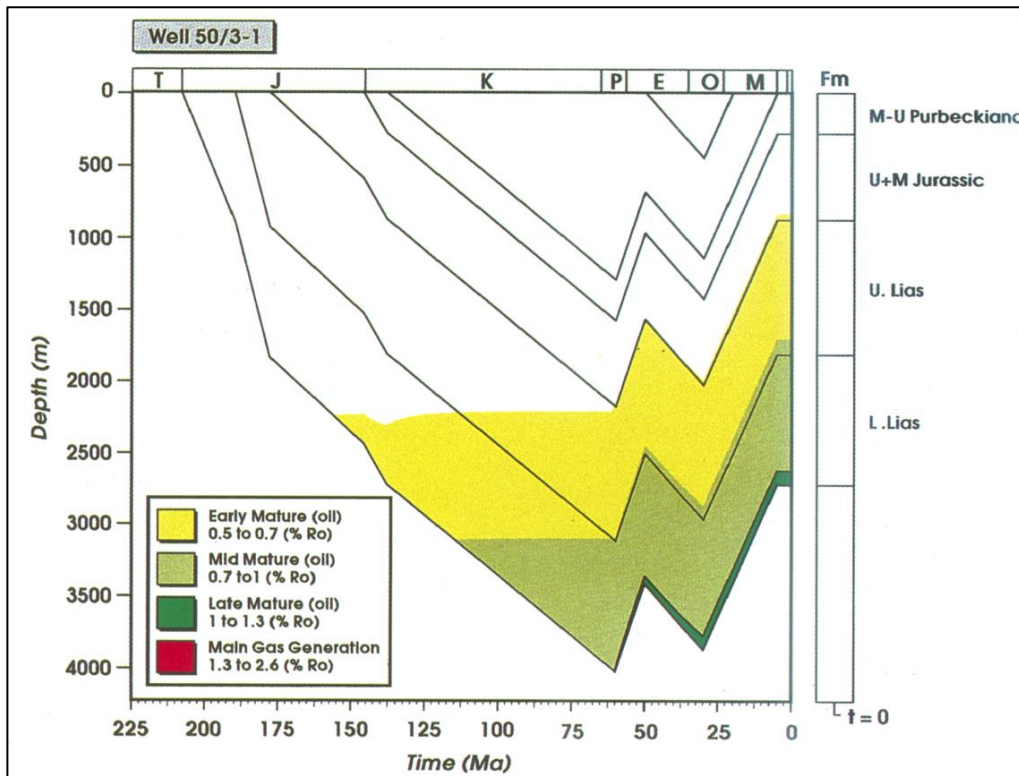


Fig 5.20. Burial history model for well 50/03-1 in the North Celtic Sea Basin which was calibrated to VR and Apatite Fission Track data (AFT). The plot is coloured by maximum experienced maturity from VR; VR reflects maximum maturity experienced and not current maturity of the interval of study.

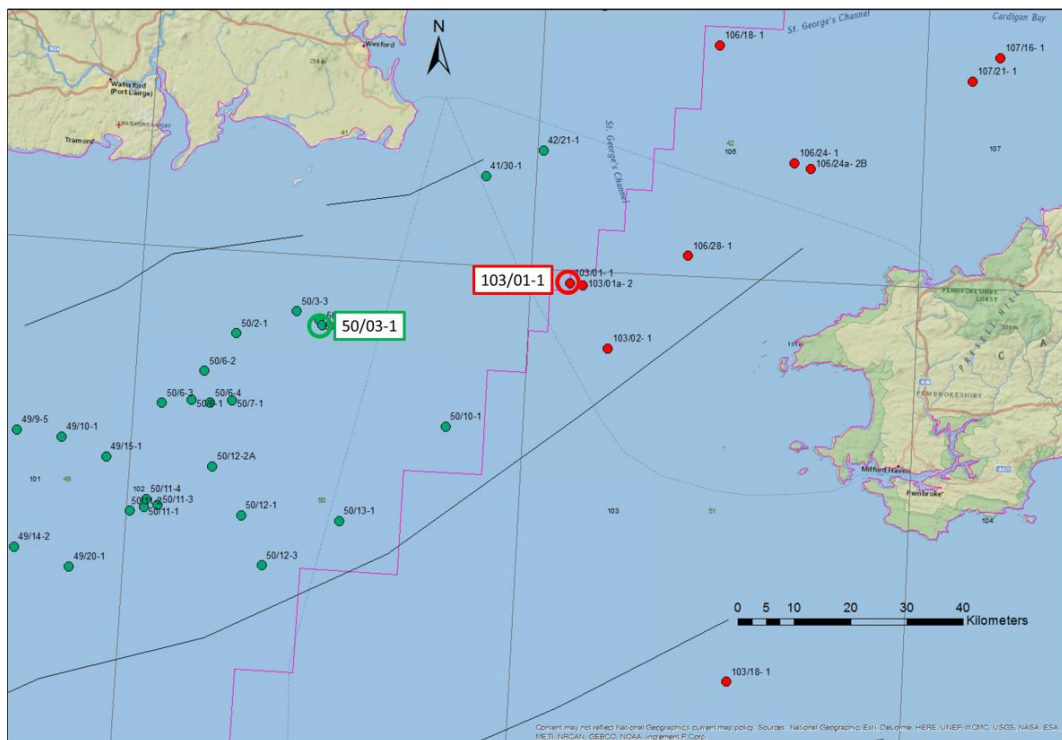
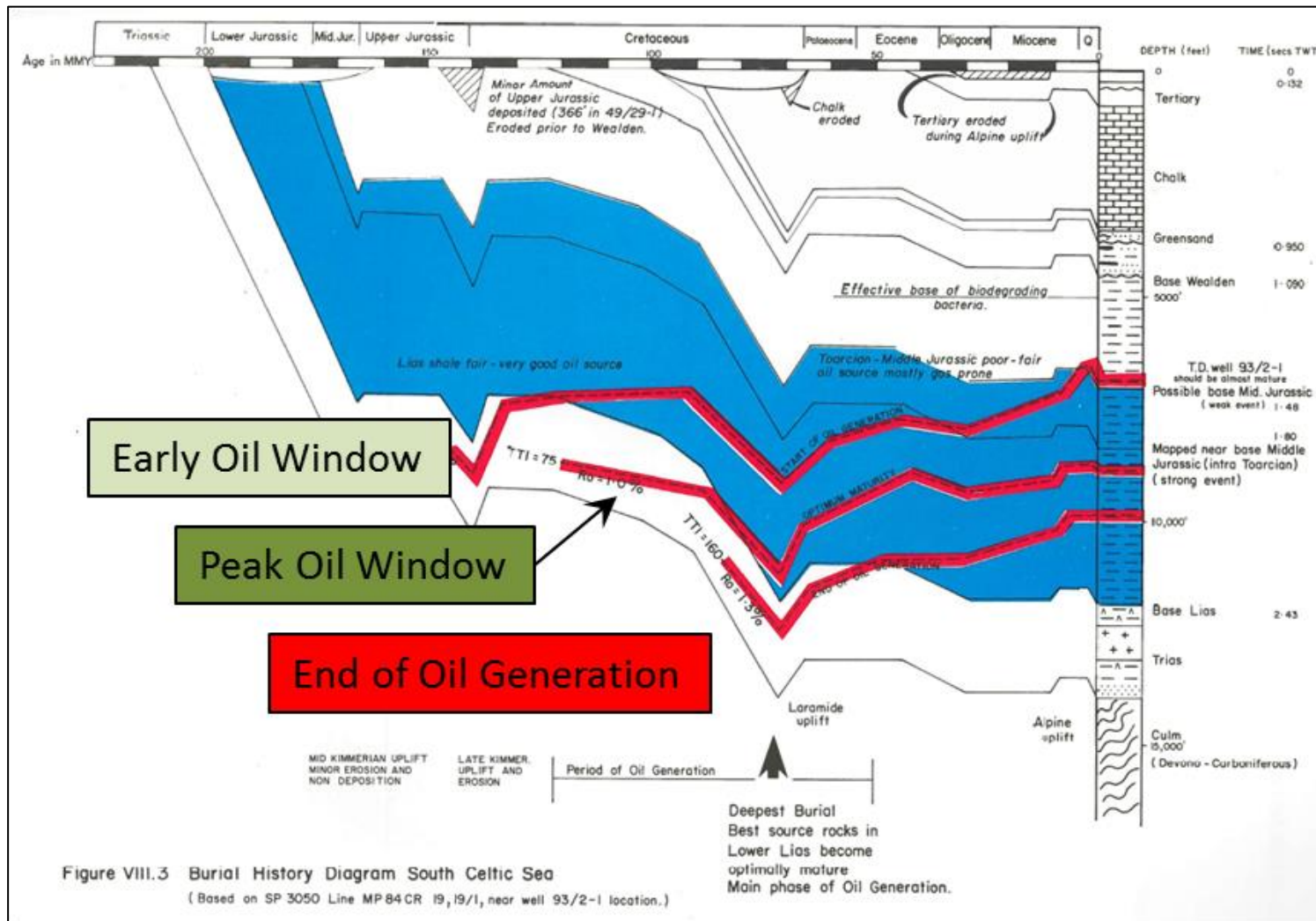


Fig 5.21. Map of the North Celtic Sea Basin showing the proximity of 50/03-1 to the Dragon Discovery (103/01-1).



5.1.1.1. Discussion of Burial History Models

The subsidence history, time-depth and burial history curves described above recognise the same major events of basin development, namely rifting, thermal subsidence and uplift, but there are several key differences primarily relating to the Cenozoic history, and the degree of uplift associated with the Top M2 Unconformity.

- Hillis (1988) indicates that maximum burial is at the present day but burial is only a few hundred metres beyond Late Jurassic burial.
- The absence of Cenozoic uplift in Ruffell's time-depth curves means that burial is at a maximum at the present day; 0.8 km deeper than maximum Jurassic burial.
- Ottaviani *et al.* (unpublished work) has a greater degree of uplift and predicts maximum burial to have occurred in the Late Jurassic; ~0.5 km deeper than present day.

Murdoch *et al.* (1995) indicate that maximum burial in the North Celtic Sea Basin occurred during the Late Cretaceous with the base Jurassic subsequently uplifted by up to 1.25 km compared to maximum burial. The Lower Jurassic reached the oil window in the Cretaceous (~130 Ma) at ~3100 m depth; however, the base Jurassic is currently at 2700 m depth at present day; potentially above the oil window.

5.3.3. Summary of Thermal Maturity

- The thermal maturity of the Jurassic interval is predominantly immature to early mature.
 - 103/01-1 – Lower Jurassic section is mature to late mature.
 - 73/13-1 – Lower Jurassic section is early mature to mature.
 - The effect of maturity on Rock-Eval is likely to be very minor except in the case of The Lower Jurassic section of 103/01-1 which has reached late maturity for oil generation. This is a potential effect on the Middle Jurassic in this well as well.
- Poor data quality means a combined approach has been used based on vitrinite reflectance, visual kerogen and spore analysis and Tmax have been used to interpret thermal maturity.

- Greater density and quality of maturity data is required to characterise the relationship between the geographical distribution and maturity.
 - The same is true if the relationship between maturity and depth is to be understood.

- The basin models and subsidence models for the Melville Basin reflect similar tectonic effects.
 - Models are not easily comparable and involve many varying methods of analysis and assumptions.
 - Variability in key events, Late Jurassic to Early Cretaceous uplift and Cenozoic uplift, lead to a high degree of uncertainty in the development of maturity through time.
 - Quantifying the effect of the uplift events is crucial to determining the development of maturity.

- Potential for the North Celtic Sea Basin wells to have experienced maximum burial in the latest Cretaceous (Fig 5.20).

- A similar basin history is shown for the South Celtic Sea Basin with additional minor Top M2 uplift.

5.4. Source Rock Richness

5.4.1. Total Organic Carbon

The objective of this section is to evaluate the source rock richness of the Jurassic interval in the Celtic Sea and Western Approaches. Source rock richness is considered in this thesis to be a factor of a rock's enrichment in organic matter as a function of weight percent Total Organic Carbon (TOC) as described in Section 4.2.3. The wells that are included in the TOC analysis are shown in Figure 5.2.

A quantitative analysis has been produced based on the guidelines (Table 5.5) laid out in Peters (1986).

Richness	TOC (wt. %)
Poor	0.0–0.5
Fair	0.5–1.0
Good	1.0–2.0
Very good	>2.0

Table 5.5. Guidelines for defining source rock richness based on weight percent TOC (Peters, 1986).

The **arithmetic average** is a method of estimating the arithmetic mean and is equally sensitive to all values so can be prone to bias in skewed populations (Fig 5.23).

The **median** of a distributed population is equal to the value of the sample that above and below which equal numbers of samples lie (Fig 5.23).

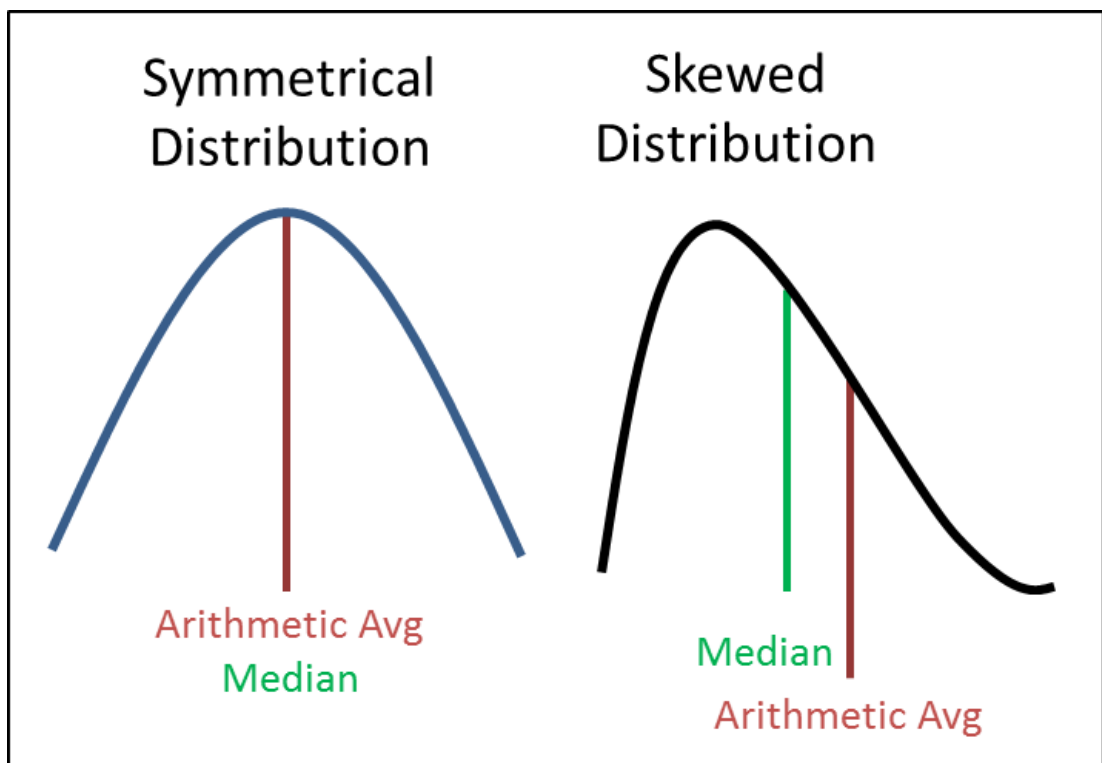


Fig 5.23. Schematic diagram showing the influence of a skewed distribution on the median and arithmetic average with the arithmetic average showing higher influence to low frequency high value samples.

The **standard deviation (St Dev)** is a measurement of mean distance of samples from the mean in the units being considered.

The **coefficient of variation (CV)** is a measurement of the heterogeneity of a sample population where:

- 0.0 < CV < 0.5** Homogeneous
- 0.5 < CV < 1.0** Heterogeneous
- CV > 1.0** Very Heterogeneous

Interval	No. Samples (N)	Arithmetic Avg	Median	ST Dev	CV
All	2364	1.45	0.73	3.96	2.72
Paleogene	56	1.38	0.28	4.97	3.61
Cretaceous	166	1.36	0.27	4.53	3.32
Jurassic	1571	1.87	0.92	4.45	2.38
Triassic	526	0.31	0.15	0.40	1.29
Unknown/Basement	24	0.81	0.24	1.05	1.29

Table 5.6 illustrating the number of TOC samples within each time period and the statistical parameters of that data.

The Paleogene, Cretaceous and Jurassic have arithmetic averages of >1.0% TOC with the Jurassic having an average of 1.87% TOC (Table 5.6). Unknown and Basement samples have an arithmetic average of 0.81% and the Triassic population has an arithmetic average of 0.31. The median values for every interval are below 1.0% with the Paleogene, Cretaceous, Triassic and Unknown/Basement intervals having median values of <0.3%. The Jurassic population has the highest median of 0.92%.

The Paleogene, Cretaceous and Jurassic intervals have standard deviations of between 4.0-5.0% with the Triassic population having a standard deviation of 0.4% and the Unknown/Basement population has a standard deviation of 1.05%. The standard deviation values correspond well with measurements of coefficient of variation. The Paleogene, Cretaceous and Jurassic all have values of CV greater than 2.0 indicating that TOC data are very heterogeneously distributed between samples. The Triassic and Unknown/Basement populations both have a CV values of 1.29 which suggest heterogeneous TOC populations.

The high degree of variation and low central tendency of samples (tendency of samples to cluster around their mean) of the Paleogene, Cretaceous and Jurassic indicates that TOC is not homogeneously distributed within an interval. The lower standard deviation values for the Triassic and Unknown/Basement correlate with the intervals of lowest arithmetic

average and median. These intervals are both poor (low median values for TOC) for source rock richness and therefore increased homogeneity is potentially linked to the deposition of more uniformly lean source rocks and/or widespread oxidisation of organic matter. Hydrocarbon generation would also decrease TOC values and values would converge on a level of irreducible type IV kerogen (Section 4.5).

The Triassic and Unknown/Basement interval are indicated as having poor organic matter richness. The arithmetic averages of 1.38% and 1.36% in the Paleogene and Cretaceous compared to median values of 0.28% and 0.27% respectively suggest that the intervals have generally poor source rock richness with some higher TOC zones/samples. This is supported by the high standard deviation >4.5% TOC in both intervals and high CV values (>3.0).

A histogram of the bulk population TOC distribution is shown in Figure 5.24. Isolated high TOC samples are present in the populations of >20% TOC. These high TOC samples contribute to the high CV and standard deviation values previously noted.

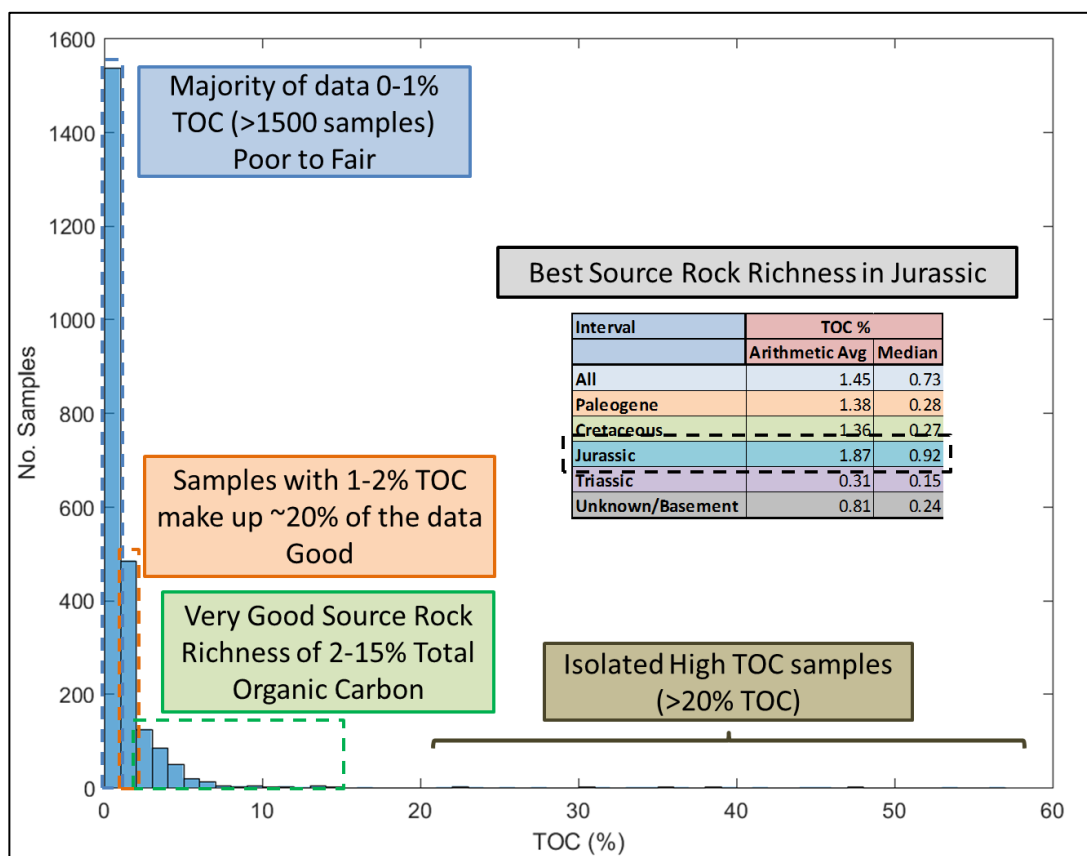


Fig 5.24. A histogram of the TOC (%) distribution for the Jurassic with the majority of data located between 0-1% TOC with very good source rocks at 2-15% and isolated samples of >20% TOC.

5.4.1.1. Jurassic

Interval	No. Samples (N)	Arithmetic Avg	Median	ST Dev	CV
Jurassic	1571	1.87	0.92	4.45	2.38
Late Jurassic	374	3.14	1.22	6.92	2.21
Middle Jurassic	555	1.26	0.77	3.53	2.81
Early Jurassic	598	1.71	1.02	3.00	1.76
Undiff Jurassic	44	1.03	0.78	0.81	0.78

Table 5.7 illustrating the number of TOC samples within each epoch of the Jurassic and the statistical parameters of that data.

The breakdown of TOC samples and the statistical parameters for the three Jurassic epochs and the undifferentiated data (values without enough data for an epoch to be assigned) are shown in Table 5.7. The undifferentiated data is included in the table but as it cannot be assigned to an epoch is not consider valid for statistical evaluation.

The Early Jurassic epoch has the most samples (598 out of 1571) with an arithmetic average of 1.71% and a median value of 1.01%. The Middle Jurassic (555 samples) has lower arithmetic average and median values of 1.26% and 0.77% respectively. In contrast, the Late Jurassic (374 samples) has an arithmetic average of 3.14% TOC (very good) and a median value of 1.22%.

The TOC enrichment as indicated by the epoch median and arithmetic average suggests that every epoch can be classified as good or better except the Middle Jurassic which has a fair median value of 0.77%. The Jurassic epochs all have standard deviations of 3.0% TOC or greater with the Late Jurassic having a value of 6.92%. The coefficient of variation for each epoch is greater than 1.0 (very heterogeneous). The question is whether the variation observed is related to stratigraphic variation or spatial variation or a factor of both.

Epoch/Interval	Celtic Sea			Western Approaches			Wytch Farm		
	No. Samples (N)	Arithmetic Avg	Median	No. Samples (N)	Arithmetic Avg	Median	No. Samples (N)	Arithmetic Avg	Median
Jurassic	677	2.02	0.87	91	3.15	1.57	768	1.64	1.00
Late Jurassic	174	4.19	0.83				200	2.27	1.54
Middle Jurassic	312	1.28	0.74				243	1.21	0.79
Early Jurassic	191	1.25	1.04	91	3.15	1.57	316	1.55	0.95
Undiff Jurassic	35	0.79	0.77				9	1.96	1.33

Table 5.8 statistical parameters and number of samples for TOC in the epochs of the Jurassic split up into the separate regions.

The variation of source rock richness between the Celtic Sea, Western Approaches and Wytch Farm in the Jurassic and the separate Jurassic epochs is shown in Table 5.8. The Celtic Sea and Wytch Farm both have greater than 650 samples for the Jurassic with more than 150 assigned to each epoch. The Western Approaches in contrast only consists of data from Early Jurassic of which 91 samples were available. The highest median value in the Celtic Sea is in the Early Jurassic (1.04%) in contrast to Wytch Farm where the Late Jurassic has the highest median (1.54%) and arithmetic average (2.27%) values. In the Celtic Sea, the Early Jurassic arithmetic average is 1.25% (only 0.21% higher than the median) in comparison to an arithmetic average of 4.19% for the Late Jurassic. This high arithmetic average is due to the effect of 21 high TOC (>10%) samples in the St George's Channel Basin (Fig 5.25). Lithology notes from the geochemistry reports suggest coal as the predominant lithology for these samples. Histograms for the Jurassic TOC distributions by basin are shown in Figure 5.25.

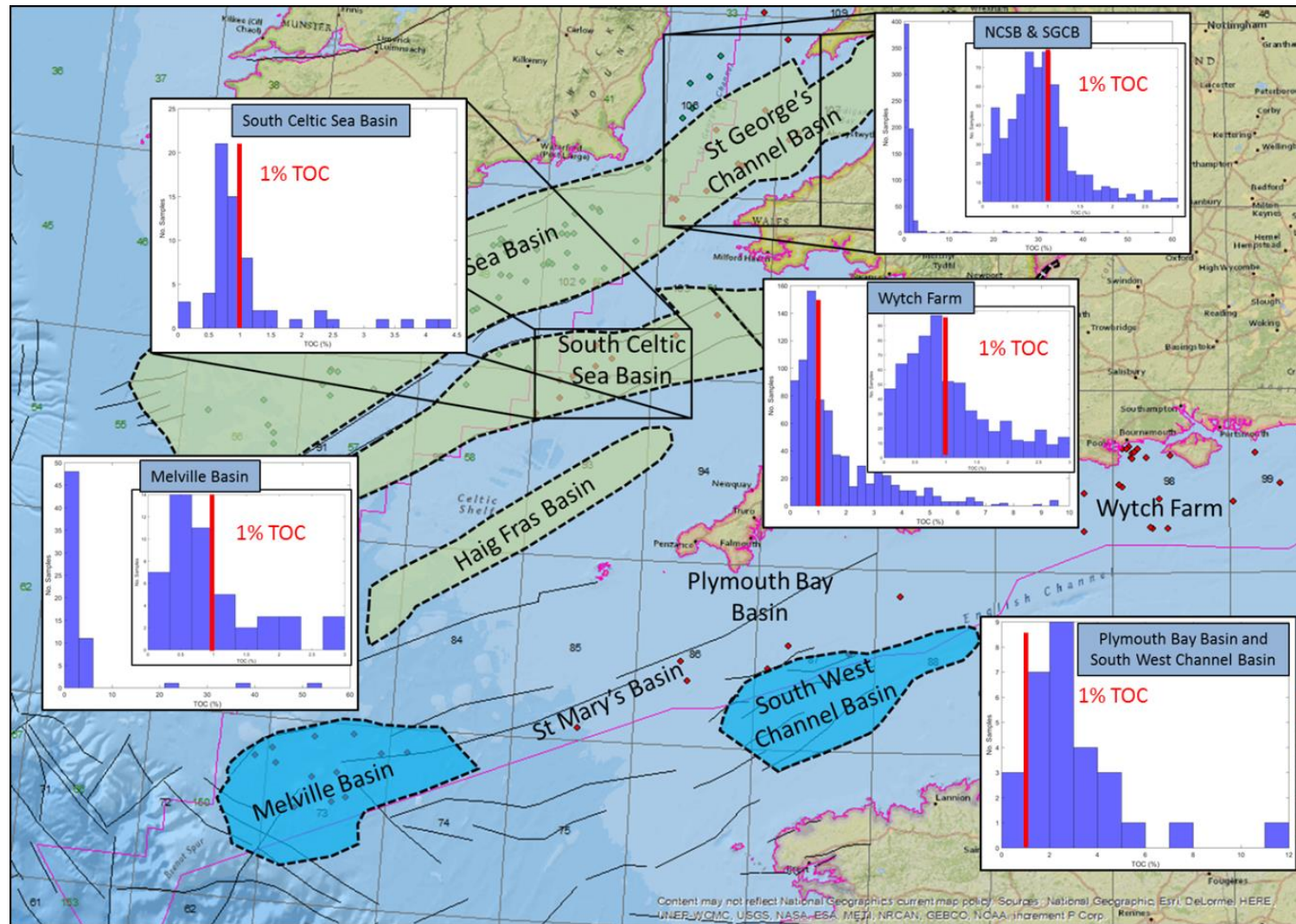


Fig 5.25. Map for the region of interest displaying histograms of the TOC distributions in the Jurassic with a red 1% TOC reference line.

The palaeontological information available for this study as discussed in Section 5.2 was not in sufficient detail to allow the analysis of the Jurassic on a sub-Epoch level which would have been preferable. In the palaeontological data or composite log interpretations (where palaeontological information was not available), Stages have been merged which does not allow consistent analysis of the geochemical information at this finer temporal resolution. The source rock richness of key wells will be described in Section 5.4 on a sub-Epoch level to determine whether trends of consistently rich source rocks exist at these scales.

5.4.2. Summary of Source Rock Richness

- The Jurassic has an arithmetic average of 1.87% TOC which would suggest good source rock richness. The median value of 0.92% in contrast would indicate only fair source rock richness for the bulk interval.
- The coefficient of variation (2.38 CV) and standard deviation (4.45%) for the Jurassic interval indicate the sample population to be very heterogeneous with high variability.
- Only Early Jurassic measurements are available for the Western Approaches due to the removal of overlying Jurassic strata by the Top M2 unconformity.
- The highest arithmetic average values for source rock richness in the Jurassic Epochs for the Celtic Sea and Wytch Farm (Table 5.6) are in the Late Jurassic (4.19% and 2.27% TOC respectively).
 - The median value for the Late Jurassic of the Celtic Sea is 0.83% (fair richness).
 - 21 samples with >10% TOC indicated to be predominantly coals.
- The analysis of key wells in Section 5.7 will describe source rock richness on a sub-Epoch scale.

5.5. Source Rock Quality

The objective of this section will be to examine qualitatively and quantitatively the source rock quality of the Jurassic intervals in the Celtic Sea and Western Approaches region.

The definition of source rock quality is discussed in Section 1.3 and is an analysis of the proportions of the petroleum generating kerogen in a potential source rock interval.

The comparison of the S2 pyrolysis peak values against Total Organic Carbon (Dembicki Jr, 2009) is used to evaluate the proportion of the organic carbon that could generate hydrocarbon. In addition the relationship between source rock richness and quality will be interrogated in an attempt to understand whether there is a clear trend between increased source rock richness and increased source rock quality. For example, a source rock could have a classification as “very good” (Peters, 1986) for source rock richness but if a high proportion of that organic carbon is inert then there is very little potential for that source rock to have produce hydrocarbons.

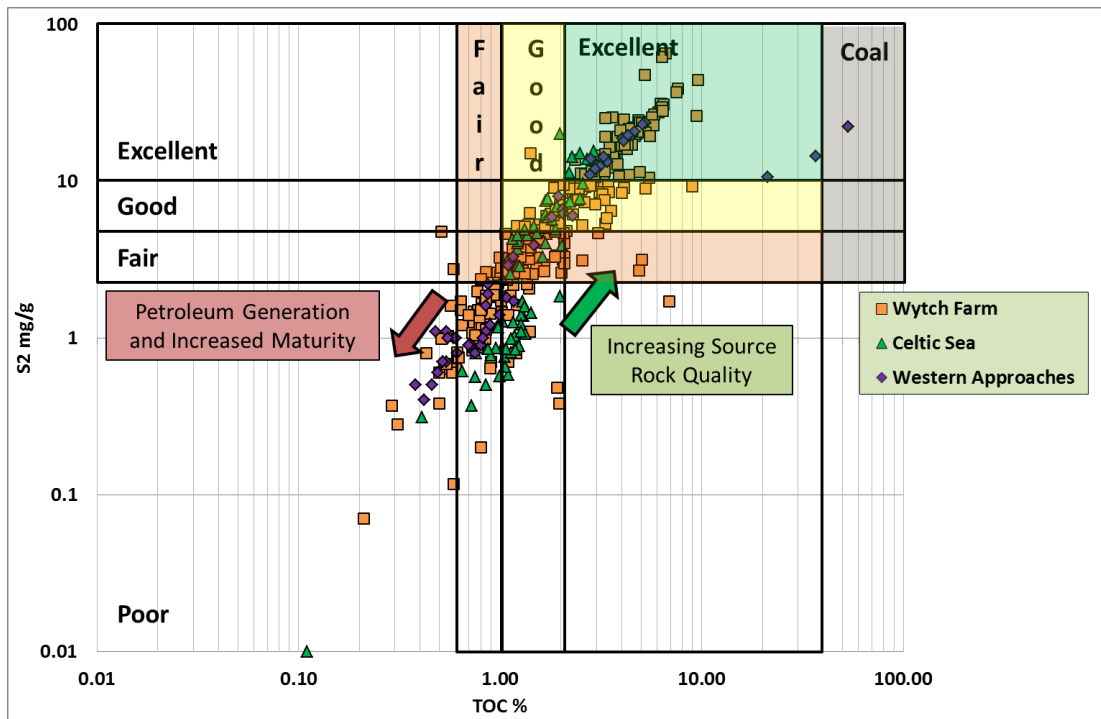


Fig 5.26. A crossplot of TOC (%) against S2 peak (mg/g) for the Jurassic (log-log axis) with overlays based on (Dembicki Jr, 2009) with data plotted for the Celtic Sea (green triangles), Western Approaches (purple diamonds) and Wytch Farm (orange squares).

A plot of TOC against S2 peaks from pyrolysis is shown in Figure 5.26, with the data coloured by region and overlays based on Dembicki Jr (2009). The TOC zones correlate well with those proposed by Peters (1986) with “Excellent” being the equivalent of what is considered here as “very good”. Data for each region exists in each zone of source rock quality. There is a clear trend between S2 peak and TOC although there is a larger degree of scatter in data from Wytch Farm. The Celtic Sea and Western Approaches data largely overlie the larger dataset from Wytch Farm. The data are typically offset to the right from Dembicki Jr’s (2009) calibration. In particular, good source rock richness (TOC) is equal to roughly good fair quality for S2 peak. The kerogen has a lower generative ability (per % TOC) which could be due to kerogen type or the presence of inertinite which would increase TOC but not contribute to S2 yield. There is an offset to the right between the trend of fair to excellent by (S2 yield) and data deemed poor based on S2 yield. This offset (0.5 % TOC) is clearest in the Celtic Sea data (Fig 5.27) and could represent a similar effect as that discussed above i.e. kerogen type or increased inertinite content. Therefore, the use of TOC alone to characterise source rocks quality would lead to an overprediction of quality.

5.5.1. Celtic Sea

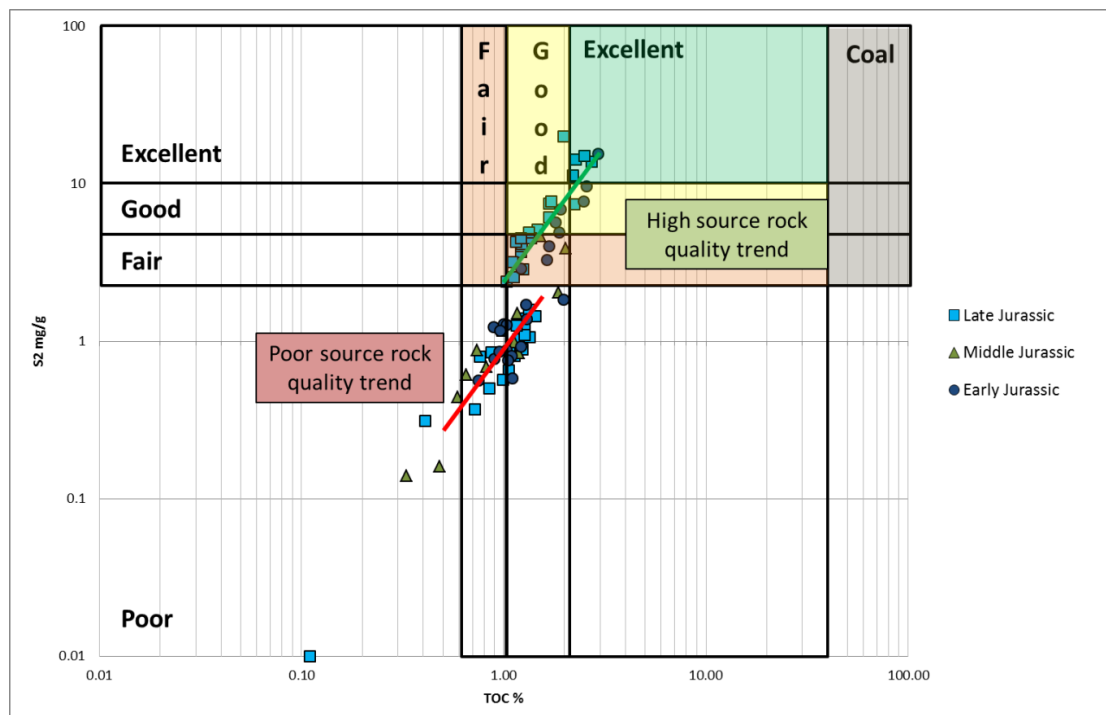


Fig 5.27. A crossplot of TOC (%) against S2 peak (mg/g) for the Jurassic (log-log axis) of the Celtic Sea with overlays based on (Dembicki Jr, 2009) with data plotted for Epoch with the Early Jurassic (dark blue circle), Middle Jurassic (green triangle) and Late Jurassic (light blue square).

The two distinct trends for TOC vs S2 peak (log-log axes) are shown in Figure 5.27. The distribution does not seem to be linked to a specific epoch within the Jurassic as Early and Late Jurassic data exist in both populations. The trend appears to be geographical with the wells included in the upper trend in the St George’s Channel Basin (including 103/01-1). A number of different companies performed the analyses for these wells suggesting the trends are not a factor of measurement error. The Middle Jurassic is less obvious as only two points of fair source rock quality (characterised by S2 yield) exist and it is unclear whether these data points are offset. The majority of the data points for the Middle Jurassic lie on the Poor source rock trend with lower S2 0.1-1.2 mg/g relative to TOC 0.5-2.0%. As discussed in Section 2.6.3 the Middle Jurassic was characterised by a marine regression from the Aalenian to Bathonian which could be linked a reduction in the limit of anoxic conditions and/or increased input of terrestrial material. The shift in TOC-S2 trend could be linked to specific changes in deposition environment, levels of terrestrial input or increased oxidation of organic matter.

5.5.2. Western Approaches

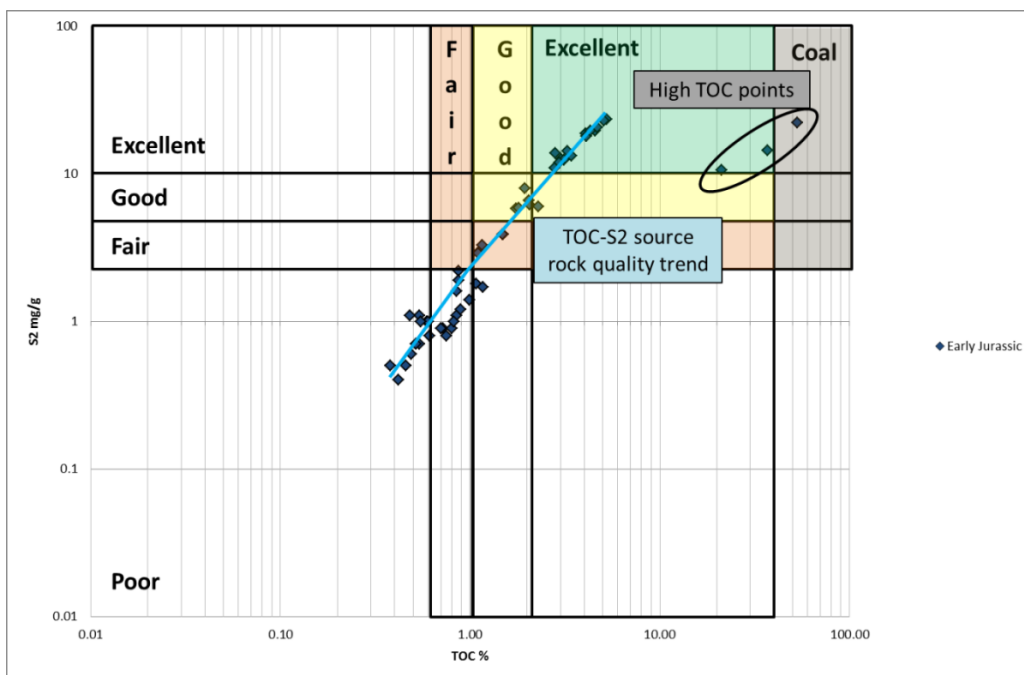


Fig 5.28. A crossplot of TOC (%) against S2 peak (mg/g) for the Jurassic (log-log axis) of the Western Approaches with overlays based on (Dembicki Jr, 2009) with data plotted for the Early Jurassic (dark blue diamonds) as no Middle Jurassic or Late Jurassic data was available.

A TOC-S2 plot for the Western Approaches is shown in Figure 5.28. Data from the Jurassic in the Western Approaches is restricted to the Early Jurassic due to the Top M2 Unconformity (Section 2.6.4). The data are generally fairly well constrained along a trend of increasing S2

yield with TOC (Fig 5.28). In addition there are some high TOC (>10% TOC) points that are significantly offset from the rest of the data population; one of these points plots in the coal zone. The data show a large range of S2 (0.3-23.3 mg/g) and TOC (0.25-56.0) values. The variation could be due to maturity, quantity of TOC deposited, kerogen type variation or oxidation of kerogen. The low degree of maturity of these sediments (Section 5.3) suggests that the variation is unlikely to be related to maturity. Tyson (2004) discusses attributes the relationship between S2 and TOC (HI) to the preservation of organic carbon with a lesser effect of terrestrial input. It is likely that the trends shown here represent variable preservation of organic matter.

5.5.3. Summary of Source Rock Quality

- Total Organic Carbon plotted against S2 yield has been used to evaluate to evaluate the fraction of generative kerogen present.
 - Hydrogen Index is the S2 yield/TOC and provides a quantitative method of evaluating source rock quality used in Section 5.7.

- There is an offset between the source rock quality as indicated from the TOC vs S2 plot (Dembicki Jr, 2009) and the source rock richness from TOC (Peters, 1986).
 - Source rock richness from TOC underpredicts source rock quality.
 - Good source rock richness roughly equivalent to fair source rock quality.

- Two trends for TOC vs S2 yield the Celtic Sea data have been described with poor S2 data plotting in the poor zone with a yield of <2 mg/g having a higher TOC relative to data plotting in fair to excellent zone.
 - Potential controls on the trend are suggested as 1) the depositional environment, 2) oxidation of organic pre-burial or soon after burial or 3) the amount of terrestrial kerogen input.
 - The trends appear have a geographical control with data in the upper trend predominantly from the St George's Channel Basin.

- The TOC vs S2 yield data plotted for the Western Approaches plots along a relatively constrained trend.
 - The data spread plots from poor to excellent (Dembicki Jr, 2009).
 - Three data points sit off the trend with high enrichment in TOC (>10%) relative to their S2 yield (10-23.3 mg/g).

5.6. Kerogen Type

The type of kerogen and the geographical and stratigraphic distribution of kerogen types will be analysed as discussed in Section 4.2.2 using a pseudo-van Krevelen plot with the objective of determining the effect of kerogen type on the source rock potential.

Figure 5.30 shows a pseudo-van Krevelen plot for the Jurassic interval of the Celtic Sea and Wytch Farm; no data are available for the Western Approaches (Table 5.2). The Jurassic of Wytch Farm is used as an analogue for the Western Approaches. The applicability of the Wytch Farm as an analogue for the Western Approaches is discussed in Section 1.4.

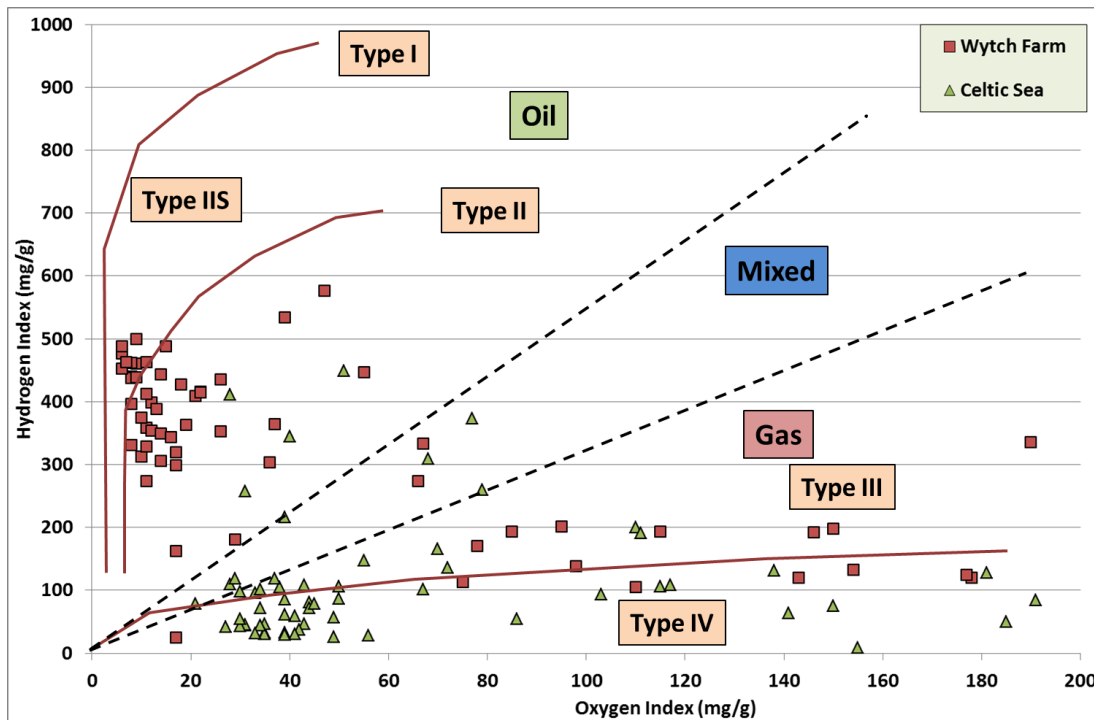


Fig 5.29. Pseudo-van Krevelen plot with Hydrogen Index values (mg/g) plotted against Oxygen Index (mg/g) for the Jurassic by region. No Jurassic samples exist for the Western Approaches. Overlays are based on Cornford *et al.* (1998) & Dembicki Jr (2009) and the applicability of the van-Krevelen plot is discussed in Section 4.2.2.

The Hydrogen Index and Oxygen Index data for the Celtic Sea are highly scattered with the bulk of the data sitting within the Type IV (inertinite) zone between 20-60 mg/g OI and 0-120 mg/g HI. These data are of Late Jurassic age or Undifferentiated Jurassic (Fig 5.30). Additional data scattered at high OI values but <200 mg/g HI are shown to be Early Jurassic of age with a four Middle Jurassic data points. Four data points also exist in the mixed kerogen zone and four data in the Type II kerogen zone of Early Jurassic age (Fig 5.30). Wytch Farm in contrast contains a significant population plotting in the Type II kerogen zone with HI values of 300-600 mg/g and OI values of 5-25 mg/g of predominantly Late Jurassic and Middle Jurassic age. The rest of the data are scattered between mixed zone and Type III/Type IV zones and are of Early Jurassic and Middle Jurassic age (Fig 5.30).

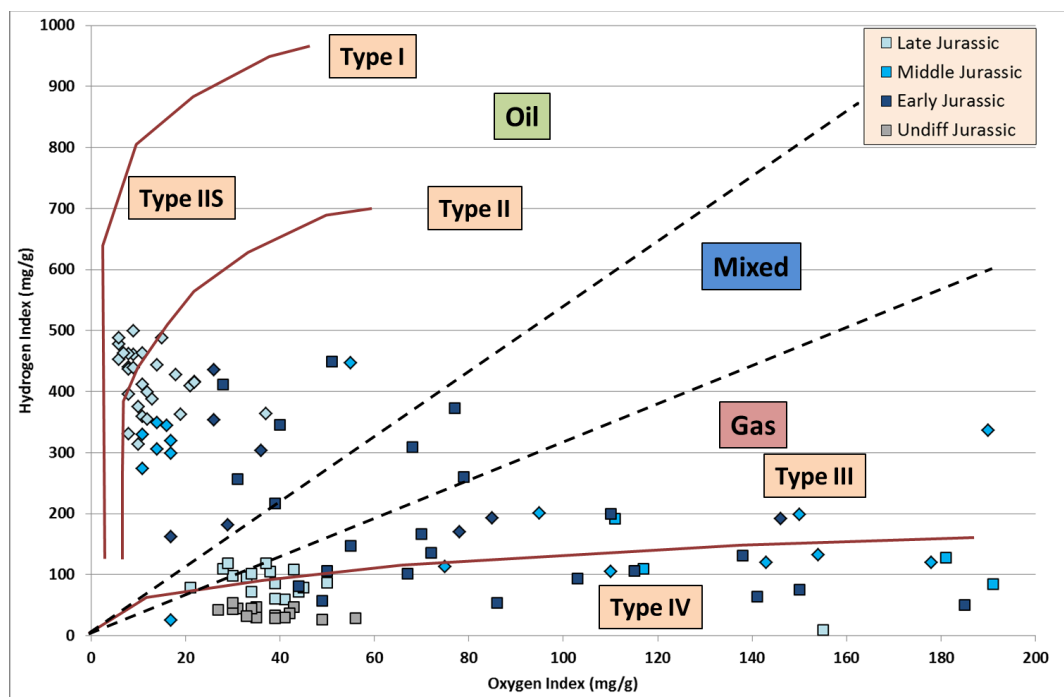


Fig 5.30. Pseudo-van Krevelen plot with Hydrogen Index values (mg/g) plotted against Oxygen Index (mg/g) for the Epochs of the Jurassic. No Jurassic samples exist for the Western Approaches. Overlays are based on Cornford *et al.* (1998) & Dembicki Jr (2009) and the applicability of the van-Krevelen plot is discussed in Section 4.2.2.

Figure 31 displays the Jurassic data on a pseudo-van Krevelen coloured by TOC. The data plotting in the Type II kerogen zone is shown to be of “Very Good” source rock richness with >2.0% TOC. The data scales with decreasing TOC to move to lower HI and high OI values i.e. Type III and Type IV kerogen zones.

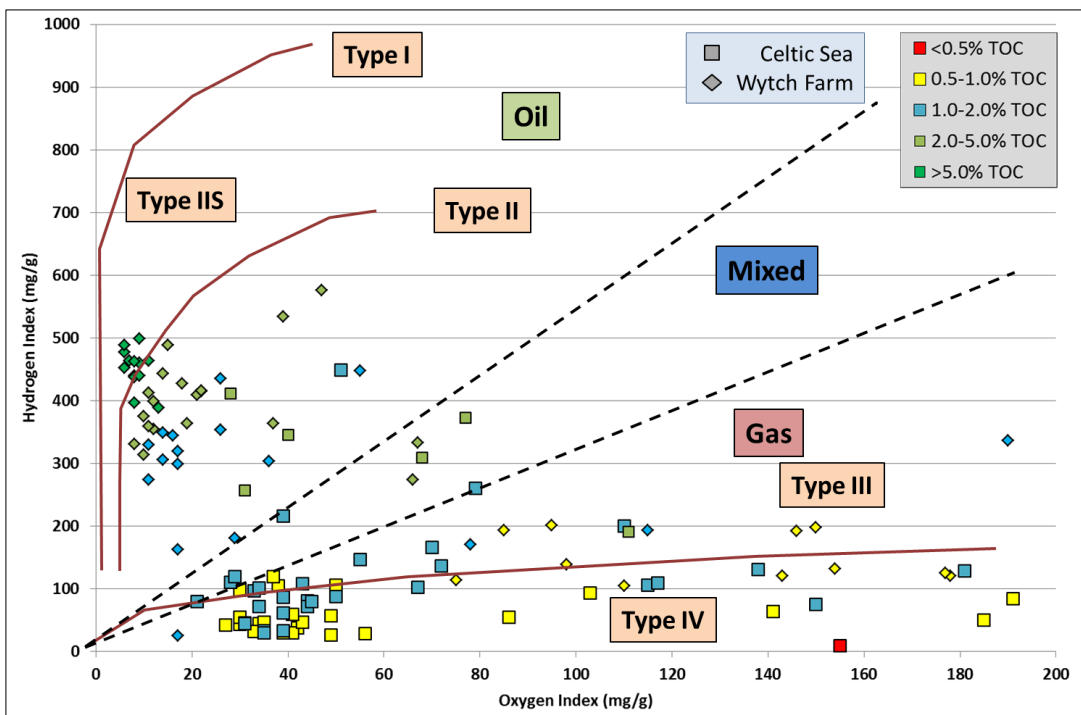


Fig 5.31. Pseudo-van Krevelen plot with Hydrogen Index values (mg/g) plotted against Oxygen Index (mg/g) for the Jurassic coloured by source rock richness (Peters, 1986). Squares represent Celtic Sea data points and diamonds represent Wytch Farm data. No Jurassic samples exist for the Western Approaches. Overlays are based on Cornford *et al.* (1998) & Dembicki Jr (2009) and the applicability of the van-Krevelen plot is discussed in Section 4.2.2.

Hydrogen Index and Oxygen Index as discussed in Section 4.2.1.2 are both normalised to TOC so that their magnitudes should be independent of increasing TOC, therefore dilution should not cause a major effect on a pseudo-van Krevelen plot. Increasing thermal maturity of the organic matter would cause the conversion of kerogen into hydrocarbons, CO₂ and water. The data would then plot towards the origin as shown by van Krevelen (1984) as oxygen and hydrogen are expelled. This effect can be largely discounted due to the predominant low thermal maturity of the sediments (Section 5.3) and in addition would not cause the left to right scaling with TOC observed in Figure 5.31. The controls on the scaling of apparent kerogen type with increasing TOC could therefore be related to:

1. Degradation or oxidation of organic carbon on the seafloor or at shallow burial (van Krevelen, 1984) which would decrease the generative fraction of kerogen (HI) and increase the levels of oxygen in the organic matter (OI).
2. The environment of deposition would be a factor that would encourage high HI values and low OI with increasing TOC as deep marine and lacustrine settings are

associated with high TOC source rock development and are typified by the deposition of hydrogen-rich oxygen and oxygen poor marine or algal material.

3. Mixing of kerogen types as suggested by Dembicki Jr (2009) could also explain the distribution seen in the van-Krevelen diagram with lower TOC sediments containing greater proportions of terrestrial lignin (low HI & high OI) relative to lipids.

Zones of high TOC and HI are therefore the most likely to represent intervals of high source rock richness and quality. In the absence of S2 peak measurements data TOC has been shown to have a scaling effect with S2. In addition high TOC sediments of >2% TOC in the Celtic Sea and >1% in the Wytch Farm have been shown to correlate with oil generating kerogen organic matter preservation (Fig 5.31).

5.6.1. Summary of Kerogen Type

- Pseudo-van Krevelen plots have been used to try and identify kerogen types from pyrolysis information (Oxygen Index and Hydrogen Index).
 - High thermal maturity, mixing of kerogen types and oxidation and degradation of kerogen also affect Oxygen Index and Hydrogen Index values.
- No Oxygen Index values are available for Jurassic strata in the Western Approaches.
 - Wytch Farm data have been used as an analogue. The validity of this comparison will be discussed in Section 1.4.
- Middle and Late Jurassic data from the Celtic Sea predominantly plot in the Type III and Type IV kerogen zones (Fig 5.30).
 - Suggests a high degree of terrestrial input or oxidation of kerogen.
- Early Jurassic data are highly scattered plotting in the Mixed, Type III and Type IV zones.
 - A high degree of scatter with terrestrial input and kerogen mixing is likely.
- The Middle and Late Jurassic of the Wytch Farm plots in the Type II kerogen zone with only relatively few Early Jurassic samples available.
- The relative position of samples on the pseudo-van Krevelen plot correlates well with the enrichment in TOC of the sample (Fig 5.31).

5.7. Source Rock Potential from key well analysis

The analyses of source rock richness (Section 5.4) and quality (Section 5.5) and kerogen type have demonstrated that TOC and HI data show a positive correlation for the region of interest, with source rocks of high potential being identified. The objective of this section is to identify specific zones of high source rock potential zones by analysing the TOC and HI data against the wireline data (Section 4.3), and to quantify the potential hydrocarbon expulsion potential of these zones. These zones of source rock potential will be correlated with zones of similar age where possible to identify basin scale and regional zones of high source rock potential. The identified zones will in addition be compared to those intervals of source rock deposition highlighted by Scotchman *et al.* (2016), and will be used to quantify potential hydrocarbon yields in the basins.

The key wells were chosen based on their geographical distribution, the presence of Jurassic strata and data availability and quality.

5.7.1. North Celtic Sea Basin

5.7.1.1. 103/01-1 (Dragon Discovery)

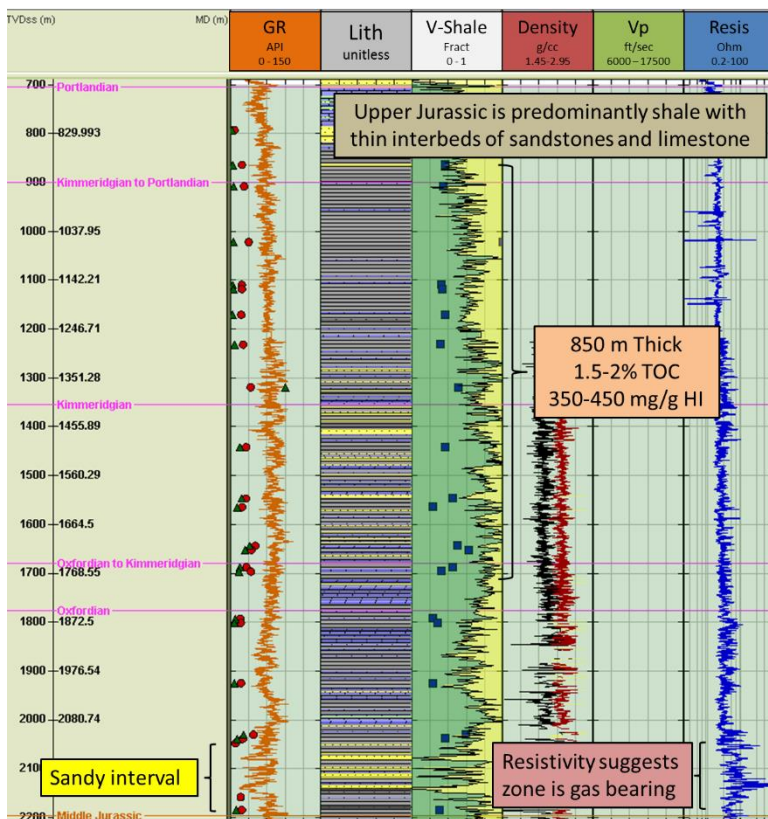


Fig 5.32. Wireline data from the Upper Jurassic section of 103/01-1 with a lithology based on the composite well log. TOC values (0-10%) are shown as red circles, HI as blue squares (1-1000 mg/g) and S1 peaks as green (0-0.1 mg/g) triangles. GR is the gamma ray tool in API, V-Shale is a volume shale log interpreted from the gamma ray log, the Density track contains

the bulk density (g/cc) in red and the neutron log (vol/vol) in black, Vp (ft/sec) is the compressional velocity and Resis is the deep resistivity in Ohmm of the formation.

The Dragon Discovery exploration well penetrated a thick section of potential Upper Jurassic (Oxfordian/Kimmeridgian to Portlandian) source rock rich shales with minor interbedded sandstones and limestones from 850-1700 m. TOC values of 1.5-2.0% are associated with HI values of 350-450 mg/g (Fig 5.32 & 5.33).

The Early Jurassic interval from 103/01-1 (Fig 5.33) has TOC values of 0.2-1.0% (poor to fair) with HI values of 20-50 mg/g which would indicate that the interval has minimal potential, S1 values of 0.35 to 0.65 mg/g in the Lower Jurassic intervals (Fig 5.33), however, suggest poor HI and TOC values are related to prior expulsion of oil and light oils (Scotchman, unpublished work). As discussed in Section 4.5, S1 yield (free hydrocarbons) increases with petroleum generation and an elevated value indicates prior petroleum generation with synchronous diminishment of remaining generative potential.

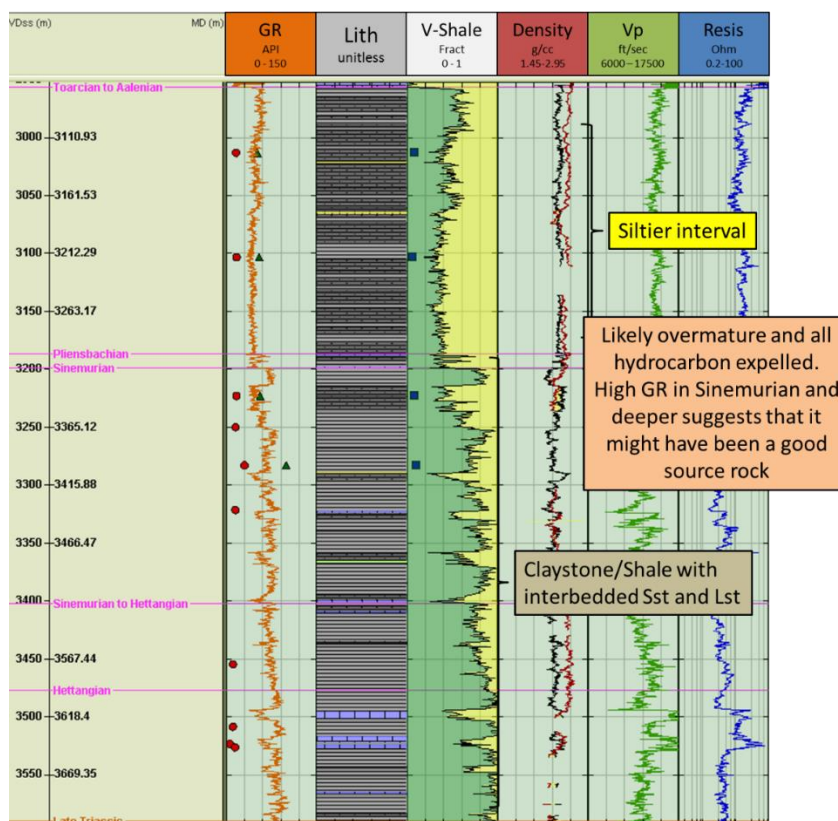


Fig 5.33. Wireline data from the Lower Jurassic section of 103/01-1 with a lithology based on the composite well log. TOC values (0-10%) are shown as red circles, HI as blue squares (1-1000 mg/g) and S1 peaks as green (0-0.1 mg/g) triangles. GR is the gamma ray tool in

API, V-Shale is a volume shale log interpreted from the gamma ray log, the Density track contains the bulk density (g/cc) in red and the neutron log (v/v) in black, Vp (ft/sec) is the compressional velocity and Resis is the deep resistivity in ohmm of the formation.

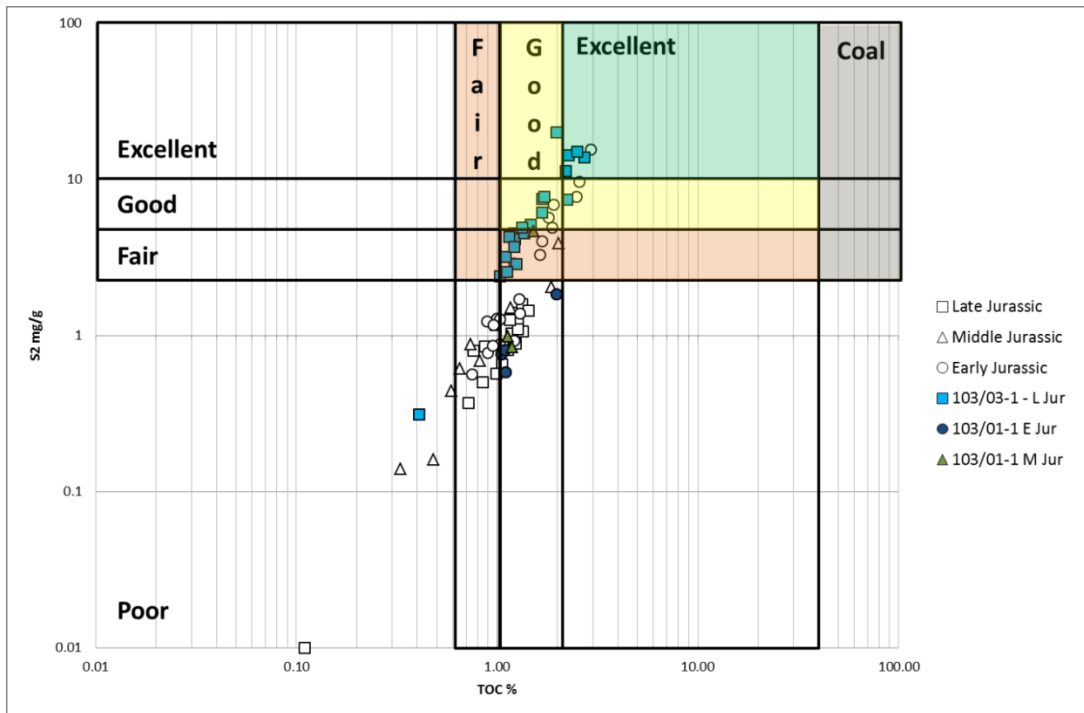


Fig 5.34. A crossplot of TOC (%) against S2 peak (mg/g) for the Jurassic (log-log axis) of the Celtic Sea with overlays based on (Dembicki Jr, 2009) with data plotted for the 103/01-1 from the Early Jurassic (dark blue circle), Middle Jurassic (green triangle) and Late Jurassic (light blue square). All other data is greyed out.

The lithology (from the composite well log) and V-Shale (interpreted from gamma ray) are suggestive of a sequence of sandstones at approximately 2060-2150 m with a high resistivity response indicative of a gas bearing reservoir that immediately underlies the zone of potential source rock and above the interpreted Middle Jurassic interval. Petroleum charge is indicated from biomarker analysis of sampled oil as being sourced from deeper equivalents to the Lower Jurassic section (Dembicki Jr, 1995).

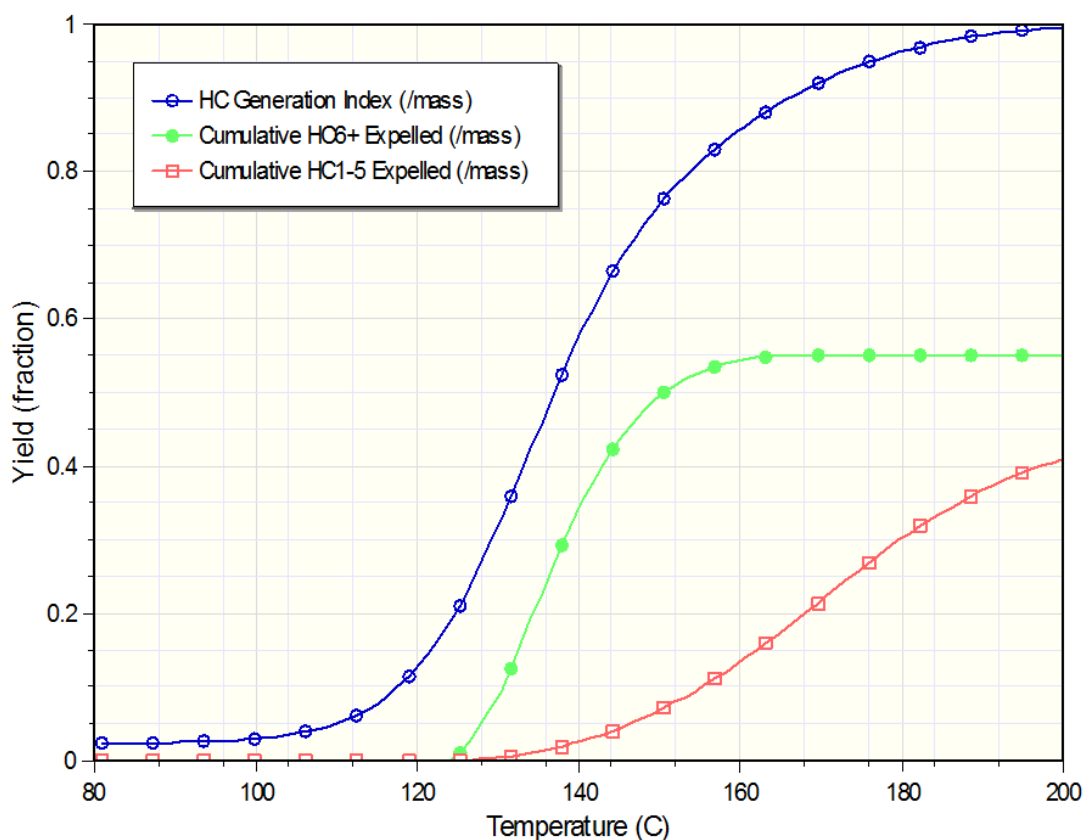


Fig 5.35. Plot of hydrocarbon yield against temperature based on the Upper Jurassic source rock section of 103/01-1 indicated using the KinEx software package with calculations based on Pepper & Corvi (1995). Kerogen type was input as algal matter (50% Type C) with high levels of terrestrial input (50% Type D/E) although Type C & Type D/E end-members were also run.

The indications in Section 5.6 that the Celtic Sea data at best plot in the mixed zone with Upper Jurassic data from 107/21-1 plotting in the zone between Type III & Type IV (Fig 5.30) suggesting a large degree of degradation or terrestrial input. In contrast Scotchman (unpublished) work suggests a lacustrine setting predominated in the Celtic Sea in the Late Jurassic. Therefore modelling of generation and expulsion for 103/01-1 has used a mixture of Type C (50%) and Type D/E (50%) organofacies with end member scenarios also run (Section 4.4).

Figure 5.34 shows an output plot from the KinEx software with plots shown for the fraction of hydrocarbon potential generated (blue), cumulative fraction of oil (green) and (gas) expelled plotted against temperature. Low amounts (0.02 CO₂/g rock) of HC initially present at temperatures <100°C represent the initial S1 peak in immature source rocks as described in Section 4.2.1. Oil generation (HC6+) is predicted to initiate at ~110°C but expulsion only begins when the kerogen sponge is saturated at ~125°C. Initially only oil is generated (125-150°C) and expelled with later gas generation (HC1-5) and cracking of oil to gas (130-200°C).

Generation is anticipated to be negligible beyond 200°C as the yield fraction has almost reached 1.0 meaning all petroleum potential has been generated.

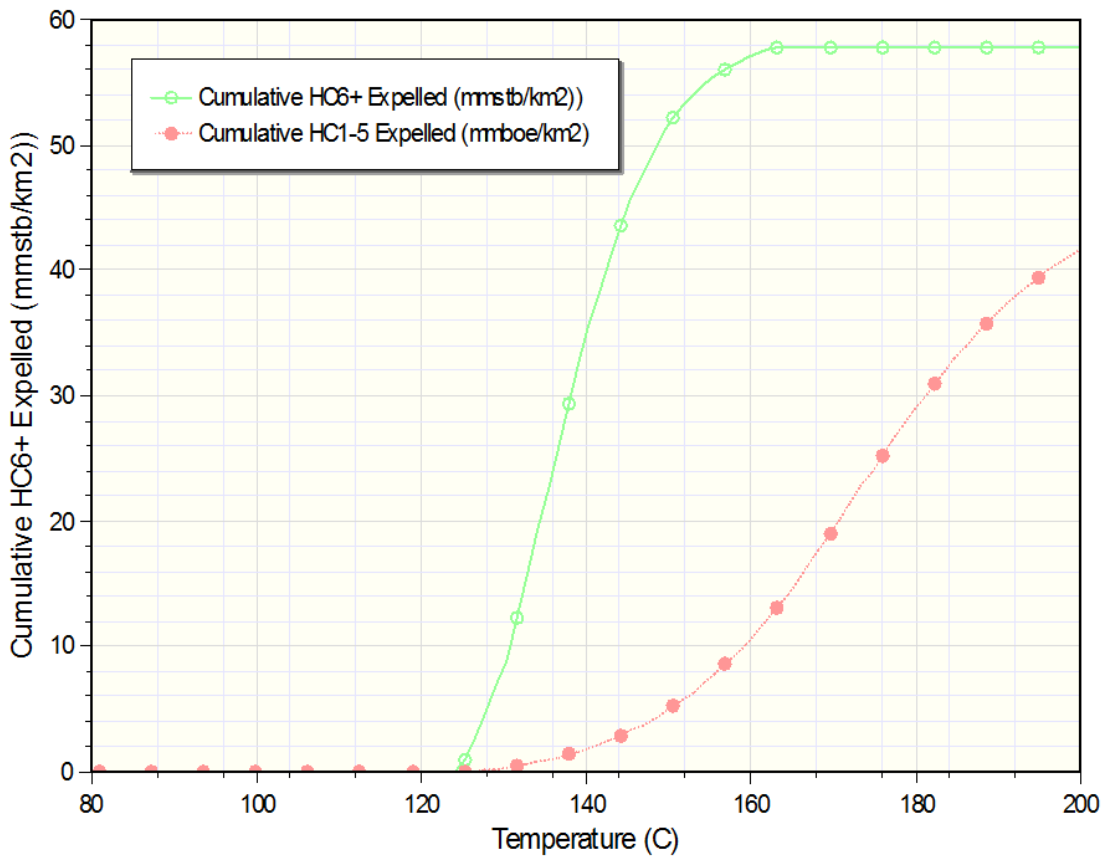


Fig 5.36. Plot of cumulative HC6+ (oil) and HC1-5 (gas) expulsion. Expulsion of oil would occur between 125-150°C with gas between 130-200°C. Early expulsion would be predominantly oil with later gas expulsion with estimates suggesting the Late Jurassic interval would be able to produce ~58 mmstb/km² of oil and ~42 mmboe/km² of gas.

Figure 5.27 indicates the likelihood that a mixture of algal and terrestrial kerogen types in the Upper Jurassic interval of 103/01-1 has the potential to produce sizeable quantities of hydrocarbon which would be dominated by oil generation and expulsion between 125-150°C with later generation and expulsion (130-200°C) of a lesser amount of gas (Fig 5.36 & 5.36).

5.7.1.2. 103/02-1

103/02-1 was drilled in the south-western section of the UK Celtic Sea in block 103/02 to appraise the Frigate Prospect with a primary objective of the Triassic Bunter Sandstones and the secondary objective the Middle Jurassic sandstones (Cooper, 1977).

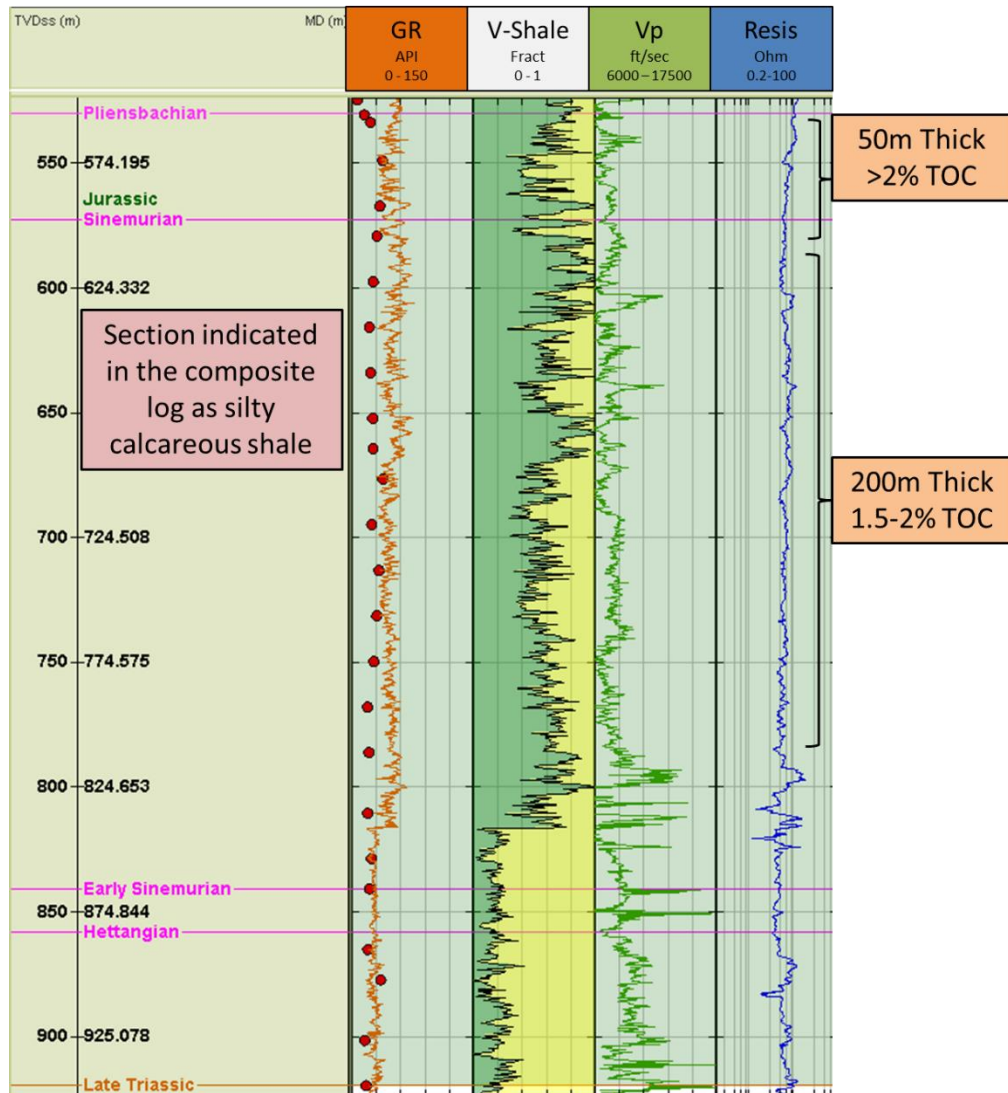


Fig 5.37. Wireline data from the Lower Jurassic section of 103/02-1. TOC values (0-10%) are shown as red circles with HI and S1 information unavailable. GR is the gamma ray tool in API, V-Shale is a volume shale log interpreted from the gamma ray log, Vp (ft/sec) is the compressional velocity and Resis is the resistivity in ohmm of the formation.

The Pliensbachian sequence consists of a 50 m thick section with TOC values greater than 2% (very good source rock richness). TOCs have decreased below 580 m TVDss at the top of the Sinemurian and vary between 1.5 to 2.0% (good source rock richness) until 820 m TVDss (Fig 5.38). No Hydrogen Index values were available for 103/02-1 so the source rock quality and potential cannot be calculated but has been estimated based on the S2-TOC

relationships described in Section 5.5. Kerogen type and organofacies have been based on the work described in Section 5.6 in which Early Jurassic data plots in the Type III & Type IV kerogen zone. The pseudo-van Krevelen plot (Fig 5.30) suggests domination by terrestrial input (Organofacies D/E – Section 4.4).

A large shift in the GR can be seen at 815 m TVDss which is not coincident with a casing point and no distinct change of lithology is indicated and the shift does not correspond to the end of a logging run. The effect present in the logs provided is not present in the interpreted composite log produced by Texaco. The GR shift might be an artefact of the wireline logging process or represent a misinterpretation of the wireline logs. Poor hole conditions, indicated in the well reports between, 2545 ft and 2900 ft MD (750-858 m TVDss) are likely causing the spikes in velocity in the Vp log (Fig 5.37).

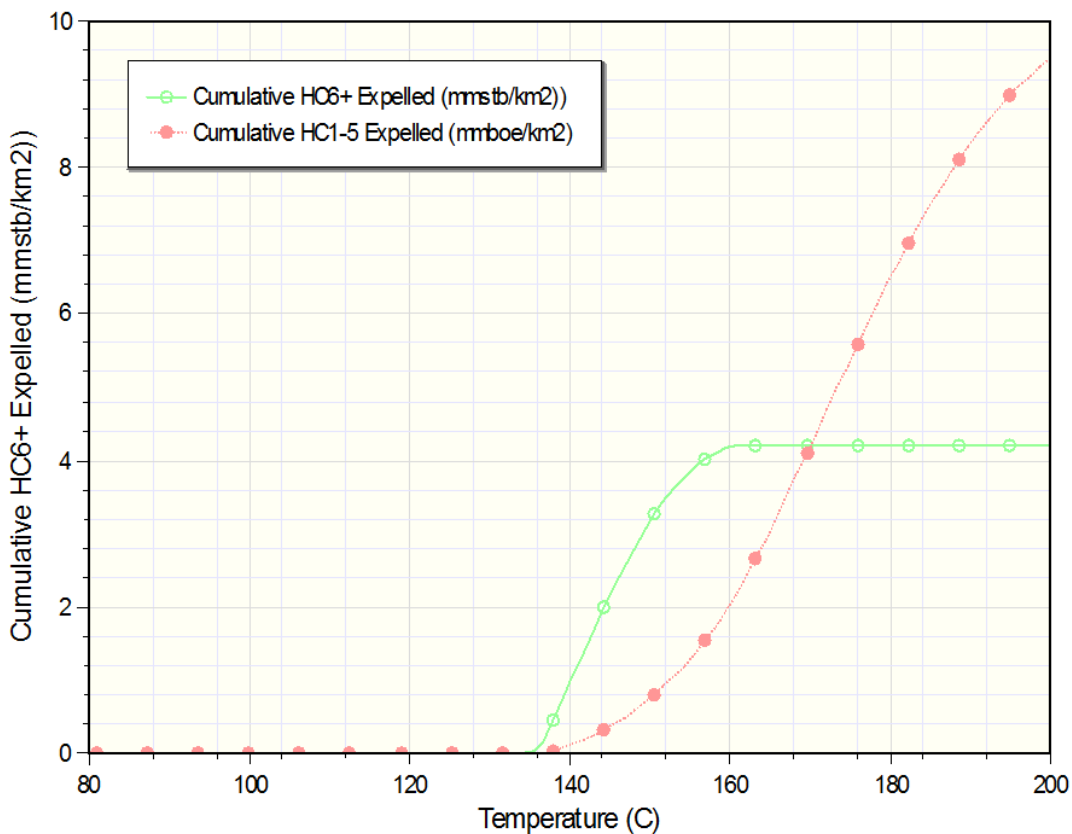


Fig 5.38. Plot of cumulative HC6+ (oil) and HC1-5 (gas) expulsion. Expulsion of oil would occur between 135-160°C with gas between 140-200°C. Early expulsion would be predominantly oil with later gas expulsion with estimates suggesting the Upper Jurassic interval would be able to produce ~4.2 mmstb/km² of oil and ~9.5 mmboe/km². Kerogen type is presumed to be predominantly Type D/E of terrestrial origin based on Early Jurassic data in the pseudo-van Krevelen diagrams (Fig 5.29. & Fig 5.30).

Modelling of the petroleum generation potential for the potential source rock zones identified in 103/02-1 (Fig 5.39) indicates that the section would expel predominantly gas 9.5 mmboe/km² (140-200°C) with ~4.2 mmstb/km² of oil expelled at a lower temperature range (138-160°C).

5.7.2. South Celtic Sea Basin

5.7.2.1. 102/29-1

102/29-1 was drilled as an exploration in partnership by Conoco, BNOB and Gulf Oil in 1977 in the South Celtic Sea (Conoco, 1977). The main objective was a Liassic (Lower Jurassic) wedge with Lower Cretaceous sandstones as secondary objectives.

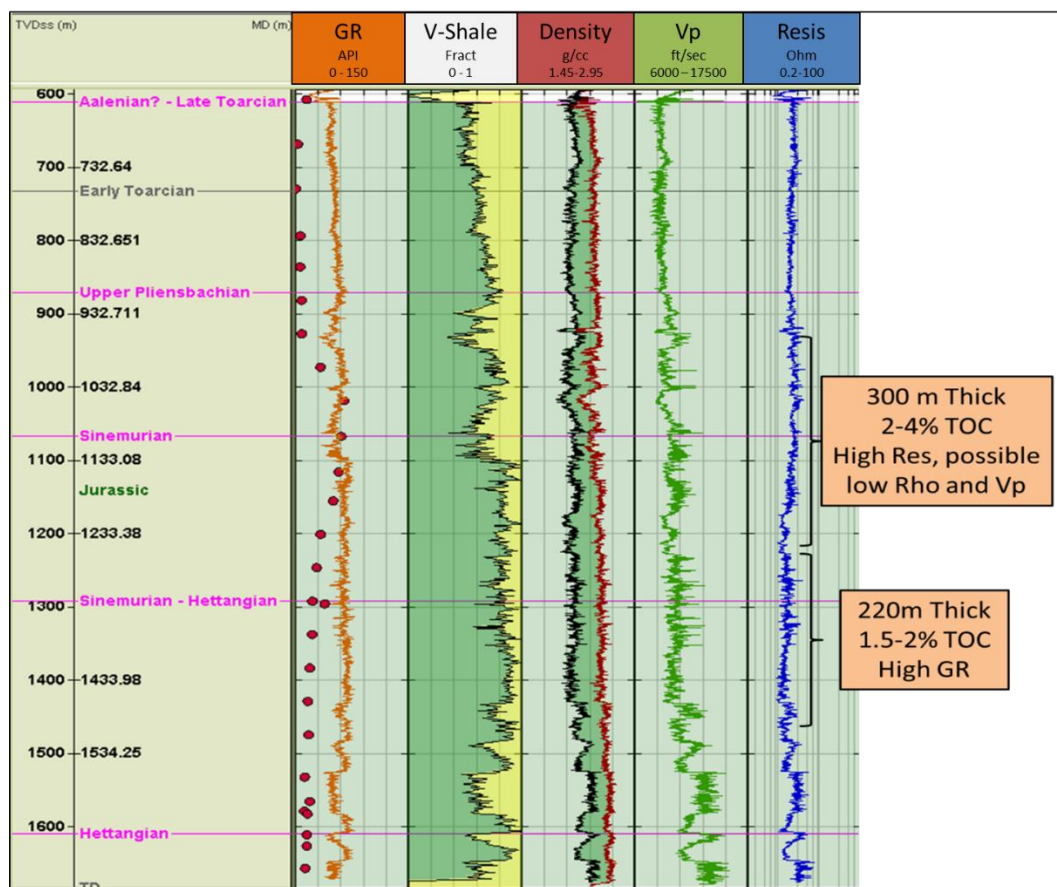


Fig 5.39. Wireline data from the Early Jurassic section of 102/29-1. TOC values (0-10%) are shown as red circles with HI and S1 information unavailable. GR is the gamma ray tool in API, V-Shale is a volume shale log interpreted from the gamma ray log, the Density track contains the bulk density (g/cc) in red and the neutron log (v/v) in black, Vp (ft/sec) is the compressional velocity and Resis is the resistivity in ohmm of the formation.

A peak of increased TOC (very good source rock richness) can be seen in the Pliensbachian to Sinemurian interval, with TOCs rising from negligible amounts to greater than 4% (600-

1050 m TVDss) and then decreasing by the Sinemurian to Hettangian interval (~1300 m TVDss) to between 1 and 1.5% (Fig 5.39). The peak described is similar in time interval to the 50 m interval of very good source rock richness described for 103/02-1. Source rock quality has been estimated due to the lack of pyrolysis information for 102/29-1 in a similar way to 103/02-1. The organofacies has been estimated similarly 103/02-1 utilising the distribution of Early Jurassic shown in Figure 5.30 (Section 5.6).

Figure 5.40 would indicate that a similar petroleum potential is estimated for 102/29-1 as 103/01-1 but hydrocarbon expulsion occurs at higher temperatures 130-160°C with more gas (~48 mmboe/km²) than oil (~40 mmstb/km²) expelled due to the expected predominance of terrestrial kerogen (Type D/E). The section in 102/29-1 is made up for two separate zones of source rock potential: 920-1220 m TVDss (2-4% TOC) and 1220-1440 m TVDss (1.5-2% TOC). This zone is 520 m thick in contrast to the 850 m thick section of Upper Jurassic source rocks described for 103/01-1 but has similar source rock potential (Fig 5.39) due to the higher TOCs in the upper 300 m section (920-1220 m TVDss).

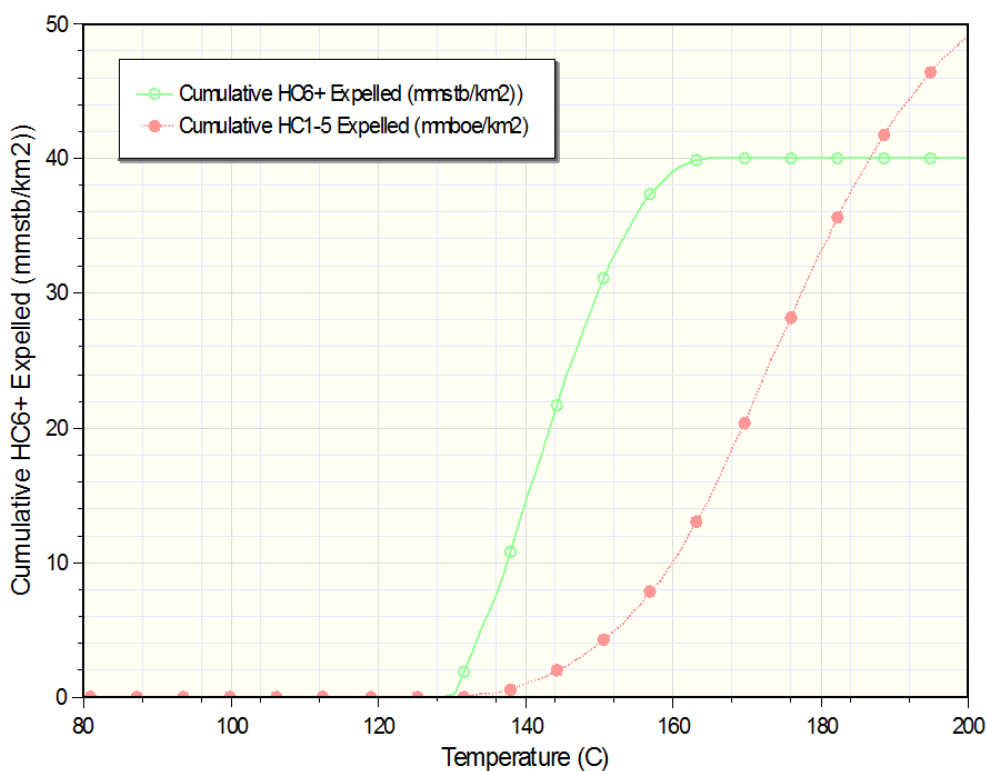


Fig 5.40. Plot of cumulative HC6+ (oil) and HC1-5 (gas) expulsion. Expulsion of oil would occur between 135-160°C with gas between 140-200°C. Early expulsion would be predominantly oil with later gas expulsion with estimates suggesting the Upper Jurassic section would be able to produce ~40 mmstb/km² of oil and ~48 mmboe/km² of gas. Kerogen type is presumed to be predominantly Type D/E of terrestrial origin based on Early Jurassic data in the pseudo-Van Krevelen diagrams (Fig 5.29 & 5.30).

5.7.2.2. 103/21-1

103/21-1 was drilled as an exploration well to test the Lower Cretaceous, Jurassic, Triassic and Permian sands and to test the stratigraphy of a poorly known area (Amoco, 1977). The Jurassic sequence penetrated in 103/21-1 has 4-5% (very good richness) TOC in the Middle Jurassic and Top Lower Jurassic 450-850 m TVDs (Fig 5.41) decreasing downwards into the Early Jurassic to ~1-2% (good richness). No pyrolysis data is available to test the source rock quality or kerogen type distribution for the well.

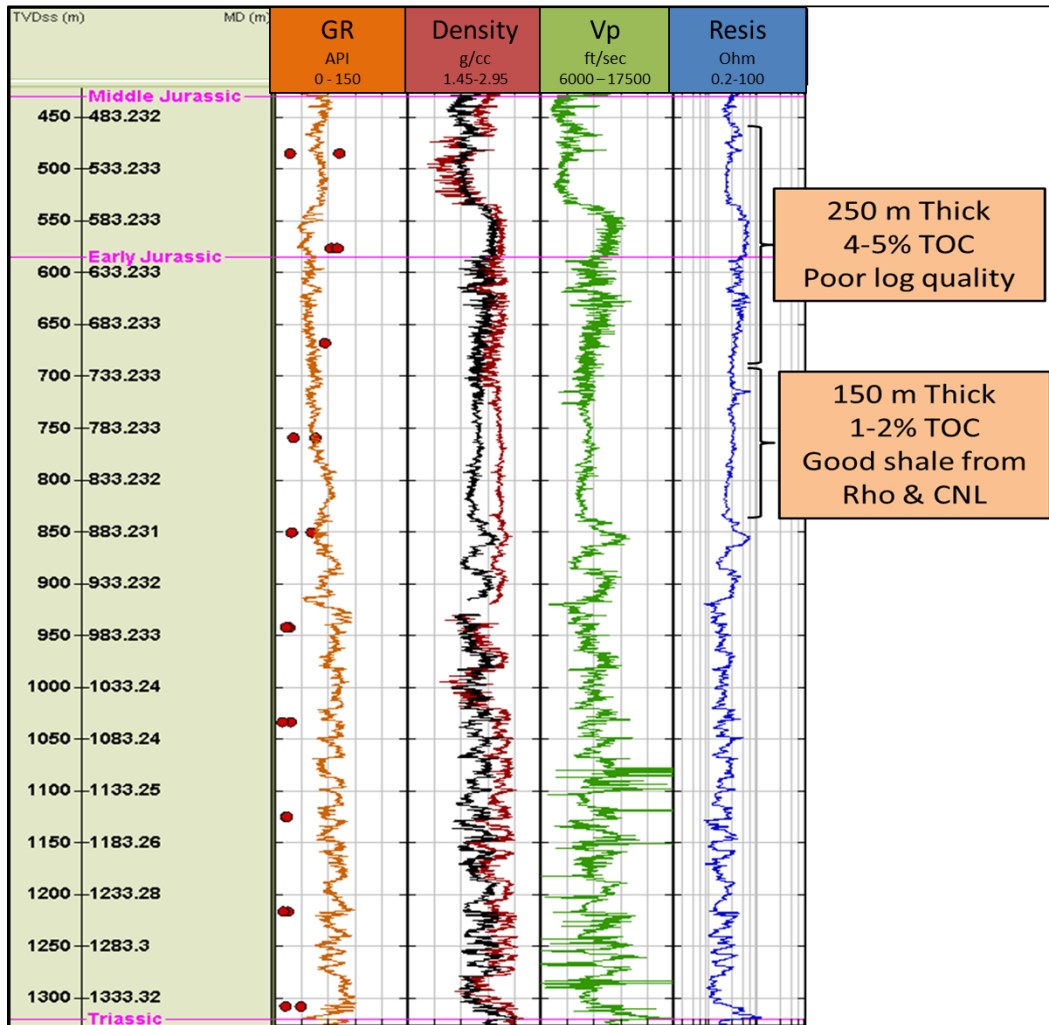


Fig 5.41. Wireline data from the Jurassic section of 103/21-1. TOC values (0-10%) are shown as red circles with HI and S1 information unavailable. GR is the gamma ray tool in API, V-Shale is a volume shale log interpreted from the gamma ray log, the Density track contains the bulk density (g/cc) in red and the neutron log (v/v) in black, Vp (ft/sec) is the compressional velocity and Resis is the deep resistivity in ohmm of the formation.

5.7.3. Western Approaches – Melville Basin

5.7.3.1. 73/13-1

73/13-1 was the first of two exploration wells drilled by Murphy Petroleum in the Melville Basin to test a faulted anticline at Jurassic/Triassic level with secondary objectives in the Lower Cretaceous and Eocene (Larsen *et al.*, 1983). The Sinemurian interval has very good source rock richness with a 150 m thick section of 2-5% TOC (1650-1800 m TVDs). Hydrogen Index values of 200 mg/g to a peak of 450 mg/g indicate very good source rock quality as well (Fig 5.42).

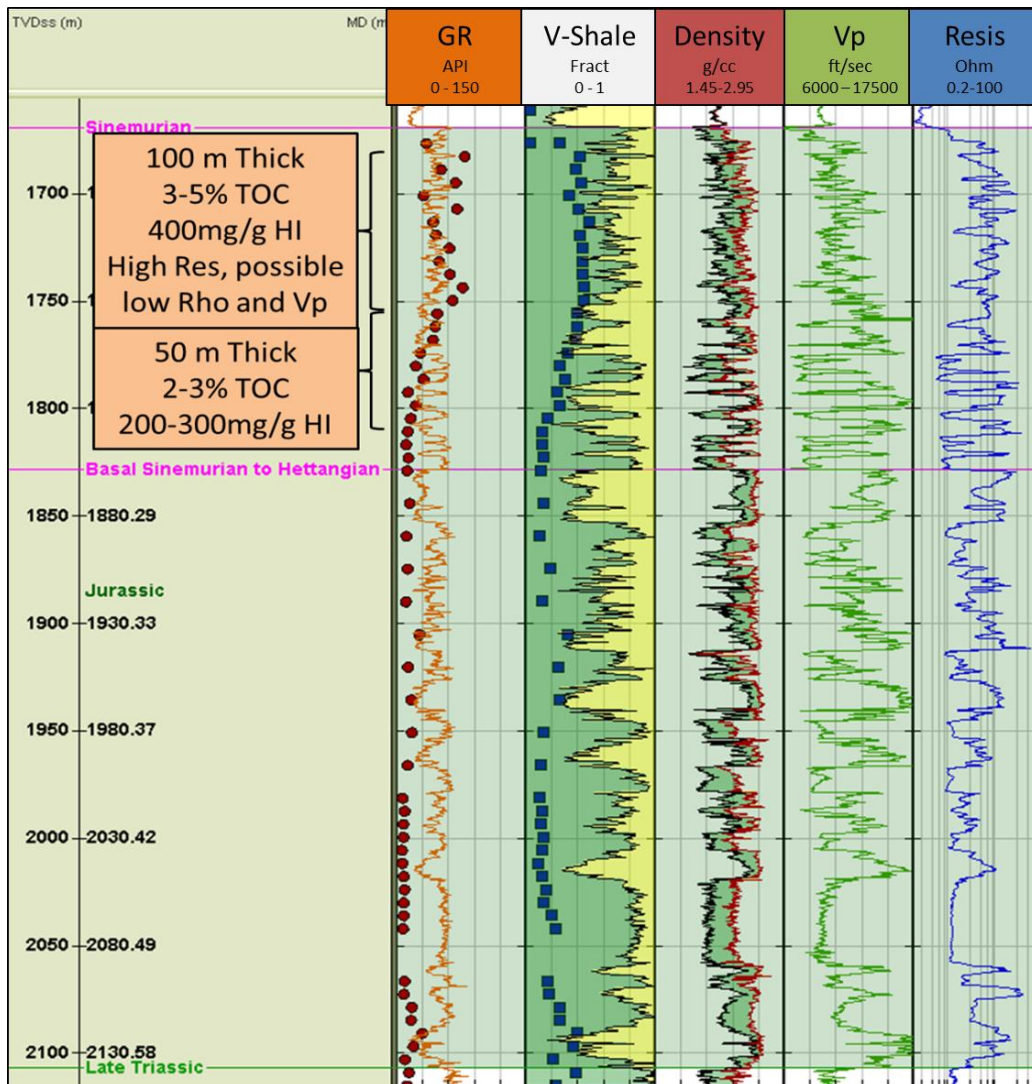


Fig 5.42. Wireline data from the Lower Jurassic section of 73/13-1. TOC values (0-10%) are shown as red circles, HI 1-1000 mg/g as blue squares GR is the gamma ray tool in API, V-Shale is a volume shale log interpreted from the gamma ray log, the Density track contains the bulk density (g/cc) in red and the neutron log (v/v) in black, Vp (ft/sec) is the compressional velocity and Resis is the resistivity in ohmm of the formation.

Gas chromatography mass spectrometry has been used to confirm that rich oil to mixed oil/gas prone source rocks are present in the Sinemurian of 73/13-1 (1670-1830 m TVDs – Fig 5.42) with analysed source extracts having similar paraffinic/naphthenic character to

sourced oils analysed from the Wytch Farm oilfield (Paleochem, 1983). The presence of sapropelic material (algal origin) in addition to the presence of abundant woody material from visual kerogen analysis (Scotchman, unpublished work) informs the assumption here that the source rocks represent marine organofacies with abundant terrestrial input (50/50 split).

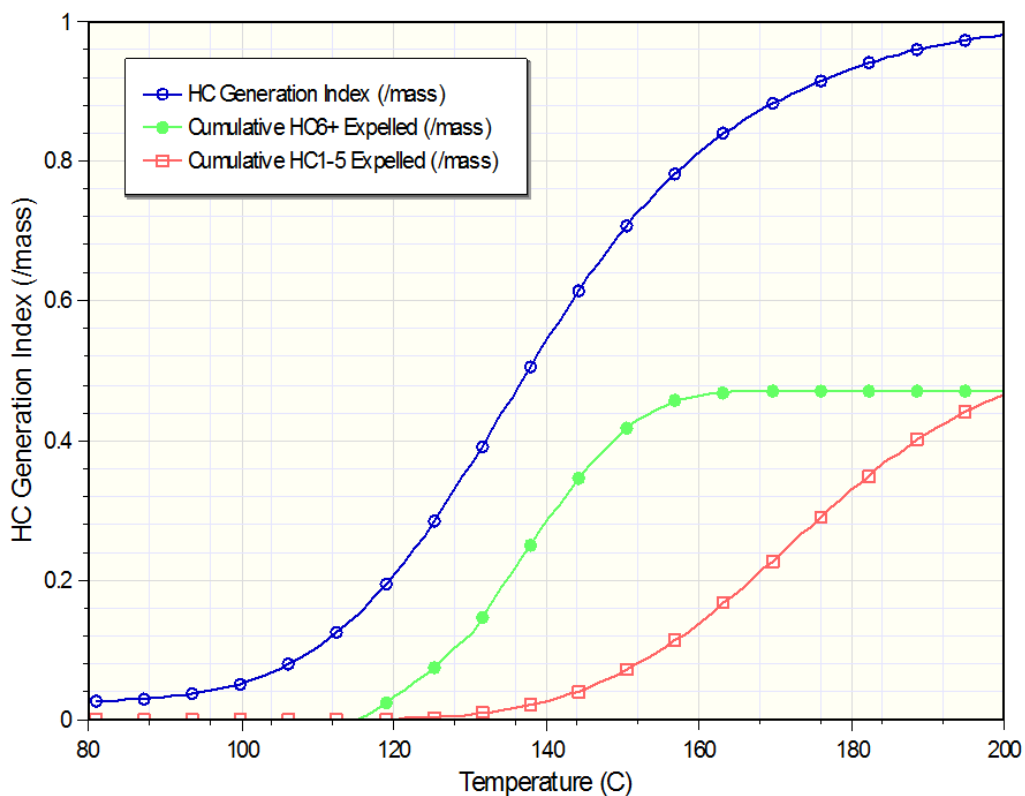


Fig 5.43. Plot of hydrocarbon yield against temperature based on the Upper Jurassic source rock section indicated in Fig 5.35 using the KinEx software package with calculations based on Pepper & Corvi (1995). Kerogen type was input based on Scotchman (unpublished work) as marine organic matter (50% Type B) with high levels of terrestrial input (50% Type D/E) although Type B & Type D/E end-members were also run.

The Lower Jurassic source rock sequence in 73/13-1 is expected, based on KinEx modelling, to have oil expulsion occurring between 115-160°C with later gas expulsion from 130 to >200°C. Approximately equal amounts of oil (~15.5 mmstb/km²) and gas (~15 mmoeb/km²) are predicted to be expelled by the source rocks analysed based on a 50/50 split of Type D/E and Type B organofacies (Fig 5.43). The split of organofacies is based on the algal and terrestrial kerogen types described by Scotchman (unpublished work).

A third of the volume hydrocarbon expelled from 103/01-1 is expelled in 73/13-1, but from a section 150 m thick compared to the 850 m section in 103/01-1, suggesting a much better quality source rock (Fig 5.44).

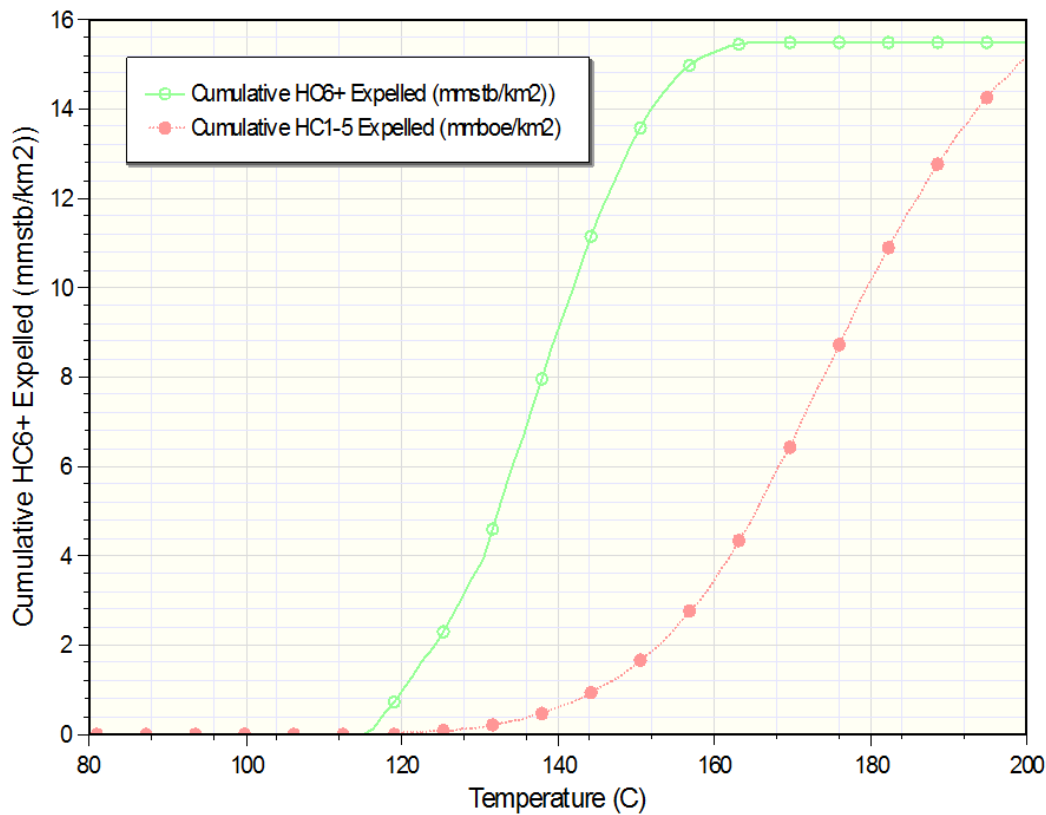


Fig 5.44. Plot of cumulative HC6+ (oil) and HC1-5 (gas) expulsion. Expulsion of oil would occur between 135-160°C with gas between 140-200°C. Early expulsion would be predominantly oil with later gas expulsion with estimates suggesting the Late Jurassic section would be able to produce ~15.5 mmstb/km² of oil and ~15 mmboe/km² of gas. Kerogen type is presumed to be composed of Type B & Type D/E.

$\delta^{13}\text{C}$ values from the Sinemurian are isotopically light with values of -30.6 to -31.2 per mil for the extract values. These values are similar to those values from Wytch Farm oils and dead oil tested from the Sherwood Sandstones in the adjacent 73/14-1 well (Paleochem, 1983). The similarity suggests a genetic links between the dead oil and the Early Jurassic interval.

5.7.3.2. 88/02-1

88/02-1 is one of four wells drilled between July and October 1977 to test the sub-Chalk (Upper Cretaceous) stratigraphy of the Western Approaches (Evans, 1977). An apparent ~30 m thick zone in the Sinemurian (520-550 m TVDss) with high GR, indicative of a high TOC “hot shale”, with TOCs in excess of 5% up to 8% is present. Figure 5.46 shows zones of >2% TOC (very good source rock richness) in the Lower Jurassic that have been identified in 88/02-1 below the Pliensbachian. The top of the Pliensbachian interval has been excluded due to the lack of wireline data and unclear extent of lithologies but the presence of TOC values of ~5% would suggest additional very good source rock richness but the extents of source rock richness is highly uncertain due to the lack of wireline data (Fig 5.45). Pyrolysis data was unavailable to interpret source rock quality in 88/02-1.

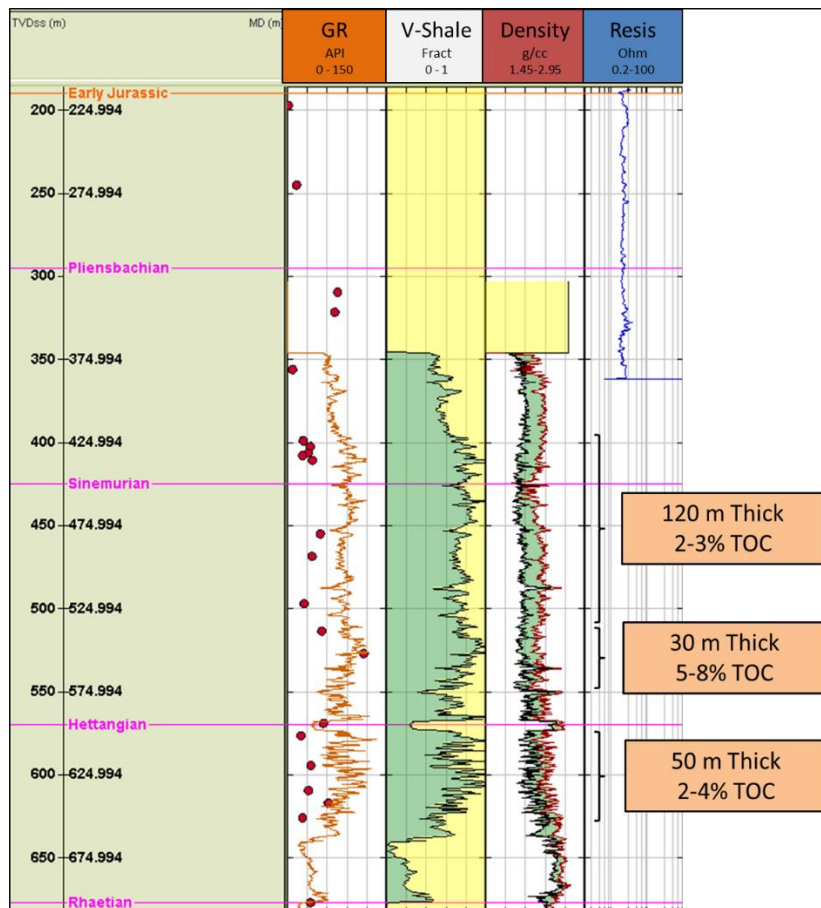


Fig 5.45. Wireline data from the Lower Jurassic interval of 88/02-1. TOC values (0-10%) are shown as red circles with HI and S1 information unavailable. GR is the gamma ray tool in API, V-Shale is a volume shale log interpreted from the gamma ray log, the Density track contains the bulk density (g/cc) in red and the neutron log (v/v) in black and Resis is the resistivity in ohmm of the formation. Wireline data is not available until 50 m into the Pliensbachian.

5.7.4. Summary of Source Rock Potential

- Six key wells have been analysed to quantify their hydrocarbon expulsion potential.
 - Pyrolysis and TOC data have been plotted against wireline data to identify zones of source rock potential.
 - The parameters of these zones have been input into KinEx to estimate the potential volume of hydrocarbons that could be expelled if they were taken to high maturity (~200°C).
- Source rock potential is variable in age but the Sinemurian, Pliensbachian and Hettangian intervals show source rock potential in 103/02-1, 102/29-1, 73/13-1 and 88/02-1.
- 103/01-1 and 102/29-1 have the highest expulsion potential analysed (100 and 88 equivalent mmstb/km² respectively).
- 73/13-1 has the highest potential per metre of source rock (0.2 equivalent mmstb/km² per m)

103/01-1

- 850 m thick source rock interval identified in the Upper Jurassic.
 - The Upper Jurassic interval has the potential to expel ~58 mmstb/km² oil and ~42 mmboe/km² of gas.
- The source rock potential of the Lower Jurassic section has been reduced due to prior generation and expulsion of hydrocarbons.

103/02-1

- 250 m thick gross source rock section of Sinemurian to Pliensbachian age which is estimated to have the potential to expel ~4.2 mmstb/km² oil and ~9.5 mmboe/km² of gas.

102/29-1

- 520 m thick source rock interval in the Hettangian to Pliensbachian with the potential to expel ~40 mmstb/km² oil and ~48 mmboe/km² of gas.

103/21-1

- 400 m thick interval with source rock potential in the Middle and Lower Jurassic.

73/13-1

- 150 m thick section of potential source rocks in the Sinemurian (>2% TOC and >200 mg/g HI).
 - Potential to expel ~15.5 mmstb/km² oil and ~15 mmboe/km² of gas.

88/02-1

- Minimum 200 m interval of source rock potential (>2% TOC) present in the Hettangian to Pliensbachian.

5.8. Discussion

Source rock richness and quality cannot be considered as a homogeneous property of a certain interval, i.e. the whole Lower Jurassic is not enriched in TOC. Zones of source rock richness can be identified in each of the key wells analysed.

5.8.1. Sinemurian to Pliensbachian

Pliensbachian and Sinemurian interval is characterised by good to very good source rock richness, such as has been observed in wells in the Western Approaches (73/13-1 & 88/02-1) and Celtic Sea (103/02-1 & 102/29-1). Figure 5.46 shows that well 98/16-1 in Western Approaches shows fair to very good source rock richness (0.5-2.5% TOC) in the Pliensbachian to Sinemurian interval (1720-1920 m TVDss), with a complimentary uranium log supporting interpretation of a source rock potential. A similar profile of TOC enrichment within this Lower Jurassic interval can be seen in Wytch Farm, based on data from 98/23-1 (Fig 5.47).

The source rock potential in the the Pliensbachian and Sinemurian correlates with a negative isotope excursion of -2 ‰ identified by Korte & Hesselbo (2011), and black shale deposition in the Wessex Basin described by Jenkins *et al.* (2012) discussed in Section 2.6.2.3. The presence of source rock enrichment in the Pliensbachian in the Celtic Sea, Western Approaches and Wytch Farm/Wessex Basin suggests widespread deposition of source rock enriched in organic matter at this time.

Scotchman (2001) and Scotchman *et al.* (2016) both indicate this period as a time of widespread source rock deposition along the Atlantic Margin, although Murphy *et al.* (1995) suggest that TOC values in the North Celtic Sea Basin for this interval are low (< 1% TOC). This good or lower source rock richness could be a factor of increased maturity as is interpreted to be the case here in 103/01-1 with the high values VR and S1 or data quality issues. Future work could look at integrating the Irish Sector Celtic Sea data with the current dataset.

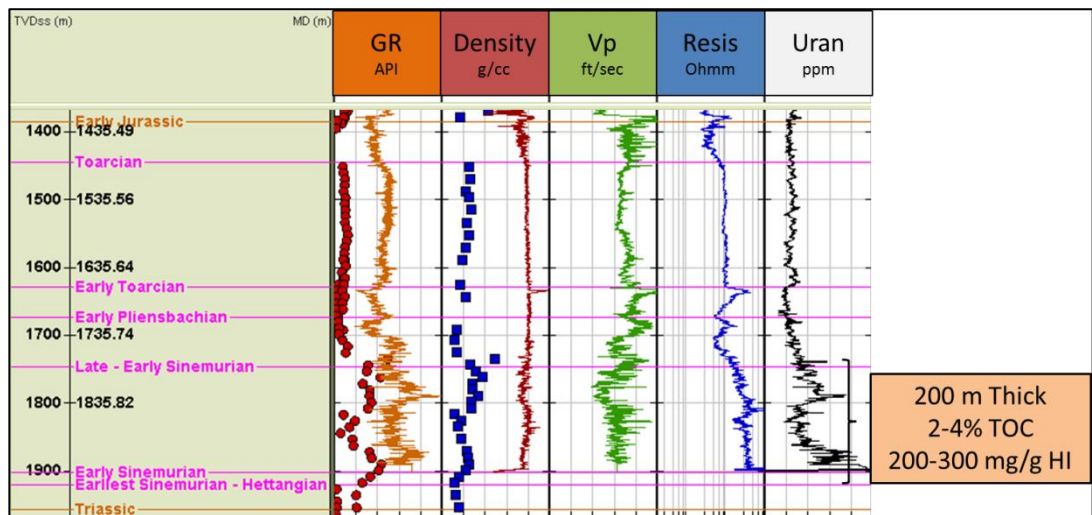


Fig 5.46. Wireline data from the Lower Jurassic section of 98/16-1. TOC values are shown as red circles, HI as blue squares. GR is the gamma ray tool in API, the Density track contains the bulk density (g/cc) in red, Vp (ft/sec) is the compressional velocity and Resis is the resistivity in ohmm of the formation. The Uran track is also included which is the uranium count from SGR in ppm as described in Section 4.3.

5.8.2. Toarcian

The presence of widespread marine shelf conditions with worldwide deposition of Early Toarcian shales is described in Section 2.6.2.4. The Top M2 Unconformity combined with a lack of accurate dating restricts the ability to analyse the Toarcian interval, with only limited well penetrations. TOC values of <0.25% (Fig 5.47) suggest the Toarcian to Aalenian section (610-880 m TVDss) of 102/29-1 to have poor source rock richness. The Top Lower Jurassic (undifferentiated) of 103/21-1, in contrast, shows TOC enrichment with values from 2-4% TOC in the top 150 m of the Lower Jurassic (Fig 5.41). Figure 5.47 demonstrates a TOC poor section in well 98/23-1 in Wytch Farm.

Good source rock richness is described in North Celtic Sea Basin by Armstrong (1988) and Murphy *et al.* (1995) but as described above good source richness is not observed in all wells in Celtic Sea and Western Approaches. Tyson (2004) suggests that the dominant control on the source rock potential of the Kimmeridge Clay Formation of onshore Dorset is the preservation of organic matter. The reason for poor source rock richness in the Toarcian of wells 88/02-1, 98/23-1 & 102/29-1 is difficult to analyse but possible causes could be restriction of organic matter input, oxidisation and breakdown of organic matter or dilution of TOC input due to increased clastic input (Aplin, pers comms.).

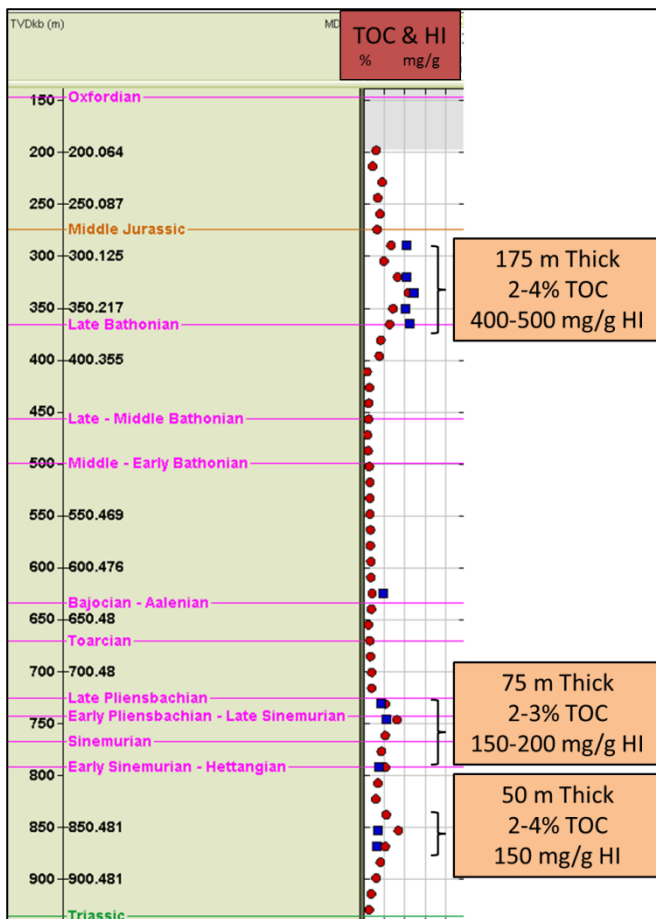


Fig 5.47. TOC (red circles) and HI (blue squares) data from Wytch Farm well 98/23-1 showing similar profiles of high TOC in the Pliensbachian to Sinemurian-Hettangian. In addition good source rock potential exists in the Middle Jurassic.

5.8.3. Middle Jurassic

The Middle Jurassic of the Atlantic Margins is characterised by a marine regression and this led to limited source rock deposition and restriction of facies between basins (Scotchman, 2016). Quantifying the extent of the marine regression is beyond the scope of this project and it is unknown whether the magnitude of regression was the same in the region of interest as in the Wytch Farm area.

Source rock analysis of the Middle Jurassic is hampered due to limited data availability and absence of Middle Jurassic strata due to the Top M2 unconformity particularly in the Western Approaches and South Celtic Sea Basin. TOC values of 1-5% (good to very good richness) are present in 103/21-1. In addition, Well 98/23-1 (Fig 5.47) in Wytch Farm displays very good source rock richness and potential (2-4% TOC with 400-450 mg/g HI values) but it seems poorly developed compared to Late Jurassic and Early Jurassic source rock potential (Appendix 3).

5.8.4. Late Jurassic

Section 2.6.4 discusses the palaeogeography of the Upper Jurassic in the Celtic Sea and Western Approaches with indications of the deposition of potential source rock facies. The presence of Upper Jurassic source rock potential, however, is possible where the Upper Jurassic has been preserved as shown by 103/01-1 but there are too few penetrations within the region of interest. Wytch Farm, however, displays significant potential in the Upper Jurassic in the Kimmeridge Clay of 98/11-4, 98/13-1 (Fig 5.48) and 98/16-1 (Appendix 3). The Lower Jurassic has been found to be predominantly immature to early mature in the region of interest so the depth of burial and maturity is similarly anticipated to be a problem for the feasibility of the Upper Jurassic as a potential expelling source rock in the region of interest.

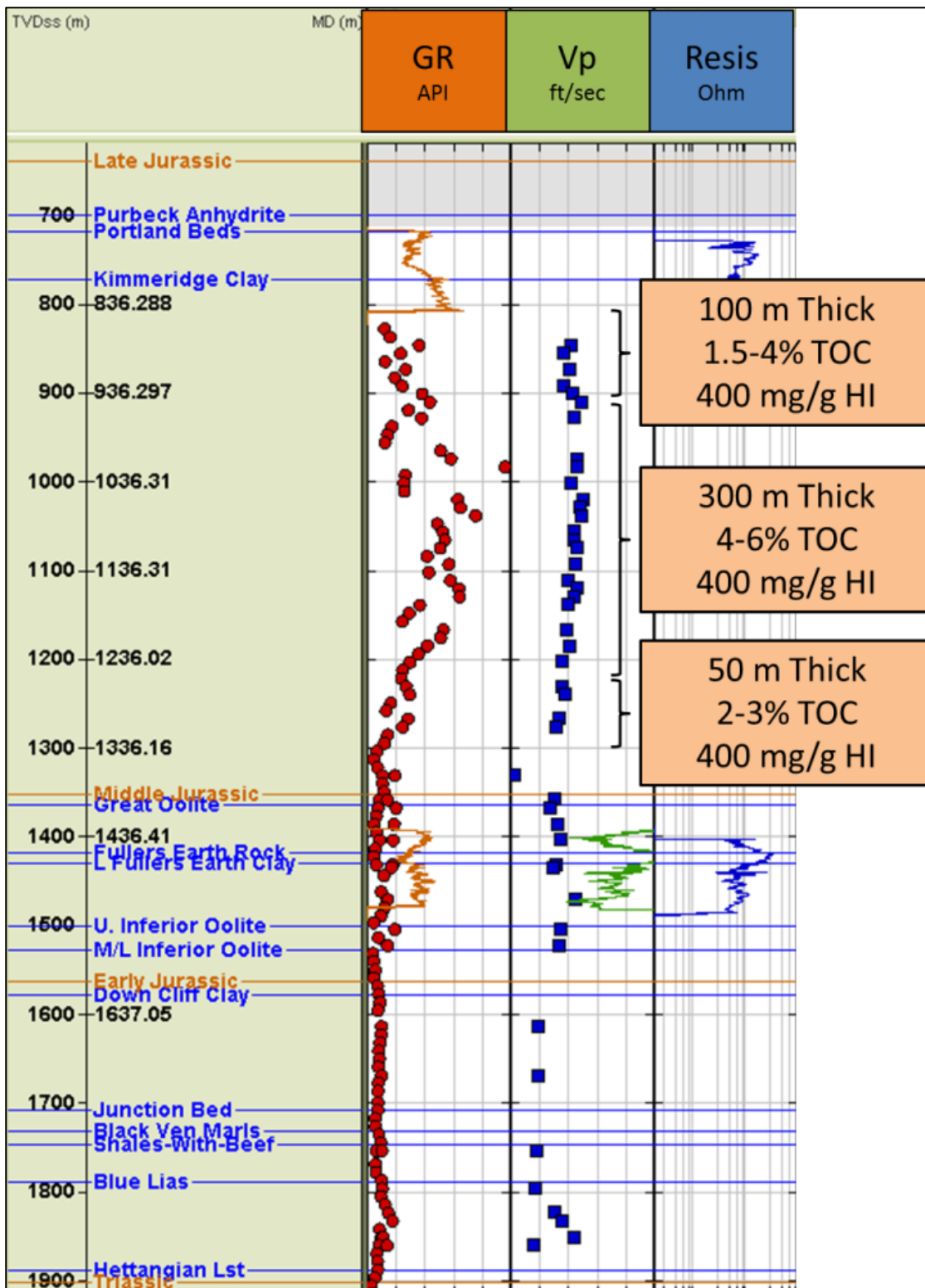


Fig 5.48. Wireline data from the Jurassic section of 98/13-1. TOC values are shown as red circles, HI as blue squares and S1 peaks as green triangles. GR is the gamma ray tool in API, Vp (ft/sec) is the compressional velocity and Resis is the resistivity in ohmm of the formation. Substantial Upper Jurassic potential exists with only minor potential in the Early Jurassic.

5.9. Conclusions

- Source Rock Potential in the Celtic Sea and Western Approaches exists (103/01-1 & 73/13-1) but is not homogenously distributed.
- Statistical analysis of Total Organic Carbon and Hydrogen Index data is useful for understanding patterns in the bulk data and understanding the distribution on a period scale.
 - Analysis of smaller time intervals along with wireline data is preferable for determining zone of enhanced source rock potential.
- Maturity in the majority of the wells analysed is low and could represent a significant risk to a working hydrocarbon system.
 - Higher maturity in Dragon Discovery 103/01-1 with generation of light oil/oil from the Lower Jurassic sequence.
 - Future work could include resampling of BGS core material from UK sector wells and wells in the Irish sector to further analyse the maturity in the region of interest.
 - Mature Jurassic present below 1654m TVDml in 73/13-1 and 2100 m TVDml in 103/01-1.
- Sinemurian to Pliensbachian source rocks have been identified in most wells and represent a potentially correlatable zone of source rock potential across the region.
- Anticipated Toarcian source rock potential that is present in the North Celtic Sea Basin cannot be demonstrated due to the lack of data availability (Section 5.7).
 - Large section of Toarcian likely removed by Top M2 Unconformity in the Western Approaches and in some South Celtic Sea Basin wells.
- The Top M2 unconformity has the potential to be an important control on the burial histories of the analysed basins and the preservation of source rock strata.
- Burial history modelling could provide future work with further understanding of the effects of the erosion possible if burial history modelling were potentially combined with the new OGA seismic lines which are beyond the scope of this study.

- Future work would require resampling of wells to increase the sample population and geographical extents of the data.
 - Analysis of data on a stage level would also require better constraint on the biostratigraphical data then is currently available.

Chapter 6

Discussion

6. Discussion

6.1. Introduction

6.1.1. Aim

The aim of the discussion chapter is to draw together the work discussed in previous chapters and discuss the important controls on source rock potential and the applicability of a potential Jurassic based petroleum system.

6.1.2. Objectives

- 1) Discuss and analyse the Top M2 Unconformity which is a key control on source rock preservation and maturity in the Western Approaches and Celtic Sea Basins.
- 2) Bring together the palaeogeography information discussed in Chapter 2 with the source rock analyses in Chapter 5 to discuss the potential effects of palaeoenvironments through the Jurassic on source rock potential.
- 3) Further discuss the maturity of the Jurassic focussing on the effect of the Late Jurassic to Early Cretaceous uplift and the implications for a working Jurassic petroleum system.
- 4) The implications and possibility of a working petroleum system in the region of interest will be a major focus of this chapter.
- 5) Discussing the potential open questions and the suggested future work are another objective of this chapter with a major focus on the work that would need to be done to constrain the potential for a working petroleum system.

6.2. Jurassic Palaeoenvironments

The evidence on which this discussion of Jurassic palaeoenvironments is based is described in Section 2.6.2.

6.2.1. Early Jurassic

Scotchman *et al.* (2016) indicated the widespread marine Hettangian to Sinemurian source rock deposition in the SW of Britain in the Wessex Basin, North Celtic Sea Basin and the Lusitania Basin (Fig 2.29). While the Western Approaches Basins and South Celtic Sea Basin are noted in grey on Figure 2.29 no source rock deposition is indicated but analysis in Section 5.7.2 and 5.7.3 indicates the presence of Pliensbachian to Sinemurian source rock potential in these basins (based on wells 102/29-1, 73/13-1 & 88/02-1).

The earliest Jurassic sea-level transgression led to marine incursions into the rift basins of the SW of England with widespread deposition of marine facies mudrocks. The marine environment is likely to have been highly influenced by the Tethyan Marine Realm to the SE in contrast to paralic source rock deposition in the Halten Terrace in the Hettangian to Sinemurian which is indicated by Scotchman *et al.* (2016) as influenced by the Boreal Marine Realm. The rich source rocks of SW England (Jenkyns *et al.*, 2002; Hallam & Wignall, 2004) are not present in the study area with carbonaceous mudstones with interbedded limestone deposition instead prevalent in the region of interest. Analysis in Section 5.7 indicates Hettangian age rocks to be typically TOC poor suggesting that the anoxic deposition environment of onshore SW England to be absent in the region of interest.

Sinemurian to Pliensbachian greenhouse conditions and a negative carbon isotope excursion of -2 ‰ (Korte & Hesselbo, 2014) are synchronous with observed widespread source rock potential in the region of interest (Section 5.7). The very good quality Sinemurian source rocks of 73/13-1 are deduced (Section 5.7.3.1) to represent marine deposition with some terrestrial input. The oxygen depleted conditions that were absent in the Hettangian were likely present at this time coinciding with increased organic matter input. The Hettangian of 73/01-1A is dominated by 15 m of sand which suggests that increased clastic input could also have contributed to poor TOC enrichment in this interval.

The Toarcian period was a period of global source rock development with Murphy *et al.* (1995) indicating maximum relative sea-level and broad marine shelf conditions in the region of interest with mudrock deposition. Much of the Toarcian sequence has been eroded from the South Celtic Sea Basin and Western Approaches Basins but in Section 5.8.2 variable source rock enrichment based on the limited well data available is suggested.

6.2.2. Middle Jurassic

In contrast to the pre-dominant marine palaeoenvironment of the Early Jurassic during the Aalenian to Bathonian relative sea-level fell in the SW of England with Scotchman *et al.* 2016 suggesting widespread marine withdrawal from the basins of the Atlantic Margin. Van Hoorn (1987) describes shallowing in the Celtic Sea at this time. During the Bathonian to Callovian the rise of sea-levels led to the deposition of limestones suggested (Baron *et al.*, 2012). Kamerling (1979) indicates the presence of marine claystones in the Bristol Channel Basin and South Celtic Sea Basin. The presence of some source rock potential in undifferentiated Middle Jurassic of well 103/21-1 in the South Celtic Sea Basin is indicated in Section 5.7. The exact palaeoenvironment of the Middle Jurassic is uncertain but shallowing likely caused a reduction of any anoxic environments in the Celtic Sea with only limited potential for source rock deposition in a shallow shelf environment as shown in Figure 2.35.

6.2.3. Late Jurassic

In the North Celtic Sea Basin the Late Jurassic is characterised by the deposition of non-marine/lacustrine source rocks (Caston, 1995; Scotchman *et al.*, 2016) with widespread anoxic conditions. The Dragon Discovery well 103/01-1 is a good example of a North Celtic Sea Basin well with a thick section (850 m) of source rock of good richness of 1.5-2% TOC (Section 5.7.1.1). The section is composed of shale with frequent interbedded sandstones and limestones. Fig 6.1 from Scotchman *et al.* (2016) suggests that the Celtic Sea was likely cut off from the Tethyan Marine Realm that influenced the Wessex Basin which underwent Late Jurassic marine source rock deposition. The basin extent shaded in grey on Figure 6.7 suggests the linkage of the Wessex Basin to the Lusitania Basin via the Western Approaches. The erosion of all Upper Jurassic strata from the Western Approaches makes testing this hypothesis impossible. It is possible, however, that if a linkage existed the Western Approaches was in a marine environment similar to that in the Wessex Basin/Wytch Farm (Fig 6.1 - Section 2.6.4).

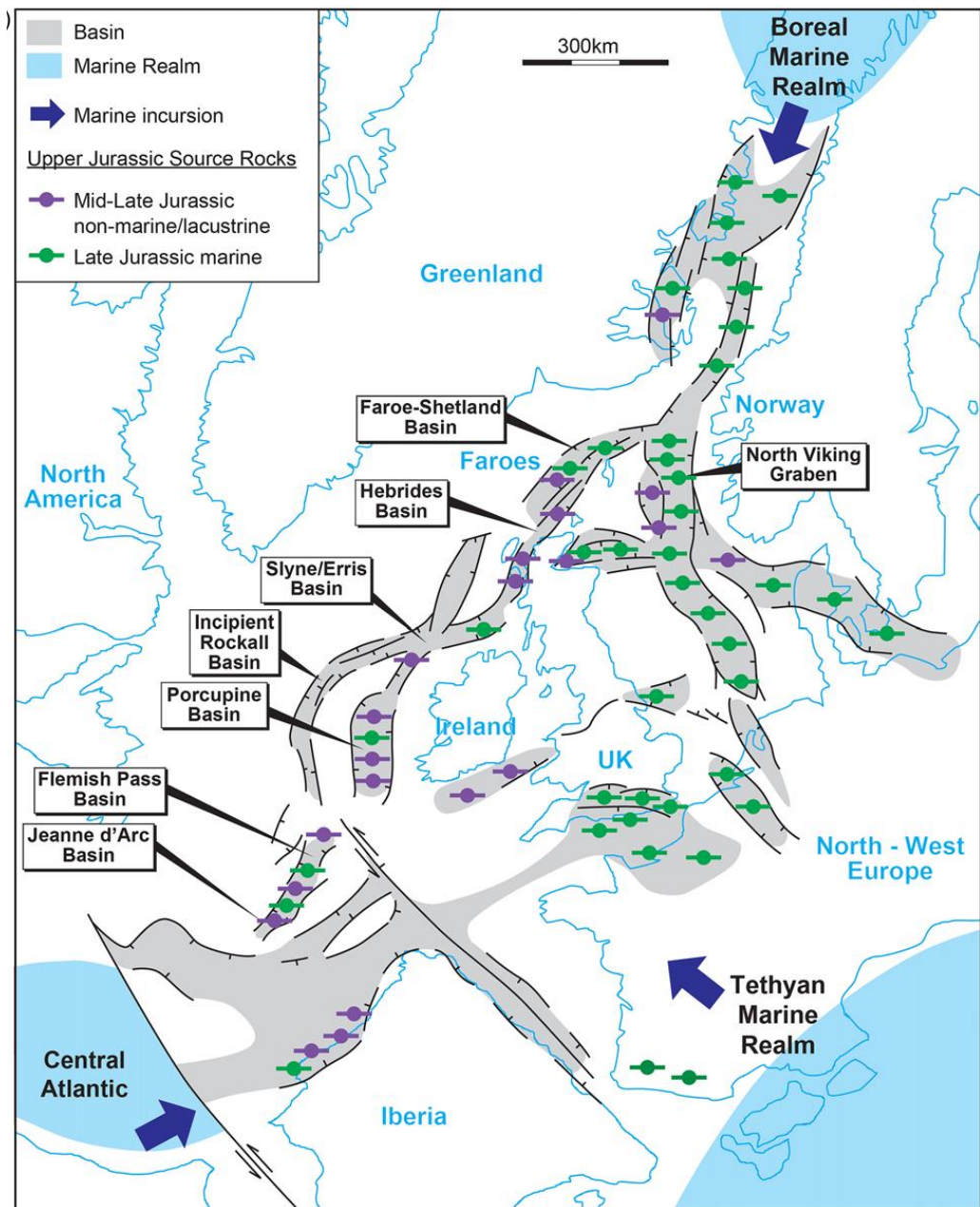


Fig 6.1. Map of the current North Atlantic margin of Europe for the Late Jurassic showing the areas of source rock deposition and Mesozoic rift basins (Scotchman *et al.*, 2016).

6.3. Top M2 Unconformity “Cimmerian”

6.3.1. Introduction

The Top M2 Unconformity is a regional scale unconformity which is described in Section 2.6.4. The unconformity truncates the underlying strata (Fig 6.2) and has removed much of the Jurassic sequence of the Western Approaches Basins and South Celtic Sea Basin and therefore is a major control on source rock distribution and burial. This section will focus on the type of unconformity present and will then discuss possible mechanisms for the development of a Late Jurassic to Early Cretaceous unconformity.

Hillis (1988) discusses what he terms the “Cimmerian Unconformity” in detail; describing the presence of complete Jurassic sequences in the adjacent Bristol Channel and South West Channel Basins and on the continental slope. Based on personal communication with Ziegler, Hillis (1988) stated that the main period of tectonic activity related to the Top M2 Unconformity was in the Late Jurassic-Early Cretaceous with marine conditions (as described in Section 2.6.4) prevalent prior to this in the Western Approaches. McMahon & Turner (1998) in addition have used chronostratigraphic dates to suggest a correlative Berriasian data for the unconformity in the Celtic Sea Basins.

The truncation of underlying strata by the Top M2 Unconformity is shown in Figure 6.2 and indicates that while the unconformity may incorporate periods of non-deposition the major effect on the Jurassic interval is erosional. Recent analysis of the OGA 2016 seismic lines suggests that the Top M2 Unconformity may in places be composed of multiple events truncating each other (J. Henderson, per comms). Underhill & Partington (1993) have been able to correlate the maximum areal extent of the Middle Jurassic doming event of the North Sea to the Aalenian. The well correlation panels (Fig 6.4 & Fig 6.5) from Stricker *et al.* (unpublished work) suggest a more complicated pattern than the Middle Jurassic event discussed by Underhill & Partington (1993). The unconformity event has variable sub- and supra-crop ages and does not narrow in on one particular age as in Underhill & Partington (1993); therefore the age of maximum areal extent cannot be determined in the Celtic Sea and Western Approaches without future work (Section 6.6).

Section 5.3.2 discussed the burial history models present for the Western Approaches and Celtic Sea. The models proposed vary widely in magnitude of Jurassic eroded: 0.7 km (Hillis, 1988; Ruffell 1995) to 2.8 km (Ottaviani *et al.*, unpublished work). The exact amount of Jurassic eroded is therefore poorly constrained but additional Vitrinite Reflectance and apatite fission track work as discussed in the Future Work (Section 6.6) could aid in constraining the possible magnitude of uplift in the Western Approaches and Celtic Sea during the Late Jurassic to Early Cretaceous.

6.3.1. Mechanisms for Uplift

Hsu (1965) used a variant on Airy's (1855) theory of isostasy to explain potential uplift and erosion of continents linking decreases in mantle density to the uplift and erosion of "ancient land masses" similar to that described as Airy-Woollard Isostasy by Wilcox (1976). This section will discuss relative density differences and crustal thicknesses in addition to plate flexure and rigidity to propose potential mechanism for the Late Jurassic to Early Cretaceous uplift in the Western Approaches and South Celtic Sea Basin.

Morgan (1983) linked typical values of rift shoulder uplift of 1 to 2 km to thermal changes in the lithosphere and asthenosphere over the period of a few tens of million years. Morgan (1983) proposed models of isostatic response to rifting with plateau or domal uplift during the main rift phase and during a post-rift phase of thermal relaxation. Montadert *et al* (1979) suggested that rift shoulder uplift is related to similar isostatic readjustments.

Rohrman *et al.* (2002) associated Neogene domal uplift in the North Atlantic to a thermal anomaly in the mantle suggesting mantle uplift as the primary mechanism driving uplift. Oyarzun *et al.* (1997) proposed a model for the opening of the Central Atlantic in which a sub-lithospheric plume channelling process occurred during the Triassic-Jurassic stage of opening. Oyarzun *et al.* (1997) suggested that a Variscan corridor of thinned lithosphere along the future Central Atlantic combined with a European lithospheric thin-spot, a Central Atlantic plume and asymmetric opening of the Central Atlantic led to north to northeast channelling of the plume as far as the Iberian Peninsula.

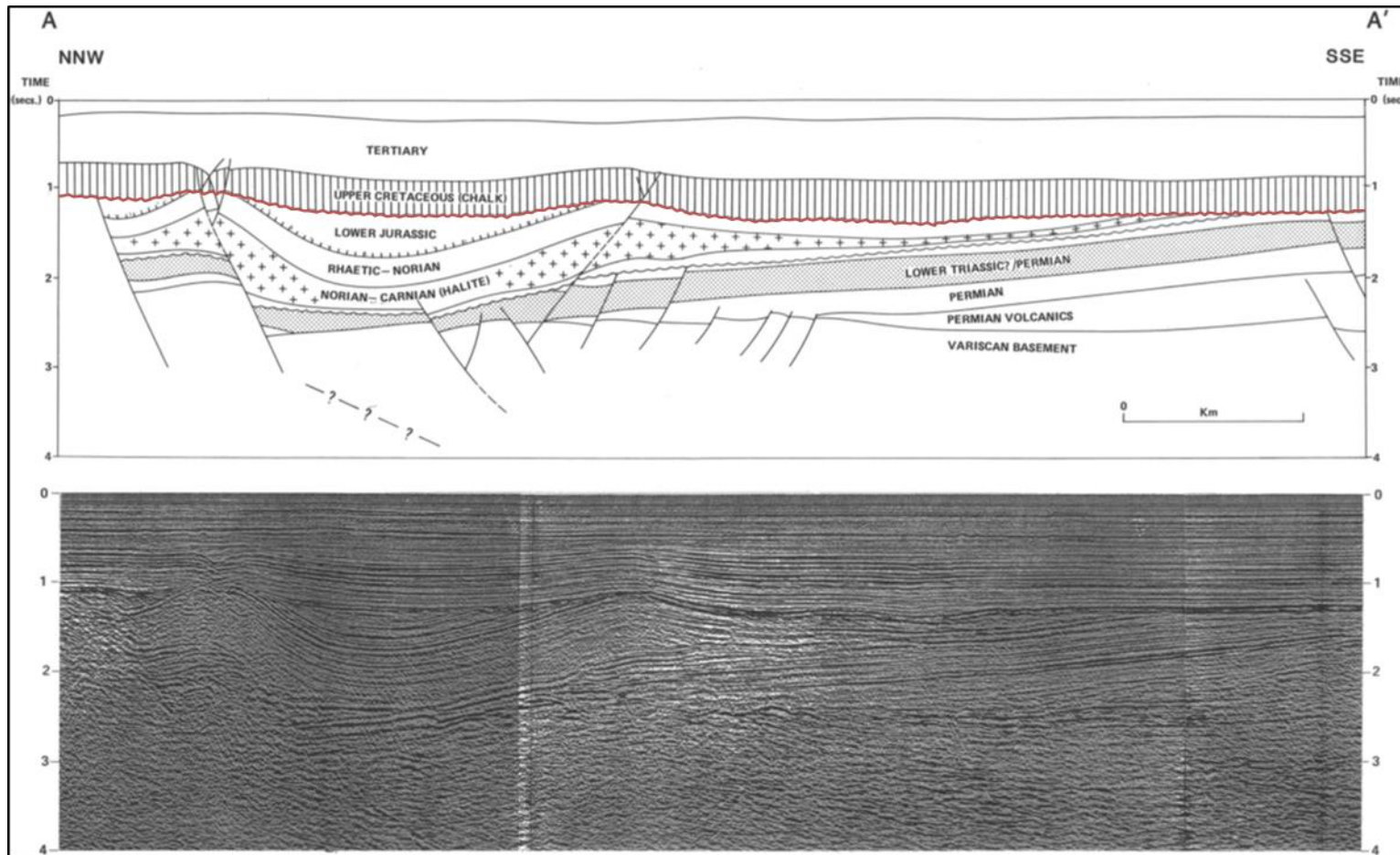


Fig 6.2. A seismic section (bottom) and an interpreted seismic profile (top) from A-A' (Chapman, 1988). The Jurassic reflectors are truncated by the Top M2 Unconformity with preservation in a syncline between salt walls.

Murrell (1986) discusses continental uplift due to shortening of the crust with shortening and compression leading to regional uplift. The literature discussed in Section 2.6.4 suggests that the Late Jurassic was a time of active rifting. In addition while Cenozoic inversion structures are described in the North Celtic Sea Basin, sub-unconformity inversion is unclear although where the Jurassic is preserved it has the synclinal structure as shown in Figure 6.2. The synclinal structure of the preserved Jurassic could be related to shortening and folding with later truncation or alternatively is related to salt withdrawal. Chapman (1989) suggests that the Upper Jurassic of the Western Approaches is characterised by transtensional sinistral rifting and therefore regional shortening of the crust seems unlikely.

6.3.2. Hypotheses for Uplift Generation

The correlation panels in Figures 6.4 & 6.5 seem to show a lack of distinct trends and the inability to find a correlative age for the Late Jurassic and Early Cretaceous uplift and erosion of the Western Approaches and South Celtic Sea Basin means that it is difficult without further work (Section 6.6) to pin down the exact cause of the regional uplift. Hillis (1988) indicates SW-NE propagation of uplift during the Late Jurassic to Early Cretaceous and connects the observed uplift and erosion to the opening of the Bay of Biscay (Section 2.7) and Central Atlantic (Section 2.6.4). Montadert *et al.* (1979) suggests, however, that the opening of the Bay of Biscay occurred without thermal doming. In addition, Tugend *et al.* (2014) indicated that the Bay of Biscay only underwent transtensional rifting in the Late Jurassic with seafloor spreading not localised until the Aptian-Albian which could be coincident with cooling and thermal subsidence of the margins (Fig 2.36). McMahon & Turner (1998) associate the opening of the Bay of Biscay with a later Aptian-Albian unconformity in the Celtic Sea Basins and suggest based on their analyses of the subsidence and uplift rates a thermal mechanism for uplift with significant vertical uplift or a similar dome to that described by Underhill & Partington (1993) for the Middle Jurassic of the North Sea.

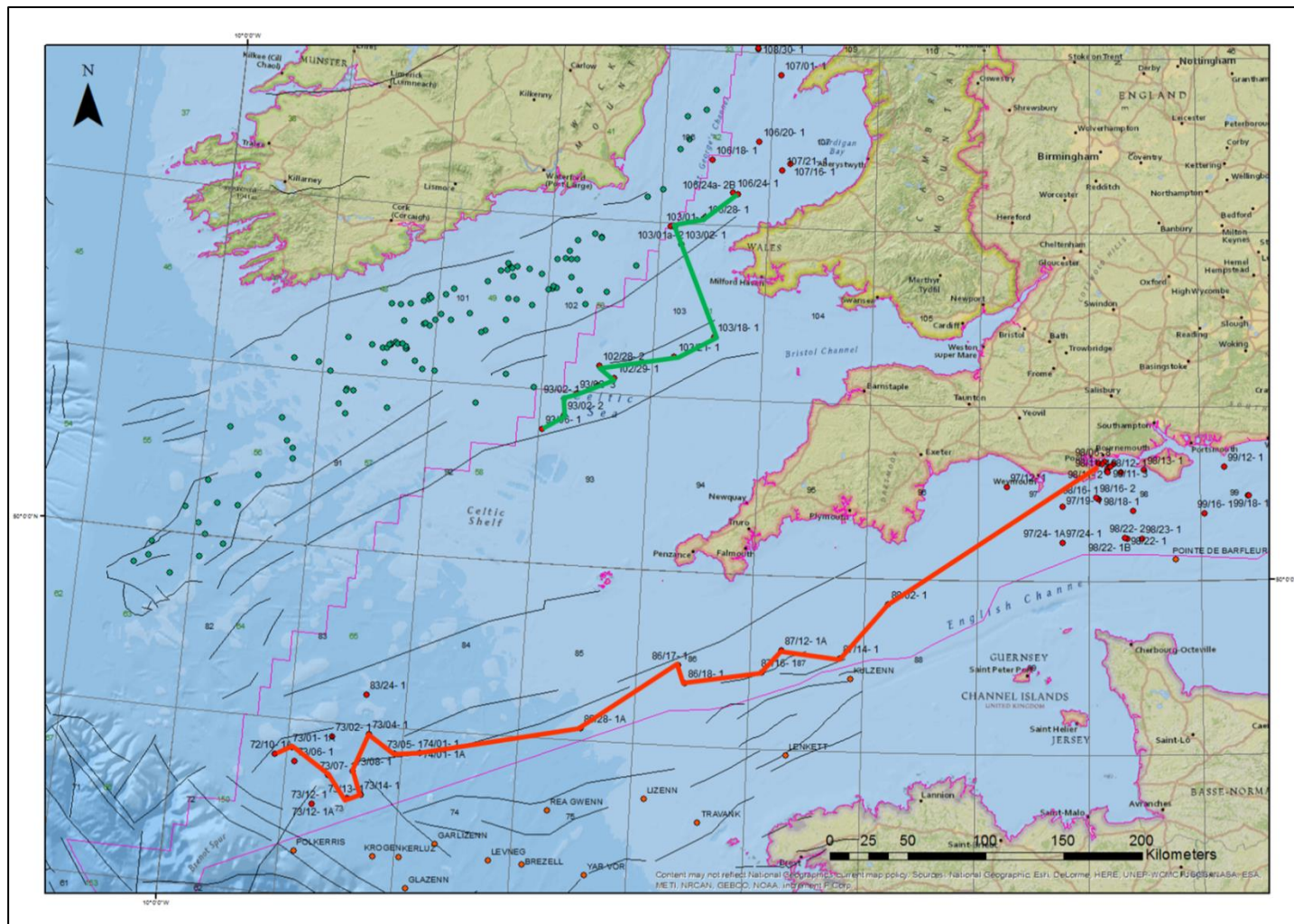


Fig 6.3. Map of the region of interest showing the lines of the correlation panels in Fig 6.4 (red) and Fig 6.5 (green).

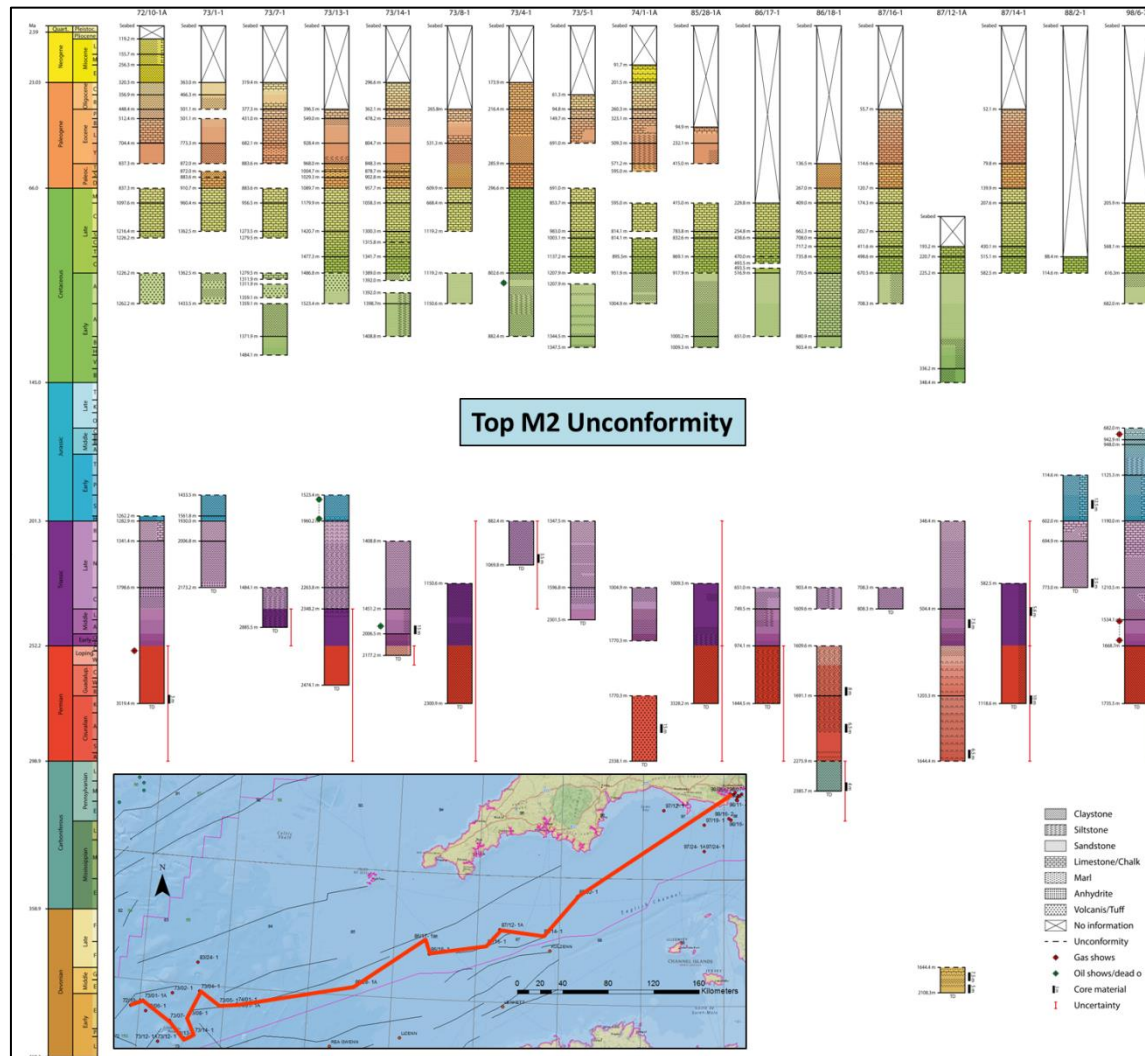


Fig 6.4. Chronostratigraphic correlation panel for the Western Approaches with oil (green) and gas (red) shows and cored sections indicated (Stricker *et al.*, unpublished work). The uncertainty range on any given interval is shown by the red bars. Where no uncertainty is stated the bar is absent.

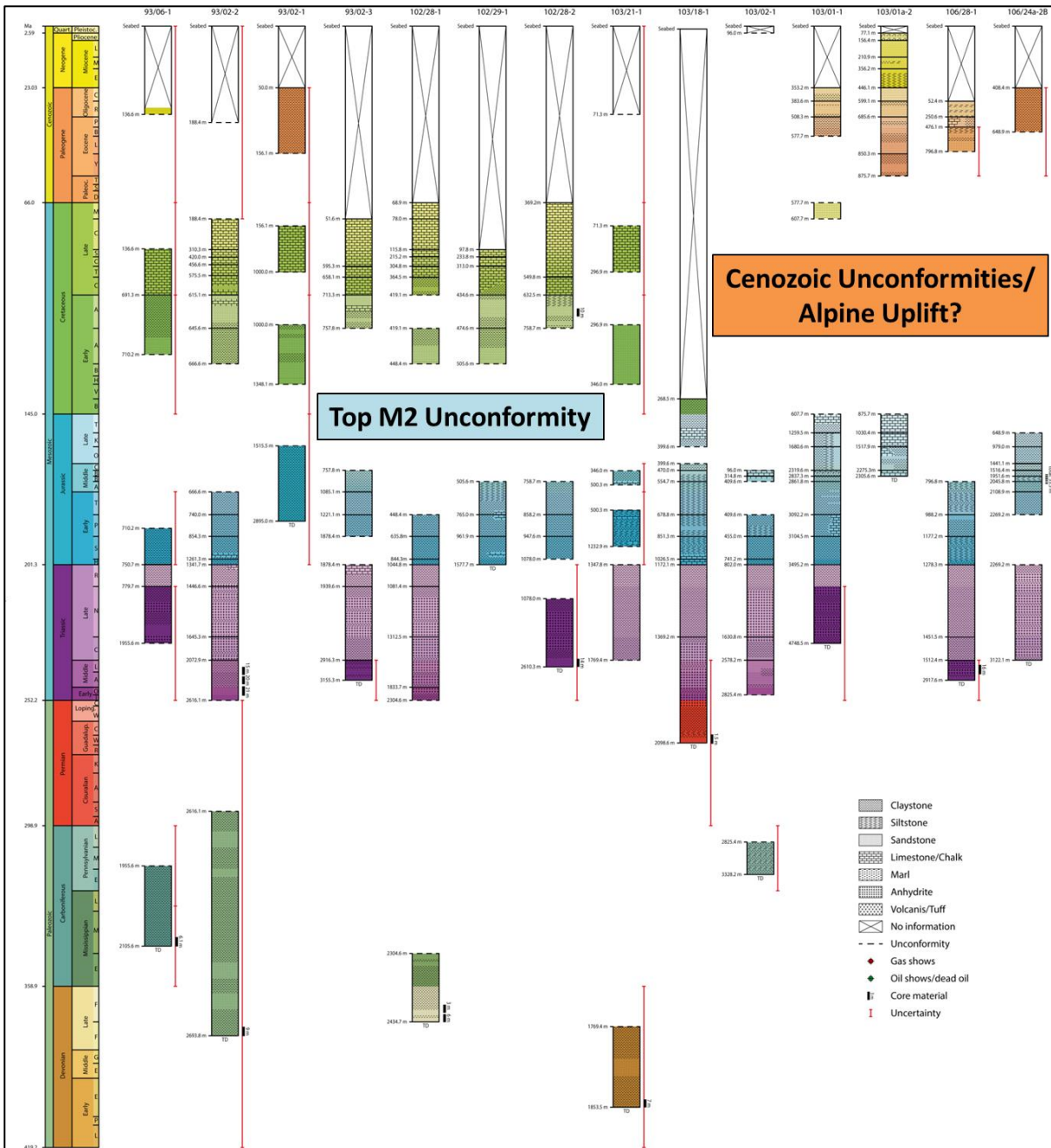


Fig 6.5. Chronostratigraphic correlation panel for the Celtic Sea with oil (green) and gas (red) shows and cored sections indicated (Stricker *et al.*, unpublished work). The uncertainty range on any given interval is shown by the red bars. Where no uncertainty is stated the bar is absent.

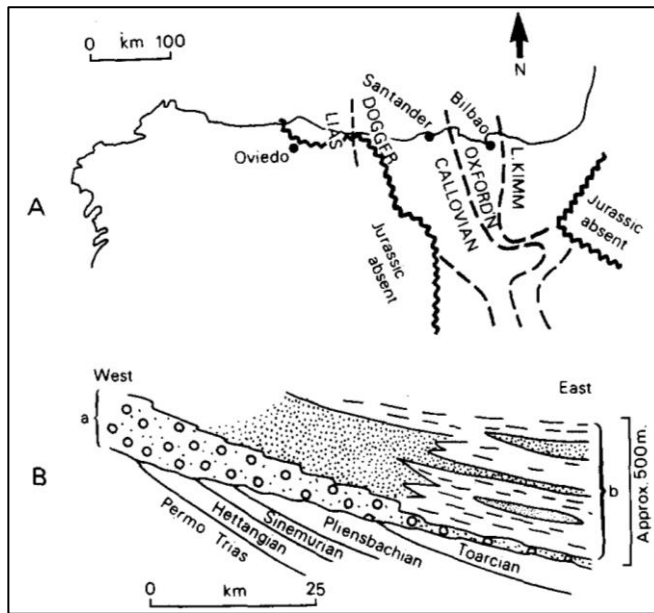


Fig 6.6. A is a map of North Spain showing the uppermost age of the stratigraphy underlying the Wealden. B. shows the overlapping relationship of the Wealden with the underlying Permian to Jurassic sediments with progressively older subcropping sediments to the West.

Wilson (1975) described the relationship of Megasequence 2 equivalent sediments in the North of Spain with progressively older strata to the West (Fig 6.6) separated by an unconformity overstepped by a Wealden Facies. The presence of the overlying Wealden Facies indicates that this unconformity is of a similar age to the proposed Top M2 unconformity in the region of interest and indicates uplift to the West. Wilson (1975) proposed a plume related triple point at the intersection of the junction of the North Pyrenean fault and the rifting axis of the Central Atlantic shown in Figure 6.7. The directions of synchronous uplift, westward in North Spain and southwest in the Western Approaches appear to suggest that the Central Atlantic or the triple point initiated the uplift and erosion during the Late Jurassic to Early Cretaceous observed in the region of interest. The exact mechanism of uplift is uncertain but as described above is likely not due to compression or shortening.

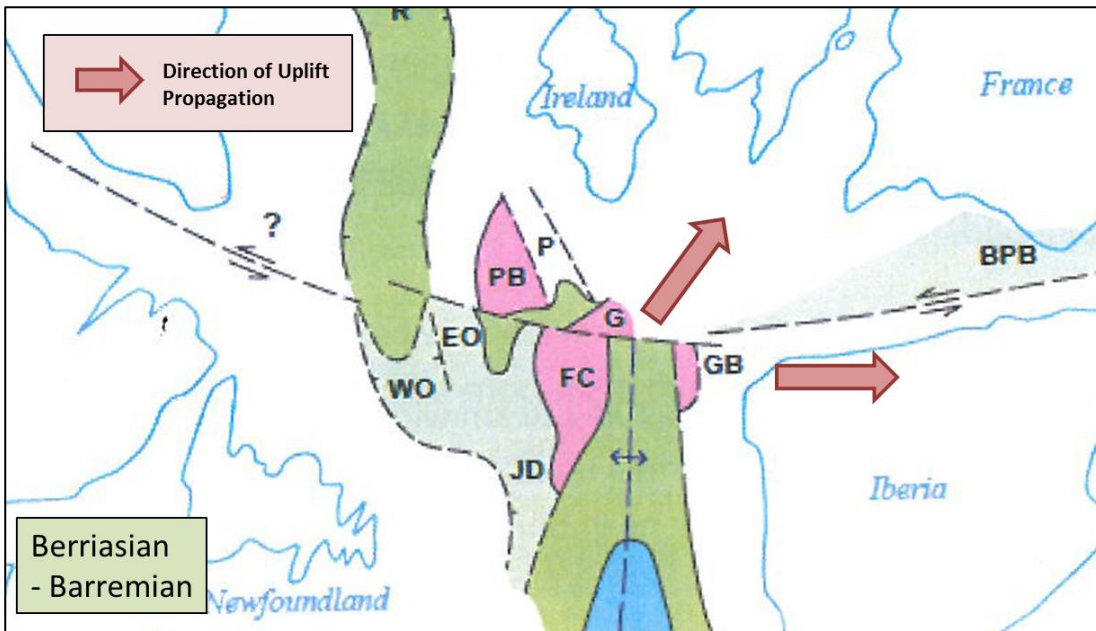


Fig 6.7. Schematic tectonic reconstruction modified from Lundin & Dore (In Press). Pink indicates highs, light green extension, darker green is hyperextension and blue indicates seafloor spreading.

6.4. Maturity

The thermal maturity of the Jurassic interval is described based on indicators from geochemical analysis of maturity (vitrinite reflectance, spore colouration and Tmax) in Section 5.3.1 with a review of the burial history models available for the basins of the Celtic Sea and Western Approaches in Section 5.3.2.

6.4.1. Effect of Top M2 Unconformity and Uplift periods

The Top M2 Unconformity as discussed in Section 6.3 had a significant effect on the preservation of source rocks in the Western Approaches and South Celtic Sea but the removal of strata in this event and Cenozoic uplift in the North Celtic Sea Basin had a large impact on the immaturity observed in the region of interest (Section 5.3). Increasing thermal maturity is a process of time and temperature and the removal of 0.7 to 2.8 km (based on burial history models discussed in Section 5.3.2) would have slowed the maturation of organic matter as temperatures decreased until the sediments are reburied to a zone of thermal maturity.

The exact impact of uplift on maturity in the region of interest is difficult to quantify as the burial history models imply different magnitudes of uplift and as discussed previously (Section 6.3) uplift during the Top M2 Unconformity is likely to have varied over the region. In Section 5.3.1 the 93/02-1, 73/13-1 and 72/10-1 wells have VR measurements and spore colouration information above and below the unconformity. The VR and SCI data shown in Figures 5.11 (93/02-1) & 5.13 (73/13-1) show no dramatic shift across the unconformity. The absence of a shift suggests that these wells are near to maximum burial. The scatter in the VR population in 72/10-1 (Fig 5.14) means it is impossible to tell whether a shift occurs.

The timing of uplift events can also have an effect on the timing of maximum burial. Ottaviani *et al.* (unpublished work) suggests maximum burial in the Late Jurassic (Fig 5.19) in contrast to Hillis (1988) who indicates burial during the Cenozoic to be close to prior maximum before the Late Jurassic (Fig 5.17). Ruffell (1995) does not include alpine (Cenozoic) uplift (Fig 5.18) and therefore predicts maximum burial at the current day. If strata have reached thermal maturity then it is unclear when petroleum expulsion is likely to have occurred without further burial history modelling (Section 6.6.3).

6.4.1. Implications for Petroleum Generation and Expulsion

The immaturity to early stage of maturity of sediments in the region of interest means that petroleum generation and expulsion is unlikely to have occurred in much of the Jurassic strata. Much of the Irish sector of the North Celtic Sea Basin is mature for oil generation at the Top Upper Jurassic with zones of peak hydrocarbon generation near the basin axis. The Dragon Well 103/01-1 has been shown to be mature to late mature in the Lower Jurassic section. It is likely that the North Celtic Sea Basin has the potential to generate and expel hydrocarbons from the majority of the Jurassic section (Fig 6.8).

The only other well analysed with a mature Jurassic section was the Lower Jurassic section of 73/13-1 which is early mature to mature. Detailed analysis of the OGA 2016 seismic lines would be needed to analysis whether deeper Jurassic strata exist in the Melville Basin that could have reached greater maturity (Section 6.6.7). Work by GTO on the French Sector indicates that the Sinemurian interval has reached hydrocarbon maturity (GTO, accessed 2017). Potential future work could look into the timing of French sector maturation and the potential of a migration pathway for petroleum to the UK sector of the Western Approaches. The brief analysis of the seismic for the Melville Basin (summarised in Section 6.6.7) suggests that wells were drilled predominantly on highs which means that the maturity observed from well information could underpredict the maturity in the main depocentres. Further analysis of the seismic will be required to quantify the actual maturity of Jurassic sediments in these depocentres.

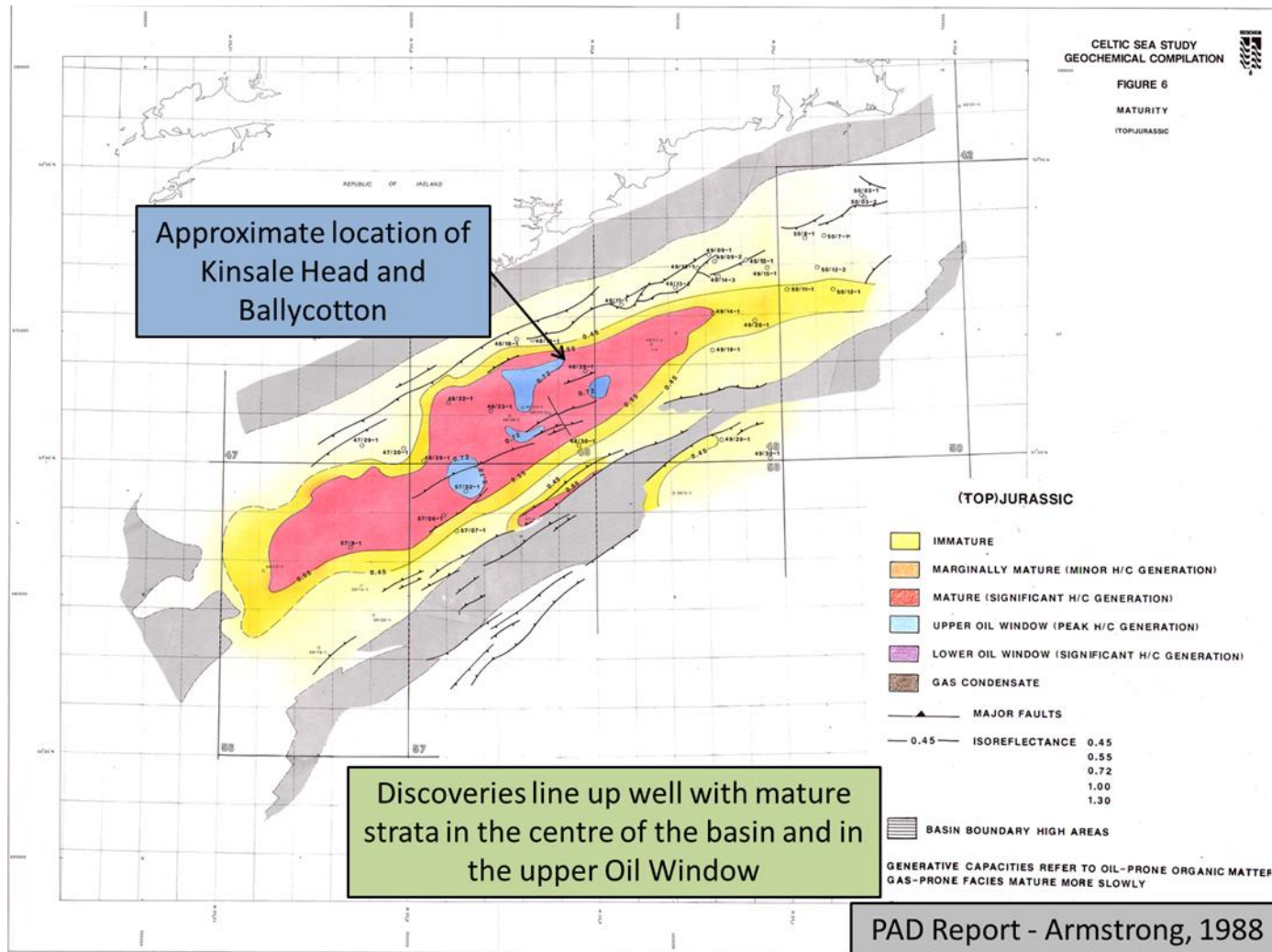


Fig 6.8. Map of maturity for the North Celtic Sea Basin for the top Upper Jurassic with highest maturity indicated in the basin centres (Armstrong, 1988).

6.5. Implications for the Petroleum System

The main aim of this project was to determine the feasibility of a petroleum system based on Jurassic source rocks. This section focuses on discussing additional evidence for a working petroleum system or the lack thereof.

6.5.1. Sea Surface Slicks (Browning-Stamp, 2017)

Sea surface slick analysis work performed by PannEx on behalf of the OGA has charted observed slicks in the SW of Britain in order to de-risk the source presence and reduce exploration risk (Fig 6.9). Optical landsat images were used to identify persistent surface slicks with anthropogenic and natural slicks screened out. Case studies identified slicks clustering around previously identified discoveries such as the Dragon Discovery and Wytch Farm (Fig 6.9).

Natural oil slicks form when petroleum and methane seep through faults and cracks in the overlying strata to the seafloor. The oil droplets and bubbles of methane then migrate through the water column with about half of the methane being dissolved and retained by the water column. The direction of the seep is also controlled at this time by prevailing currents. The oil then forms a slick on the surface with the methane being released in to the atmosphere. The surface slick is then subject to effects of wind and currents on the surface with heavier hydrocarbon components sinking back down to the seabed. The processes involved in forming a slick suggest that natural processes such as sea currents and wind need to be understood as potential controls on slick location.

The slicks shown in Figure 6.9 generally correlate well with the known basin extents suggesting they are a geologically phenomenon. The sea surface slicks are absent in the Melville Basin and St Mary's Basin where substantial sections of Jurassic have been eroded. The presence of numerous slicks in the North Celtic Sea Basin, St Mary's Basin and South West Channel Basin suggest the presence of a working petroleum system. Slicks in the South Celtic Sea Basin and Bristol Channel Basin are less numerous and scattered but also suggest the generation and expulsion of hydrocarbons. In addition the Haig Fras for which no data was available for this project has four slicks suggesting a potential working petroleum system. The slicks also demonstrate a trend of increasing number away from the southwest Western Approaches which is interpreted to be the location of the maximum degree of Late Jurassic to Early Cretaceous uplift and erosion (Section 6.3). Future work could be done to tie the distribution of the slicks into the new OGA 2D seismic to analyse the correlation between deeply buried potentially mature Jurassic and the slicks observed.

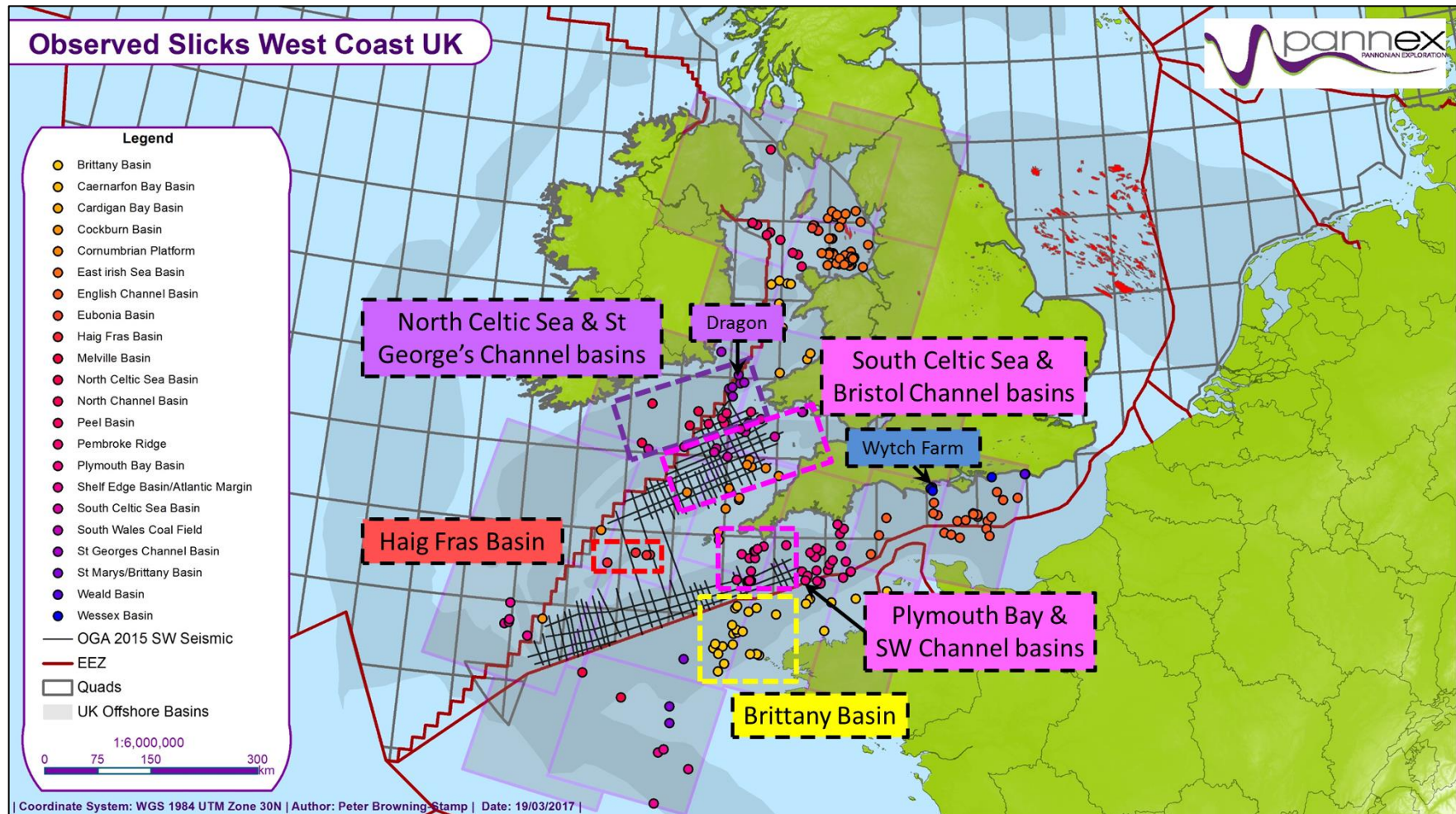


Fig 6.9. Map of observed sea surface slicks identified from landsat (Browning-Stamp, 2017).

6.5.2. Summary of Work

As discussed in Chapter 3 the only area of the region of interest where a working petroleum system must be working is the Dragon Discovery. Analysis of the palaeogeographic and tectonic history of the region in Chapter 2 suggests that the SW of England has had a complicated pre-Mesozoic history followed by basin formation and rifting events followed by multiple uplift and inversion events that vary in magnitude across the region of interest. As is summarised in Section 6.2 the Jurassic was a time of widespread source rock deposition with regional source rock development in the Early and Late Jurassic developing known petroleum systems in the Wessex Basin and North Celtic Sea Basin respectively.

Analysis of source rock richness, quality and kerogen type within the Jurassic intervals (Sections 5.4-5.6) demonstrate that source rock potential is highly heterogeneous. Significant potential is present in the Jurassic. Estimations of the potential of UK sector Western Approaches and Celtic Sea Jurassic organic matter-rich rocks to generate and expel hydrocarbons indicate that thick sections Jurassic such as the Upper Jurassic of the Dragon Discovery well 103/01-1 have the potential to generate substantial quantities of hydrocarbons (~58 mmstb/km² of oil and ~42 mmboe/km² of gas). In addition it has been demonstrated that the Lower Jurassic in 103/01-1 has already generated hydrocarbons.

The two largest factors in source rock potential appear to be maturity and preservation. As discussed in Section 6.4 source rock maturity in the Jurassic is typically poorly developed with little or no source rock generation or expulsion likely to have occurred from the wells analysed in the UK sector of the Western Approaches or South Celtic Sea Basin. Preservation in addition is a major factor, especially in the UK sector of the Western Approaches. The extents of the Lower Jurassic are limited (Fig. 2.31) with removal of the overlying Jurassic intervals (Section 6.3). Where the Lower Jurassic (Sinemurian to Pliensbachian in particular) has been preserved, source rock potential is present such as in 73/13-1. 73/13-1 has just reached maturity in the Lower Jurassic below 1830 m but this is below the Sinemurian interval of source rock potential (Section 5.8.1).

Hillis (1988) suggests that current burial in the Western Approaches is close to the maximum burial of the strata with 1-2 km of Permian-Jurassic strata eroded during Late Jurassic to Early Cretaceous uplift and erosion. Truncation of underlying strata due to erosion during the Late Jurassic to Early Cretaceous is shown in Figure 6.2, 6.11 & 6.12. The absence of a break or shift in the trend of maturity indicators across the Top M2 Unconformity (Section 6.3.1) supports the hypothesis that sediments are close to or at maximum burial at the current day.

If a significant thickness of strata has been removed at the Top M2 Unconformity such as the 1-2 km suggested by Hillis (1988) then the Late Jurassic to Early Cretaceous uplift and erosional event would have caused a significant hiatus/break in burial and the increase thermal maturity. It is hypothesised here that the removal of Jurassic source rocks and potential hiatus in thermal maturity mean that the Top M2 Unconformity is the primary control on the presence of a Jurassic based petroleum system in Western Approaches and Celtic Sea region. Further work described later in Section 6.6 would be needed to further understand the Top M2 Unconformity and its effect on the burial history of source strata and their preservation.

6.6. Recommendations/Future Work

The focus of this section will be to discuss what future work could be carried out to add to this project and advance the understanding laid out here.

6.6.1. Rhenium-Osmium Geochronology

Selby & Creaser (2003) describe methodology by which Rhenium and Osmium geochronology can be used to constrain accurate dates of organic matter deposition. If a similar method could be used to date the zones of good to very good source rock richness (Chapter 5) then further constraint could lead to better understanding of time intervals of increased source rock potential. These time periods could then be closely linked to the known periods of ocean bottom anoxia described in Section 2.6.2.

6.6.2. Resampling

A significant issue with this project was the availability of data and the quality of the data where it existed. The availability of data is outlined in Section 5.2.

6.6.2.1. TOC

Additional TOC sampling on every Celtic Sea and Western Approaches well where cuttings samples and core sections could be obtained would add to the sample population analysed in Section 5.4.

6.6.2.2. Rock-Eval

Similar to TOC and increased population of Rock-Eval data such as HI and OI (Section 5.2.1) would aid in the identification of source rock quality (HI) and in kerogen type analysis (OI). This project only had three wells available with S3 pyrolysis peak data in the Celtic Sea and

Western Approaches which led to a reliance on Western Approaches and St George's Channel Basin data to increase the sample population. Extra S3 peak data would provide invaluable knowledge into the kerogen type distribution in the region of interest.

6.6.2.3. Vitrinite Reflectance

VR data was available for 23 wells in the region of interest but as demonstrated in Section 5.2.2 the sample populations were often scattered with other indicators of maturity (Tmax, SCI...etc.) required to constrain the likely thermal maturity. Further analyses on additional wells or re-run sample populations that were particularly difficult to interpret would help constrain the regional thermal maturity.

6.6.3. 2D Burial History Analysis

The burial history models available for the Celtic Sea and Western Approaches Basins were discussed in Section 5.3.2. The models for the Melville Basin are highly variable and all the models run were 1 dimensional. Further basin modelling work to constrain the burial history with this analysis tied into the new OGA seismic would be invaluable in modelling thermal maturity in the Western Approaches and the potential timing of maturity.

6.6.4. Backstripping and Regional Structural Analysis

As discussed in Chapter 2 the SW of England has a complex tectonic and structural history. Backstripping of well and seismic lines combined with a regional structural analysis including quantification of uplift could lead to further understanding of the controls the structural history had on source rock development and preservation. Uplift quantification could be done through resampled (R_o trend - Corcoran & Clayton, 2001), Apatite Fission Track Analysis as carried out by Holford *et al.* (2005) of the Irish Sea or porosity-depth trends as discussed in Hillis (1988) and Hillis (1995).

6.6.5. Further Petroleum System Analysis

If a mature source rock could be proven within the Western Approaches and Celtic Sea Basins then additional work could focus on constraining the other aspects of a working petroleum system i.e. timing, seal, reservoir, trapping mechanisms.

The potential for generation and expulsion of hydrocarbons from the French Sector of the Western Approaches could be tested in the future. The presence of higher maturity dead oil in 73/14-1 that is isotopically similar to the Lower Jurassic of 73/13-1 has to have come from somewhere and could potentially have migrated from deeper in the Melville Basin or have come from higher maturity source rocks in the French sector of the Western Approaches. Integration of available seismic lines and analysis of the French well data could help to constrain whether source rock generation and expulsion has occurred in the French Sector and then migrated to the Melville Basin.

6.6.6. Additional Source Rock Potential

In Section 2.5 and 2.7 additional potential in the Carboniferous/Devonian and Cretaceous is discussed. A similar process as described in Chapter 5 could be used to analysis additional hydrocarbon generation and expulsion potential within the Cretaceous and Devonian/Carboniferous intervals. Figure 5.6 indicates that significantly fewer samples are available in the Devonian/Carboniferous (24 TOC & 9 HI values) and Cretaceous (166 TOC & 32 HI values) compared to the Jurassic (1571 TOC & 434 HI values). Resampling would be a key component for any statistically viable analysis of these intervals.

6.6.7. Seismic Interpretation

Seismic analysis and interpretation would be a significant part of any future work to be done with interpretation feeding into the 2D burial history analysis, backstripping and structural analysis. Figure 6.10 shows the available seismic data for the Western Approaches with the lines shown in Figure 6.11 & 6.13 highlighted in red. Figure 6.11 & 6.12 show a strike-line and a dip-line through the southern Melville Basin with the Top M2 Unconformity highlighted in green. The Jurassic can be seen as a series of synclinal reflectors below the Top M2 Unconformity. As described in Section 5.3 the base of the Lower Jurassic sediments in the 73/13-1 are mature and the presence of potentially deeper Jurassic between well 73/13-1 and 73/14-1 suggests that this section of Jurassic has likely produced some petroleum.

Future work would focus on understanding the distribution and relationships of the Top M2 Unconformity with the development of an integrated understanding of the cause and effects of the regional uplift and erosion. Figure 6.11 & 6.12 indicate that Jurassic strata are present below the Top M2 Unconformity in an “egg box” setting with apparent 3D bowl and synclinal geometry. This “egg box” geometry could be caused due to salt-withdrawal, multiple orthogonal rift directions or transtensional rifting with anything above the 3D synclines peneplained during the Late Jurassic to Early Cretaceous erosion. A residual isostatic gravity map (Getech, 2017) is shown in Figure 6.13 which shows the changes in lateral crustal thickness. The variation in the Western Approaches picks out this “egg box” geometry. Future work could focus on integrating the isostatic residual gravity data with the available OGA 2016 seismic lines. The exact nature of this relationship is the key to figuring out where Jurassic source rocks have been preserved at sufficient maturity to have generated and expelled source rocks.

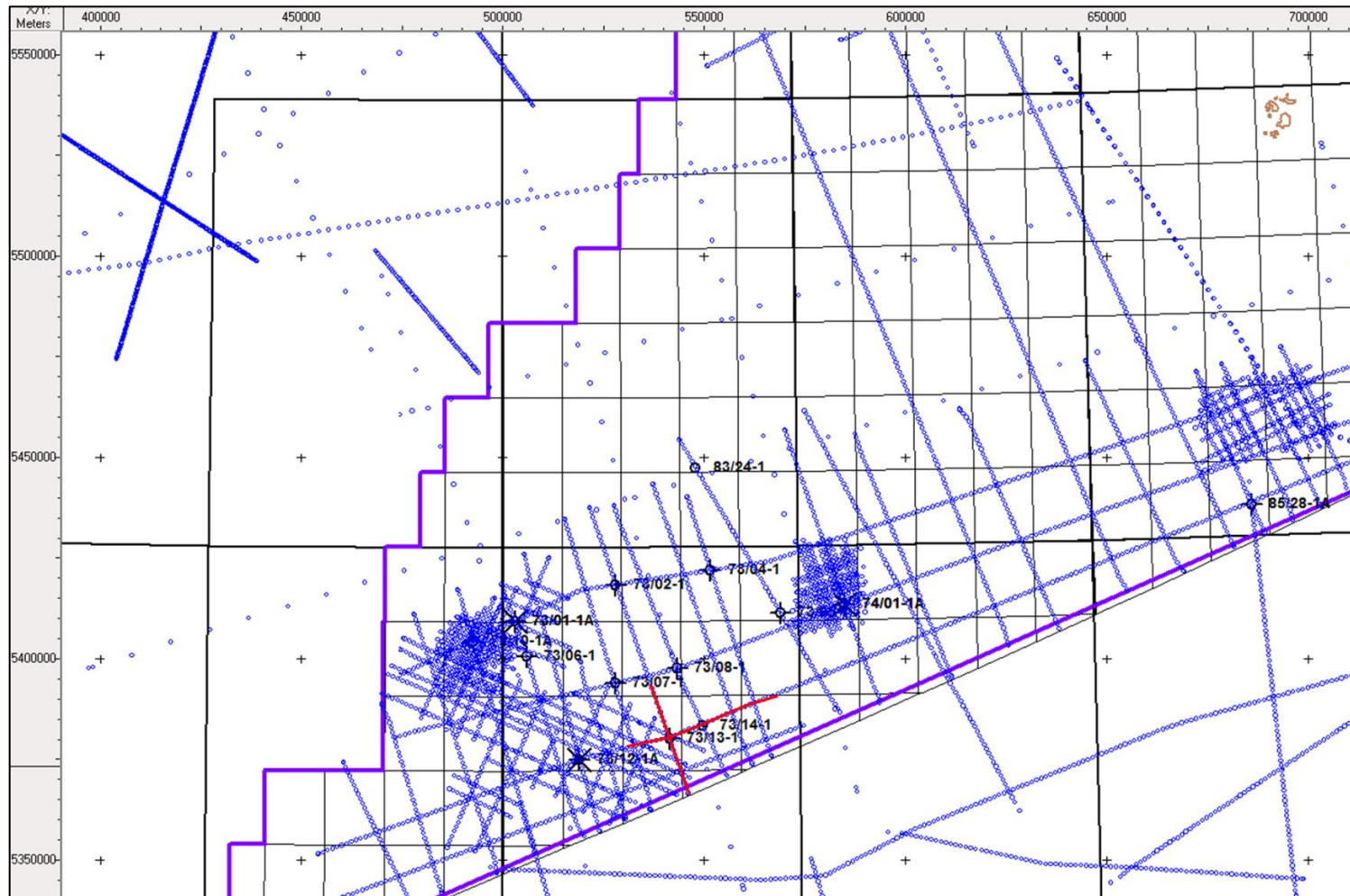


Fig 6.10. Map of the available seismic lines in the Western Approaches for future analysis and interpretation. The locations of Fig 6.11 & 6.12 are shown in red.

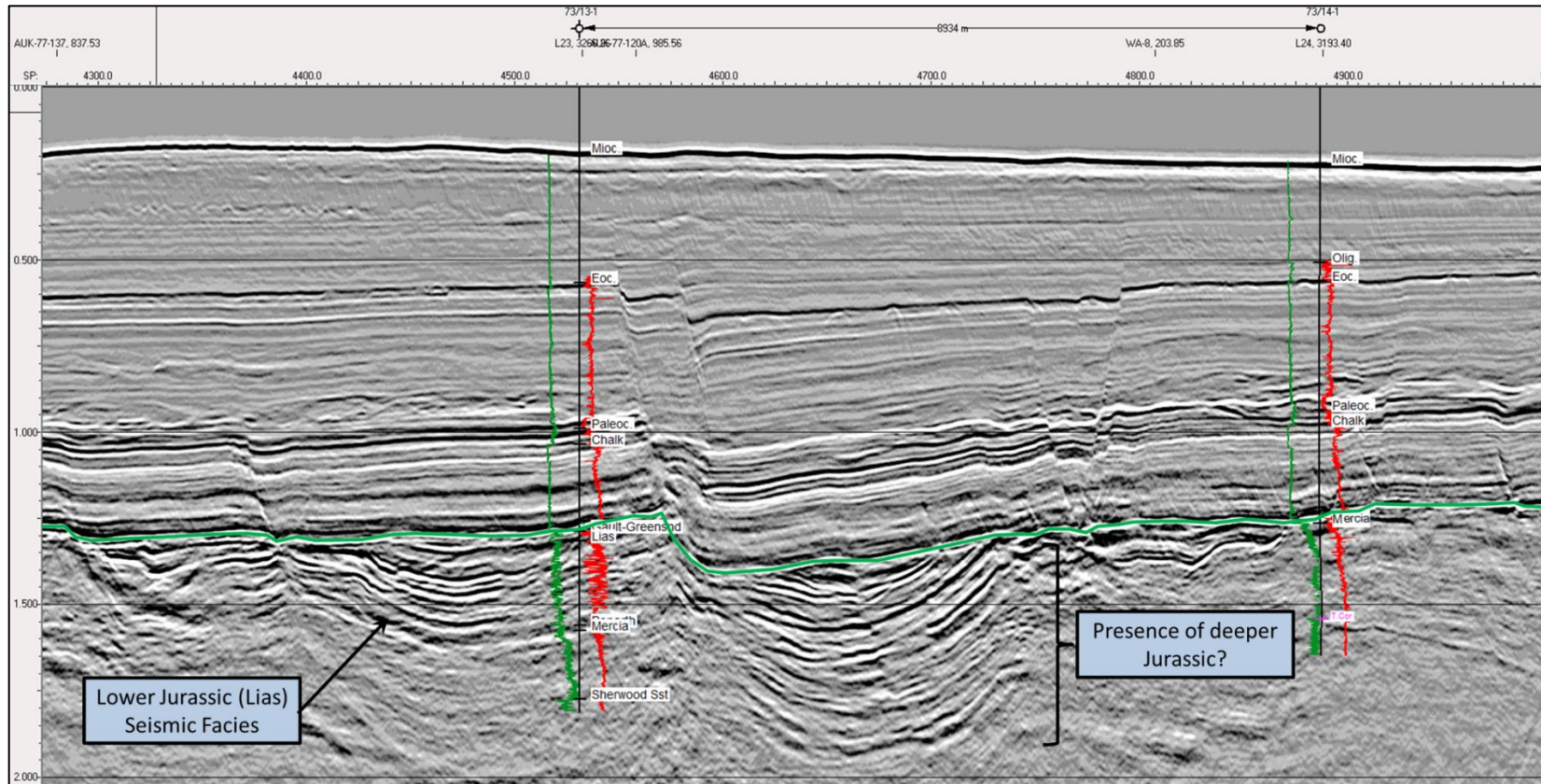


Fig 6.11. Strike-line seismic profile from the southern section of the Melville Basin with stratigraphic tops and wireline gamma ray (green) and compression sonic (red) shown for wells 73/13-1 & 73/13-1. The green marker is interpreted to represent the Top M2 Unconformity with underlying synclinal Jurassic strata truncated. The Lower Jurassic (Lias) is considered to be represented by a high reflective seismic facies which might represent an interbedded sand and shale sequence as discussed in Section 2.6.2.

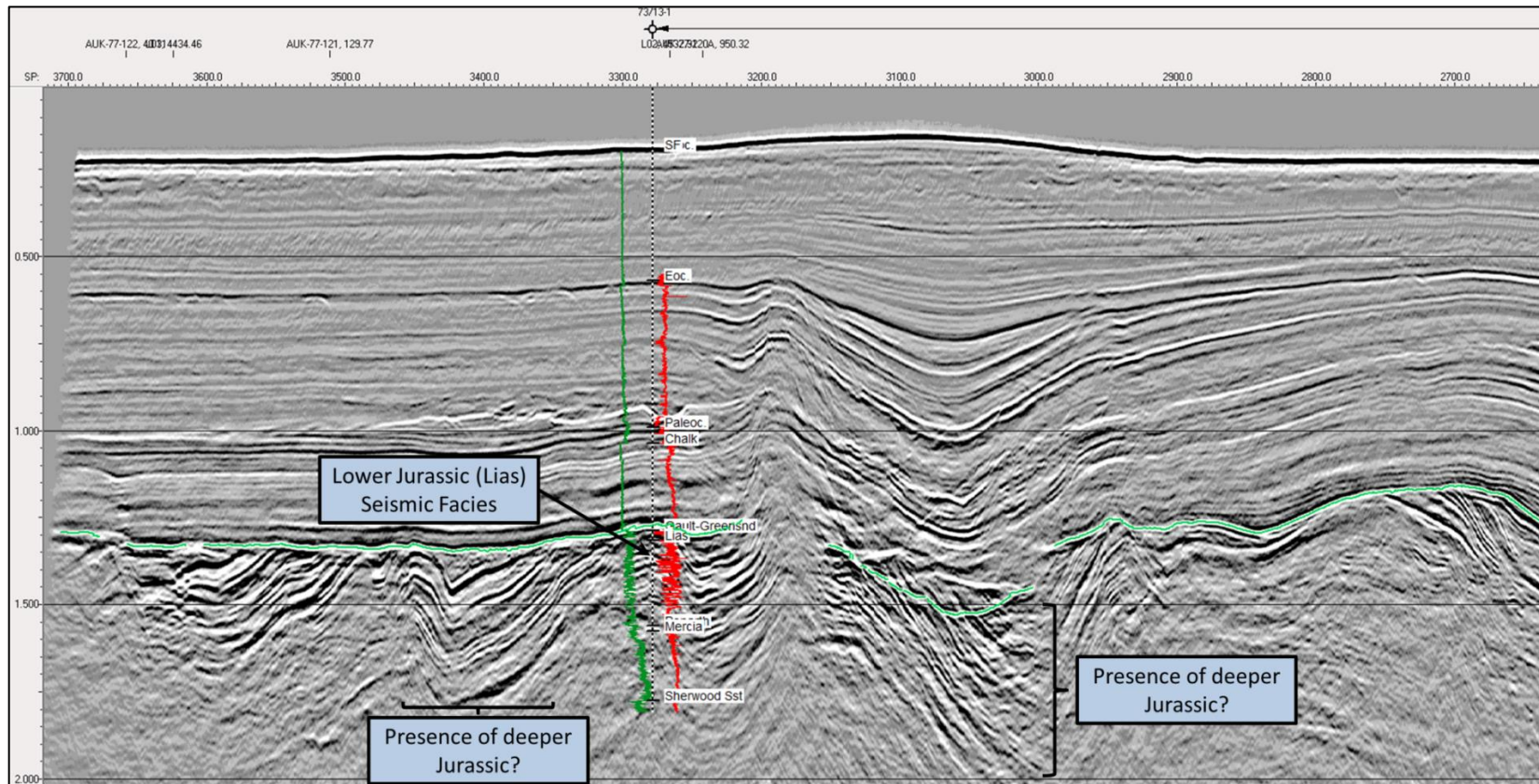


Fig 6.12. Dip-line seismic profile from the southern section of the Melville Basin with stratigraphic tops and wireline gamma ray (green) and compression sonic (red) shown for well 73/13-1. The green marker is interpreted to represent the Top M2 Unconformity with underlying synclinal Jurassic strata truncated. The Lower Jurassic (Lias) is considered to be represented by a high reflective seismic facies which might represent an interbedded sand and shale sequence as discussed in Section 2.6.2.

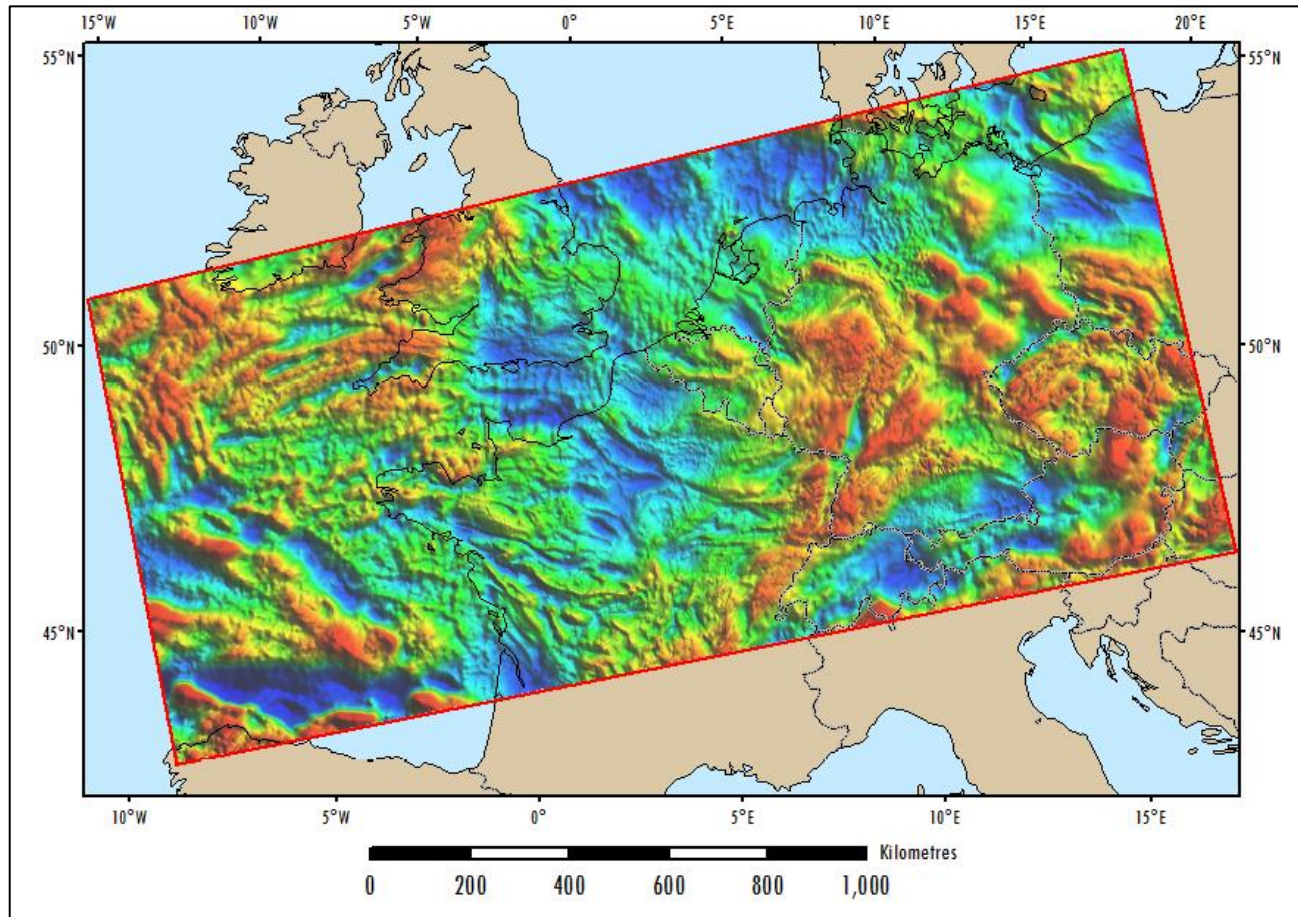


Fig 6.13. Isostatic residual gravity map for Ireland, southern Britain and western Europe. The map has been corrected to remove the influence of crustal thickness by making an assumption of the depth to the Moho based on Airy's isostasy (Getech, 2017).

Chapter 7

Conclusions

7. Conclusions

The basins of the Western Approaches and Celtic Sea record a history of sedimentation from the Permian to Recent. This thesis has undertaken new work to analyse the potential presence of source rock intervals combining palaeogeographic and tectonostratigraphic analysis with the detailed appraisal of geochemical data from unpublished well reports and regional data.

- The basins of the Western Approaches and Celtic Sea record multiple stages of Mesozoic rifting and Late Jurassic to Early Cretaceous and Cenozoic uplift and erosional events, which are vital to understanding the preservation of source rock intervals and the burial history of the potential source rock units.
- The Carboniferous, Jurassic and Cretaceous periods all led to the deposition of potential source rock facies which are characterised by zones of good to very good source rock richness (>1.0% TOC). In particular the Jurassic demonstrates the greatest potential but is highly heterogeneous with multiple, intercalated zones that could act as potential source rocks (see below).
- The Jurassic contains zones of high source rock potential with the Sinemurian-Pliensbachian representing an interval of significant source rock potential with Toarcian and Upper Jurassic source rock potential in the North Celtic Sea Basin. These source rock intervals are capable of generating and expelling significant quantities of hydrocarbon if present in sufficient quantities and at maturity to support a Jurassic sourced petroleum system.
- The Top M2 (or “Cimmerian”) Unconformity has been linked to regional uplift and erosion during the Late Jurassic to Early Cretaceous, causing the removal of large sections of the Jurassic interval in the Western Approaches and South Celtic Sea Basin. Smaller magnitudes of uplift and erosion in the North Celtic Sea Basin, which led to greater burial and, in places, preservation of the rich Toarcian source rock interval, mean that greater hydrocarbon potential could exist here, as exemplified by the Dragon Discovery.

- Jurassic strata across the Western Approaches are typically immature for petroleum generation with only the 103/01-1 and 73/13-1 wells demonstrating Jurassic age rocks of significant maturity (0.3-0.6% R_o). Cessation of burial related to uplift by the Top M2 Unconformity is likely to have led to the regional immaturity of the Jurassic.
- The Top M2 Unconformity is suggested to be the major control on source rock maturity and preservation in the Western Approaches and South Celtic Sea Basin. The potential exists for the presence of thicker Jurassic sections of more mature source rocks beneath the Top M2 Unconformity in preserved small, locally salt-related depocentres within the Melville Basin and further south within the Brittany Trough.

Future Research

1. Future research using the Oil and Gas Authority's 2016 broadband, 2D seismic reflection data is proposed in order to investigate the locations and sizes of the inferred, more deeply buried Jurassic depocentres. The seismic data will also allow better characterisation of the nature and extent of the Top M2 Unconformity across the Western Approaches and Celtic Sea regions.
2. Resampling of the geochemical datasets are put forward to better identify and analyse the potential of source rock zones along with Re-Os geochronology to better constrain the timing of organic matter deposition and identify times of ocean bottom anoxia. The project would also be expanded to focus on Carboniferous and Cretaceous source rock potential to quantify the total source rock potential of the regions.
3. Structural and seismically driven 2D basin modelling could be produced to enhance the understanding of source rock maturity and potential preservation below the Top M2 Unconformity.
4. Access to French and Irish well data and reports would facilitate expansion of the project into the French and Irish Sector. The Irish and UK Sectors of the Celtic Sea could be compared and contrasted with similar work done to compare the French and UK Sectors of the Western Approaches.

References

- Airy, G.B., 1855. On the Computation of the effect of the attraction of mountain masses disturbing the apparent astronomical latitude of stations in geodetic surveys. *Royal Society of London*, 145, pp.101–104.
- Alexander, A.C. & Shail, R.K., 1995. Late Variscan structures on the coast between Perranporth and St. Ives, Cornwall. In *Annual conference of the Ussher Society*. pp. 398–404.
- Alexander, A.C. & Shall, R.K., 1996. Late- to Post-Variscan Structures on the coast between Penzance and Pentewan, South Cornwall. In *Annual Conference of the Ussher Society*. pp. 72–78.
- Allen, J.R., 1986. Pedogenic calcretes in the Old Red Sandstone facies (late Silurian–early Carboniferous) of the Anglo-Welsh area, southern Britain. *Paleosols. Their recognition and interpretation*, pp.58–86.
- Allen, M.E., 1977. Texaco Production Services Ltd - Final Geological Report for U.K. Well 103/2-1 Wildcat. , pp.1–11.
- Allen, P.A. & Allen, J.R., 2013. *Basin analysis: Principles and application to petroleum play assessment*, John Wiley & Sons.
- Amoco, 1977. 103/21-1 W28: Geological Report. , pp.1–21.
- Anell, I., Thybo, H. & Artemieva, I.M., 2009. Tectonophysics Cenozoic uplift and subsidence in the North Atlantic region: Geological evidence revisited. *Tectonophysics*, 474(1–2), pp.78–105. Available at: <http://dx.doi.org/10.1016/j.tecto.2009.04.006>.
- Arche, A. & Lopex-Gomez, J., 1996. Origin of the Permian-Triassic Iberian Basin, central-eastern Spain. *Tectonophysics*, 266, pp.443–464.
- Armstrong, J.P., 1988. Compilation of Geochemical Data Relating to the Celtic Sea Basin. , pp.1–152.
- Bailey, N.J.L., 1981. 73/07-1: Geochemical Evaluation. , pp.1–46.
- Barnard, P.C., Cooper, B.S. & Fisher, M.J., 1976. Organic maturation and hydrocarbon generation in the Mesozoic sediments of the Sverdrup basin, Arctic Canada. In *4th International Palynology Conference*. Lucknow, pp. 581–588.
- Barron, A.J.M., Lott, G.K. & Riding, J.B., 2012. *Stratigraphical framework for the Middle Jurassic strata of Great Britain and the adjoining continental shelf*,
- Batten, D.J., 1980. Use of transmitted light microscopy of sedimentary organic matter for evaluation of hydrocarbon source potential. In *4th International Palynology Conference Vol 2*. Lucknow, pp. 589–594.
- Bennet, G., Copestake, P. & Hooker, N.P., 1985. Stratigraphy of the Britoil 72/10-1A well, Western Approaches. *Proceedings of the Geologists Association*, 96(3), pp.255–261. Available at: [http://dx.doi.org/10.1016/S0016-7878\(85\)80007-9](http://dx.doi.org/10.1016/S0016-7878(85)80007-9).

- Bluck, B.J., Gibbons, W. & Ingham, J.K., 1992. Terranes. *Geological Society of London, Memoirs*, 13(1), pp.1–4.
- Blundell, D.J., 2002. Cenozoic inversion and uplift of southern Britain. In A. G. Doré et al., eds. *Exhumation of the North Atlantic Margin: Timing, Mechanisms and Implications for Petroleum Exploration. Geological Society, London, Special Publications*. Geological Society of London, pp. 85–101.
- BNO Development Ltd, 1979. 72/10-1A/W28: Geological Completion Report. , pp.1–72.
- Bois, C. & ECORS Scientific Party, 1990. Major geodynamic processes studied from the ECORS deep seismic profiles in France and adjacent areas. *Tectonophysics*, 173, pp.397–410.
- Browning-Stamp, P., 2017. Sea Surface Slick Study - Western UK: Initial Project Presentation and Results Summary. pp.1–14.
- Bulnes, M. & McClay, K.R., 1998. Structural analysis and kinematic evolution of the inverted central South Celtic Sea Basin. *Marine and Petroleum Geology*, 15(7), pp.667–687.
- Burnham, A.K. & Sweeney, J.J., 1989. A chemical kinetic model of vitrinite maturation and reflectance. *Geochimica et Cosmochimica Acta*, 53, pp.2649–2657.
- Butler, R.W.H., Holdsworth, R.E. & Lloyd, G.E., 1997. The role of basement reactivation in continental deformation. *Journal of the Geological Society of London*, 154, pp.69–71.
- Byrne, K., 2014. Revised Structural Evolution of the North Celtic Sea Basin Based on Modern 2D and 3D Seismic Data - Poster.
- Chapman, T.J., 1989. The Permian to Cretaceous structural evolution of the Western Approaches Basin (Melville sub-basin), UK. In M. A. Cooper & G. D. Williams, eds. *Inversion Tectonics*. pp. 177–200.
- Cheadle, M.J. et al., 1987. Extensional structures on the western UK continental shelf: a review of evidence from deep seismic profiling. *Geological Society, London, Special Publications*, 28(1), pp.445–465.
- Conoco Phillips, 1977. UK Celtic Sea Well 102/29-1 Final Report. pp.1–117.
- Cooles, G.P., Mackenzie, A.S. & Quigley, T.M., 1986. Calculation of petroleum masses generated and expelled from source rocks. *Organic Geochemistry*, 10, pp.235–245.
- Cooper, B.S., 1977. Petrographic and Chemical Analyses of a Coal from 10280 Feet Depth in the Texaco 103/2-1 Well. pp.1–6.
- Cooper, B.S. & Collins, A.G., 1979. Geochemistry of The B.N.O.C 72/10-1 Well, Western Approaches. pp.1–20.
- Cooper, M. a et al., 2015. Recognizing inversion structures. *Geological Society Special Publications - Inversion Tectonics*, (44), pp.335–347.
- Corcoran, D. V & Clayton, G., 2001. Interpretation of vitrinite reflectance profiles in sedimentary basins, onshore and offshore Ireland. In P. M. Shannon, P. D. W. Houghton, & D. V Corcoran, eds. *The Petroleum Exploration of Ireland's Offshore Basins. Geological Society, London, Special Publications*. pp. 61–90.

- Corfield, S.M. et al., 1996. Inversion tectonics of the Variscan foreland of the British Isles. *Journal of the Geological Society of London*, 153(1987), pp.17–32.
- Cornford, C., Gardiner, P. & Burgess, C., 1998. Geochemical truths in large data sets. I: Geochemical screening data. *Organic Geochemistry*, 29(1), pp.519–530.
- Cornford, C., Jones, M. & Scrivener, R.C., 2011. Towards an Origin for Bideford Black. *Geoscience in South-West England*, 12, pp.356–363.
- Coward, M.P., 1995. Structural and tectonic setting of the Permo-Triassic basins of northwest Europe. In B. S. A. R, ed. *Permian and Triassic Rifting in Northwest Europe*, *Geological Society Special Publication*. pp. 7–39.
- Coward, M.P. et al., 2003. Tectonic evolution. In D. Evans et al., eds. *Millennium Atlas: Petroleum geology of the central and northern North Sea*. London, UK, pp. 17–33.
- Dembicki Jr, H., 2009. Three common source rock evaluation errors made by geologists during prospect or play appraisals. *American Association of Petroleum Geologists Bulletin*, 93(3), pp.341–356.
- Dembicki Jr, H., 1995. Dragon Prospect Geochemistry. pp.1–74.
- Dera, G. et al., 2011. Climatic ups and downs in a disturbed Jurassic world. *Geology*, 39(3), pp.215–218.
- Dewey, J.F. & Burke, K.C.A., 1973. Tibetan , Variscan , and Precambrian Basement Reactivation : Products of Continental Collision Author (s): John F . Dewey and Kevin C . A . Burke Published by : The University of Chicago Press Stable URL : <http://www.jstor.org/stable/30058995>. *The University of Chicago Press Journals*, 81(6), pp.683–692. Available at: <http://www.jstor.org/stable/30058995>.
- Dodson, M.H. & Rex, D.C., 1971. Potassium-argon ages of slates and phyllites from south-west England. *Journal of the Geological Society of London*, 126, pp.465–499.
- Doré, A.G. et al., 1999. Principal tectonic events in the evolution of the northwest European Atlantic margin. In A. J. Fleet & S. A. R. Boldy, eds. *Petroleum Geology of Northwest Europe: Proceedings of the 5th Conference*. Geological Society of London, pp. 41–61.
- Dungworth, G., Abernethy, I. & McGarva, R., 1986. Well 73/14-1: Petroleum Geochemical Report (Interval 7017'16" -7054'8"). pp.1–42.
- Espitalié, J. et al., 1977. Source Rock Characterisation: Method for Petroleum Exploration. In *9th Annual Offshore Technology Conference*. Houston Texas, pp. 439–445.
- Evans, C.D.R., Lott, G.K. & Warrington, G., 1981. *The Zephyr (1977) wells, south-western approaches and western English Channel*,
- Evans, D.J. & Thompson, M.S., 1979. The geology of the central Bristol Channel and the Lundy area, South Western Approaches, British Isles. *Proceedings of the Geologists' Association*, 90(1–2), pp.1–14. Available at: <http://www.sciencedirect.com/science/article/pii/S0016787879800267>.
- Ewins, N.P. & Shannon, P.M., 1995. Sedimentology and diagenesis of the Jurassic and Cretaceous of the North Celtic Sea and Fastnet Basins. *Geological Society, London, Special Publications*, 93(1), pp.139–169.

- Fisher, J.M. & Jeans, C. V., 1982. Clay Mineral Stratigraphy Permo-Triassic Red Bed Sequences of BNOC 72/10-1A, Western Approaches, and the South Devon Coast. *Clay Minerals*, 17, pp.79–89.
- Gardiner, P.R.R. & Sheridan, D.J.R., 1981. Tectonic framework of the Celtic Sea and adjacent areas with special reference to the location of the Variscan Front. *Journal of Structural Geology*, 3(3), pp.317–331.
- Gedenk, R., 1977. Organic Geochemical Evaluation Source Rock Study Celtic Sea UK Texaco 103/2-1. pp.1–8.
- Getech Group plc, 2017. *Gravity and Magnetic Data SW Approaches and Western Europe - G1701*.
- Geochem Laboratories, 1976. Geochemical Service Report: Hydrocarbon Source Character of Amoco's 103/21-1 Well, Celtic Sea. pp.1–42.
- Gibbs, A.D., 1987. Linked tectonics of the northern North Sea basins. In *Sedimentary Basins and Basin-Forming Mechanisms*. pp. 163–171.
- Glen, R.A., Hancock, P.L. & Whittaker, A., 2005. Basin inversion by distributed deformation: The southern margin of the Bristol Channel Basin, England. *Journal of Structural Geology*, 27(12), pp.2113–2134.
- Gray, J. & Harvey, T., 2014. *South West Approaches prospectivity*, Available at: http://www.kis-orca.eu/media/9348/2016_SWA_LRes.pdf.
- Greenhalgh, E., 2016. *The Jurassic Shales of the Wessex Area: Geology and Shale Oil and Shale Gas Resource Estimation*, London, UK.
- Hallam, A. et al., 2004. Discussion on sea-level change and facies development across potential Triassic–Jurassic boundary horizons, SW Britain. *Journal of the Geological Society*, 161(6), pp.1053–1056.
- Harland, B.W., 1990. *A geologic time scale 1989*,
- Hartley, A.J. & Warr, L.N., 1990. Upper Carboniferous foreland basin evolution in SW Britain. In *Proceedings of the Ussher Society 7.3*. pp. 212–216.
- Harvey, M.J. et al., 1994. Tectonic evolution of the Plymouth Bay Basin. *Geoscience in South-West England*, 8(3), pp.271–278.
- Hesselbo, S.P. et al., 2017. Mochras borehole revisited: a new global standard for Early Jurassic earth history. *Scientific Drilling*, 16(2013), pp.81–91.
- Hesselbo, S.P. et al., 2007. Carbon-isotope record of the Early Jurassic (Toarcian) Oceanic Anoxic Event from fossil wood and marine carbonate (Lusitanian Basin, Portugal). *Earth and Planetary Science Letters*, 253, pp.455–470.
- Hillis, R.R., 1988. *The Geology and Tectonic Evolution of the Western Approaches Trough*. University of Edinburgh.
- Holdsworth, R.E., Butler, C.A. & Roberts, A.M., 1997. The recognition of reactivation during continental deformation. *Journal of the Geological Society of London*, 154, pp.69–71.

- Holdsworth, R.E., 1989. Short Paper: The Start-Perranporth line: a Devonian terrane boundary in the Variscan orogen of SW England? *Journal of the Geological Society*, 146(3), pp.419–421. Available at: <http://jgs.lyellcollection.org/cgi/doi/10.1144/gsjgs.146.3.0419>.
- Holford, S., Turner, J., & Green, P. (2005). Reconstructing the Mesozoic – Cenozoic exhumation history of the Irish Sea basin system using apatite fission track analysis and vitrinite reflectance data. In A. G. Doré & B. A. Vining (Eds.), *Petroleum Geology: North-West Europe and Global Perspectives - Proceedings of the 6th Petroleum Geology Conference*, pp. 1095–1110. <http://doi.org/10.1144/0061095>
- Houchen, M.A., Eustance, N.P. & Dernie, P.J., 1991. BP Exploration - Geological Well Evaluation Report 93/2-3. pp.1–57.
- Howell, T.J. & Griffiths, P., 1995. A study of the hydrocarbon distribution and Lower Cretaceous North Celtic Sea Basin. In P. F. Croker & P. M. Shannon, eds. *The Petroleum Geology of Ireland's Offshore Basins, Geological Society Special Publication*. pp. 261–275.
- Hsu, J.K., 1965. Isostasy, Crustal Thinning, Mantle Changes, and the Disappearance of Ancient Land Masses. *American Journal of Science*, 263, pp.97–109.
- Hubbard, R.J., Pape, J. & Roberts, D.G., 1985. Depositional Sequence Mapping as a Technique to Establish Tectonic and Stratigraphic Framework and Evaluate Hydrocarbon Potential on a Passive Continental Margin: Chapter 5. In *Seismic Stratigraphy II: An Integrated Approach to Hydrocarbon Exploration*. pp. 79–91.
- James Armstrong and Associates, 1995. A Geochemical Evaluation of Interval 2700' -11960' Well 103/1-1. , pp.1–26.
- Jammes, S. et al., 2009. Tectonosedimentary evolution related to extreme crustal thinning ahead of a propagating ocean: Example of the western Pyrenees. *Tectonics*, 28, pp.1–24.
- Jenkyns, H.C. & Clayton, C.J., 1986. Black shales and carbon isotopes in pelagic sediments from the Tethyan Lower Jurassic. *Sedimentology*, 33, pp.87–106.
- Jenkyns, H.C. et al., 2002. Chemostratigraphy of the Jurassic System: applications, limitations and implications for palaeoceanography. *Journal of the Geological Society*, 159, pp.351–378.
- Jones, D.G., Miller, J.M. & Roberts, P.D., 1988. A seabed radiometric survey of Haig Fras, S. Celtic Sea, U.K. *Proceedings of the Geologists' Association*, 99(3), pp.193–203. Available at: [http://dx.doi.org/10.1016/S0016-7878\(88\)80035-X](http://dx.doi.org/10.1016/S0016-7878(88)80035-X).
- GTO, accessed 12/09/2017, France: The Brittany Basin - GTO Flyer. pp.1–4. Available at: <http://gto-limited.co.uk/wp-content/uploads/2016/02/France-Flyer.pdf>.
- Kamerling, P., 1979. The geology and hydrocarbon habitat of the Bristol Channel Basin. *Journal of Petroleum Geology*, 2(1), pp.75–93.
- Kelling, G., 1988. Silesian sedimentation and tectonics in the South Wales Basin: a brief review. In *Sedimentation in a Synorogenic Basin Complex: the Upper Carboniferous of North-west Europe*. Glasgow: Blackie, pp. 38–42.

- Klemperer, S.L. & Hobbs, R., 1991. *The BIRPS Atlas: Deep Seismic Reflections Profiles Around the British Isles*, Cambridge University Press.
- Korte, C. & Hesselbo, S.P., 2011. Shallow marine carbon and oxygen isotope and elemental records indicate icehouse-greenhouse cycles during the Early Jurassic. *Palaeoceanography*, 26, pp.1–18.
- Korte, C. et al., 2015. Jurassic climate mode governed by ocean gateway. *Nature communications*, 6, pp.1–7.
- Labails, C., 2010. An alternative early opening scenario for the Central Atlantic Ocean. 297(September), pp.355–368.
- Labails, C. & Roest, W.R., 2010. Comment on “Breakup of Pangaea and plate kinematics of the central Atlantic and Atlas regions” by Antonio Schettino and Eugenio Turco. 183, pp.96–98.
- Larsen, N., Hayes, T. & Rogowski, C., 1983. 73/13-1 Well Completion Report. , pp.1–76.
- Leveridge, B.E. & Hartley, A.J., 2006. The Variscan Orogeny: the development and deformation of Devonian/Carboniferous basins in SW England and South Wales. In P. J. Benchley & P. F. Rawson, eds. *The geology of England and Wales*. Geological Society of London.
- Lewis, J.H., 1976. 93/2-1: Thermal Alteration and Source Rock. pp.1–8.
- Lundin, E.R., 2002. North Atlantic – Arctic : Overview of sea-floor spreading and rifting history. In *BATLAS–Mid Norway plate reconstruction atlas with global and Atlantic perspectives*. Coordinated by EA Eide. Trondheim, Norway: Geological Survey of Norway, pp. 40–47.
- Lundin, E.R. & Doré, A.G., Non-Wilsonian break-up, pre-disposed by transforms: examples from the North Atlantic and Arctic.
- Marathon Oil, 1994. Marathon Oil UK Ltd Composite Log - Well 103/1-1. p.1.
- Marathon Oil, Licence P804 , Block 103 / 01a ALL , Relinquishment Report. , pp.1–5.
- Masson, D.G. & Miles, P.R., 1986. Development and Hydrocarbon Potential of Mesozoic Sedimentary Basins Around Margins of North Atlantic. *The American Association of Petroleum Geologists Bulletin*, 70(6), pp.721–729.
- McKenzie, D., 1978. Some remarks on the development of sedimentary basins. *Earth and Planetary Science Letters*, 40(1), pp.25–32.
- Mckerrow, W.S., Niocaill, C.M.A.C. & Dewey, J.F., 2000. The Caledonian Orogeny redefined. *Journal of the Geological Society of London*, 157, pp.1149–1154.
- McKie, T., 2017. Palaeogeographic Evolution of latest Permian and Triassic Salt Basins in North West Europe. In J. I. Soto, J. Flinch, & G. Tari, eds. *Permo-Triassic Salt Provinces of Europe, North Africa and the Atlantic Margins*, Chapter: 7. Elsevier.

- McMahon, N.A & Turner, J. 1998. The documentation of a latest Jurassic-earliest Cretaceous uplift throughout southern England and adjacent offshore areas. In: Underhill, J. R., ed. *Development, Evolution and Petroleum Geology of the Wessex Basin*, Geological Society, London, Special Publications, 133, pp.215-240.
- Melvin, A., 2005. *Sedimentology and sequence stratigraphy Greensand Formation North Celtic Sea Basin, Ireland: A Predictive Model for Exploration Volume I of II*,
- Menpes, R.J. & Hillis, R.R., 1995. Quantification of Tertiary exhumation from sonic velocity data, Celtic Sea/Southwestern Approaches. *Geological Society, London, Special Publications, Basin Inversion*, 88, pp.191–207.
- Montadert, L. et al., 1979. Rifting and subsidence of the northern continental margin of the Bay of Biscay. *Initial Reports of the Deep Sea Drilling Project*, pp.1025–1060. Available at: http://www.deepseadrilling.org/48/volume/dsdp48_54.pdf.
- Morgan, P., 1983. Constraints on rift thermal processes from heat flow and uplift. *Developments in Geotectonics*, 19(C), pp.277–298.
- Murdoch, L.M., Musgrove, F.W. & Perry, J.S., 1995. Tertiary uplift and inversion history in the north Celtic Sea Basin and its influence on source rock maturity. In P. F. Croker & P. M. Shannon, eds. *The Petroleum Geology of Ireland's Offshore Basins*, Geological Society Special Publication. pp. 297–319. Available at: <http://sp.lyellcollection.org/cgi/doi/10.1144/GSL.SP.1995.093.01.22>.
- Murphy, J.B., 1989. Model for the evolution of the Avalonian-Cadomian belt. *Geology*, 17, pp.735–738.
- Murphy, N.J., Sauer, M.J. & Armstrong, J.P., 1995. Toarcian source rock potential in the North Celtic Sea Basin, offshore Ireland. *The Petroleum Geology of Ireland's Offshore Basins*, 93(93), pp.193–207.
- Murrell, S.A.F., 1986. Mechanics of tectogenesis in plate collision zones. *Geological Society, London, Special Publications*, 19(1), pp.95–111. Available at: <http://sp.lyellcollection.org/lookup/doi/10.1144/GSL.SP.1986.019.01.06>.
- O'Reilly, C., Shannon, P.M. & Feely, M., 1998. A fluid inclusion study of cement and vein minerals from the Celtic Sea basins, offshore Ireland. *Marine and Petroleum Geology*, 15(6), pp.519–533.
- Ottaviani, A. et al., Burial History and Thermal Maturity evaluation of the Western Approaches Basin, SW UK. pp.1–20.
- Oyarzun, R., 1997. Opening of the central Atlantic and asymmetric mantle upwelling phenomena: Implications for long-lived magmatism in western North Africa and Europe. *Geology*, 25(8), pp.727–730.
- Paleochem Ltd, 1983. Geochemical Evaluation of Sediments from the S.W. Approaches Well: 73/13-1. pp.1–102.
- Pálffy, J., Smith, P.L. & Mortensen, J.K., 2000. A U-Pb and ⁴⁰Ar/³⁹Ar time scale for the Jurassic. *Canadian Journal of Earth Sciences*, 37(6), pp.923–944.

- Passey, Q.R. et al., 1990. A Practical Model for Organic Richness from Porosity and Resistivity Logs. *American Association of Petroleum Geologists Bulletin*, 74(12), pp.1777–1794.
- Peace, A. et al., The role of pre-existing structures during rifting, continental breakup and transform system development, offshore West Greenland. *Basin Research*, pp.1–49.
- Pepper, A.S., 1995. Simple kinetic models of petroleum formation . Part II : oil-gas cracking. *Marine and Petroleum Geology*, 12(3), pp.321–340.
- Pepper, A.S., 1991. Estimating the petroleum expulsion behaviour of source rocks: a novel quantitative approach. *Geological Society, London, Special Publications*, 59(1), pp.9–31.
- Pepper, A.S. & Corvi, P.J., 1995. Simple kinetic models of petroleum formation Part III: modelling an open system. *Marine and Petroleum Geology*, 12(4), pp.417–452.
- Pepper, A.S. & Corvi, P.J., 1995. Simple kinetic models of petroleum formation. Part I: oil and gas generation from kerogen. *Marine and Petroleum Geology*, 12(3), pp.291–319.
- Peters, K.E., 1980. Guidelines for Evaluating Petroleum Source Rock Using Programmed Pyrolysis. *American Association of Petroleum Geologists Bulletin*, 70(3), pp.318–329.
- Petra-Chem Limited, 1983. Source Rock Evaluation of Sediments from Western Approaches Well: 73/2-1. pp.1–41.
- Pharaoh, T.C. et al., 2017. *South-West Approaches Study Phase 1 Lot 2: A Review of Late- and Post- Variscan basins and source potential in Western Europe. Energy and Marine Geoscience Programme Commissioned Report CR/17/031*, Keyworth, Nottingham.
- Providence, 2016. Licence P1930 St Georges Channel Basin UKCS Relinquishment Report June 2016. (June), pp.1–18.
- Readman, P.W. et al., 1995. A gravity map of Ireland and surrounding waters. In P. F. Croker & P. M. Shannon, eds. *The Petroleum Geology of Ireland's Offshore Basins Offshore Basins, Geological Society Special Publication*. pp. 9–16.
- Rider, M.H., 1996. *The geological interpretation of well logs - 2nd Edition*, Whittles Publishing.
- Robertson Research International Limited, 1974. Celtic Sea Geochemical Study. pp.1–12.
- Robertson Research International Limited, 1977. Report on a Geochemical Evaluation of Part of the 102/29-1 Well, Celtic Sea. In *UK Celtic Sea Well 102/29-1 Final Report*. pp. 42–58.
- Rohrman, M. et al., 2002. Timing and mechanisms of North Atlantic Cenozoic uplift: evidence for mantle upwelling. *Geological Society, London, Special Publications*, 196, pp.27–43.
- Rowell, P., 1995. Tectono-stratigraphy of the North Celtic Sea Basin. In P. F. Croker & P. M. Shannon, eds. *The Petroleum Geology of Ireland's Offshore Basins, Geological Society Special Publication*. pp. 101–137. Available at: <http://sp.lyellcollection.org/cgi/content/abstract/93/1/101>.

- Ruffell, A., 1995. Evolution and hydrocarbon prospectivity of the Brittany Basin (Western Approaches Trough), offshore north-west France. *Marine and Petroleum Geology*, 12(4), pp.387–407.
- Ruhl, M. et al., 2016. Astronomical constraints on the duration of the Early Jurassic Pliensbachian Stage and global climatic fluctuations. *Earth and Planetary Science Letters*, 1, pp.1–17. Available at: <http://dx.doi.org/10.1016/j.epsl.2016.08.038>.
- Sauer, M.J. & Bailey, N.J.L., 1978. Geochemical Evaluation of the BNOC 72/10A-1 Well, Western Approaches.
- Scotchman, I.C., 2017. *Evaluation of Hydrocarbon Source Potential of UK Western Approaches, based on vintage released well geochemistry reports*,
- Scotchman, I.C., 2001. Petroleum geochemistry of the Lower and Middle Jurassic in Atlantic margin basins of Ireland and the UK. In P. M. Shannon, P. D. W. Haughton, & D. V Corcoran, eds. *The Petroleum Exploration of Ireland's Offshore Basins. Geological Society, London, Special Publications, 188*. pp. 31–60.
- Scotchman, I.C., Doré, A.G. & Spencer, A.M., 2016. Petroleum systems and results of exploration on the Atlantic margins of the UK, Faroes & Ireland: what have we learnt? In M. Bowman & B. Levell, eds. *Petroleum Geology of NW Europe: 50 Years of Learning – Proceedings of the 8th Petroleum Geology Conference*. Geological Society of London, pp. 1–11.
- Scotese, C.R., 2001. *Atlas of Earth History*, PALEOMAP Project.
- Selby, D. & Creaser, R.A., 2003. Re-Os geochronology of organic rich sediments: An evaluation of organic matter analysis methods. *Chemical Geology*, 200(3–4), pp.225–240.
- Sellwood, B.W. & Valdes, P.J., 2006. Mesozoic climates : General circulation models and the rock record. *Sedimentary Geology*, 190, pp.269–287.
- Shail, R.K. & Leveridge, B.E., 2009. The Rhenohercynian passive margin of SW England: development, inversion and extensional reactivation. *Comptes Rendus Geoscience*, 341(2), pp.140–155.
- Sibuet, J. et al., 2017. Early Cretaceous motion of Flemish Cap with respect to North America: implications on the formation of Orphan Basin and SE Flemish Cap – Galicia Bank conjugate margins Natural Resources Canada, Geological Survey of Canada, Bedford Institute of. In G. D. Karner, G. Manatschal, & L. M. Penheiro, eds. *Imaging, Mapping and Modelling Continental Lithosphere Extension and Breakup*. pp. 63–76.
- Simms, M.J. et al., 2004. British Lower Jurassic stratigraphy: an introduction. *Geological Conservation Review Series, No. 30, Joint Nature Conservation Committee, Peterborough*, pp.1–25.
- Smith, P.M.R., 1983. Spectral Correlation of Spore Coloration Standards. *Geological Society, London, Special Publications*, 12(1), pp.289–294.
- Soper, N.J. & England, R.W., 1992. The Iapetus suture zone in England, Scotland and eastern Ireland: a reconciliation of geological and. *Journal of the Geological Society of London*, 149, pp.697–700.

- Soper, N.J. & Hutton, D.H.W., 1984. Late Caledonian Sinistral Displacements in Britain: Implications for a Threeplate Collision Model. *Tectonics*, 3(7), pp.781–794.
- Soper, N.J. et al., Sinistral transpression and the Silurian closure of Iapetus. *Journal of the Geological Society of London*, 149, pp.871–880.
- Staplin, F.L., 1969. Sedimentary organic matter, organic metamorphism, and oil and gas occurrence. *Bulletin of Canadian Petroleum Geology*, 17(1), p.47-66.
- Staplin, F.L., 1977. Interpretation of Thermal History from Color of Particulate Organic Matter: A Review. *Palynology, Proceedings of the 8th Annual Meeting*, 1, pp.9–18.
- Steckler, M.S. & Watts, A.B., 1978. Subsidence of the Atlantic-type Continental Margin off New York. *Earth and Planetary Science Letters*, 41, pp.1–13.
- Stricker, S. et al., Well Correlation Panels of the Western Approaches and Celtic Sea.
- Styles, A.J., 1997. The nature and significance of Late-Orogenic extensional structures in the Variscan Orogen of SW England and comparison to equivalent features from the Italian Apennines. *Durham E-Theses*.
- Taylor, G.K., 2007. Pluton shapes in the Cornubian Batholith: new perspectives from gravity modelling. *Journal of the Geological Society of London*, 164, pp.525–528.
- Tissot, B.P., Pelet, R. & Ungerer, P.H., 1987. Thermal History of Sedimentary Basins, Maturation Indices, and Kinetics of Oil and Gas Generation. *The American Association of Petroleum Geologists Bulletin*, 71(12), pp.1445–1466.
- Tissot, B. et al., 1974. Influence of Nature and Diagenesis of Organic Matter in Formation of Petroleum. *The American Association of Petroleum Geologists Bulletin*, 58(3), pp.499–506.
- Torsvik, T.H. & Cocks, R.M., 2017. *Earth History and Palaeogeography*, Cambridge University Press.
- Torsvik, T.H. et al., 1996. Continental break-up and collision in the Neoproterozoic and Palaeozoic - A tale of Baltica and Laurentia. *Earth-Science Reviews*, 40, pp.229–258.
- Tucker, R.M. & Arter, G., 1987. The tectonic evolution of the North Celtic Sea and Cardigan Bay basins with special reference to basin inversion. *Tectonophysics*, 137, pp.291–307.
- Tugend, J., Manatschal, G. & Kusznir, N.J., 2015. Spatial and temporal evolution of hyperextended rift systems : Implication for the nature , kinematics , and timing of the Iberian- European plate boundary. , 43(1), pp.15–18.
- Tugend, J. et al., 2014. Formation and deformation of hyperextended rift systems: Insights from rift domain mapping in the Bay of Biscay-Pyrenees. *Tectonics*, 33, pp.1239–1276.
- Tyson, R. V, 2017. Variation in marine total organic carbon through the type Kimmeridge Clay Formation (Late Jurassic), Dorset, UK. *Journal of the Geological Society*, 161, pp.667–673.

- Underhill, J.R & Partington, M.A 1993. Jurassic thermal doming and deflation in the North Sea: implications of the sequence stratigraphic evidence. In J. R. Parker, ed. *Petroleum Geology of Northwest Europe: Proceedings of the 4th Conference*. Geological Society of London, pp. 337–345.
- Van Hoorn, B., 1987. The South Celtic Sea/Bristol Channel Basin: origin, deformation and inversion history. *Tectonophysics*, 137(1–4), pp.309–334.
- van Krevelen, D.W., 1984. Organic geochemistry - old and new. *Organic Geochemistry*, 6, pp.1–10.
- Vissers, R.L.M. et al., 2016. Cretaceous slab break-off in the Pyrenees: Iberian plate kinematics in paleomagnetic and mantle reference frames. *Gondwana Research*, 34, pp.49–59. Available at: <http://dx.doi.org/10.1016/j.gr.2016.03.006>.
- Waters, C.N. & Davies, S.J., 2006. Carboniferous: extensional basins, advancing deltas and. In P. J. Brenchley & P. F. Rawson, eds. *The geology of England and Wales*. Geological Society of London, pp. 173–223.
- Waters, C. et al., 2009. *A lithostratigraphical framework for the Carboniferous successions of southern Great Britain (onshore)*,
- Wilcox, L.E., 1976. Airy-Woollard isostasy. In *The Geophysics of the Pacific Ocean Basin and its Margin*. pp. 53–58.
- Woodcock, H. & Johnson, E., 1988. Acadian Tectonics of Wales during Avalonia/Laurentia Convergence. *Tectonics*, 7(3), pp.483–495.
- Woodcock, N.H. & Strachan, R.A., 2012. *Geological history of Britain and Ireland*, John Wiley & Sons.
- Ziegler, P.A., 1987. Evolution of the Western Approaches. *Tectonophysics*, 137, pp.341–346.
- Ziegler, P.A., 1987. Celtic Sea-Western Approaches area: an overview. *Tectonophysics*, 137(1–4), pp.285–289.
- Anon, *Evolution of the Celtic Sea Basins - Unknown Celtex S Celtic Sea Report*,